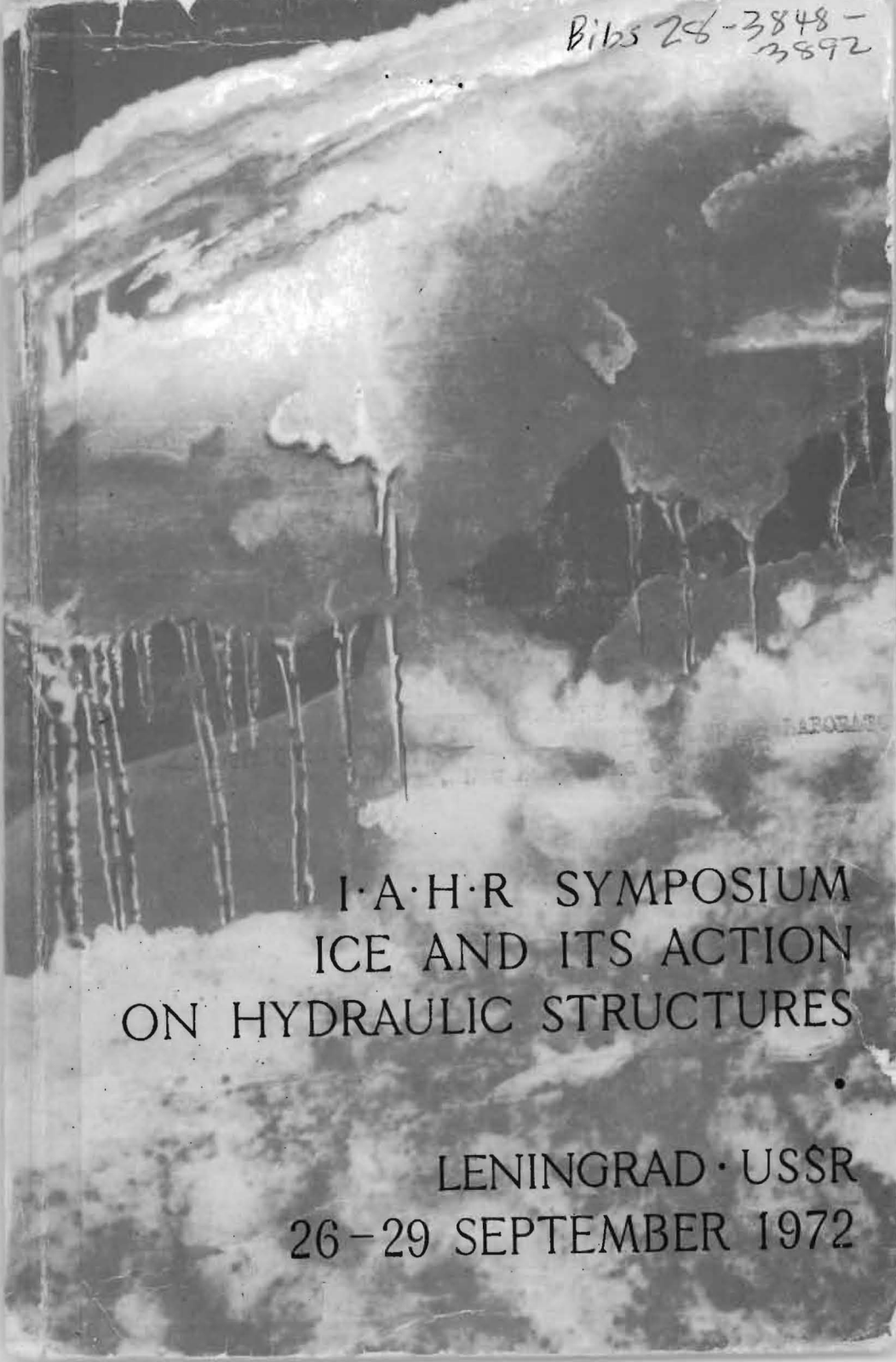
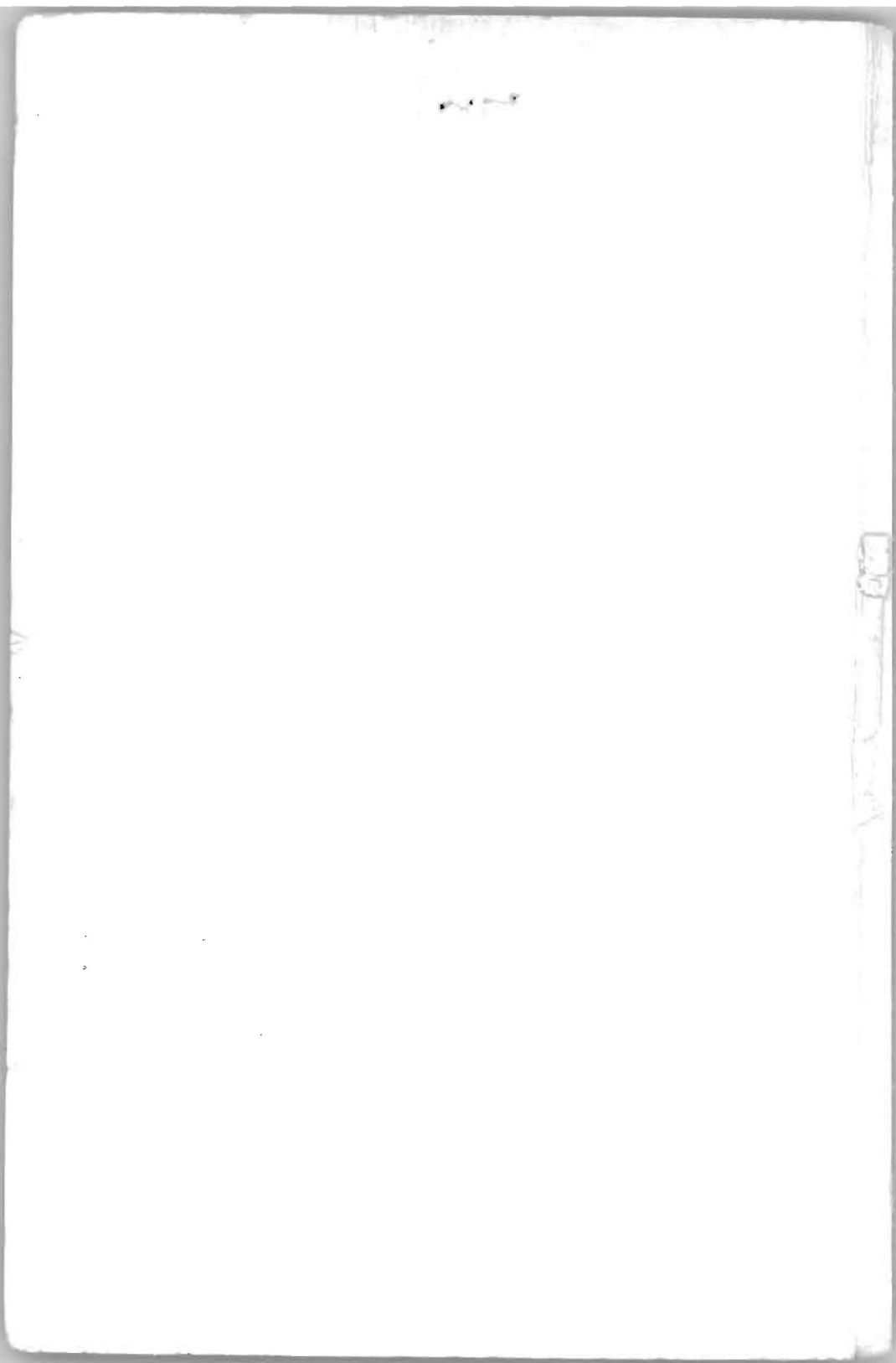


Bibs 26-3848 -
3892



I·A·H·R SYMPOSIUM
ICE AND ITS ACTION
ON HYDRAULIC STRUCTURES

LENINGRAD · USSR
26 - 29 SEPTEMBER 1972



GF



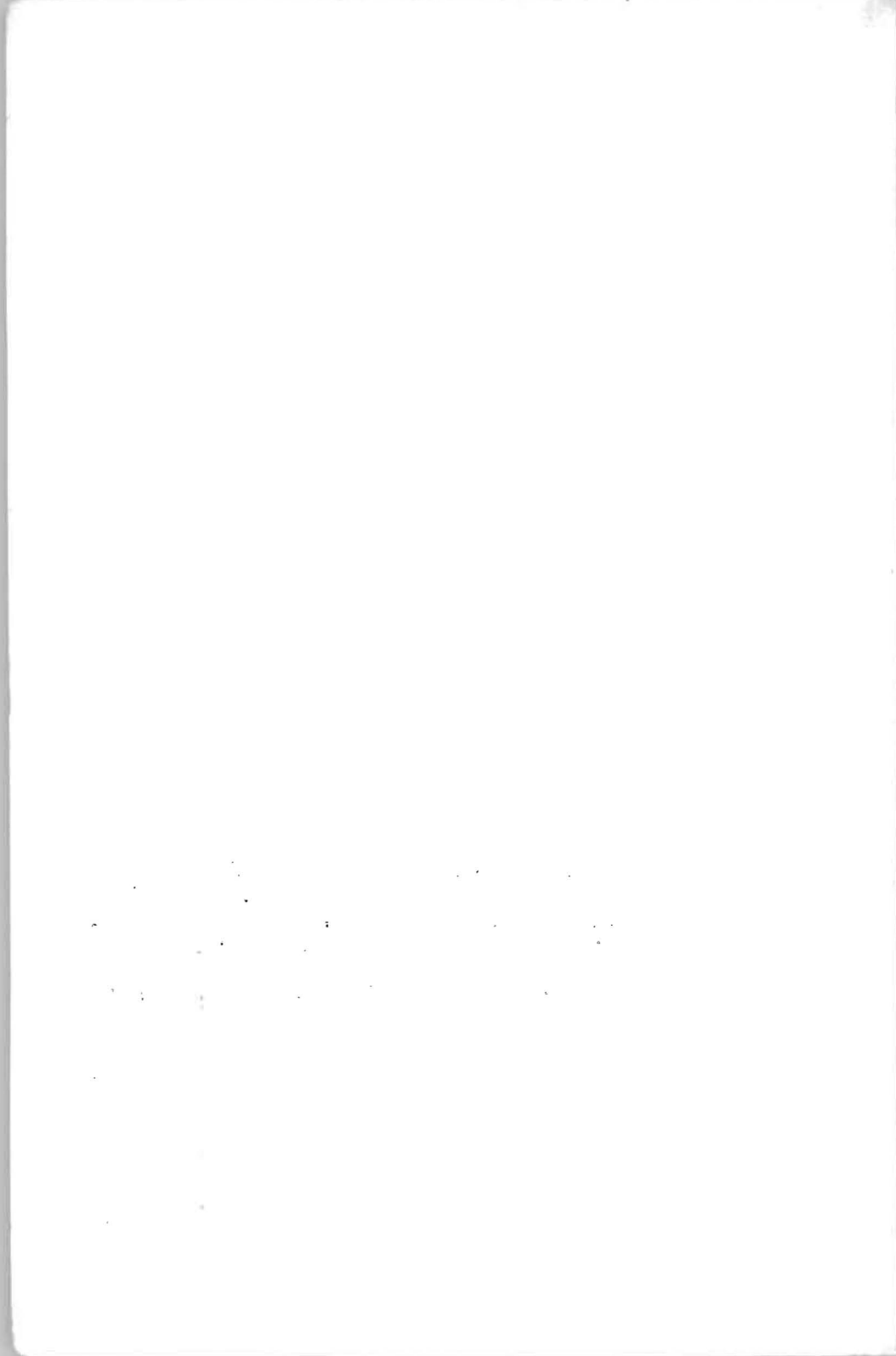
U. S. ARMY

ENGINEERING LABORATORY
REGULATIONS 03765

I·A·H·R SYMPOSIUM
ICE AND ITS ACTION
ON HYDRAULIC STRUCTURES

•

LENINGRAD · USSR
26 - 29 SEPTEMBER 1972





ICE SYMPOSIUM 1972
LENINGRAD

DEPENDENCE OF MECHANICAL PROPERTIES
OF ICE ON ITS STRUCTURE

K.F. Voitkovsky, Dr. Sc. (Eng.), Prof. Moscow Moscow
V.N. Golubev, Engr State University U.S.S.R.

SYNOPSIS

An attempt has been made to generalize the data on the dependence of the mechanical properties of ice on its structure which, in its turn, is governed by the conditions of ice formation and existence. The influence of ice structure on its deformation and failure mechanism as well as on creep parameters, strength characteristics and adhesion forces has been shown. Three stages of recrystallization of polycrystalline ice during creep process, namely crystal growth, relative structure stabilization and crushing have been pointed out. It is proposed to use the obtained dependences for forecasting the ice strength based on the conditions of ice formation and for changing ice mechanical properties by ensuring adequate thermodynamic conditions during ice formation.

RESUME

La tentative a été faite de généraliser les connaissances sur la dépendance entre les propriétés mécaniques de la glace et sa structure, qui est déterminée par les conditions de formation et d'existence de la glace. L'influence de la structure de la glace sur le mécanisme de sa déformation et destruction, de même que sur les paramètres du fluage, les caractéristiques de la résistance et les forces adhésives a été démontrée. Trois stades de la recristallisation de la glace polycristalline au cours de sa fluage ont été distingués - la croissance des cristaux, la stabilisation relative de la structure et le morcellement. On propose d'employer ces régularités pour la prévision des caractéristiques de la résistance de la glace conformément aux conditions de sa formation et pour le changement à but précis des propriétés mécaniques de la glace par le moyen de la création des conditions thermodynamiques respectives lors de sa formation.

The deformation mechanism, strength and mechanical properties of ice depend largely on its structure which, in its turn, is governed by the thermodynamic conditions of ice formation and existence. Ice of different structure is formed according to the degree of supercooling of water, the temperature gradient, the intensity of diffusion of water or vapour towards the air-water interface, and the presence of impurities. In solving ice engineering problems we most often have to deal with the following cases of ice formation: 1) ice formation at the air-water interface with subsequent growth of the ice cover due to temperature gradient; 2) ice formation and growth on the surface of a cold solid body in contact with a large mass of supercooled water; 3) ice growth from drops of supercooled water on a cold surface; 4) successive freezing of thin water layers on the ice surface.

In the first and second cases, coarse- and medium-grained ice of prismatic structure is formed, the prisms growing in the direction of temperature gradient, with the optical axes of crystals parallel to the surface of freezing (Fig.1a). In the third and fourth cases, fine- and medium-grained hypidiomorphic ice with random or slightly oriented crystal optical axes is generally formed (Fig.1b,c).

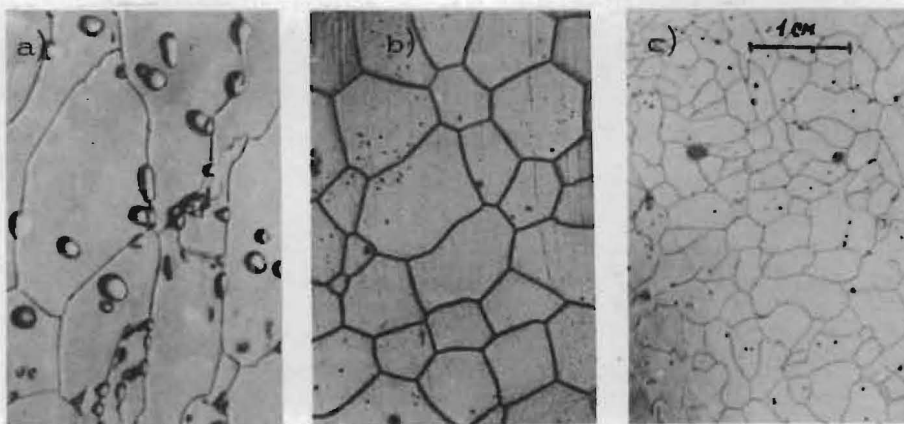


Fig. 1. Microphotos of ice structure

- a - coarse-grained prismatic ice;
- b - medium-grained hypidiomorphic ice;
- c - fine-grained hypidiomorphic ice.

Thorough crystal-optic investigations of deformed ice have shown that the deformation of monocrystals and blocks consisting of a few large crystals is due to sliding along the basal and prismatic planes, while during the deformation of polycrystalline ice microdisplacement of the crystals with respect to each other, the appearance of microcrevices with gliding of crystal groups, and recrystallization are predominant.

The study of light interference at the boundaries of deformed crystals has shown that the bigger the crystals, the more intensive the stress concentration at the contacts. Accordingly, the possibility of crystal discontinuity and formation of crevices at the contacts increases, thus reducing ice strength. The crevices formed in fine-grained ice may end at the crystal contacts without causing brittle failure of an ice sample. The crevices formed in coarse-grained ice and in monocrystals grow quickly, and the deformed sample desintegrates. Therefore, fine-grained ice has the greatest strength (Table 1).

Table 1

Compressive Strength of Ice (kgf/cm^2)
(Strain rate $\dot{\epsilon} = 0.03 \text{ 1/min, } t = -10^\circ\text{C}$)

Average size of crystals, mm	Crystal orientation		
	random	clearly defined σ_{\parallel}	defined σ_{\perp}
fine $d < 1$	49.5	52.0	47.5
medium $d = 2 - 5$	-	42.7	36.4
coarse $d > 5$	-	31.2	27.9

Note: σ_{\parallel} - compression in the direction of optical axes;
 σ_{\perp} - compression perpendicular to the optical axes.

To establish the relationship between the ice strength characteristics and its structure it is necessary to take into consideration three main characteristics: the size of crystals, their isometricity and orientation of optical axes. At present it is obvious that the smaller the crystals, the greater compressive ice strength. The strength of ice is also the higher, the more intricate the crystal boundaries and the greater the number of crystals whose optical axes orientation coincides with the direction of compression. The ice structure is not a constant characteristic and even under permanent environmental conditions it undergoes considerable alterations with time. These changes embrace the whole complex of structural characteristics: the size, the form and the orientation of ice optical axes as well as the character of distribution of air bubbles, brine cells and mineral particles. The temperature gradient and strain forces speed up the process of ice structure rearrangement.

The experiments on compression of polycrystalline ice with random distribution of crystal optical axes under a constant load showed that structural changes due to deformation are determined both by the time of deformation and the magnitude of the load and relative strain applied (Fig. 2).

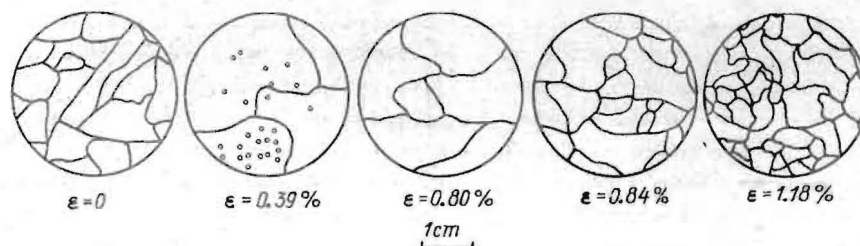


Fig. 2. Structural changes of polycrystalline ice in creep ($\sigma = 2 \text{ kgf/cm}^2$)

According to the three main stages of creep we can distinguish three main stages of recrystallization, namely crystal growth, relative structure stabilization and crystal crushing (Fig. 3c,d). A few moments after the application of the load the crystals are adapted, as it were, to the new thermodynamic conditions. Some rotations and displacements of the crystals and their partial destruction are observed, which leads to simplification of the form of crystals. The intensity of this process decreases gradually, and any further modification of the deformed ice structure is caused by the tendency of the system to minimize the surface and free energy. The less stressed crystals grow at the expense of the more stressed ones, and the small crystals are absorbed by the bigger ones. Hence, the total number of crystals decreases, with the average crystal volume essentially increasing. The rate of crystal growth slows down with increasing ice strain and after a time a relative stabilization of the ice structure occurs, which is characterized by a distinct crystal orientation. Subsequent deformation leads to progressive cracking and crushing of crystals. This stage is observed only when shear stresses exceed a certain limit, which is 1.5 kgf/cm^2 at the ice temperature -1°C , and 3 kgf/cm^2 at the ice temperature -4°C .

The rate and the magnitude of relative creep deformation of ice depend on the size of crystals as well as on the direction of shear stress with respect to the predominant directions of crystal axes. The lowest rates of creep are observed in fine-grained ice with random crystal orientation (Fig. 3a,b), and the highest rates in the ice of prismatic structure when maximum shear stresses occur in the planes coinciding with the prism axes (Curves 2,3). For other directions of shear stresses the creep rate values fall within the two extreme cases indicated above (Curve 1).

In solving ice engineering problems the relationships established between the physico-mechanical properties of ice and its structure permit to forecast ice strength characteristics according to ice formation conditions or to change these characteristics by providing adequate thermodynamic conditions during ice formation.

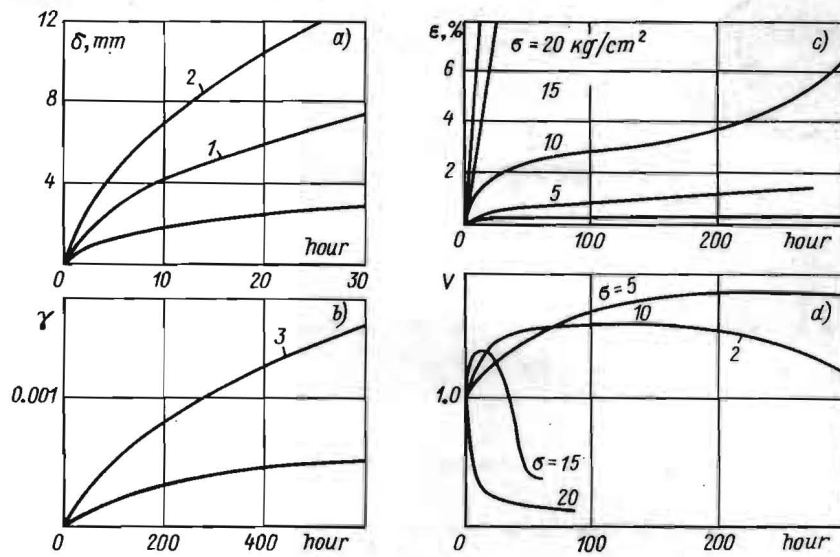


Fig. 3. Creep curves of polycrystalline ice:

- a) in bending (a beam of 10×10 cm cross-section, span $l = 100$ cm, load 40 kgf);
- b) in pure shear (torsion of tubes at $\tau = 0.25 \text{ kgf/cm}^2$);
- c) in compression; and
- d) for changing volumes of average crystals.
 - 1 - vertical direction of crystal axes in the beam;
 - 2 - horizontal direction of crystal axes in the beam;
 - 3 - radial direction of crystal axes in the tube. Other curves refer to samples of random structure.



ICE SYMPOSIUM 1972
LENINGRAD

THE MODULUS OF ELASTICITY OF SEA ICE
SHOWN BY DIRECT TENSION AND COMPRESSION
TESTS OF SMALL SPECIMENS

Philip R. Johnson, Civil Engineer Phil Johnson Engineering Box 80337
College
Alaska 99701

SYNOPSIS

E , the modulus of elasticity of sea ice, was studied using some of Peyton's published data. His tests were of small specimens of sea ice tested in direct compression and direct tension. The compression data shows that all data can be thrown together and E expressed as a simple linear function of ultimate strength. The tension data shows two separate E -strength relationships. For ice which can fail on the brine-basal plane, a strong linear relationship exists between E and strength. All other orientations have an essentially constant E unaffected by strength. E in tension may be as much as an order of magnitude greater than E in compression. The problem of evaluating beam or plate tests and ring tensile tests is now seen to be more complex than had been previously assumed.

INTRODUCTION

Strength and stiffness are two characteristics of a material of basic interest to engineers. Sea ice, as a material, has proven to be unusually difficult to describe and define as it exhibits both viscous and elastic behavior and has an unusual internal structure containing liquid inclusions in the already relatively weak basal plane. While the strength of sea ice has been studied extensively, a really good definition of this strength has not yet been obtained. The state of knowledge regarding the stiffness of the material as measured by E, the modulus of elasticity, is even less satisfactory.

The classic method of determining the E for elastic materials is by measuring the slope of a stress-strain curve. For materials which do not behave in a purely elastic manner, an apparent modulus can be and is used. For a visco-elastic material such as ice, it is either necessary to separately define the viscous and elastic properties or to use an apparent modulus which combines both functions.

CHARACTERISTICS OF SEA ICE

Peyton carried out an extensive testing program on sea ice at Point Barrow during the period 1958-1962 and made about 3800 direct compression and direct tension tests on small specimens. This data and a partial analysis was published in 1966*. The analysis concentrated on identifying and measuring the parameters governing ultimate strength and, while the data includes both the stress-strain raw data and computed moduli of elasticity, little work had previously been done on the elasticity data. This paper reports on an investigation into part of this stress-strain data. However, some background and description of the data is required.

In examining sea ice both at Point Barrow and elsewhere, Peyton found that below a depth of about 20 inches, the sea ice had an ordered structure. Calling this ordered ice "bottom ice," he reported that it was composed of relatively large vertical crystals with horizontal c-axes which showed a preferential orientation. In a sample three meters square, he found that the orientation of the c-axes throughout the entire specimen were oriented in the same direction. Because of this preferred orientation, the orientation of the specimens was included in the testing data. He developed a notation consisting, for each specimen, of two

*Peyton, H. R., 1966. Sea Ice Strength, Geophysical Institute, University of Alaska, College, Alaska 99701

angles: the angle between the applied force during testing and the zenith, and the angle between the applied force and the c-axis of the specimen. Thus, an orientation of 00:90 shows a zero angle between the force and the zenith (vertical specimen) and 90 degrees between the force and the c-axis. An orientation of 90:00 shows 90 degrees between the force and zenith (horizontal specimen) and with the force applied along the c-axis. In analyzing ultimate or failure strength of this ice in both tension and compression, orientation was found to be extremely important. Figure 1 shows the strength of sea ice under standard conditions for different orientations in both tension and compression. In addition to orientation, ice strength was affected by ice type, brine volume, rate of loading and, possibly, by depth and the presence of solid salts.

THE E-STRENGTH RELATIONSHIPS IN COMPRESSION & TENSION

The stress-strain curves from Peyton's tests were curved, so the apparent modulus was defined as a line secant to this curve at the origin and a stress equal to one-third the failure strength of replicate tests. Peyton reported that, on the basis of a cursory examination of the data, E was generally strongly dependent on the rate of loading, strength and orientation, and that E in tension is approximately five times that in compression. Figure 2 shows E in both tension and compression under standard conditions as a function of orientation. This figure shows a strong similarity to the strength-orientation pattern in Figure 1. However, in his report Peyton inadvertently mis-labeled the tension and compression curves in Figure 2 so that the apparent close relationship in the upper curves is between the strength-orientation relationship in compression and the E-orientation relationship in tension. The relationships between these curves, while striking, are not easily explained at this time.

This study examined the relationship between strength and E. Since the data was in British units, the analysis was carried out in those units but the regression equations are also given in metric units.

In the study of compression data, 330 selected tests were used. They were all of bottom ice at a depth of 44 inches in the ice sheet and most were obtained from a single sample just off Point Barrow. Four orientations (00:90, 90:00, 90:45 and 90:90), four temperatures (-2, -5, -10, and -21°C) and about six rates of loading were used. Each set, constant in the above parameters, contained 3-4 data which were averaged. It was found that all of the data, when plotted on the same graph, showed a good linear relationship. The least squares line through this data, shown in Figure 3, is:

$$E = 60630 + 148.6 \sigma \text{ psi} \quad (1)$$

where σ is failure strength in psi. The correlation is .84 and the standard error is 74,000 psi. In metric units, this is:

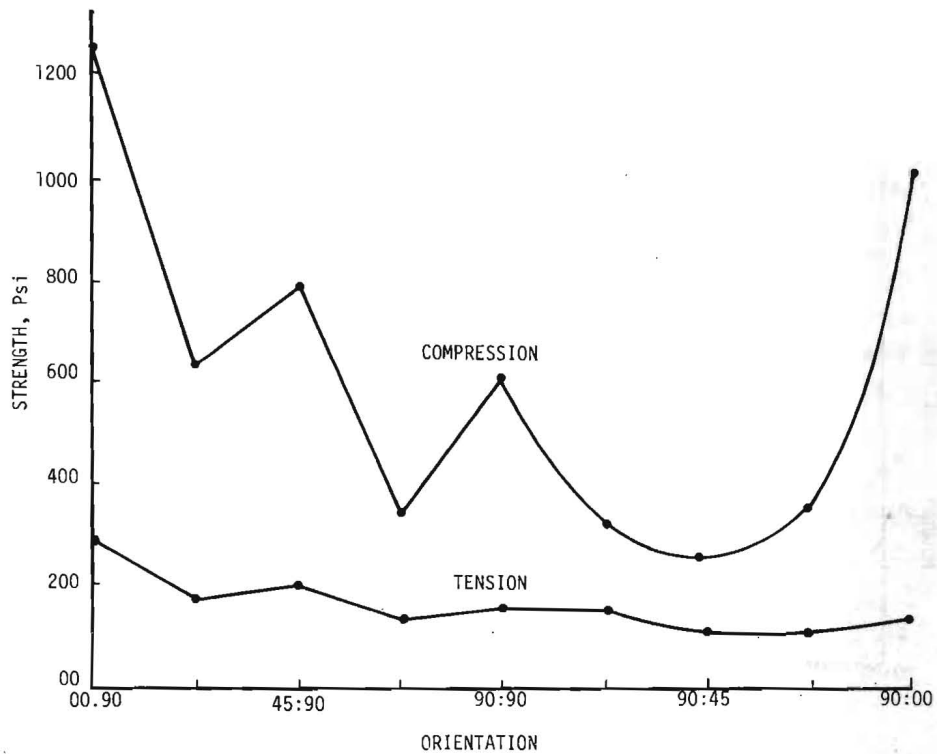


FIG. 1 SEA ICE STRENGTH AT VARIOUS ORIENTATIONS UNDER STANDARD CONDITIONS (After Peyton)

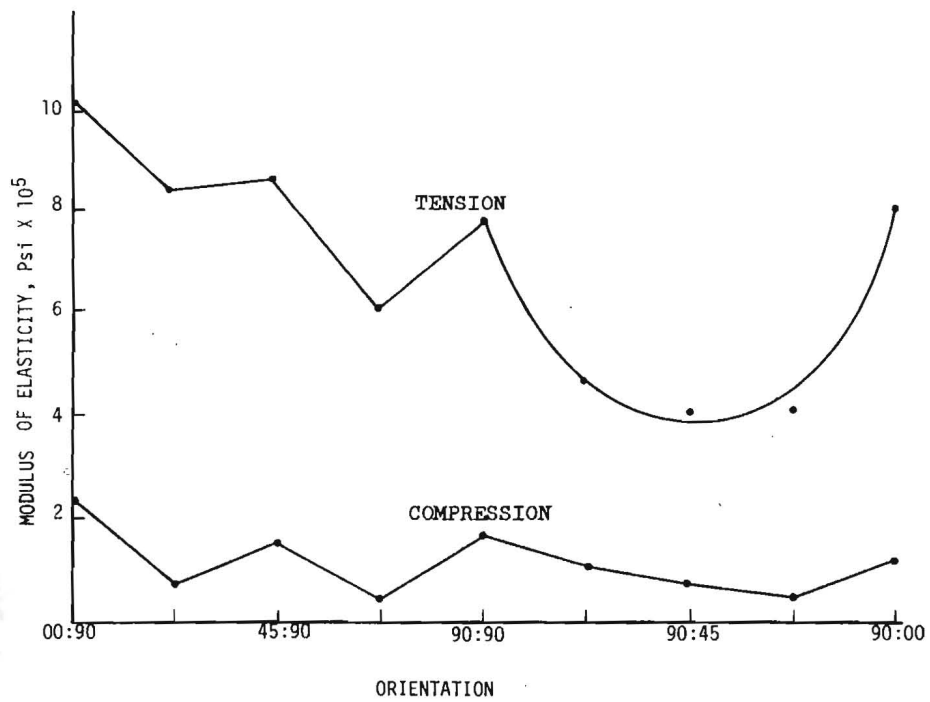


FIG. 2. MODULUS OF ELASTICITY OF SEA ICE AT VARIOUS ORIENTATIONS UNDER STANDARD CONDITIONS(after Peyton, corrected)

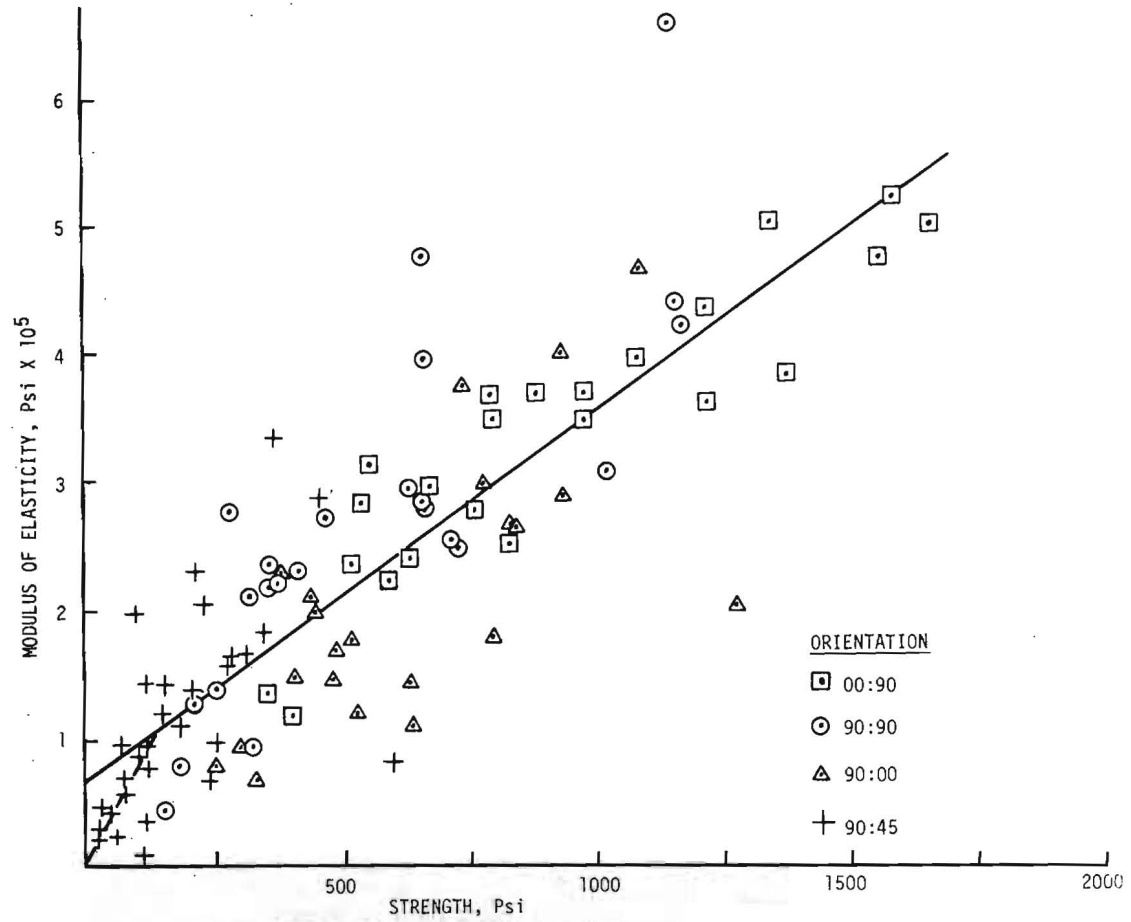


FIG. 3. MODULUS OF ELASTICITY vs STRENGTH FOR COMPRESSION DATA.

$$E = (4.18 + 0.001 \bar{\sigma}_m) \times 10^9 \text{ dynes/cm}^2 \quad (2)$$

where $\bar{\sigma}_m$ is strength also expressed in dynes/cm².

A similar study of tensile data was also carried out. 184 tests from the same ice with the same orientations and temperatures and, generally, three rates of loading, were grouped into 50 sets. Strength and E were again averaged for each set. This data is plotted in Figure 4. It shows that two types of behavior exist in sea ice when loaded in tension. Ice which can fail on the weak brine-basal plane (90:45) shows a strong positive correlation between E and strength. This behavior also seems characteristic of the 90:00 and 90:90 ice until a transition point is reached at $E = 10 \times 10^5$ and strength = 185 psi. Beyond that point, E can be considered to be constant with a value of 10×10^5 psi (6.9×10^{10} dynes/cm²). The least squares equation for the 90:45 data is:

$$E = -446,000 + 7,800 \bar{\sigma} \text{ psi} \quad (3)$$

with a correlation coefficient of .95 and standard error of 67,000 psi. In metric units, this equation is:

$$E = (-3.075 + 0.054 \bar{\sigma}_m) \times 10^{10} \text{ dynes/cm}^2. \quad (4)$$

The three lines described above have been plotted on Figure 5 with the lines extending over the strength ranges found for the data. It is seen that E in tension is indeed much greater than in compression and, in the area where ice will fail in tension, may be an order of magnitude greater. Thus Peyton's statement is confirmed and amplified by the results of this study.

DISCUSSION

It is seen that E can be expressed in terms of strength in both compression and tension. In compression, E can be expressed as a single linear function of strength for the data studied. On the other hand, the tension data shows two separate types of behavior. The 90:45 specimens, which can easily fail by sliding on the brine-basal plane show an extremely strong linear relationship between E and strength. This behavior also occurs in other warm weak horizontal specimens. Stronger horizontal specimens and all vertical specimens show a constant E throughout the strength range that ice experiences in tension.

Despite the relationships shown above, it is not felt that strength controls E in sea ice. Instead, the same parameters that control strength also control the modulus of elasticity with the result that E can be found in terms of strength

These relationships provide a means of evaluating E and its variability within a beam or the ice sheet. However, the great difference between E in tension and E in compression must complicate the analysis of loaded beams or plates and ring tensile tests. In addition, the effect of ice type and orientation now

becomes of greater importance. Weeks and Assur* approached the problem of a variable property in an ice sheet based on the vertical variation of brine volume. It would be possible to expand this approach to include the difference in E in tension and compression; however, these variations seem to be so extreme that the entire problem should be re-examined.

*Weeks, W., and Assur, A., 1967. The Mechanical Properties of Sea Ice, p. 61-66, U. S. Army CRREL Monograph II-C3, Hanover, New Hampshire.

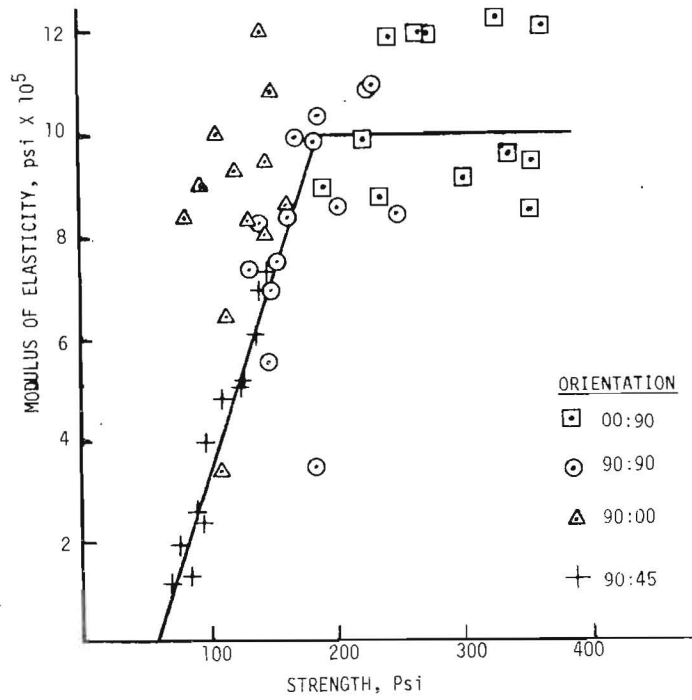


FIG. 4. MODULUS OF ELASTICITY vs STRENGTH, TENSION

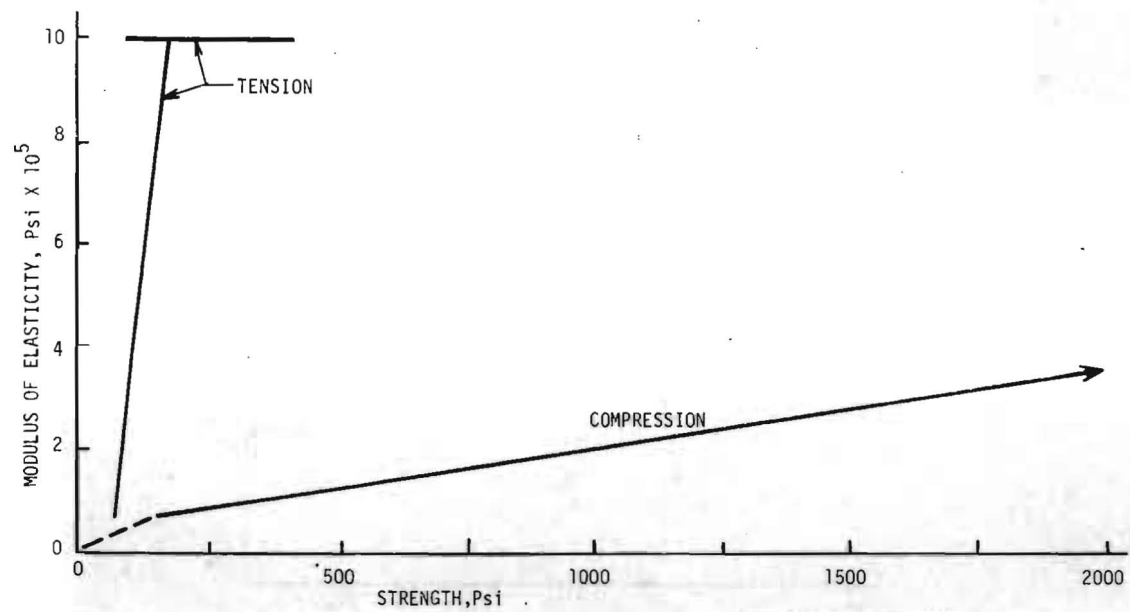


FIG. 5. MODULUS OF ELASTICITY vs STRENGTH, FOR SEA ICE IN TENSION AND COMPRESSION.



THE ULTIMATE FAILURE OF A FLOATING
ICE SHEET

Donald E. Nevel, Research Civil Engineer	U.S. Army Cold Regions Research and Engineering Laboratory,	Hanover, New Hamp- shire, U.S.A.
---------------------------------------------	----------------------------------------------------------------	----------------------------------------------

SYNOPSIS

When a floating ice sheet impinges on a sloping structure, the ice will fail in bending. To obtain a theoretical approach to this problem, a review is given of the way in which a vertical load will ultimately break through the ice. New theoretical equations are given for the breaking of wedges and the results compare favorably with published data on the ultimate load carrying capacity of ice sheets. For a sloping structure, a wedge with both vertically and horizontally applied loads has been solved, but numerical results are still being calculated.

H. Hertz¹ was the first to solve the problem of the load carrying capacity of a floating plate. His analysis predicted the initial crack for a load uniformly distributed over a circular area. He recognized that the plate theory incorrectly predicted the stress in the vicinity of the load when the radius a of the loading is small compared to the plate thickness h . This problem was solved by A. Nadai² who matched a three-dimensional *theory of elasticity* solution of a loaded disk to the floating plate solution. H. Westergaard³ numerically evaluated this solution and presented the result with an approximate equation. D. Nevel⁴ solved the floating plate problem by using the three dimensional *theory of elasticity*. These results verified that Westergaard's equation was sufficiently accurate for engineering purposes.

The above theories predict the initial, single radial crack of a floating plate, but they do not predict the ultimate break-through. Observations show that, as the load increases, additional radial cracks occur after the initial crack. Each additional crack tries to divide the remaining section of plate in half. Theoretically, the second radial crack should be perpendicular to the first and would create four 90° sections of ice. Under further load, the four 90° sections will crack in half creating eight 45° sections or wedges. This cracking pattern has been observed, but more frequently only six wedges are formed. This is most probably due to nonuniform ice properties.

The ultimate load carrying capacity is associated with breaking off tips of these wedges. Even after these tips have cracked, the load will sometimes not fall through the ice. The load is transferred through the crack to the truncated portion of the wedge which must be broken to cause break-through. For wedges whose angles are less than 90°, observations show that these tip-breaking cracks are straight. This effect indicates that the wedges may be analyzed as beams rather than as plates.

D. Nevel^{5,6,7} has solved the problem of a floating wedge. The wedge was considered a beam whose width b varied linearly with the distance x measured along the wedge bisector from the tip, i.e. $b = b_0 x$ where b_0 is a constant. The tip of the wedge was uniformly loaded for a distance $x = a$. The predicted distance where the wedge should break is shown in Figure 1 as a function of the loading distance a . The characteristic length $\lambda = [(Eh^3)/(12k)]^{1/4}$ where E is Young's modulus, h is the plate thickness, and k is the unit weight of the water.

The load factor $(6P_w)/(b_0 \sigma h^2)$ required to break the uniformly loaded wedge is shown in Figure 2 where P_w is the load on the wedge and σ is the bending tensile strength. An approximate equation for this relation is

$$\frac{6 P_w}{b_0 \sigma h^2} = 1.05 + 2.00 \left(\frac{a}{\lambda}\right) + 0.50 \left(\frac{a}{\lambda}\right)^3. \quad (1)$$

The exact values are given in Table I.

D. Panfilov⁸ has performed ultimate load carrying capacity experiments with the load P applied at the corners of a square whose side is of length $2a$. The results were linear and expressed as

$$\frac{P}{\sigma h^2} = 1.25 + 2.10 \left(\frac{a}{\lambda}\right) \quad (2)$$

where a/λ was as large as 0.4 in the tests. Eight wedges were observed and hence equation 2 becomes

$$\frac{6 P_w}{b_0 \sigma h^2} = 1.13 + 1.90 \left(\frac{a}{\lambda}\right) \quad (3)$$

which agrees remarkably well with equation 1.

The solution of the problem for the truncated wedge can easily be solved by using the previous general solutions. At the truncated distance $x = a$, the applied vertical load is P_w and the applied moment is zero. As x goes to infinity the deflection and slope of the wedge are zero. These boundary conditions yield a solution whose stress is

$$\frac{b_0 \sigma h^2}{6 P_w} = \frac{-1}{(a/l)} \left[\frac{Dn_3'(a/l)Dn_2'(x/l) - Dn_2'(a/l)Dn_3'(x/l)}{Dn_2''(a/l)Dn_3'(a/l) - Dn_2'(a/l)Dn_3''(a/l)} \right] \quad (4)$$

where Dn_2 and Dn_3 are two of the general solutions⁶ for the floating wedge problem. The primes indicate derivatives. The maximum stress occurs when x/l satisfies

$$\frac{Dn_3'''(x/l)}{Dn_2'''(x/l)} = \frac{Dn_3''(a/l)}{Dn_2''(a/l)} \quad (5)$$

The position of the maximum stress is shown in Figure 1, and the load factor $(6P_w)/(b_0 \sigma h^2)$ at this position is shown in Figure 2. An approximate equation for this is

$$\frac{6 P_w}{b_0 \sigma h^2} = 1.10 + 2.40 \left(\frac{a}{l}\right) - 0.10 \left(\frac{a}{l}\right)^3 \quad (6)$$

The exact values are shown in Table II.

It is of interest to compare the previous results with the position of the circumferential crack as predicted from the plate theory. M. Wyman⁹ has expressed Hertz's solution in terms of modified Bessel functions. For the deflection w not under the load, he gives

$$w = \frac{P}{k l^2} \frac{1}{\pi (a/l)^2} [\text{ber}'(a/l) \text{ker}(x/l) - \text{bei}'(a/l) \text{kei}(x/l)] \quad (7)$$

where a is the radius of the loaded area and x is the radial coordinate. The radial bending stress σ_r is determined by

$$\sigma_r = -\frac{6 k l^2}{h^2} \left[\frac{\partial^2 w}{\partial x^2} + \nu \frac{\partial w}{\partial x} \right] \quad (8)$$

where ν is Poisson's ratio. To determine the position of the maximum stress σ_r , equation 8 is differentiated with respect to x and set equal to zero. This produces an equation linear in ν , but transcendental in x/l and a/l . The results of numerically solving for x/l are shown in Figure 1. For $\nu = 1/4$ and $a/l = 0$, the distance that maximizes the stress is $x/l = 2.06$. A Taylor's series expansion of the modified Bessel function about the points $x/l = 2.06$ and $a/l = 0$, yields the equation for the position of the maximum stress as

$$x/l = 1.83 + 0.916\nu + 0.292(a/l)^2 \quad (9)$$

In this expansion terms of the order $(\nu - 1/4)^2$, $(x/l - 2.06)^2$, $(a/l)^4$ and higher, have been neglected. If a similar Taylor's series expansion is made of equation 8 and the result from equation 9 is used, the maximum radial bending stress factor is

$$\frac{\sigma_r h^2}{P} = -0.1432 + 0.0977\nu + 0.0266(a/l)^2 \quad (10)$$

These plate theory results are most useful in predicting stresses near shorelines. If two loads P are placed on an infinite ice sheet as shown in Figure 3, there is zero deflection and bending moment along a straight line midway between these loads. Hence the line acts as a simple support and represents a shoreline at which the ice has been cracked. The radial stress distribution for the two loads in Figure 3 is shown in Figure 4. As the distance between the two loads

becomes smaller, the stresses will superimpose. A maximum stress occurs when the loads are at $\frac{1}{2}$ of the distance calculated from equation 9 from the shoreline.

Because the results of the wedge analysis have been useful for predicting the ultimate load carrying capacity of a floating ice sheet, it is anticipated that the results from a similar approach would be useful for predicting the ultimate load that an ice sheet can apply to a sloping structure. The author has solved the floating wedge problem for loads applied both vertically and horizontally. Numerical evaluation of this solution is presently being performed.

Table I. Uniformly loaded wedge.

$\frac{a}{l}$	$\frac{x}{l}$	$\frac{6 P_w}{b_0 \sigma h^2}$
.00	.00	1.00
.01	.22	1.05
.02	.28	1.08
.05	.39	1.15
.10	.51	1.26
.15	.60	1.35
.20	.68	1.45
.25	.75	1.55
.30	.81	1.65
.35	.87	1.76
.40	.93	1.87
.45	.98	1.98
.50	1.04	2.10
.55	1.09	2.23
.60	1.14	2.36
.65	1.19	2.50
.70	1.24	2.64
.75	1.29	2.80
.80	1.34	2.96
.85	1.39	3.13
.90	1.44	3.31
.95	1.49	3.50
1.00	1.54	3.70

Table II. Truncated wedge.

$\frac{a}{l}$	$\frac{x}{l}$	$\frac{6 P_w}{b_0 \sigma h^2}$
.00	.00	1.00
.01	.25	1.06
.02	.32	1.10
.03	.38	1.14
.04	.42	1.17
.05	.46	1.20
.06	.49	1.23
.07	.52	1.26
.08	.55	1.29
.09	.58	1.31
.10	.60	1.34
.12	.64	1.39
.14	.69	1.44
.16	.73	1.49
.18	.77	1.54
.20	.81	1.59
.25	.89	1.72
.30	.97	1.83
.35	1.04	1.95
.40	1.12	2.06
.45	1.19	2.17
.50	1.25	2.29
.55	1.31	2.40
.60	1.38	2.52
.65	1.44	2.63
.70	1.50	2.74
.75	1.57	2.85
.80	1.63	2.96
.85	1.68	3.08
.90	1.74	3.19
.95	1.80	3.29
1.00	1.86	3.41

References

1. H. Hertz, Über das Gleichgewicht schwimmender elastischer Platten. *Annalen der Physik und Chemie*, New Series, 1884.
2. A. Nadai, Die Biegungsbeanspruchung von Platten durch Einzelkräfte, *Schweizerische Bauzeitung*, band 76, 1920. See also *J. Springer, Die elastischen Platten*, 1925.
3. H. Westergaard, Stresses in concrete pavements computed by theoretical analysis. *Public Roads*, vol. 7, no. 2, 1926.
4. D. Nevel, Concentrated loads on plates. U.S. Army Cold Regions Research and Engineering Laboratory (USACRREL) Research Report 265, 1970.

5. D. Nevel, the narrow infinite wedge on an elastic foundation. U.S. Army Snow, Ice and Permafrost Research Establishment (USA SIPRE) Technical Report 56, 1958.
6. D. Nevel, The narrow free infinite wedge on an elastic foundation. USACRREL Research Report 79, 1961.
7. D. Nevel, The general solution of a wedge on an elastic foundation. USACRREL Research Report 247, 1968.
8. D.F. Panfilov, Experimental investigation of carrying capacity of an ice cover. *Instituta Gidrotechniki*, 64:101-115, 1960.
9. M. Wyman, Deflections of an infinite plate. *Canadian Journal of Research*, vol. A28, 1950.

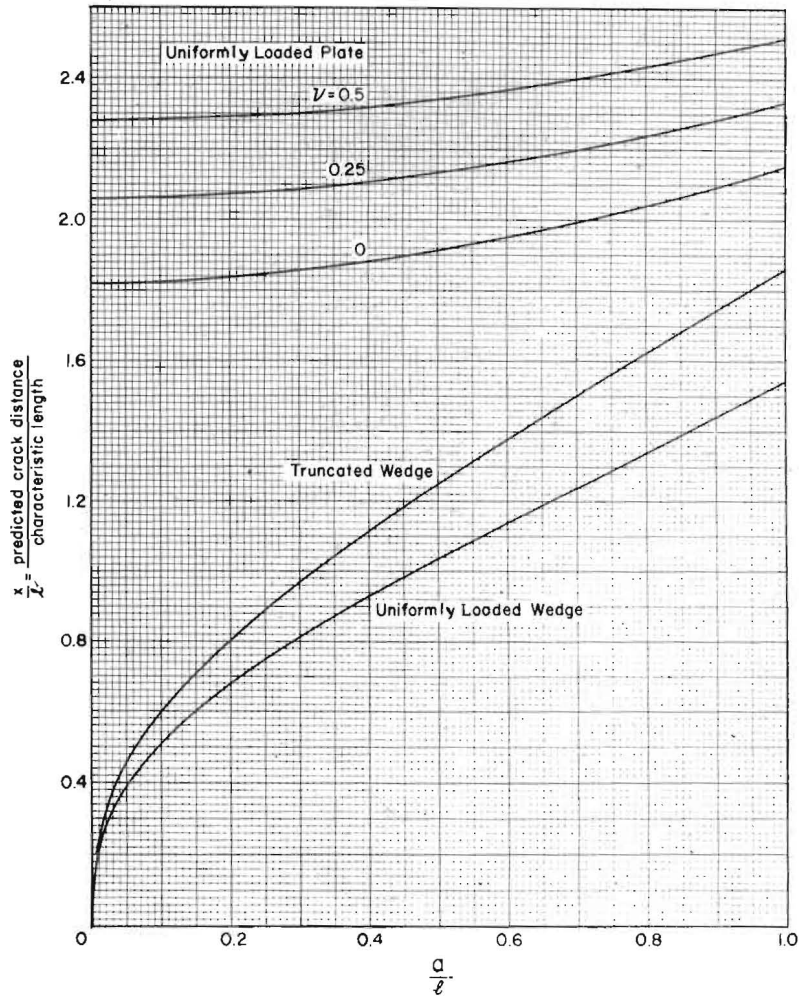


Figure 1. Position of crack.

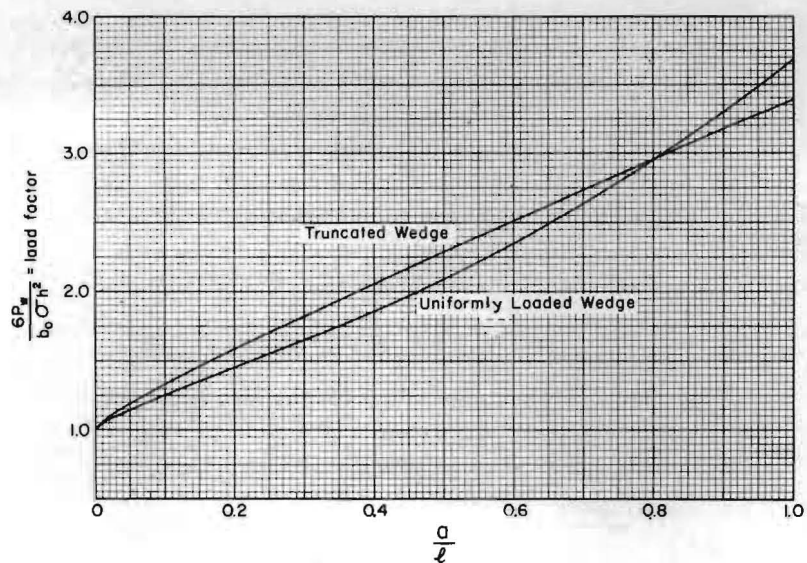


Figure 2. Ultimate load.

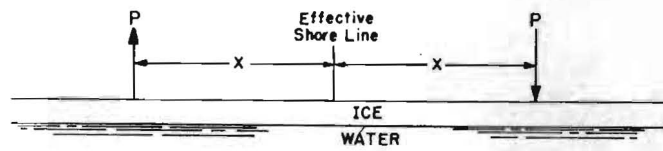


Figure 3. Effective shoreline.

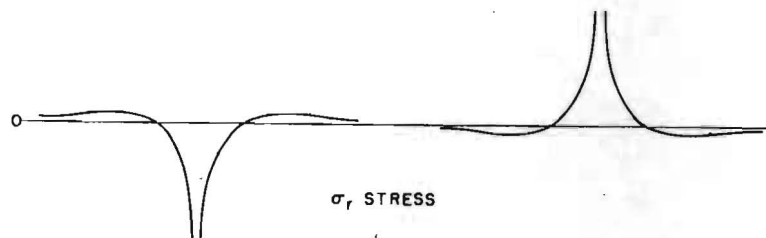


Figure 4. Stress for effective shoreline.



PRELIMINARY RESULTS OF PLANE STRAIN
COMPRESSION TESTS ON COLUMNAR-GRAINED
ICE

R. Frederking

Division of Building Research,
National Research Council of Canada

Ottawa, Canada

SYNOPSIS

A subpress designed to produce plane strain deformation was used to perform constant strain rate compression tests on columnar-grained ice. The failure stress, for the case of plane strain compression with the second principal stress direction perpendicular to the columnar-grain axes, was at least double that for uniaxial compression. A difference in the deformation mechanism between the two modes of compression is suggested as the reason for the variation in failure stress.

RESUME

Des essais de compression à vitesse de déformation constante ont été effectués sur la glace colonnaire en se servant d'une presse conçue pour produire des déformations biaxiales. On a trouvé dans le cas de la compression biaxiale et avec le deuxième axe principal de contrainte perpendiculaire sur le sens de la longueur des cristaux que la contrainte de rupture était d'au moins le double de celle obtenue lors d'une compression uniaxiale. La raison de la variation dans la contrainte de rupture peut être la différence dans le mécanisme de déformation entre les deux modes de compression.

In recognition of the anisotropic nature of columnar-grained ice, it was thought that its mechanical properties should be investigated under loading conditions comparable to those that occur under certain field conditions. Ice in contact with a long straight structure, for example, is subject to plane strain loading conditions. This paper describes the techniques used for performing plane strain compression tests and presents the preliminary results of a comparison of the strain rate dependence of the failure strength for plane strain compression and simple compression.

APPARATUS

A subpress designed to permit loading in a plane strain mode is shown in Figure 1. Ideally, the press should be sufficiently rigid to prevent any strain in one of the coordinate directions but in practice this is impossible. The press was designed, therefore, to reduce strain in the constrained direction to one tenth of that for simple compression, a more realistic condition. The distance between the confining sides was 101.20 mm. They were parallel to one another, perpendicular to the bottom surface of the cavity, and ground to obtain a smooth surface. The upper platten is movable and load is transferred to it via a column passing through the upper cross-member of the subpress.

The press was used in a 10,000-kg capacity test machine which had cross-head rates ranging from 5 cm/min to 5×10^{-5} cm/min. Transducers used to

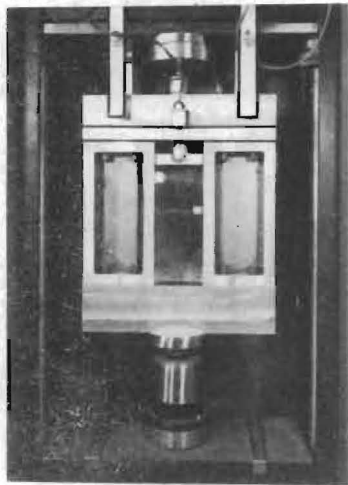
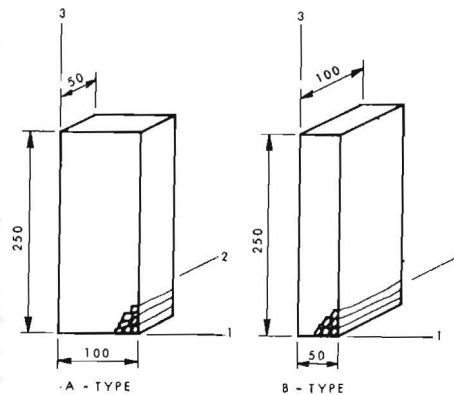


Figure 1. Plane strain compression subpress.



NOTE: Dimensions in mm

Figure 2. Schematic of two specimen types.

measure the motion of the upper platten and lateral expansion of the cavity are shown in Figure 1.

SPECIMEN PREPARATION

The tests were performed on columnar-grained ice with the axis of crystallographic symmetry tending to be perpendicular to the long axis of the grains. The ice, which was grown from the local supply of drinking water, had an average grain size of 20 mm^2 on a plane perpendicular to the long direction of the columnar grains.

The specimens were prismatic with nominal dimensions 50 by 100 by 250 mm. Two types of specimens were machined: A-type with columnar grains perpendicular to the 100- by 250-mm face and B-type with the columnar grains perpendicular to the 50- by 250-mm face. The two types of specimens are shown schematically in Figure 2. Because the specimens had to fit exactly into the subpress cavity it was necessary that they be machined with a high degree of precision, i. e. to within 0.025 mm. The required degree of precision was achieved with special jiggling techniques and a commercial milling machine.

TEST PROCEDURE

The subpress was used in two modes: a confined one yielding plane strain compression, and an unconfined one yielding simple compression. In the confined mode, the 50- by 250-mm faces of the specimen were in contact with the side walls of the cavity. For the unconfined mode the specimens were rotated 90 degrees about their long axis to avoid contact with the sides of the cavity. Load was applied to the specimen at a constant rate of cross-head motion until the specimen was crushed, in cases of brittle failure; or until a strain of about 3 per cent was reached, in cases of ductile failure. Specimens were prepared and tested at a temperature of -10°C . There was a thin film of kerosine on all of the specimens but no attempt was made to explore the use of lubricants to reduce friction on the interfaces between the ice and the subpress.

ANALYSIS TECHNIQUE

In analysing the results it would be desirable to have a consistent means of comparing the stresses and strain rates for the two types of specimens and the two loading conditions under which they were tested. Hill¹ has considered

¹R. Hill. The mathematical theory of plasticity. Oxford University Press, 1950.

the theory for plane strain deformation of an anisotropic material and more recently Venter et al² have reported on a theoretical and experimental study of plane strain compression of an anisotropic material. As indicated by the discussion in ref. 2, the relation between theory and experiment is open to further investigation. A comparison between experimental results and the plastic anisotropy theory appropriate to columnar-grained ice, however, is beyond the scope of this paper.

Simple definitions of stress and strain rate are used in this report.

Failure stress is given by

$$\sigma = P/A \quad (1)$$

where P is the maximum force sustained by the ice and A is the area on which it was applied (nominally 5000 mm^2). The strain rate is given by

$$\dot{\epsilon} = \dot{u}/l_0 \quad (2)$$

where \dot{u} is the rate of deformation at the instant of maximum force and l_0 is the initial length of the specimen (nominally 250 mm). The direction of the applied force and measured deflection is in the 3-coordinate direction as shown in Figure 2.

DISCUSSION OF RESULTS

Figure 3 is a plot of the maximum stress at failure versus the strain rate. This figure shows that the failure stress for A-type specimens in the confined mode is about twice the failure stress obtained from the unconfined mode tests. B-type specimens in the confined mode yield results identical to those of the unconfined mode.

While specimens were deforming it was observed that, for the cases of the unconfined mode, the deformation mechanism consisted of relative movement of the columnar grains primarily in a direction at right angles to their axes. Cracks appeared and propagated between and through columnar grains parallel to the long direction of the grains. Cavities opened up and the surface developed a corded texture, particularly at lower strain rates. For A-type

²R. Venter, W. Johnson and M.C. De Malherbe. The plane strain compression of anisotropic aluminum using a frictionless flat rectangular punch. J. Mech. Eng. Sci., Vol. 13, No. 6, p. 416-428, 1971.

specimens in the confined mode, however, the deformation was forced to occur in the long direction of the columnar grains. At high strain rates this resulted in the formation of plate-like cracks which tended to propagate in a plane perpendicular to the columnar-grain axes. At low strain rates elongation and extrusion of the columnar grains resulted in a cobbled texture on the specimen surface. It was clear that two distinct deformation mechanisms were involved.

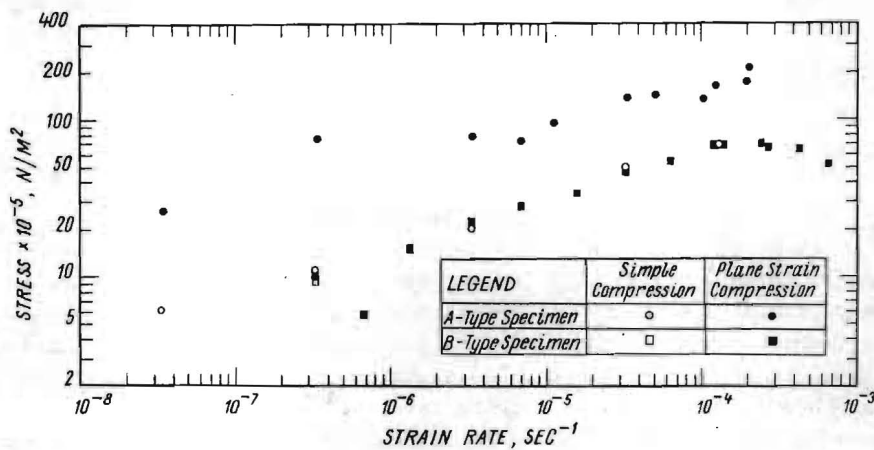


Figure 3. Strain rate influence on failure stress of columnar-grained ice at -10°C .

CONCLUSIONS

The deformation mechanism that occurs in plane strain compression of specimens, in which the second principal stress direction is perpendicular to the columnar-grain axes, is fundamentally different from the one that occurs in simple compression. The failure stress for this plane strain case is at least twice that for simple compression; the difference in deformation mechanism is primarily responsible for the variation in failure stress. In plane strain compression of specimens in which the second principal stress direction is parallel to the columnar-grain axes, the deformation mechanism is similar to the one that occurs in simple compression, and thus the failure stresses are equivalent.

This paper is a contribution from the Division of Building Research, National Research Council of Canada, and is published with the approval of the Director of the Division.



STRESSED ICE COVER STATE DUE TO THERMAL
WAVE AND RELATED UNDERWATER NOISE IN THE
OCEAN

V.V. Bogorodsky, Dept. Chief, the Arctic and Antarctic Leningrad,
Corresp. Member of the Academy, Research Institute, U.S.S.R.
V.P. Gavrilov, S.Sc.-s, Cand. states of Sc.,
A.V. Gusev, S.Sc. Cand. of Sc.,
Z.M. Gudkovich, S.Sc. Cand. of Sc.,
A.P. Polyakov, J.Sc., Cand. of Sc.

SYNOPSIS

Physical-statistical relationships of the underwater noise, recorded under the ice, with the variations of the air temperature and surface wind speeds are discussed, the underwater noise being caused by thermal cracks appearing in the ice cover of the Arctic Ocean. On the basis of the experiments the equation of multiple correlations was obtained which correlates the level of the underwater noise pressure (db) at a depth of 20 cm in the 200-400 Hz band with air temperature ($^{\circ}\text{C}$) and wind speeds (cm/sec) $P = P_0 + 1.13 \Delta \bar{v}_{15}^* + 0.33 V$, where P_0 a certain constant coefficient and $\Delta \bar{v}_{15}^* = \begin{cases} \Delta \bar{v}_{15} = \bar{v}_t - \frac{1}{30} \sum_{t-15 \Delta t}^{t+15 \Delta t} \bar{v}_t \\ 0 \end{cases}$ $\Delta \bar{v}_t \leq 0$
 $\Delta \bar{v}_t \geq 0$ corresponds to temperature deviations from those smoothed by 15-day intervals.

RESUME

Le rapport physico-statistique des bruits acoustiques sous-marins avec les variations de température et de vitesse de vent est discuté, des bruits acoustiques sous-marins étant enregistrés sous la glace par suite de la formation des crevasses thermiques formées dans la couverture de glace de l'océan Arctique. A la base de l'expérimentation l'équation de correlations multiples est obtenue. Elle relie le niveau de la pression sonore P(dB) à la profondeur de 20 m avec la température de l'air \bar{v}_t ($^{\circ}\text{C}$) et la vitesse de vent V (m/sec) $P = P_0 + 1.13 \Delta \bar{v}_{15}^* + 0.33 V$ où $P_0 = \text{const.}$, et $\Delta \bar{v}_{15}^* = \begin{cases} \Delta \bar{v}_{15} = \bar{v}_t - \frac{1}{30} \sum_{t-15 \Delta t}^{t+15 \Delta t} \bar{v}_t \\ 0 \end{cases}$ $\Delta \bar{v}_t \leq 0$
 $\Delta \bar{v}_t \geq 0$ correspond aux déviations de la température de celle aplanie par les intervalles de 15 jours.

Ice cover becomes stressed and eventually breaks up under the influence of many factors, stresses and strains, however, seem to be crucial among them. Strains in the ice cover are caused by its temperature variations due to the changes of thermal balance of the sea ice surface. Thermal stresses which exceed the tensile strength of the ice might cause the crack formation in the ice cover with accompanying elastic oscillations which propagate further through the ice cover and are then reflected to the underlying water column, where it is possible to record them by acoustic sensors.

Let us consider physical and thermal processes taking place in the floating ice sheet, assuming that air temperature changes induce only vertical temperature variations in the ice sheet. Were the edges of the ice plate free, the plate should have a format of a spherical surface portion, there should be no strains, if the temperature changes through the thickness obey the linear law. The experimental data, however, have shown that the temperature changes within the ice sheet do not cause its bending [1]. While the horizontal dimensions of the ice sheet actually change with temperature. The mechanism of this phenomenon involves the following processes. The upper layers of the floe shrink when the air temperature drops. Inner stresses in the horizontal planes cause the appearance of compressive stresses in the bottom layers, while at the surface tensile stresses are applied due to resistance force.

The value of the tensile and compressive stresses in each layer of dZ thickness is determined by equation (1)

$$\sigma(Z) = (\epsilon - \alpha \cdot \vartheta) \cdot E \cdot (1 - \nu)^{-1} \quad (1)$$

where α - linear coefficient of thermal deformation

E - elastic modulus

ν - Poisson's ratio

ϑ - temperature deviation from the initial value

ϵ - relative linear deformation which is constant for all the layers, if the floe is not bent, it can be calculated from the balance of tensile and compressive stresses:

$$\epsilon = \left(\int_0^h E \cdot \alpha \cdot \vartheta \cdot dZ \right) \left(\int_0^h E \cdot dZ \right)^{-1} \quad (2)$$

1. Legenkov A.P. On the problem of thermal stresses and strains of ice sheets. Fizika atmosfery i okeana, Vol VI, N°8, 1970.

Assuming E and α constant, this holds true especially for bottom ice layers, which do not show large temperature variations, we may write eq.(3) from eq.(1) and eq (2) to calculate normal stresses within the ice sheet

$$\sigma(z) = \frac{\alpha \cdot E}{1-\nu} \left(\frac{1}{h} \int_0^h \bar{v} \cdot dz - \bar{v} \right) \quad (3)$$

To solve eq.(3) we should know the law of temperature distribution within its thickness and its temporal variations. Thermal wave within the ice sheet is described by the equation of thermal conductivity

$$\frac{\partial \bar{v}}{\partial t} = a \frac{\partial^2 \bar{v}}{\partial z^2} \quad (4)$$

where $a = \frac{k}{\rho c}$ coefficient of temperature conductivity (k - thermal conductivity coefficient, ρ - density, c - ice heat capacity)

The equation of the temperature of snow-and-ice surface and that of the air (the latter changing by the harmonic law) is taken as a boundary condition in our problem,²⁾

$$\bar{v}(0,t) = \bar{v}_0 + \Theta \cdot \sin \omega t \quad (5)$$

where \bar{v}_0 - mean air temperature; Θ and $T = \frac{2\pi}{\omega}$ - amplitude and period of its oscillation.

If the ice thickness is not limited the solution of eq.(4) together with eq.(5) for a quasi-stationary case can be made by eq.(6):

$$\bar{v}_z = \bar{v}_z + \Theta \cdot e^{-\beta z} \cdot \sin(\omega t - \beta z) \quad (6)$$

where \bar{v}_z - mean temperature at a depth of z and $\beta = \sqrt{\frac{\pi \rho c}{k T}}$. For the limited ice thickness eq.(7) $\bar{v}(h,t) = \text{Const}$ is valid.

According to F. Malmgren and V.V. Shuleykin /2/ eq(7) holds true if temperature wave at each layer can be expressed as a sum of two waves: incident and reflected from the bottom. With $k = 5 \cdot 10^{-3}$ cal/cm at the ice bottom with $h = 300$ cm the amplitude of the incident wave ($T=1$ day) comprises 0.01 per cent of the surface wave amplitude, that is the effect of its reflection is negligible.

The calculations show that semidiurnal temperature variations actually are not felt at a depth of 50 cm, while the amplitude of variations with $T = 4-5$ days equals at this layer 20-25 per cent of the amplitude of the corresponding air temperature changes.

2. Shuleykin V.V. Fizika morya (Physics of the Sea) AN SSSR M., 1953.

The effect of the snow cover can be taken into account introducing the equivalent ice thickness proportional to the depth of the snow layer/3/. By integrating the second term in the right-hand part of eq (6) and assuming that $e^{-\beta h} \leq 10^{-4}$ in accordance with eq.(3) we can obtain the final expression for determination of thermal stresses

$$\sigma(z,t) = \frac{\alpha \cdot E \cdot \Theta}{1-\nu} \left[\frac{\sin \omega t - \cos \omega t}{2\beta h} - e^{-\beta h} \sin(\omega t - \beta z) \right] \quad (8)$$

For example, with $h = 300$ cm, by eq. (8) we can make a plot which shows that with the temperature increase there appear compressive stresses in the upper layers and when the temperature drops with depth the larger is the wave period the deeper penetrates the wave of thermal stresses. The peak of thermal stresses lags behind the peaks and lows of the air temperature. This time delay is larger, the deeper is the layer of ice. If we assume that the ultimate ice resistance to the compression at low temperatures two or three times higher than that of tensile stress (the latter being equal to $\sim 10 \text{ kg/cm}^2$) we may then conclude that thermal compression of the upper layers with a 10° air temperature rise does not cause the crack formation in the ice sheet. And conversely, tensions in the ice upper layers with similar temperature decrease reach the limit of strength. Thus, according to our calculations with a snow depth of 10 cm the cracks may form within 5-10 cm (at $T = 1$ day), within 15-20 cm (at $T = 3$ days), within 25-30 cm (at $T = 5$ days). Due to the fact that thermal crack formation diminishes the corresponding stresses in the ice the time interval during which the crack formations occurs starts when these stresses reach the limit of strength at the ice surface and it is over when this strength limit is reached at the ice bottom.

If we consider the elastic properties of the ice, then the effect of short-period air temperature variations on the crack formation is not large due to the penetration depth limit and the effect of long-period variations is weakened due to stress relaxation. This allows us to suggest that there are optimum frequency of temperature variations which result in the intense (maximum) crack formation and the corresponding underwater noise. It is possible to determine these optimum frequencies empirically, comparing observational data on under water noise and air temperature over a considerable time period.

3. Pekhovich A.I. The calculation of the statistic ice pressure. Izv. VNIIG vol. 49, 1953.

Series of observations on the underwater noise level at a depth of 20 meters, air temperature and wind speed during autumn months (September-October) were treated in this way. Measurements were taken during hourly intervals twice a day. Underwater acoustic signals were recorded in the active band, with an average frequency of 320 Hz. /4/.

Figure 1 shows the oscillations of the actual noise level (curve 1) against the estimated variations (curve 2) calculated by the equation of multiple correlation, given in the abstract. As it is seen from this Figure the air temperature from the start of the observed period till its end decreased from -4°C to 30°C . No progressive increase of the noise level was observed.

All the periods of considerable noise increase, i.e. 29 September and 11 October correspond to pronounced air cooling, continuing from several hours to 2-3 days, (the period of thermal wave is 1-6 days).

Relative role of different factors, affecting the formation of the underwater noise in the ocean (hummocking, wind etc.) changes from season to season. Notwithstanding the complicated interrelationships of these physical phenomena, which make the simple interpretation difficult, because the observational data were obtained in separate time intervals, the present study made it possible to reveal a number of regularities of thermal stresses in the ice cover and to show the advantages of the acoustic method of detecting the critical stressed state of the ice cover.

4. Gavrilov V.P., Gusev A.V., Polyakov A.P. On the feasibility of acoustic detecting of the critical stressed state of the ice cover. Trudy AANII vol.295, Gidrometeoizdat, L., 1970.

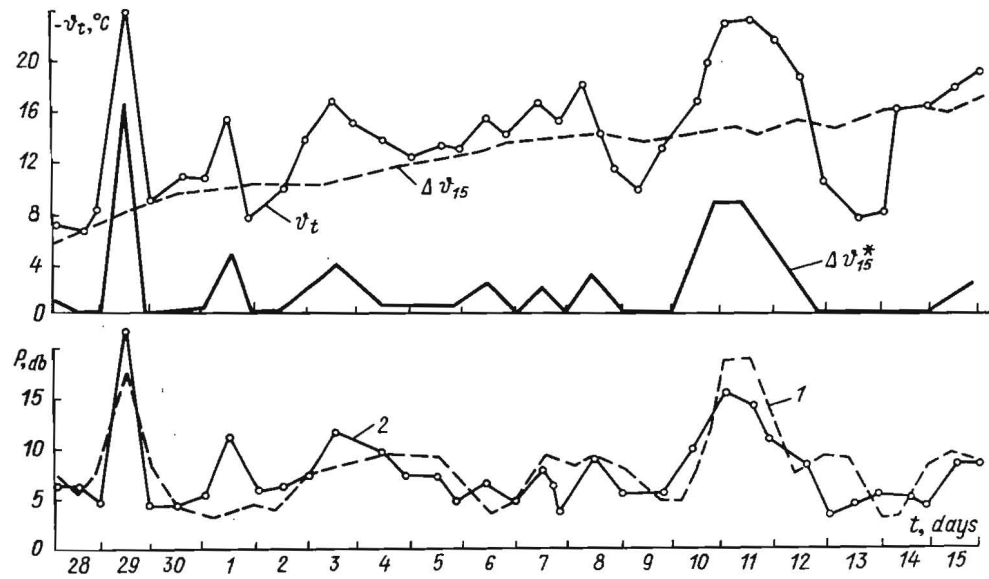


Figure I.

The air temperature data should be filtered first, cutting off certain frequencies. The simplest way of filtration (with a low-pass filter) is a running smoothing with a subsequent subtraction of the smoothed line from the initial.



ICE SYMPOSIUM 1972
LENINGRAD

STRUCTURAL FEATURES OF ICE ADHESION
TO SOLIDS

B.A. Savelyev, Prof.

V.N. Golubev, Eng.

M.N. Laptev, Eng.

I.B. Savelyev, Eng.

The Moscow State University Moscow, U.S.S.R.

SYNOPSIS

Experiments pertaining to ice formation on different materials, viz. metals, wood, plastics, concrete, and frozen soils have been carried out and the thermodynamics of the icing process examined. The presence of an ice contact layer formed under the influence of the substratum material is established by means of crystallo-optical research. Adhesion strength is considered arguing from the hypothesis of a quasi-liquid transition layer. "Plane" and "volumetric" adhesion are defined. The correlation is discussed between adhesion strength and ice structure and phase composition on the one hand, and temperature and substratum material on the other. It is revealed that the adhesion strength of fresh ice grows with an increase in crystal dimensions, while that of the salt ice decreases. The main requirements to the methods for determining adhesion strength are discussed.

RESUME

Les expériences sur la formation de la couverture de glace sur les matériaux différents (comme métaux, bois, matières plastiques, bétons, sols congelés) ont été faites et la thermodynamique de ce processus a été étudiée. Se basant sur les essais cristallographiques on a mis en évidence la présence de la glace près du contact, cette glace étant formée sous l'influence du substratum. Les forces adhésives ont été examinées du point de vue de l'hypothèse de la couche transitoire quasiliquide. On distingue deux formes de l'adhésion, "plane" et "volumique". On démontre la corrélation entre les forces adhésives et la structure et la composition de phase de la glace, d'une part, et de la température et du matériau du substratum, d'autre part. On a mis en évidence qu'avec l'augmentation des dimensions des cristaux les forces adhésives de la glace douce croissent et celles de la glace saline diminuent. Les exigences principales de la méthode de détermination des forces adhésives sont examinées.

The structure, composition and adhesion of ice to the substratum depend on the thermodynamic conditions of the system at the time of ice formation, on the physical and chemical processes on the interface, as well as on the structure and composition of the substratum material.

The ice structure is a function of thermodynamic conditions of icing. The size of crystals diminishes, their forms become more ideomorphic, the optical axes orientation grows more random as the ambient, air and water temperature drop, the wind velocity increases, while the rate of the liquid phase entering the crystallization front decreases. The structure of ice in proximity to the contact with the substratum is governed not only by the thermodynamic conditions of icing, but also by the physical and chemical characteristics of the substratum material. Under the same thermodynamic conditions the larger the ice crystals, the greater the cryophobic properties of the substratum material, the fewer crystallization nuclei develop on the surface. Therefore structural characteristics of the ice layer formed at the contact differ from the remaining part of the ice. As a rule, the ice crystals in this layer are considerably smaller than those further removed from the substratum (Fig. 1). The influence of the substratum material weakens with the distance from the contact, and the ice structure at a 2 or 3 cm distance from the contact is determined only by the thermodynamic conditions of the environment (Fig. 1).

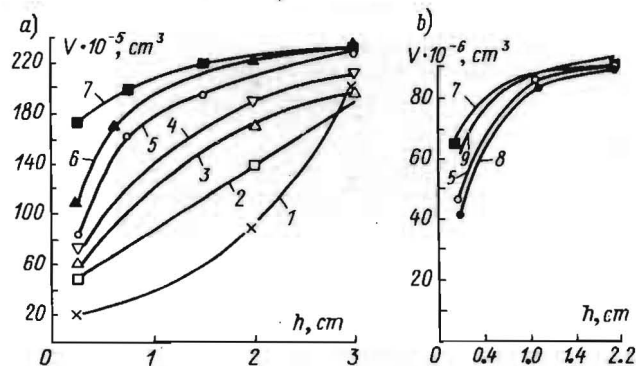


Fig. 1. The average volume of the ice crystal (V) versus the distance (h) from the interface.

- a - fresh ice; b - salt ice; - steel-3; 0 - painted steel;
 - wood; - teflon; 5 - special paint N 5; - sand;
 - concrete; - kaolin; - montmorillonite.

The quasi-liquid transition layer on the ice-substratum interface is the main factor which affects adhesion in the temperature range from 0°C to 15°C . At lower temperatures ice adhesion is in the main controlled by the dielectric, thermal and mechanical characteristics of the substratum material. "Sticking" of ice to smooth monolithic surfaces due to surface tension of the transition layer is termed "plane

adhesion. "Volumetric" adhesion occurs in case the pores of the substratum material are commensurable with the minimum crystal dimensions, the crystals grow into the pores of the substratum layer.

Ice structure on the ice-substratum interface is one of the main factors determining adhesion strength. Defects on the interface, the largest of which are boundaries between crystals, engender new defects in the structure of the quasi-liquid layer causing an irregular stress distribution across the displacement or rupture plane and, consequently, a reduction in adhesion strength as compared to theoretical values. An inverse dependence is observed between the adhesion forces and the crystal boundary length per unit of contact area.

The results of field and laboratory studies of the adhesion strength of fresh and salt ice to the substratum reveal a pronounced difference in the relationship of adhesion strength versus structure for fresh and salt ice.

The adhesion strength of fresh ice grows with the crystal size owing to an increase in the crystal contact surface area and a decrease of the pore surface and the intercrystal layers (Fig. 2). Hence, a weakening of adhesion is noted when a temperature drop occurs during freezing of fresh water (Table 1).

Table 1
Dependence of adhesion strength on the temperature of ice
freezing on plexiglass

Freezing temperature ($^{\circ}\text{C}$)	-5	-10	-15	-20
Crystal cross-section area (cm^2)	0,17	0,05	0,02	0,003
Adhesion strength at -10°C (kg/cm^2)	0,63	0,50	0,23	0,17

With salt water freezing, a temperature drop also leads to crystal size reduction. We have established that salt ice adhesion increases simultaneously governed both by the dimensions of the ice contact surface and by the presence of a brine layer. Other things being equal, the total quantity of brine is a function of the specific crystal surface, the strengthening or weakening of adhesion of salt ice to the substratum observed depending on the correlation between the contact and specific crystal surfaces.

A temperature drop in the ice-substratum system increases the adhesion strength of both fresh and salt ice.

When fresh ice freezes on rough surfaces (frozen dispersive rocks and concrete) adhesion assumes a volumetric character and strengthens due to a sharp increase in the number of crystallization nuclei. For this reason, direct

adhesion strength measurement at temperatures below -5°C is difficult and results, as a rule, in ice rupture.

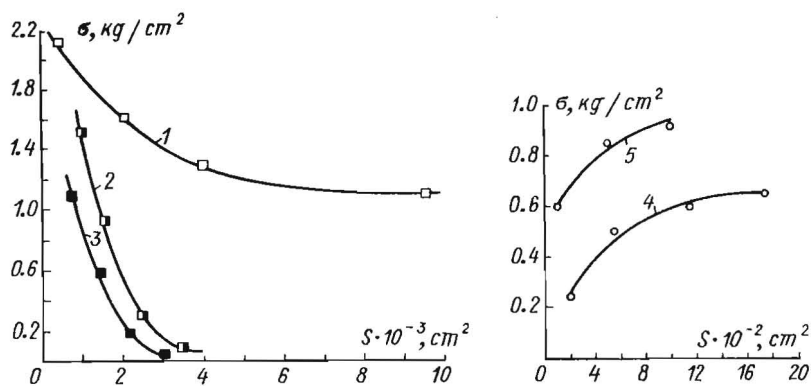


Fig. 2. Cohesion and adhesion of fresh and salt ice to different substrata as a function of crystal cross-section area in the rupture plane.
 1 - fresh ice cohesion; 2 - salt 15% ice adhesion;
 3 - salt 30% ice adhesion; 4,5 - fresh ice adhesion.

Structural research carried out on frozen specimens of two monomineral clays, fine-grained sands and concrete of the strength 300 kg/cm^2 demonstrated a marked dependence of crystal sizes over the ice contact on the activity of the substratum. A regularity, which holds true for the contact layer 3 cm thick (Fig. 1), is established in the successive growth of crystal sizes at the surface of the substrata studied (montmorillonite, caolinite, concrete, sand). Since adhesion depends on the ice structure and is correlated with cohesion strength, cohesion measurements in the contact layer were made at three different temperatures under a deformation rate of 2 mm/min. Cohesion was found to increase inversely to ice crystal size and ice temperature (Fig. 2).

No standard technique for measuring adhesion strength being accepted at present, the results of individual studies cannot be compared. With any design of the loading device, selection of optimal specimen dimensions and forms, adequate sample preparation conditions, accurate measurement of the deformation rate and of the test temperature are the basic principles of any method for adhesion strength measurement, i.e.:

1. Minimum specimen dimensions are determined by the size of structural and textural heterogeneities of the ice under investigation. Experimental data indicate that the rupture area must be not less than 40 cm^2 with a specimen about 5 cm thick prepared under optimal conditions.

2. Deviations from the test temperature regime and the accuracy of load

application should not exceed 5%.

3. The optimal deformation or loading rate of the specimen is established for each individual problem. When deformation or loading rate is reduced, the adhesion strength decreases due to changes in the ice structure and phase composition in the stress field, which in its turn affects the relaxation process (Table 2).

Table 2
Change of ice salinity at rupture

Deformation rate mm/min	Ice salinity before rupture of specimen g/l	Salinity of ice contact layer after rupture of the specimen g/l
60	13.088	18.455
30	18.103	21.105
6	18.080	26.629

CONCLUSIONS

1. The effect is established of the contact ice layer structure and the percentage of the liquid phase in ice and over the contact on ice strength, adhesion and cohesion.

2. The structure of the ice in the 30 mm thick contact layer differs from that of the rest of the ice and is conditioned by the substratum material.

3. Two kinds of adhesion can be distinguished: the plane and the volumetric.

4. An appreciable difference is marked in the dependence of adhesion strength on fresh or salt ice layer structure.

5. At the temperature of below -5°C at ice contact with different dispersive rocks, ice rupture has a cohesive character and is determined by the presence of an ice contact layer.

6. Other conditions being equal, minimum ice adhesion is to be observed with materials covered by organic epoxy and organosilicon films.



ICE SYMPOSIUM 1972
LENINGRAD

PREDICTION OF SEA ICE PHYSICAL PROPERTIES
BY USE OF RADAR

R.C. Byrd, Graduate Research Assistant,	Institute of Arctic	Alaska,
M. Yerkes, Student Assistant,	Environmental Engi-	United
W.M. Sackinger, Principal Investigator,	neering, University	States of
Associate Professor	of Alaska, Fairbanks.	America.
of Electrical Engineering,		
T.E. Osterkamp, Co-investigator, Assistant		
Professor of Physics.		

SYNOPSIS

The information which can be determined from radar returns from sea ice is discussed. The possibility of predicting age and strength is discussed and current data on the electromagnetic properties of sea ice which supports this possibility are presented.

RESUME

L'information qui peut être déterminée de réflexions de radar de la glace de mer est discutée. La possibilité de prédire l'âge et la force est discutée et des faits qui décrivent de qualités électromagnétique de la glace de mer qui supportent cette possibilité sont présentés.

INTRODUCTION *

A definite need exists today to be able to determine the physical properties of the arctic ice cover remotely, both for the purposes of large area surveillance and for gaining information about specific small areas of immediate interest. Tests conducted in recent years have shown that it is possible to acquire a large amount of information about surface topography from side-looking airborne radar (SLAR) and scatterometer presentations.¹ General features of the ice cover such as pressure ridges, hummock fields, relative smoothness, and open leads can be readily distinguished. Correlation of radar return data with the ice floes thus represented have shown that new and old ice fields under similar conditions have different reflective characteristics.¹ Recent experiments by the authors have resulted in information which shows that these differences are the result of variations in the dielectric properties of sea ice with changes in temperature and salinity.

PROPERTIES OF ARCTIC ICE: PHYSICAL-ELECTROMAGNETIC

Sea ice differs from fresh water ice in that it has liquid brine inclusions contained in its ice matrix. The rate at which the freezing process takes place and the original water salinity determines to a great extent the amount of salt initially trapped in the ice, and therefore the percent of the brine volume.² Rapid freezing produces more included brine. As the ice temperature decreases, the relative volume of the included brine decreases. More of the water in the inclusion freezes out, with an increase in salt concentration in the brine remaining.

¹ Rouse, J. W., Arctic Ice Type Identification by Radar, Proc. of the I.E.E.E., Vol. 57, No. 4, 1969.

² Lofgren, G. and Weeks, W. F., Effect of Growth Parameters on Substructure Spacing in NaCl Ice, J. of Glaciology, 7, 153, 1969.

* Supported by the Advanced Research Projects Agency through the Office of Naval Research, Arctic Program Office, under Contract No. N00014-71-A-0365-0001.

At about -22°C , solid salts (predominantly NaCl) begin to precipitate out of the brine.³ At temperatures warmer than -22°C , the liquid brine inclusions tend to gravity drain to a lower point and eventually out of the ice. If the ice is subjected to the annual temperature cycles, the brine drainage is great, resulting in decreasing salinity, with age.

Several investigators^{4,5} have shown that the various facets of physical strength (i.e., tension, compression, etc.) are closely related to brine volume, which is a function of temperature and salinity. Although much remains to be done before the exact relationships can be determined, strength in sea ice has been shown to generally decrease with an increase in temperature or salinity.^{4,5}

The complex permittivity, an electromagnetic property which partially dictates the nature of the radar reflection from a substance, also varies with ice temperature and salinity. The ratio of the imaginary to the real part of the complex permittivity is defined as the "loss tangent." Figure I shows the change in loss tangent with temperature and salinity for a frequency of 34 GHz. The normalized real part of the complex permittivity has been found to be nearly constant, having a value of about 3.10, for the frequency range from 26 to 40 GHz.⁶ The loss tangent was found to vary by a factor of approximately 4, with the change in the brine cell vertical axis orientation from perpendicular to parallel to the incident electric field.⁶ This effect has been averaged out in the figure to show the values of loss that would be

³ Weeks, W. F., Studies of Salt Ice, USACRREL Research Report 80, 1961.

⁴ Assur, A., Composition of Sea Ice and its Tensile Strength, USACRREL Research Report 44, 1969.

⁵ Weeks, W.F., and Assur, A., Fracture of Lake and Sea Ice, USACRREL Research Report 269, 1969.

⁶ Sackinger, W.M., and Byrd, R.C., Reflection of Millimeter Waves from Snow and Sea Ice, Institute of Arctic Environmental Engineering, University of Alaska, Report 7203, 1972.

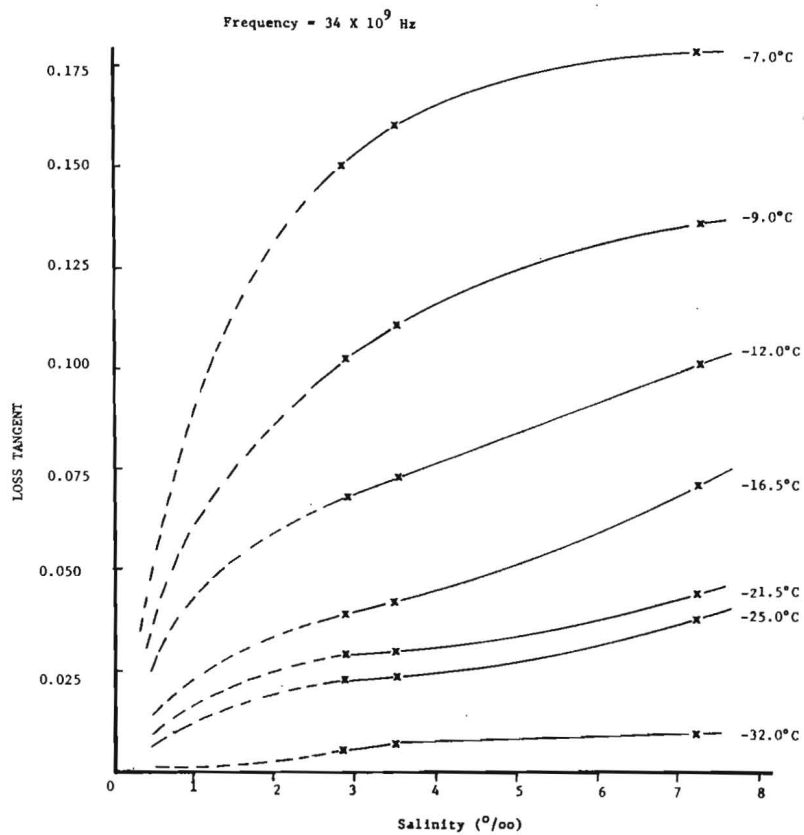


Figure 1. Loss Tangent versus Salinity for several temperatures in natural sea ice.

expected in field conditions. The plotted data represents the influence of salinity and temperature averaged from a large number of tested samples, coupled with the expectation that the loss tangent for fresh water ice, zero salinity, will be very small.⁷

The effect of these changes can be summarized by the fact that cold, low salinity ice will not reflect electromagnetic waves as strongly as warm, high salinity ice. For a given temperature, the higher salinity ice will produce a stronger reflection. This, of course, assumes that the other physical characteristics such as average surface roughness are the same. From the detailed information which has been obtained on the electromagnetic properties of sea ice at representative salinities in the frequency range from 26-40 GHz, and at temperatures between -7°C and -32°C, many of the physical properties should be predictable from remote sensing data. Detailed calculations and field measurements are in progress to confirm this.

CONCLUSIONS

The interpretation of radar returns from sea ice is complicated by variations in the composition and topography. However, several groups, including the authors, are working to separate these two contributions, so that the physical properties may be measured by remote sensing techniques. The measurements reported here of the complex dielectric constant as a function of temperature and salinity are the first steps in the interpretation process.

⁷ Evans, S., Dielectric Properties of Ice and Snow - A Review, J. of Glaciology, 5, 773, 1965.



ICE SYMPOSIUM 1972
LENINGRAD

FORCE FLUCTUATIONS DURING ICE-FLOE
IMPACT ON PIERS

C.R. Neill, Hydraulic Engineer Research Council of Alberta Edmonton,
Canada

SYNOPSIS

A communication to the 1970 Symposium described two field installations designed to measure dynamic ice forces on bridge piers. In April 1971 both installations were subjected to repeated impacts from ice-floes of varying sizes. Synchronization of force recording and movie photography at one site enabled force fluctuations to be compared with the nature of the ice failure. Peak instantaneous forces were generally several times larger than mean forces averaged over durations in the order of one second. Peak unit pressures on a vertical pier appear to have been comparable with ice strength in compression.

RESUME

Dans un rapport au Symposium de 1970 nous avons décrit deux installations dans la nature qui ont été établies pour mesurer les forces dynamiques de la glace sur les piles de ponts. En Avril 1971 les deux installations ont soutenu des impacts de la glace en blocs d'une grandeur variable. Parce que les enregistrements des forces ont été synchronisés avec des photographies cinématographiques, nous avons pu comparer les fluctuations de la force avec le caractère de la rupture de la glace. Les forces maximales instantanées ont été plus grandes par plusieurs fois que les forces moyennes pendant des intervalles de temps à peu près d'une seconde. Les pressions par unité de surface sur une pile verticale, qui sont calculées des forces maximales, ont été d'une grandeur similaire à la résistance compressive de la glace.

PREVIOUS DESCRIPTION OF TEST INSTALLATIONS

We have previously described (1) two field installations for measuring break-up forces on bridge piers, and have presented a summary of data obtained 1967-70. This paper presents further data from April 1971 concerning force fluctuations and the relationships between peak and mean forces during ice-floe impacts. More details are available in a local report (2).

OBSERVATIONAL TECHNIQUES

The most interesting data were obtained at Pembridge, where forces are measured on a 0.9 m diameter vertical test pile (Fig. 2 of ref. 1). Forces were recorded during a two-hour ice run, and movie film was taken from above the test pile. The recorder and camera could be switched on and off simultaneously to record significant episodes. One electric clock with a targeted second hand was mounted in view of the camera, and a duplicate clock was mounted beside the load recorder. By means of this system it was possible to compare the force fluctuations with the behaviour of the ice as seen on film.

It was intended to use the same system at Hondo, where forces are measured on a 2.3 m wide pier provided with a hinged nose (Fig. 1 of ref. 1). Unfortunately break-up at this site occurred only a few hours after break-up at Pembridge, and we did not succeed in setting up the synchronization system in time. Force recordings and some unsynchronized film were however obtained for the most significant part of the ice run.

NATURE OF ICE ACTION AT TWO SITES

The ice at Pembridge was mostly in the form of separated floes of widely varying size, of which the largest were in the order of 30 m diameter. Approach velocities were mostly in the range of 1 to 2 m/sec. On striking the vertical pile, some of the floes came to a complete halt as the edge of the ice crushed against the pile. Others split immediately on impact, and some rotated or sheared obliquely after initial crushing.

At Hondo, where the pier nose is inclined at 23° to the vertical, the initial part of the ice-run consisted of a dense mass of ice-floes, including some of up to about 70 m diameter. Approach velocities were generally in the range of 1.5 to 2.5 m/sec. The mode of ice failure was noticeably different from Pembridge. All the larger floes rode up the pier after impact and appeared

-
- (1) Neill, C.R. "Ice pressure on bridge piers in Alberta, Canada". Proceedings 1970 IAHR Ice Symposium, Reykjavik, Paper no. 6.1.
 - (2) Neill, C.R., H.D. Saunders and H. Schultz. "Measurements of ice forces on bridge piers, 1970 and 1971". Report of Alberta Cooperative Research Program in Highway and River Engineering, Edmonton, Sept. 1971.

to fail by bending or splitting (Fig. 1). Some pieces were lifted to a height of over 3 m above water level.

FORCE FLUCTUATIONS AT PEMBRIDGE SITE

Impact forces were generally in the order of one second duration. The peak signal was often of virtually zero duration, sometimes occurring at the beginning of the impact episode, and sometimes in the middle (Fig. 2).

Thirty of the most significant events were picked out on the recorder chart and analyzed in detail, together with the corresponding movie film. Table 1 presents data and descriptions covering twelve of these events, and Fig. 2 shows oscillographic traces for three of them. The "mean force over duration of chart event" values were estimated from the average height of the chart trace during each event. Unit pressures were calculated on the basis of average ice-sheet thickness. It is interesting to note that instantaneous peak forces are mostly from 2 to 6 times larger than mean forces.

In the case of events nos. 6, 9 and 12 of Table 1, when ice-floes of known dimensions and approach velocities came to rest against the pile in known time intervals, estimates were made of mean impact force by applying the impulse-momentum equation

$$M \cdot \Delta V = \bar{F} \cdot \Delta t \quad \dots \quad \text{Eq. (1)}$$

- where M = mass of ice-floe
- ΔV = change in velocity during impact
- \bar{F} = mean stopping force
- Δt = time interval from initial impact to rest.

Table 2 compares mean forces so calculated with those estimated from the load recorder traces. The agreement is surprisingly good.

FORCE FLUCTUATIONS AT HONDO SITE

At Hondo the more severe impact episodes were generally of several seconds duration. Table 3 presents data for four episodes, and Fig. 3 shows oscillographic traces for three of them. Again, it is interesting to note that instantaneous peak forces were from 2 to 4 times higher than maximum one-second-mean forces. Fig. 1 shows three photographic sequences illustrating typical episodes.

ICE STRENGTH

A few blocks of ice from Pembridge were collected immediately before and during the ice-run. Samples were cut and tested in the laboratory in uni-axial compression at a temperature of -1.5°C and at strain rates in the range of 10^{-5} to 10^{-3} sec^{-1} . Strengths were generally in the range of 14 to 28 kgf/cm^2 . It is interesting to note that peak unit pressures for six of the events listed in

Table 1 fall into this range; the other six fall below it.

GENERAL REMARKS

There has been some controversy concerning discrepancies between ice strengths as normally measured in the laboratory, and the successful performance of actual structures apparently incapable of sustaining comparable pressures. One explanation for such discrepancies may be that in many dynamic situations peak ice strengths are mobilized only for very brief intervals of time. In such circumstances massive piers would not require such high design pressures as lighter structures. Consideration should be given to investigations of how much work would be involved in significant displacement of large piers, and to whether the ice floes liable to occur at a particular site would have sufficient kinetic energy to cause damage.

ACKNOWLEDGMENTS

The observations described formed part of a continuing program of investigations supported by the Alberta Department of Highways and Transport and initiated by E. J. Sanden, Chief Bridge Engineer. Ice strength testing was conducted by Professor J. B. Nuttall, University of Alberta.



Fig. 1 - Movie film sequences illustrating three episodes at Hondo.
Frames in each sequence are 1/24 second apart.
Ice is rising to approximately 3 m above surface.

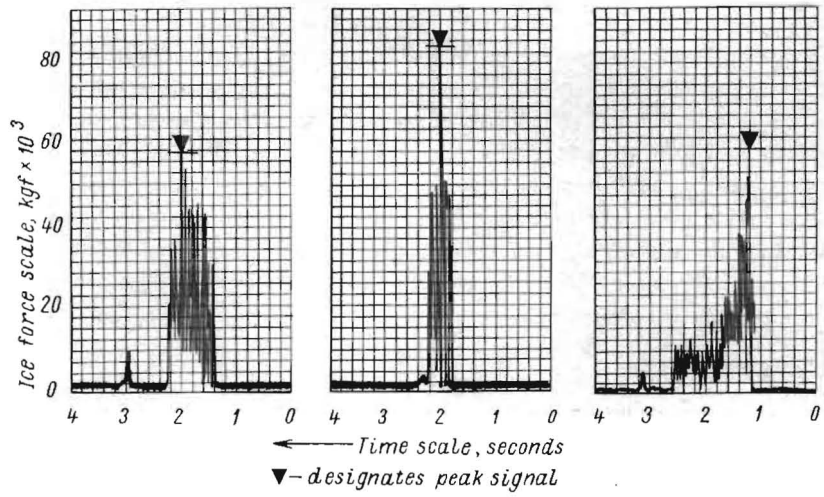


Fig. 2 - Oscillographic records of Pembridge impact events nos. 6, 7, and 9 (Table 1)

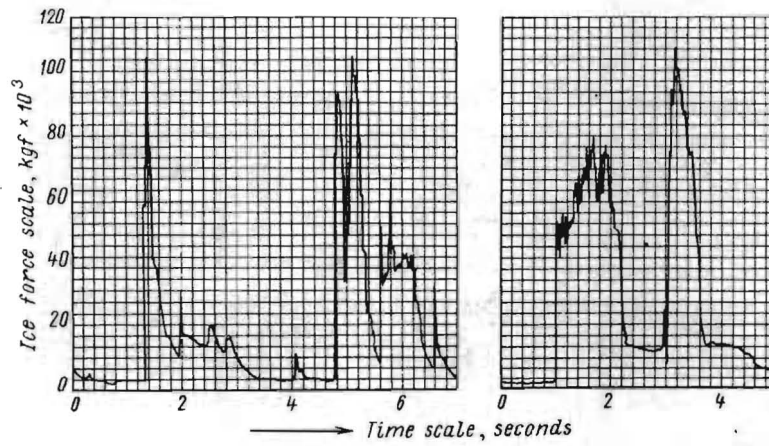


Fig. 3 - Oscillographic records of Hondo episodes nos. 2, 3 and 4 (Table 3)

TABLE 1 - DATA FOR SELECTED IMPACT EVENTS AT PEMBRIDGE

Pier width 0.86 m; assumed ice thickness 0.46 m

Event no.	Instantaneous peak force kgf	Corresponding unit pressure kgf/cm ²	Duration of event seconds	Approx. mean force over duration kgf	Corresponding unit pressure kgf/cm ²	Ratio of peak/mean force	Ice-floe velocity m/sec	Approximate floe dimensions m	Nature of impact and ice failure (as viewed on film)
1	35,800	9.1	3.0	11,900	3.0	3.0	1.4	> 10 x 30	Sheet slid along pier : crushing for 2 seconds.
2	58,700	14.9	0.1	9,300	2.4	6.3	1.4	6 x 9	15 cm penetration, then floe rotated and moved clear.
3	47,400	12.0	4.0	9,900	2.5	4.8	1.6	> 10 x 12	4 m penetration : peak force at zero velocity of incision.
4	37,200	9.2	1.0	14,000	3.5	2.7	1.9	12 x 15	0.6 m crushing penetration, then floe split.
5	39,200	9.9	1.0	14,000	3.5	2.8	1.9	> 12 x 27	Initial crushing followed by a sharp blow.
6	58,700	14.9	0.8	31,400	7.9	1.9	1.7	15 x 15	15 cm penetration, then floe rotated and moved clear.
7	83,900	21.2	0.3	34,900	8.8	2.4	1.8	>> 12 x 15	Abrupt crushing followed by splitting.
8	47,400	12.0	0.2	19,600	4.9	2.4	1.6	9 x 9	Abrupt crushing followed by rotation.
9	58,700	14.9	1.4	11,000	2.8	5.3	1.7	9 x 12	Grazing contact followed by rotation and splitting.
10	83,900	21.2	0.4	36,300	9.2	2.3	1.5	> 9 x 12	Crushing followed by rotation.
11	47,400	12.0	1.8	14,600	3.7	3.2	1.7	Unknown	Splitting along line of impact.
12	58,700	14.9	0.5	9,800	2.5	6.0	1.2	9 x 12	30 cm crushing penetration, followed by rotation.

TABLE 2 - MEAN FORCES AS ESTIMATED FROM RECORDER CHART
 COMPARED WITH KINEMATIC ESTIMATES

Event no. (Table 1)	Mean force (kgf) from recorder chart (Table 1)	Mean force (kgf) by impulse-momentum (Eq. 1)
6	31,400	29,400
9	11,000	12,900
12	9,800	11,500

TABLE 3 - DATA FOR SELECTED IMPACT EPISODES AT HONDO

Pier width 2.34 m; assumed ice thickness 0.46 m

Event no.	Indicated peak instan- taneous force kgf	Corre- sponding unit pressure kgf/cm ²	Approx. duration of episode seconds	Mean force over total duration kgf	Corre- sponding unit pressure kgf/cm ²	Mean force over highest one-sec. interval kgf	Corre- sponding unit pressure kgf/cm ²	Ratio of peak/ one- sec. force
1	69,000	6.4	6.5	14,700	1.4	21,000	2.0	3.3
2	105,000	9.7	2.0	29,000	2.7	23,900	2.2	4.4
3	105,000	9.7	2.2	29,000	2.7	44,900	4.2	2.3
4	123,000	11.4	4.0	17,800	1.7	61,600	5.7	2.0



EXPERIMENTAL DETERMINATION OF ICE IMPACT
LOADS ON MARINE VEHICLES

Roderick Y. Edwards, Jr., ARCTEC, Incorporated, Columbia, Maryland, USA
Vice President,
James W. Wheaton, Teledyne Materials Waltham, Massachusetts,
Section Manager, Research, USA

SYNOPSIS

An experiment to determine the magnitude of ice impact loads experienced by the hull structure of the U.S. Coast Guard Icebreaker MACKINAW was conducted in Lakes Huron and Michigan during the winter of 1970-1971 under the sponsorship of the Office of Research and Development, U.S. Coast Guard (U.S. Department of Transportation). The impact load was estimated from the response of a strain gauged portion of the bow structure. The results indicated that the loads were of very short duration. The peak value of the load correlated well with the product of ship speed and ice thickness. The dimensionless impact load ($F_i/p_w gh^3$) correlated reasonably well with the product of Froude number and dimensionless flexural strength ($\sigma_f/p_w gh$). The successful use of dimensionless groups to reduce the data suggests that the hull-ice impact phenomenon may be modeled on a small scale.

RESUME

Les forces dues à l'impact des lames de glace sur la coque du brise-glace U.S. Coast Guard MACKINAW ont été mesurées au cours d'essais conduits pendant l'hiver 1970-71 dans les lacs Huron et Michigan. Ces essais ont été effectués sous contrat de l'Office of Research and Development, U.S. Coast Guard (U.S. Department of Transportation). Une partie de l'avant de la coque était pourvue de capteurs de contrainte de sorte que les forces dues à l'impact pouvaient en être estimées. Les résultats ont montré que celles-ci étaient de courte durée et que leurs valeurs maximales étaient fonction du produit de la vitesse du navire et de l'épaisseur de la glace. Une corrélation satisfaisante entre les forces d'impact adimensionnelles ($F_i/p_w gh^3$) et le produit du nombre de Froude et de la contrainte de flexion adimensionnelle ($\sigma_f/p_w gh$) a été établie. L'excellent recouplement des résultats obtenu avec ces variables réduites suggère que le phénomène d'impact entre coque et glace peut être étudié en échelle réduite.

Motivation

The structural steel content of icebreaking ships accounts for as much as fifty percent of their cost. One of the primary goals of designers of future ships for Arctic service will be the reduction in the bulk of the structure while maintaining an acceptable level of reliability under expected operating conditions. The scantlings of present icebreaking ships are chosen on the basis of classification society rules, on the basis of load criteria extracted empirically from failure data¹, on the basis of analytical calculations of ice loads², or on the basis of a combination of all of these approaches. Ideally, a designer requires an estimate of ice loads which will be experienced by a ship's hull. To be useful these loads should be expressed statistically as functions of environmental parameters (ice thickness, ice compressive strength, flexural strength, elastic modulus, snow cover, etc.) and designer controlled parameters (ship mass, speed, power, and hull surface angles).

The full scale experiment described in this paper was, to the authors knowledge, the first attempt at estimating full scale ice loads (as opposed to stress levels³) on ships and at relating them to some of the environmental and operating parameters mentioned above. The experiment was designed to assess the feasibility of "measuring" ice impact loads and reducing the results to a body of information which would be useful to designers of ships for service in ice covered waters.

Physical Concepts

The load experienced by a ship's hull when it contacts the edge of an ice sheet may be expressed in functional notation as follows:

$$F_i = f_1 (h, v_i, \sigma_f, \sigma_{cr}, f, E, \beta, \alpha, \psi, M_g, I_g, \rho_i, \rho_w, g, x) \quad [1]$$

- | | |
|--------------------------------------------------------------------------------------|-----------------------------------------------------------------------------------------------------------------|
| F_i = peak normal force on hull surface | I_g = longitudinal moment of inertia of the ship about the axis normal to the water surface |
| h = ice thickness | g = gravitational constant |
| v_i = impact velocity | f = friction coefficient between hull and ice |
| σ_f = flexural strength of ice | β = angle between a plane tangent to the ship's side at the contact point and a normal to the ice surface |
| σ_{cr} = unconfined compression strength of ice | |
| E = elastic modulus of ice (bending) | |
| ψ = spread angle of the wedge shaped ice slab with which the hull makes contact | |

1. Johansson, B.M. "On The Ice-strengthening of Ship Hulls", International Shipbuilding Progress, Vol. 14, June 1967 - No. 154.
2. Y.N. Popov, O.V. Faddeyev, D.Y. Kheysin, and A.A. Yakovlev. Strength of Ships Sailing on Ice, Sudostroenie Publishing House, Leningrad.
3. Waterman, R. Structural Tests of Coast Guard Icebreaker WESTWIND (WAGB-281) DTMB Report No. 2134, January 1966.

α = angle between a plane tangent to the ship's side at the contact point and the ship's center line

M_s = mass of the ship

ρ_i = mass density of ice

ρ_w = mass density of water

\bar{x} = distance from the ship's center of gravity to the contact point

Our experiment treated the loads on a ship which was moving at a steady speed in uniformly thick ice. Hence, M_s , I_s , and \bar{x} are not a consideration and [1] becomes

$$F_i = f_2 (h, v_i, \sigma_f, \sigma_{\sigma}, E, \beta, \alpha, \psi, \rho_i, \rho_w, g, f) \quad [2]$$

If the principles of dimensional analysis are applied to equation [2] several important dimensionless groups may be extracted from it.

$$\frac{F_i}{\rho_w g h^3} = f_3 \left[\left(\frac{v^2}{gh} \right), \left(\frac{E}{\rho_w g h} \right), \left(\frac{\sigma_f}{E} \right), \left(\frac{\sigma_{\sigma}}{\sigma_f} \right), \left(\frac{\rho_i}{\rho_w} \right), \beta, \alpha, \psi, f \right] \quad [3]$$

We were able to measure only v , h , and σ_f carefully for each experiment. β and α remained constant. f and σ_{σ} did not vary appreciably. ψ , the ice slab angle, was a random variable which could not be observed. Hence our experiment consisted of attempting to document the following functional relationship:

$$\frac{F_i}{\rho_w g h^3} = f_4 \left[\left(\frac{v_i}{\sqrt{gh}} \right), \left(\frac{\sigma_f}{\rho_w g h} \right) \right] \quad [4]$$

$$\bar{f} = 0.145 \quad \beta = 35^\circ \quad \alpha = 17^\circ$$

DESCRIPTION OF THE EXPERIMENT

Test Procedure

The ice load experiments were conducted in conjunction with experiments to determine the resistance offered by the ice cover to the continuous motion of the U.S. Coast Guard Cutter MACKINAW. The ship was run at constant speed through uniformly thick fresh ice. During each run the strains in an instrumented portion of the ship's forward hull structure were monitored continuously. The average velocity of the ship was measured. The ice thickness along the track and the depth of snow cover were measured at the end of each run. The flexural strength of the ice sheet was determined by in situ cantilever tests. During periods in which ship speed and ice thickness were steady, the five highest sets of strains were chosen from the out put of the strain gauged panel. These strains were used in conjunction with external calibration data for the panel to determine the normal force acting on the hull surface. Mean values of estimated normal force and their corresponding values of ice thickness, ship speed, and ice strength, are tabulated in Table I.

TABLE I. RESULTS OF ICE IMPACT EXPERIMENTS

Data Point No.	Ice Thickness (h) ft.	Velocity (v) ft/sec	Flexural Strength (σ_f) lb/in ²	Impact Load (F_i) lbs.	Dimen'less Impact Load $F_i/\rho_w g h^3$	$\frac{\sigma_f}{\rho_w g h} \cdot \frac{v}{\sqrt{g h}}$
2-2	1.81	11.97	74	16,600	44.86	141.40
3-4	1.56	15.73	88	22,200	93.71	286.40
4-4	1.89	15.45	187	22,200	52.69	433.70
4-5	1.71	9.55	187	26,000	83.33	302.80
5-2	0.35	17.53	98	3,800	1420.34	3359.70
5-3	1.65	13.70	98	27,800	99.18	246.00
5-4	1.77	3.53	98	12,000	34.67	51.00
5-5	1.60	8.38	98	18,800	73.55	155.40
5-6	1.66	12.03	98	20,000	70.06	224.00
6-4	1.22	13.53	139	18,000	158.85	565.30
6-6	1.28	17.71	139	15,600	119.20	689.00
6-2	1.24	18.45	139	19,800	166.42	753.60
7-1	1.18	1.57	137	7,000	68.27	66.97
7-1a	1.77	4.89	137	4,200	12.13	114.30
9-1	0.39	8.09	154	4,200	1134.60	2077.53
18-1	0.32	5.89	137	3,992	1952.34	1807.80
18-3	0.30	10.71	137	3,400	2018.04	3625.20
18-4	0.34	12.18	137	4,000	1630.94	3422.00
19-1	0.32	12.28	137	6,200	3032.19	3773.00
20-1	0.34	8.50	137	3,000	1223.20	2380.00
25-1	1.71	6.28	128	12,800	41.02	145.09
26-3	1.46	5.16	128	10,600	54.58	151.72
28-2	0.86	10.77	126	31,200	786.09	689.00
29-1	0.90	17.14	126	13,400	294.57	1027.36
29-2	0.82	19.96	126	9,400	273.21	1377.00
30-1	0.84	22.11	126	13,000	351.49	1470.00
30-2	0.82	23.12	126	11,000	319.71	1592.10
30-3	0.87	23.79	126	25,000	608.41	1500.00
31-5	0.94	18.61	126	20,400	393.60	1045.00
32-3	0.88	22.65	107	8,800	206.94	1190.00
33-1	0.87	9.42	56	13,600	330.97	262.00
34-1	0.87	4.42	56	7,600	184.95	123.20
35-7	0.87	15.93	56	10,200	248.23	447.00

Test Results

The data in Table I were plotted in Figure 1. Ship speed was plotted against ice thickness with impact load as a parameter. Four regions of relatively constant ice thickness appear on the plot. Impact force was plotted against ship speed for each of the regions of relatively constant ice thickness. The slopes of those force versus velocity curves were plotted against ice thickness. The results indicated that impact force was a function of the product of velocity and ice thickness. Hence the data was manipulated to produce the plot of the impact load versus the product of ship speed and ice thickness which is shown in Figure 2. Figure 2 suggested that a product of the dimensionless groups v/\sqrt{gh} and $\sigma_f/\rho_w gh$ would be best used to explain the data. Figure 3 is a plot of dimensionless impact load $F_i/\rho_w gh^3$ versus the product of Froude number v/\sqrt{gh} and dimensionless flexural strength $\sigma_f/\rho_w gh$. An approximate fit to the data produces:

$$\frac{F_i}{\rho_w gh^3} = 9.6 \left[\frac{v_i}{\sqrt{gh}} \cdot \frac{\sigma_f}{\rho_w gh} \right]^{1.2} \quad [5]$$

It appears that the important dimensionless parameters controlling the impact load are Froude number and dimensionless strength. The scatter in the data is probably caused by uncontrolled variation in ψ , f , σ_{ox} , and snow cover depth.

DESCRIPTION OF INSTRUMENTATION SYSTEM

Strain Gauge Array

The data discussed in this paper was acquired from an array of 12 semiconductor strain gauges applied to hull stiffeners. The area of the hull which was chosen to be instrumented was between Stations 1 and 3. Mathematical techniques developed by Popov, et al were used to predict the portion of the hull which would encounter the greatest ice load.

The array of gauges is shown schematically in Figure 4, which also shows the locations of the calibration loads which will be discussed later. The upper insert in Figure 4 is a photograph taken during strain gauge installation. The lower insert shows the location of the gauged frame on the exterior of the hull. The gauges were connected as half-bridges, with the vertical element sensing the strain due to ice impact, and the horizontal element sensing the transverse strain due to the Poisson effect, and providing temperature compensation.

Recording Apparatus

The twelve gauges were connected to a standard signal-conditioning system for bridge completion, calibration, and amplification. The amplified signals, in turn, were applied to the inputs of twelve separate channels of a Teledyne Geotech slow-speed FM tape recorder. The thirteenth channel recorded a timing signal used in measurement of ship velocity, which acted as an event reference.

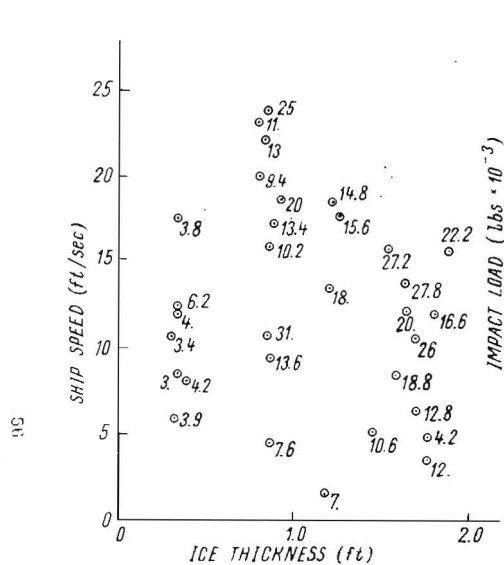


FIGURE 1. PLOT OF SHIP SPEED
VERSUS ICE THICKNESS

Trials of USCGC MACKINAW,
February-March 1971
Subscript numbers indicate
Impact Load (lbs x 10^{-3})

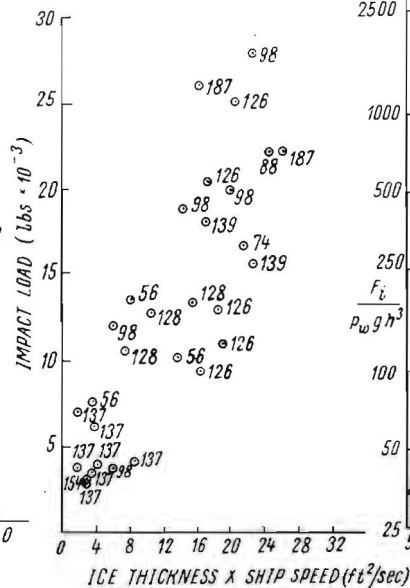


FIGURE 2. PLOT OF IM-
PACT LOAD
VERSUS THE
PRODUCT OF
ICE THICKNESS
AND SHIP
SPEED

Trials of USCGC MACKINAW,
Feb-March 1971

Subscript numbers indicate
Flexural Strength lbs/in²

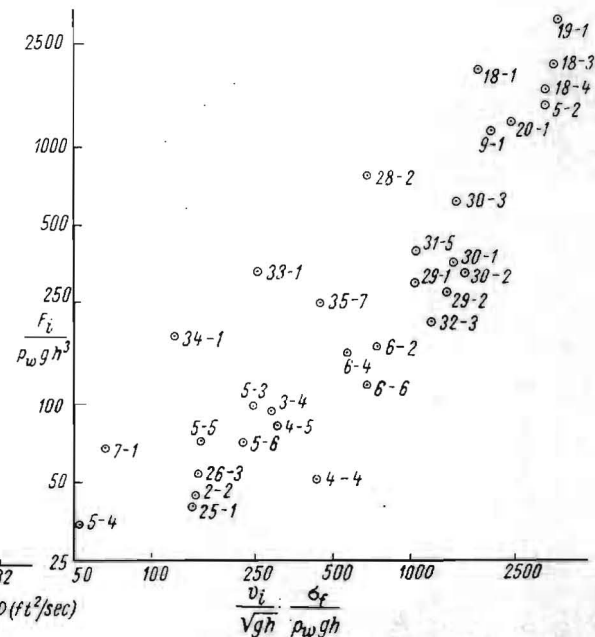
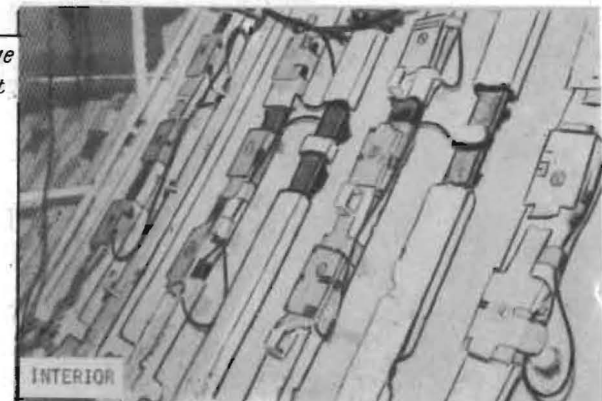
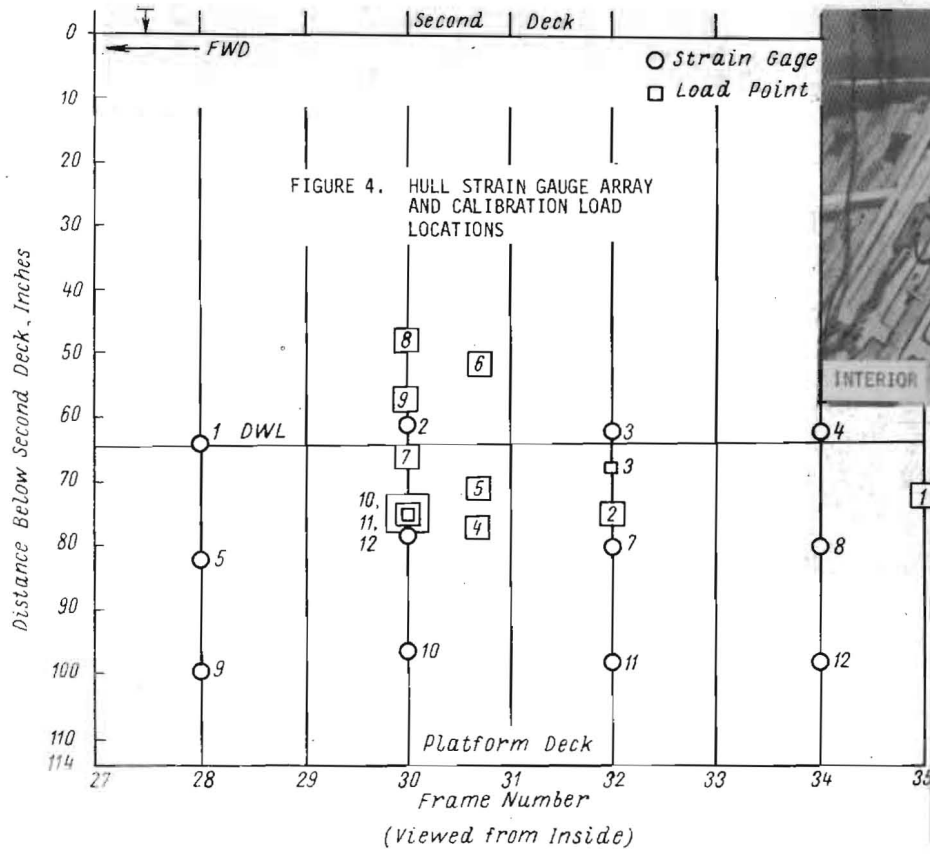


FIGURE 3. PLOT OF DIMENSIONLESS IMPACT
LOAD VERSUS PRODUCT OF FROUDE
NUMBER AND DIMENSIONLESS
STRENGTH

Full Scale Trials of USCGC MACKINAW,
February-March 1971

Subscript numbers indicate Data Point Number

57



During each of the experimental runs the outputs of the twelve hull gauges and the velocity signal were recorded. Figure 5 is a reproduction of the strain time-history from gauges 2, 6, and 10 on Frame 30 during a typical test. The strain impulses are the result of the impact of a cusp of unbroken ice against the hull, or the grinding and crushing of already broken pieces.

CALIBRATION OF HULL

In order to relate the recorded strains to applied icebreaking loads, a calibration of the instrumented portion of the hull was performed by applying known loads and measuring the response of the strain gauge array.

Loading Procedure

The hull was loaded with a 20-ton hydraulic jack set into a frame on a floating raft which was positioned next to the hull and braced against a set of pilings. Figure 4 shows the load locations for the twelve calibration cases.

Each calibration test case was performed by establishing the location of the jack on the panel, taking a set of zero and calibration readings on the gauges, applying loads to the hull and reading the gauge output voltage. Figure 6 shows the placement of the hydraulic jack in position against the hull.

Analysis of Calibration Data

A regression analysis was performed on the raw output voltage versus observed hydraulic jack force from each gauge for each load location. The zero intercept was subtracted from the data, and the regression performed again, with the output expressed in units of micro strain per ton of force by incorporating the calibration factor for each gauge and the hydraulic jack calibration results.

In order to gain perspective on the pattern of strain distribution, the data were plotted as functions of the panel geometry and load locations. The results indicated that the distribution of strain along a vertical stiffener is essentially linear, but that the distribution horizontally is an exponential decay. Figure 7 illustrates the extrapolation of the strain sensitivity under the load from the data of calibration case 2.

Conversions of Strains to Force

Analysis of all of the calibration data showed that strain distribution along the frames was linear and symmetrical about the point of load. The strain decayed exponentially away from the load point in the horizontal direction (see Figure 7). The sensitivity directly under the load was essentially invariant with load location at 18 micro strain per short ton of normal force. To cut down on the data reduction, a test was made to determine if, over a long run, the four frames in the panel experienced different stresses. They did not appear to. Hence the five highest strains were obtained from the gauges on a single frame (Frame 30). A symmetrical linear extrapolation was performed for each set of strains to obtain the maximum value of strain (see Figure 8). This value was divided by 18 micro

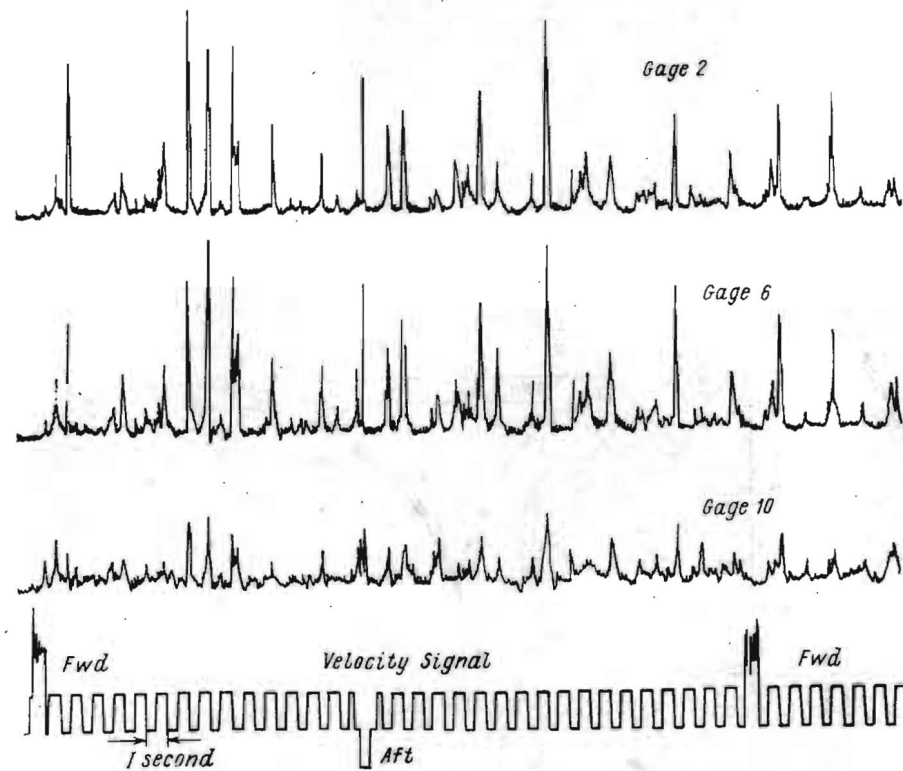


FIGURE 5. Strain vs. time, Gages 2, 6, 10 during test



FIGURE 6. ARRANGEMENT FOR HULL CALIBRATION BY EXTERNAL LOADING

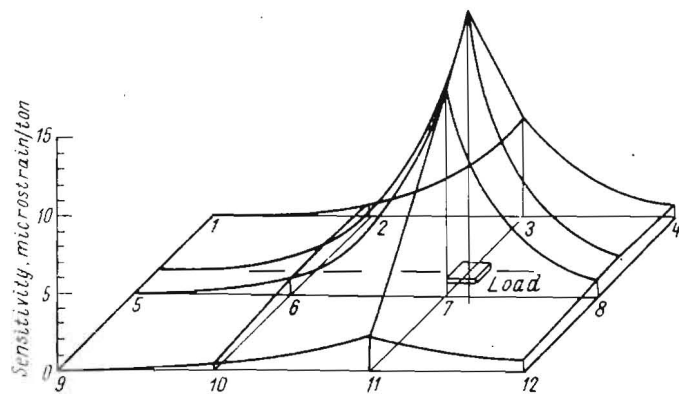


FIGURE 7. EXTRAPOLATION OF CALIBRATION DATA TO DETERMINE HULL STRAIN SENSITIVITY; CASE 2

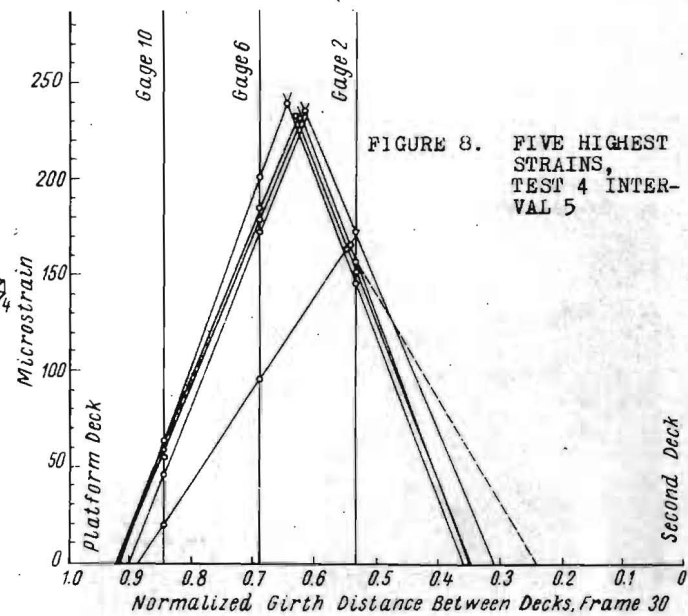


FIGURE 8. FIVE HIGHEST STRAINS, TEST 4 INTERVAL 5

strain per ton to obtain normal impact force. The average of these five force values have been tabulated in Table I for thirty-three intervals during which the ship traveled at a steady speed in uniformly thick ice.

CONCLUSIONS

This experiment demonstrated that with reasonable care it is possible to develop a body of data, expressed in dimensionless terms, which will provide designers of future ice going ships with rational hull design criteria.

RECOMMENDATIONS

Experiments such as the one discussed herein should be conducted in conjunction with ice resistance tests whenever possible. The effect of the variation in hull surface slopes β and α must be investigated before data such as we have reported is useful. The experiment described herein has treated a very limited problem relevant to ships moving in thin ice. Ramming mode structural tests should be performed in thick ice to obtain hull force criteria germane to the design of polar icebreakers. Elastic modulus should be measured carefully in all future hull-ice impact load experiments and included in the dimensional analysis.

The feasibility of modeling the ice impact phenomenon should be investigated. The successful use of dimensionless variables to explain the full scale data suggests that modeling may be a useful and inexpensive way of expanding the body of hull-ice impact data.

ACKNOWLEDGMENTS

The authors wish to thank the Office of Research and Development of the U.S. Coast Guard for permission to publish this paper. The cooperation of the Officers and Crew of the U.S. Coast Guard Cutter MACKINAW was vital to the acquisition of the data in this paper; we wish also to thank them for a job well done.



BRITTLE FRACTURE OF POLYCRYSTALLINE ICE
UNDER COMPRESSIVE LOADINGS

Donald S. Carter, D. Sc.	Defence Research Board	Ottawa
Scientific Officer	Defence Research Estab- lishment Ottawa	Canada

SYNOPSIS

By considering the energy dissipated in the plastic region at the head of a crack under compressive loadings, the author derives the criterion for the quasi-brittle propagation of this elastic-plastic crack. It is shown that when unstable fracture occurs the ratio of brittle fracture stress to maximum ductile stress must be 0.6. This analysis both predicts and provides a theoretical explanation of the marked decrease in strength observed when polycrystalline ice undergoes a transition from ductile to brittle behaviour under increasing strain rates.

RESUME

En considérant l'énergie dissipée dans la zone plastique à l'extrémité d'une fissure sous des contraintes de compression, l'auteur dérive le critère de propagation quasi-fragile d'une fissure élasto-plastique. On montre aussi que la contrainte de fracture fragile doit être égale à 0.6 de la contrainte maximale ductile. La présente analyse prévoit et explique théoriquement la forte diminution de résistance observée quand le comportement de la glace polycristalline passe de ductile à fragile sous une augmentation des taux de déformation.

INTRODUCTION

For a long time, the effect of strain rate on the strength of ice was not clear, since some tests show increasing strength with increasing load rates, while others show decreasing strength with increasing load rates [1],[2]. However, the recent results of systematic tests carried out on river and lake ice by Ramseier [3] show that, under low strain rates, the yield strength, σ_Y , increases with increasing strain rates, $\dot{\epsilon}$, according to a law of the following form:

$$\sigma_Y = K \dot{\epsilon}^{1/m} \exp \left[\frac{Q}{m k T} \right] \quad (1)$$

where K, m are constants, k is the Boltzman's constant, Q the activation energy and T the absolute temperature. This increase in strength can hardly continue indefinitely, beyond a certain critical strain rate, the yield strength, σ_Y , will equal or exceed the stress required to initiate and propagate catastrophically a crack through the ice sample and fracture will precede yielding. By distinguishing between the two important stages of crack growth, initiation and propagation, Carter [4] has shown that, under compressive loads, once nucleated the crack will come to rest at a finite length and the fracture stress will be the stress required to start this stable crack. The present paper is a theoretical and experimental study of the transition from ductile to brittle behaviour which manifests itself in a marked decrease of strength as observed by Korzhavin [5] under high strain rates.

PROPAGATION OF AN ELASTIC-PLASTIC CRACK

As shown by Ingis [6], a highly concentrated tensile stress occurs at the tips of a favourably oriented crack under compressive loadings. This stress concentration is then damped by plastic deformation as soon as the yielding strength is reached. A model of an elastic-plastic crack, proposed by Dugdale [7] is shown in Figure 1.

Yielding is assumed to be confined to a narrow zone directly ahead of the crack tip, and the model is analyzed by viewing the effect of yielding as making the crack longer by an amount equal to the plastic zone size, s, with cohesive stresses, σ_0 , in the plastic zone acting on the extended crack surface so as to restrain the opening. Sanders [8], in an effort to establish the equivalence of the energy and stress criteria for fracture, reformulated the two-dimensional theory of Griffith and obtained an equivalent criterion involving a certain integral around any contour enclosing the crack tip. His result suggests that the determination of the energy release rate requires only the stress and displacement fields in a small zone around the crack tip. Rice [9], by making the convenient choice of shrinking the path-independent integral down to the upper and lower surfaces of the cohesive zone obtained the potential energy decrease rate $\frac{dP}{da}$ in the following simple form:

$$\frac{dP}{da} = \sigma_0 \delta \quad (2)$$

where σ_0 is the cohesive stress in the plastic zone, δ the separation distance at the crack tip and a the half-length of the crack.

By assigning the potential energy decrease dP to the new surface energy, we can write:

$$\sigma_0 \delta da = 2 \gamma dc \quad (3)$$

where c is the half-length of the crack including the plastic zone and the surface energy.

To go further we now need the geometrical characteristics of the plastic zone as a function of the ratio of applied stress σ to yield stress σ_Y . Independent calculations of Dugdale [7], Bilby et al. [10] and Rice [9] enable us to write the two following equations:

$$\frac{c}{a} = \sec \left\{ \frac{\pi}{2} \cdot \frac{\sigma}{\sigma_Y} \right\} \quad (4)$$

$$\delta = \frac{2(\kappa+1)(1+\nu) \sigma_Y a}{\pi E} \log \sec \left\{ \frac{\pi}{2} \cdot \frac{\sigma}{\sigma_Y} \right\} \quad (5)$$

which differ from the Hult and McClintock [11] results based on the mathematical theory of plasticity by less than 5%. In these equations, E is the elastic modulus and κ , the material constant, is $(3-\nu)(1+\nu)^{-1}$ for plane stress, $(3-4\nu)$ for plane strain, ν being the Poisson's ratio. By the use of equations 4 and 5, the criterion for unstable elastic-plastic fracture (3) can be rewritten:

$$\frac{\sigma_0 \sigma_Y a}{E} > \frac{\pi \delta \sec \left\{ \frac{\pi}{2} \cdot \frac{\sigma}{\sigma_Y} \right\}}{(\kappa+1)(1+\nu) \log \sec \left\{ \frac{\pi}{2} \cdot \frac{\sigma}{\sigma_Y} \right\}} \quad (6)$$

Knowing that $\sigma_0 = \alpha \sigma_Y$, α being the stress concentration factor under test conditions, then equation 6 takes the following form:

$$\frac{\sigma_Y^2 a}{E} > f\left(\frac{\sigma}{\sigma_Y}\right) \quad (7)$$

or expressed in an adimensional form:

$$\frac{(\sigma_Y^2 a)}{(\sigma_Y^2 a)_{\min}} > \frac{f\left(\frac{\sigma}{\sigma_Y}\right)}{f\left(\frac{\sigma}{\sigma_Y}\right)_{\min}} \quad (8)$$

where $(\sigma_Y^2 a)_{\min}$ and $f\left(\frac{\sigma}{\sigma_Y}\right)_{\min}$ are the minimum values which satisfy equation (7). Figure 2 shows the ratio of $f\left(\frac{\sigma}{\sigma_Y}\right)$ to $f\left(\frac{\sigma}{\sigma_Y}\right)_{\min}$ as a function of $\left(\frac{\sigma}{\sigma_Y}\right)$. We can see that Equation (8) has real roots for $\left(\frac{\sigma}{\sigma_Y}\right)$ when $\left(\frac{\sigma_Y^2 a}{(\sigma_Y^2 a)_{\min}}\right) > 1$. In this case, as σ is increase from zero continuously, the length of the plastic zone increases until σ reaches the value σ_c corresponding to the intersection U, in Figure 2, and then under the stress σ_c the crack extends. It can be seen in Figure 2 that the propagation of an elastic-plastic crack always occurs at a stress level $\left(\frac{\sigma}{\sigma_Y}\right)$ lower than 0.7. As an example when, under particular conditions of temperature and strain rate, the

ratio $\frac{\sigma_Y^2 a}{(\sigma_Y^2 a)_{\min}} = 4$ the elastic-plastic crack will propagate when $(\frac{\sigma}{\sigma_Y}) = 0.3$.
 On the contrary, when $\frac{\sigma_Y^2 a}{(\sigma_Y^2 a)_{\min}} < 1$, Equation (8) has no real roots, and the plastic zone increases its length with increase of σ until σ reaches σ_Y , that is, general yielding will occur. Although we can evaluate the theoretical yield stress for any temperatures and strain rates by the use of Equation (1), the maximum yield stress, $\sigma_{Y \text{ crit}}$, that we can observe experimentally is given by $\frac{\sigma_{Y \text{ crit}}^2 a}{(\sigma_Y^2 a)_{\min}} = 1$ which determines the onset of the ductile-to-brittle transition.
 The Equation (8) may be rewritten:

$$\frac{\sigma_Y^2 a}{\sigma_{Y \text{ crit}}^2 a} > \frac{f(\frac{\sigma}{\sigma_Y})}{f(\frac{\sigma}{\sigma_Y})_{\min}} \quad (9)$$

As shown in Figure 2, when the fracture criterion is satisfied, the function, $\frac{f(\frac{\sigma}{\sigma_Y})}{f(\frac{\sigma}{\sigma_Y})_{\min}}$ of the right hand side of Equation (8) is satisfactorily approximated by the experimental relation:

$$\frac{f(\frac{\sigma}{\sigma_Y})}{f(\frac{\sigma}{\sigma_Y})_{\min}} = 0.36 \left(\frac{\sigma_Y}{\sigma}\right)^2 \quad (10)$$

Incorporating Equation (10) into Equation (9), we get:

$$\frac{\sigma^2 a}{\sigma_{Y \text{ crit}}^2 a} > 0.36 \quad (11)$$

The results obtained by Gold [12] on columnar-grained ice indicate that a is dependent on the temperature. However, under increasing strain rates and constant temperature, the stress required to propagate an elastic-plastic crack, when the fracture criterion is satisfied, $(\sigma_Y^2 a > \sigma_{Y \text{ crit}}^2 a)$ will be given, according to Equation (11), by:

$$\frac{\sigma}{\sigma_{Y \text{ crit}}} > 0.6 \quad (12)$$

Therefore the transition from ductile to brittle behaviour under increasing strain rates must be accompanied by a marked decrease in ice strength from $\sigma_{Y \text{ crit}}$ to $0.6 \sigma_{Y \text{ crit}}$. When the strain rate is increased beyond the transition zone, a constant strength equal to 0.6 of the maximum strength of ice must be exhibited.

COMPARISON WITH EXPERIMENTAL RESULTS

All tests were performed on cylindrical samples (5 cm x 15 cm) taken horizontally in ice covers of the three most common distinctive types: frazil ice,

snow ice and columnar-grained ice. The physical characteristics of these three types of fresh water ice are summarized in Table 1. Figures 3, 4 and 5 show the relation proposed by Ramseier [3] for the ductile behaviour and the experimental data obtained by Carter [4] in the ductile-to-brittle transition zone and in the brittle range. For each type of ice at each temperature the theoretical ratio (0.6) of the brittle fracture stress to the maximum strength is very well verified.

CONCLUSION

By energy considerations, a criterion is derived for the propagation of an elastic-plastic crack. Unstable brittle fracture will occur if:

$$\sigma_y^2 a > \text{constant}$$

σ_y being the yield stress for test conditions and $2a$ the length of the elastic-plastic crack. For polycrystalline ice tested under increasing strain rates and constant temperature, the brittle fracture stress is given by:

$$\sigma = 0.6 \sigma_{y \text{ crit}}$$

where $\sigma_{y \text{ crit}}$ is the maximum strength which is observed experimentally at this temperature. These theoretical deductions are in very good agreement with experimental data obtained by Carter [4], Korzhavin [5], Schwarz [13] and Peyton [14] on various types of ice.

ACKNOWLEDGEMENT

The present study was done at Laval University as part of a doctoral thesis supervised by Professor Bernard Michel.

REFERENCES

- 1- VOITKOVSKII, K.F. (1962)- "The Mechanical Properties of Ice", Moscow transl. by Am. Met. Soc.
- 2- MASER, K.R. (1971)- "The Interpretation of Small Scale Strength Data for Ice", POAC - Conference Norway 1971.
- 3- RAMSEIER, R.O. (1972)- Doctoral thesis, Université Laval, Québec, Canada.
- 4- CARTER, D. (1971)- "Fracture Fragile de la Glace d'Eau Douce", Doctoral thesis, Université Laval, Québec, Canada.
- 5- KORZHAVIN, K.N. (1962)- "Action of Ice on Engineering Structures", Novosibirsk, Akad, Navk, SSSR.
- 6- INGLIS, C.E. (1913)- Trans. Inst. Naval Arch. London, Vol. 55, Part 1.
- 7- DUGDALE, D.S. (1963)- Journ. Mech. Phys. Solids, 8, p. 100.
- 8- SANDERS, J.L. (1960)- Journ. Appl. Mech. 27, 352.
- 9- RICE, J.R. (1968)- in "Fracture", Vol. 2, edited by H. Liebowitz Acad. Press, New York and London.
- 10- BILBY, B.A., COTTRELL, A.H. and SWIDEN, K.H. (1962)- Adv. Appl. Mech., Vol. 7, p. 55.
- 11- HULT, J.A.H and McCLINTOCK, F.A. (1957)- 9th Int. Cong. Appl. Mech., Vol. 8, p. 51

- 12- GOLD, L.W. (1970)- "The Failure Process in Columnar-Grained Ice", Ph.D. Thesis, McGill University, Montreal, Canada.
- 13- SCHWARZ, K. (1970)- "The Pressure of Floating Ice-Fields on Piles", Ice Symposium 1970, Reykjavik, Iceland.
- 14- PEYTON, H.R. (1966)- "Sea Ice Strength", Geophy. Inst., University of Alaska, U.S.A.

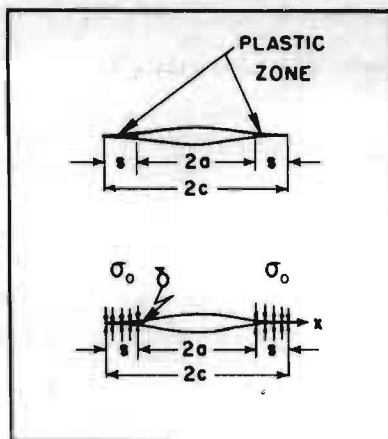


FIGURE 1: Elastic-Plastic Crack Model.

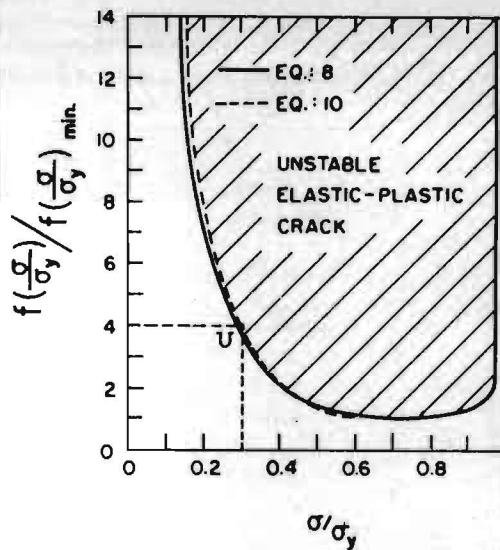


FIGURE 2: Criterion for Elastic-Plastic Fracture.

TYPE OF ICE	GRAIN SHAPE	GRAIN SIZE	C-AXIS DISTRIBUTION	DENSITY	ELASTIC MODULUS (Kg/cm ²)
Frazil Ice	Angular	0.09 cm	Random	0.89	$E = 40148 - 666\theta$ (°C)
Snow Ice	Spherical	0.1 cm	Random	0.89	$E = 52423 - 673\theta$ (°C)
Columnar Ice	Columnar-grained	0.4 cm	Random in horizontal plane	0.91	$E = 57000 - 649\theta$ (°C)

* θ is the temperature expressed in (°C).

TABLE 1: Physical Constants of the Three Types of Ice Used in our Experiments.

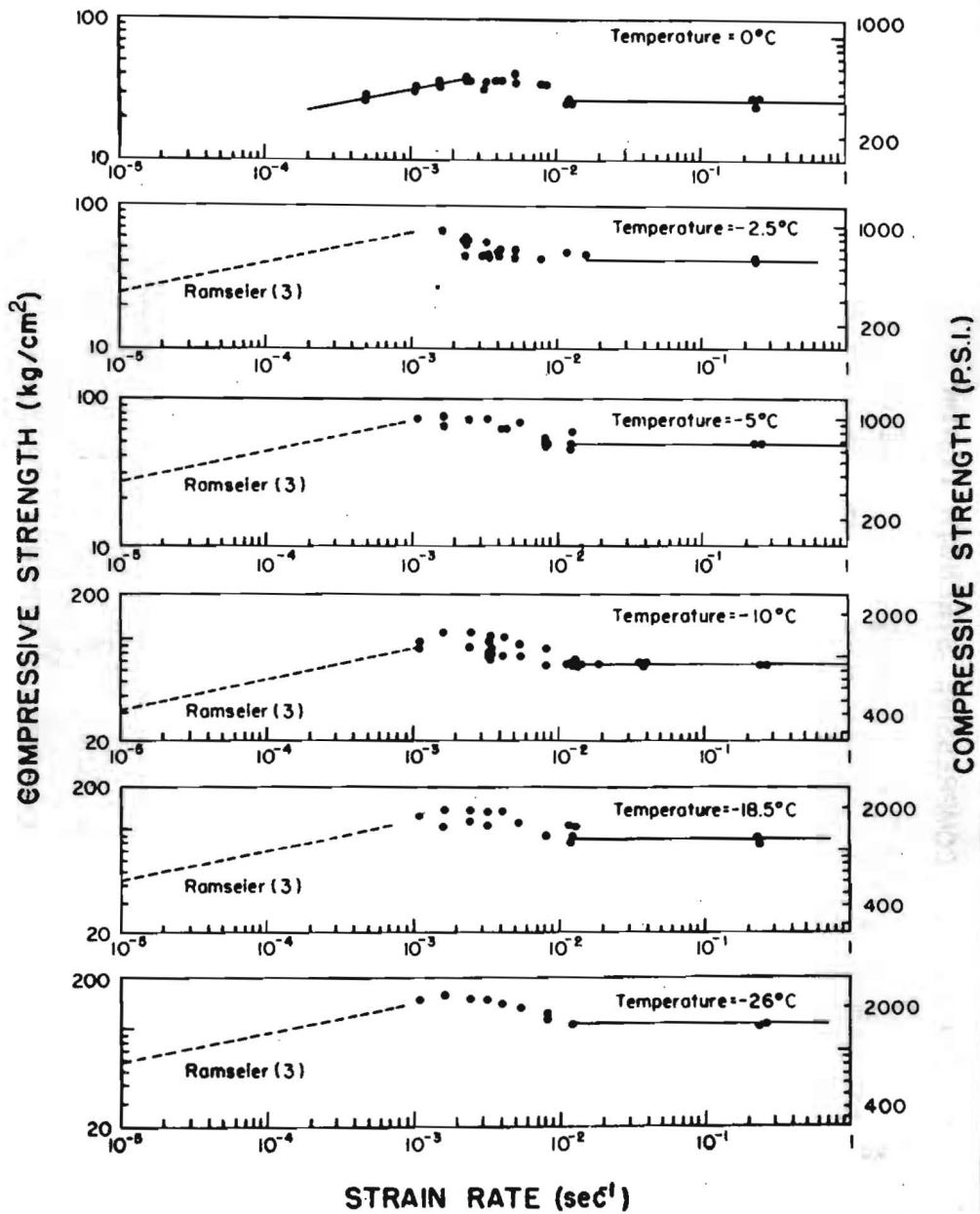


FIGURE 3: Compressive strength of frazil ice under increasing strain rates at various temperatures:

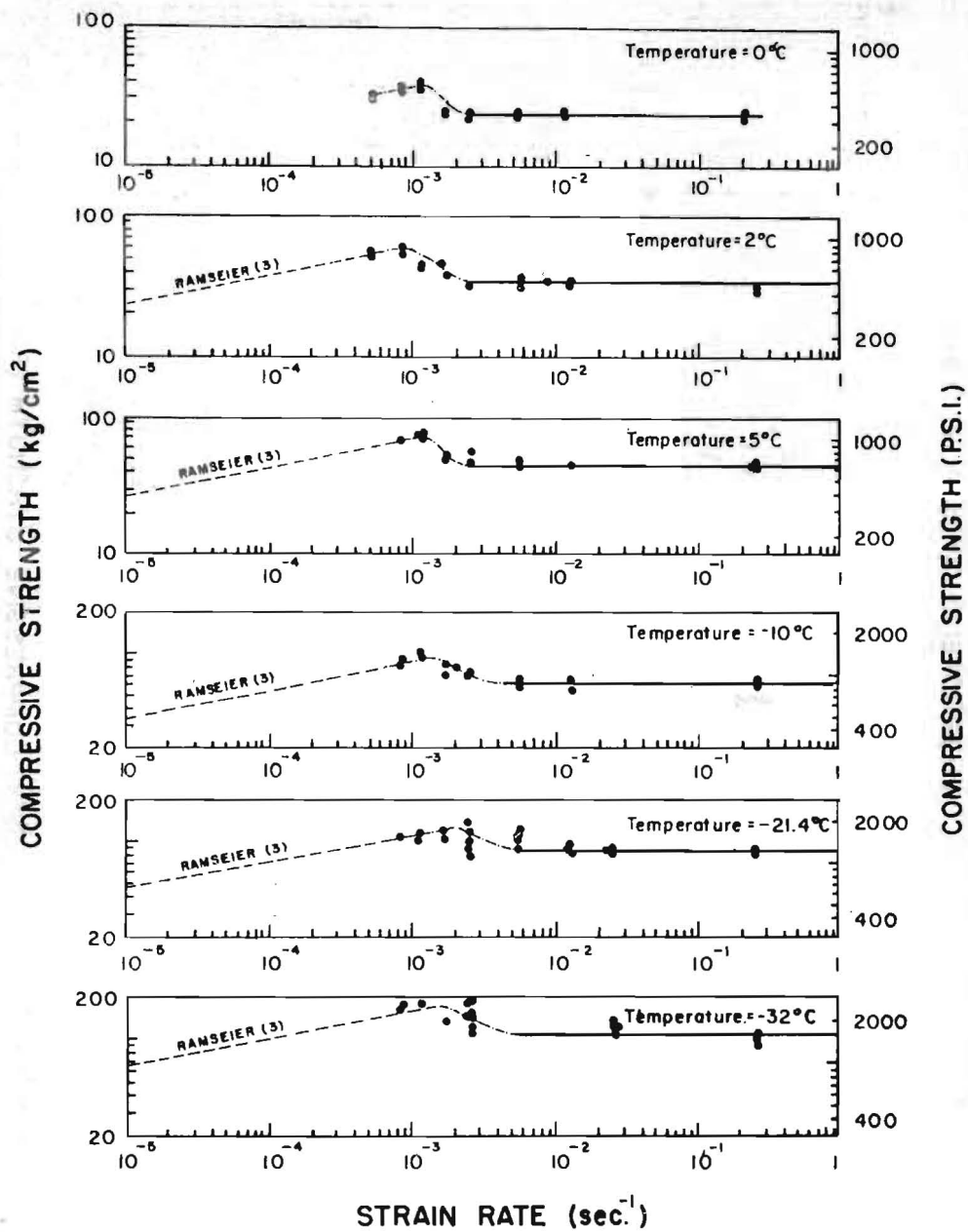


FIGURE 4: Compressive strength of snow ice under increasing strain rates at various temperatures.

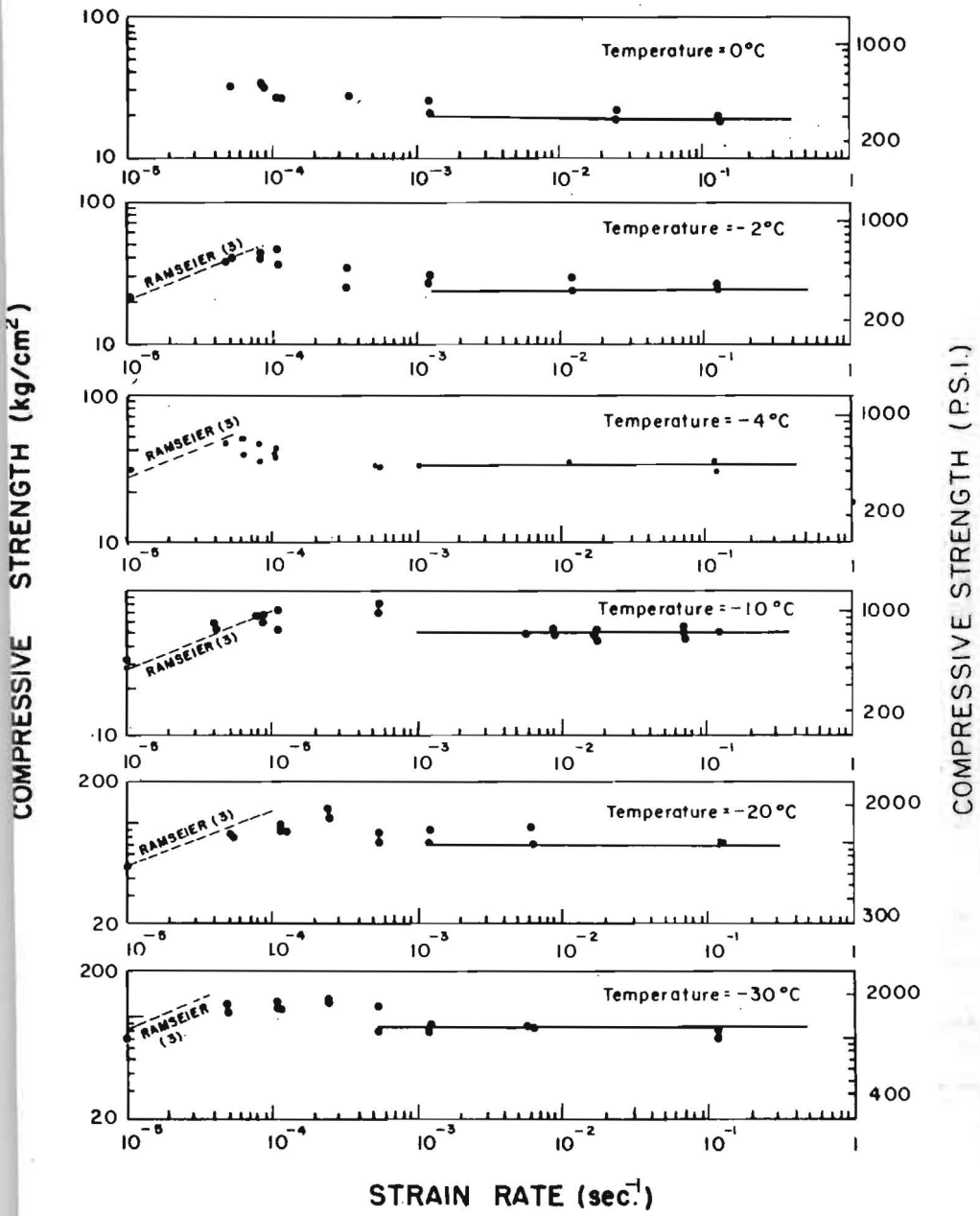


FIGURE 5: Compressive strength of columnar-grained ice under increasing strain rates at various temperatures.



ICE SYMPOSIUM 1972
LENINGRAD

LABORATORY INVESTIGATION ON ICE THERMAL
PRESSURES

Marc Drouin, Research Associate Ice Mechanics Laboratory Quebec, Canada
University Laval

SYNOPSIS

The usual technique used to estimate the thermal stresses exerted by ice has consisted in immobilizing the extremities of samples during temperature increases. A second technique consists in doing constant strain rate tests at different temperatures. This method has advantages over the first one in that it is done at constant temperatures and it enables one to relate the thermal stresses to the fundamental creep laws of ice. The paper describes the results of constant strain rate tests of three types of ice deformed at rates of 10^{-8} sec^{-1} and presents the rheological model which fits the stress-strain curves and which is used to calculate the thermal stresses exerted by thick ice covers restrained in one direction.

RESUME

Parmi les méthodes expérimentales pour déterminer les valeurs des contraintes induites sous l'effet des variations de température, la plus évidente consiste à utiliser une éprouvette mécaniquement immobilisée à ses extrémités. Une deuxième méthode consiste à effectuer, à différentes températures, des essais de déformation à taux constants. Cette méthode comporte de nombreux avantages comme celui de procéder à des essais à des températures constantes et celui de rattacher les contraintes d'origine thermique aux lois fondamentales du fluage de la glace. L'article décrit les résultats d'essais de déformation à taux constants de l'ordre 10^{-8} sec^{-1} obtenus pour trois types de glace et présente un modèle rhéologique décrivant les courbes contrainte-déformation qui est utilisé par la suite pour calculer les contraintes d'origine thermique exercées par les couverts de glace épais dont l'expansion est limitée dans une direction.

INTRODUCTION

The strain rates of an ice cover submitted to temperature rises are given by the general equation:

$$\dot{\epsilon}(t, z) = \alpha(t) \dot{\theta}(t, z) \quad (1)$$

where $\dot{\epsilon}(t, z)$ is the strain rate at time t and depth z under the ice surface, α is the linear expansion coefficient which is a function of the temperature θ and $\dot{\theta}$ is the rate of the temperature rise for the time and the depth considered. Taking for α a value of $50 \times 10^{-6} \text{ } ^\circ\text{C}^{-1}$ at -20°C , the strain rates corresponding to constant rates of temperature rises between 0.1 and 10°C/h are the followings: $\dot{\theta} = 0.1^\circ\text{C/h}$, $\dot{\epsilon} = 1.39 \times 10^{-9} \text{ sec}^{-1}$; $\dot{\theta} = 0.5^\circ\text{C/h}$, $\dot{\epsilon} = 6.95 \times 10^{-9} \text{ sec}^{-1}$; $\dot{\theta} = 2^\circ\text{C/h}$, $\dot{\epsilon} = 2.78 \times 10^{-8} \text{ sec}^{-1}$; $\dot{\theta} = 10^\circ\text{C/h}$, $\dot{\epsilon} = 1.39 \times 10^{-7} \text{ sec}^{-1}$. A theoretical solution of the problem relative to the thermal pressures exerted by ice covers should take into account the rheological properties of ice deformed at strain rates lower than 10^{-7} sec^{-1} .

CONSTANT STRAIN RATE TESTS

Constant strain rate tests, totalizing some 4000 hours of testing machine operation, have been made for three types of ice¹: snow ice and columnar ice with vertical and with horizontal optic axis. From previously undeformed ice covers, cylindrical samples were cut with the axis of the cylinder horizontal, and the deformation was applied in the direction of the long axis of the cylinder. The sample dimensions, the ice characteristics and the direction of the deformation relative to the c -axis were as follows:

Type of ice	Density	Strain direction Relative to the c -axis	Grain diameter	Sample dimensions
Snow	≈ 0.90	Random to c	$\approx 1 \text{ mm}$	$l \approx 76 \text{ mm}$, $d \approx 25 \text{ mm}$
*Columnar	≈ 0.91	Perpendicular to c	$> 80 \text{ mm}$	$l \approx 76 \text{ mm}$, $d \approx 25 \text{ mm}$
Columnar	≈ 0.91	Parallel to c	$\approx 2.3 \text{ mm}$	$l \approx 100 \text{ mm}$, $d \approx 50 \text{ mm}$

*Such an ice sample is part of a natural monocrystal machined out of a columnar ice grain and deformed in a direction parallel to the basal plane.

Typical test results are shown in figure 1. The stress-time curves for snow ice (figure 1 a) and columnar ice with horizontal c -axis (figure 1 c) have the same shape, i.e. the stress increases initially at a constant rate, reaches a maximum value which decreases very slowly as the strain is increased at a constant rate. For columnar ice with horizontal c -axis (figure 1 c) the yield stress corresponds to a strain of 1% in contrast to a strain of 0.2% for snow ice. For the case of columnar ice with vertical c -axis* (figure 1 b) the stress increases initially at a constant rate but a large yield drop appears followed by a constant stress value as the strain continues to increase. The yield stress corresponds to a strain of the order of 0.2%. The yield drop observed for that type of ice

follows upon the formation of double kink band as shown on figure 1 b.

A very interesting characteristic of so-called constant strain rate tests is the fact that the strain rate of a sample is not truly constant throughout the duration of a test. The change in the strain-time curves are caused by the elastic deformation of the testing machine and the loading cell when the stress is increasing or decreasing. The calculated and measured strain rates are equal only when the stress-time curve levels off.

EXPERIMENTAL STRESS-TIME CURVE FITTING

A general equation to fit experimental stress-time curves, like those shown on figure 1, taking into account the plastic properties of the ice sample tested and the characteristics of the testing machine used has been deduced from the work of Johnston² on LiF crystals which has been commented on by many ice physicists^{3, 4, 5, 6}. This equation is based on Cottrell's⁷ fundamental equation which gives the plastic strain rate of a crystal as equal to the product of the Burgers vector by the number of mobile dislocations by the dislocation velocity. Johnston² assumed, on the basis of observations made on the movement of dislocations due to a shear stress, that the number of dislocations increased linearly with strain and their velocity was proportional to τ^m . The equation written in function of the axial stress applied on the sample^{1, 2} is:

$$\frac{d\sigma}{dt} = \frac{S_c K}{A} - \frac{2b K \beta}{A} \left[\left(\frac{n_0 \ell}{\beta} + S_c t \right) - \frac{\sigma(t)A}{K} \right] \left(\frac{\sigma(t)}{2P} \right)^m \quad (2)$$

where: S_c is the crosshead speed in cm/min, ℓ is the length of the ice sample in cm, A is the area of the ice sample in cm^2 , K is the effective spring constant depicting the apparent elastic deformation of the ice sample and the elastic deformation of the testing machine in kg/cm ($dF/dt = \text{const.} = K S_c$), F is the applied load at time t taken in the linear part of the load increase, in kg, b is the Burgers vector in cm, n_0 is the number of mobile dislocations initially present per cm^2 , β is the dislocation multiplication rate per cm^2 , P is a parameter to be adjusted for each stress-time curve and m is the exponent associated with stress in the general equation of secondary creep as a function of the applied stress and the temperature.

For a given test the following parameters are known: S_c , ℓ , A , K , b and m . The only parameters to be determined for a particular type of ice are n_0 and β . The parameter P which is a function of the test temperature is determined by successive trials. The values used for each of the three tests of figure 1 are the following:

Parameters	Snow ice strain random to c-axis (figure 1 a)	Columnar ice strain \perp to c-axis (figure 1 b)	Columnar ice strain // to c-axis (figure 1 c)
S_c (cm/min)	2.54×10^{-5}	2.54×10^{-5}	4.23×10^{-5}
ℓ (cm)	7.60	7.70	10.20
A (cm ²)	5.04	5.11	20.27
K (kg/cm)	7750	8880	4073
b (cm)	4.523 Å	4.523 Å	4.523 Å
m	4	2.7	4
n_0 (cm ⁻²)	10^9	5×10^{-5} (ref:6)	10^9
β (cm ⁻²)	10^9 (ref: 2)	10^9 (ref:2)	10^9 (ref:2)
P	1100	1100	490
θ °C	-27.4	-26.1	-20.6

The dotted point shown in figure 1 are values calculated with equation (2). The fitting with experimental stress-time curves for columnar ice where the strain is perpendicular to the optic axis is limited to the first part of the curve. The formation of a double kink band cannot be considered in the rheological model because it is a rupture of the basal plane (figure 1 b).

STRESS-STRAIN CURVES

From an experimental stress-time curve it is possible to calculate the stress-strain curve relative to an infinitely rigid testing machine, i.e. the true stress-strain curve for a given rate of deformation. In this case the effective spring constant K become only a function of the material tested. The new value for K is written as a function of the apparent Young's modulus E_a of the material i.e. $K = (E_a \times A) / \ell$. The stress-strain curve equation becomes:

$$\frac{d\sigma}{d\varepsilon} = E_a \left[1 - \frac{2b\beta}{\dot{\varepsilon}} \left(\left(\frac{n_0}{\beta} + \dot{\varepsilon}t \right) - \frac{\sigma(t)}{E_a} \right) \left(\frac{\sigma(t)}{2P} \right)^m \right] \quad (3)$$

For strain-rates between 10^{-7}sec^{-1} and 10^{-8}sec^{-1} the following equations for E_a and P have been determined from the tests.

Type of ice	Apparent Young's modulus	Parameter P
Snow ice	$E_a = 4.52 e^{2060/T(^{\circ}\text{K})}$	$P = 18 \times 10^{-3} e^{2710/T(^{\circ}\text{K})}$
Columnar ice strain \perp to c- axis	$E_a = c \cdot 0.079 e^{1335/T(^{\circ}\text{K})}$ $c = 249$ if $\dot{\varepsilon}$ en min^{-1} $c = 344$ if $\dot{\varepsilon}$ en sec^{-1}	$P = 18 \times 10^{-3} e^{2710/T(^{\circ}\text{K})}$
Columnar ice strain // to c- axis	Tests not completed	

THERMAL STRESS

Ice sample

Equation (3) can be used to calculate the thermal stress relative to an ice sample, restrained in one direction, initially at a uniform temperature which increases with time. Stress-time curves for two types of temperature rises are shown on figure 2 for columnar ice sample where the strain is perpendicular to the optic axis and snow ice sample¹.

Ice cover

Similar stress-time curves can also be computed for ice covers subjected to temperature rises. Such results¹ are shown in figure 3 for a columnar ice cover 100 cm thick with vertical c-axis and in figure 4 for a snow ice cover of the same thickness. For this example, the ice surface temperature is rising from -40°C to 0°C in 10 hours according to a sinusoidal function limited by $-\frac{\pi}{2}$ ($t = 0\text{h}$, $\theta = -40^{\circ}\text{C}$) and $+\frac{\pi}{2}$ ($t = 10\text{h}$, $\theta = 0^{\circ}\text{C}$). The initial temperature distribution in the ice is considered as being linear. The ice cover is clear of snow and contains no cracks. For these severe conditions, the maximum forces are 54,180 kg/linear meter (36,300 lb/linear foot) for the columnar ice cover (figure 3) and 38,690 kg/linear meter (25,900 lb/linear foot) for the snow ice cover (figure 4). If there is on the ice cover a layer of snow 10 cm thick of density 0.20, the above maximum forces are reduced by a factor of about 3. Surface cracks will reduce again the thermal pressure.

CONCLUSION

The estimation of thermal ice stresses exerted by ice covers has always been a controversial problem in ice mechanics research. Even if an acceptable solution can be deduced from laboratory investigations taking into account the texture and the structure of ice covers, field conditions have to be considered when evaluating this force for a given application. In particular, snow layers on ice covers and surface cracks reduce drastically the thermal forces exerted by ice covers.

Measurements of thermal ice forces in nature should now be planned which will take into consideration the texture and the structure of the ice, the ice surface cracks, the meteorological variables and the type of shores restraining the ice cover. Such results analyzed in terms of the rheological properties of ice deformed at strain rates lower than 10^{-7}sec^{-1} will make it possible to calculate realistic values of the maximum thermal pressures exerted by ice covers for given applications.

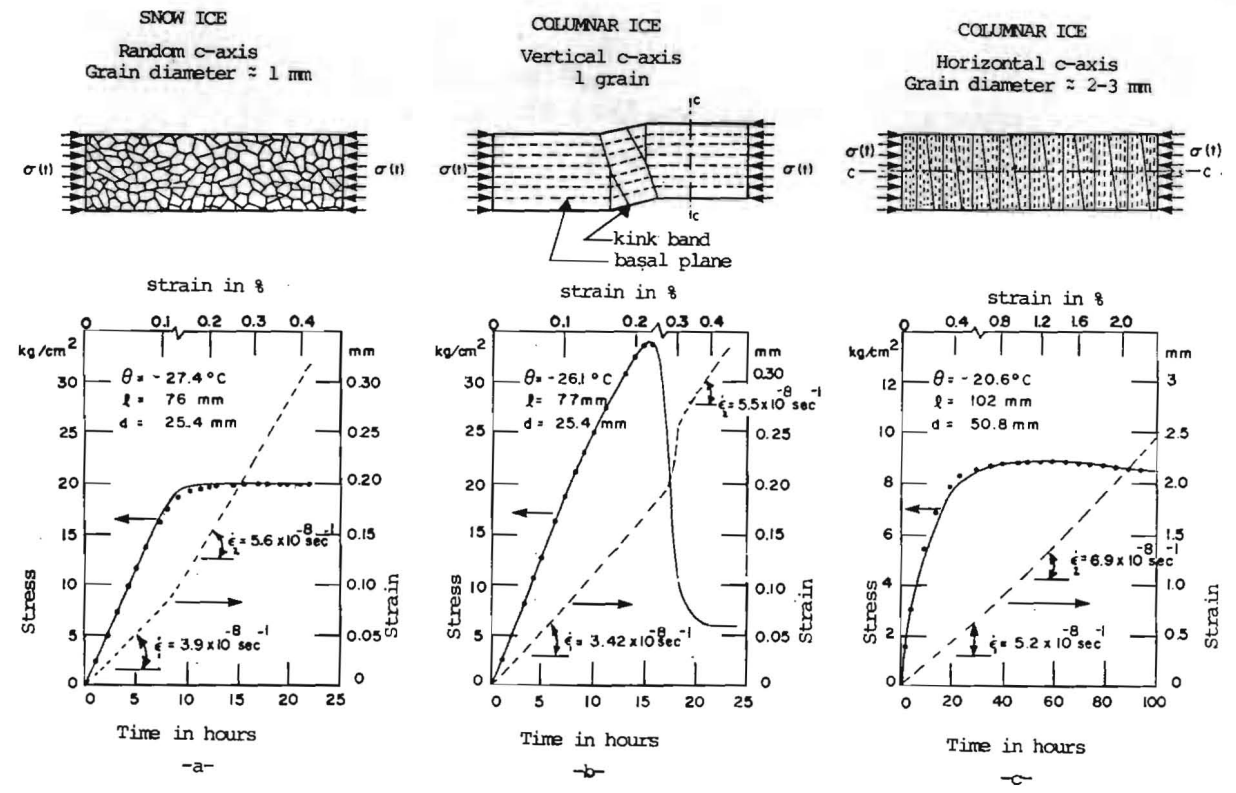


FIGURE 1- STRESS-TIME AND STRESS-STRAIN CURVES OBTAINED BY ACTING ON ICE SPECIMENS WITH A CONSTANT SPEED CROSSHEAD TESTING MACHINE.
 (Experimental curves ————)
 (Calculated values from equation 2)

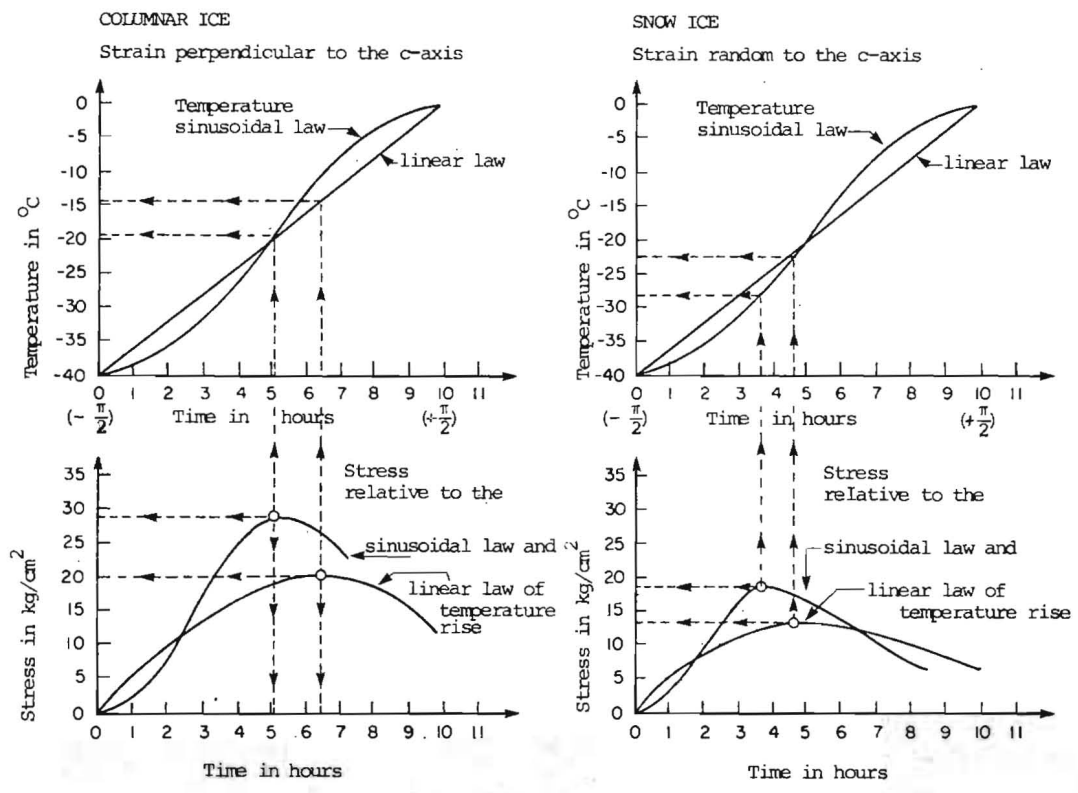


FIGURE 2- THERMAL STRESS-TIME CURVES RELATIVE TO CYLINDRICAL ICE SAMPLES RESTRAINED IN ONE DIRECTION.

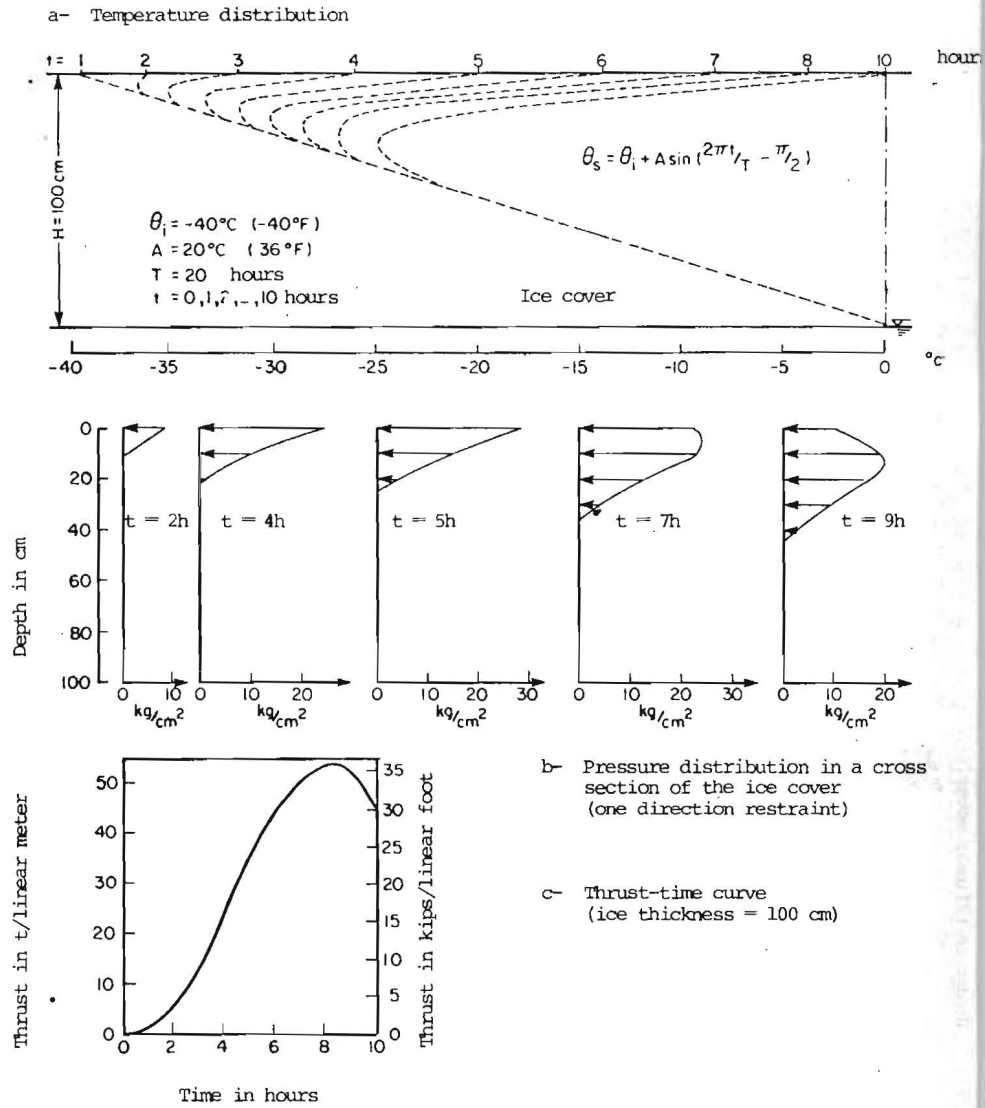
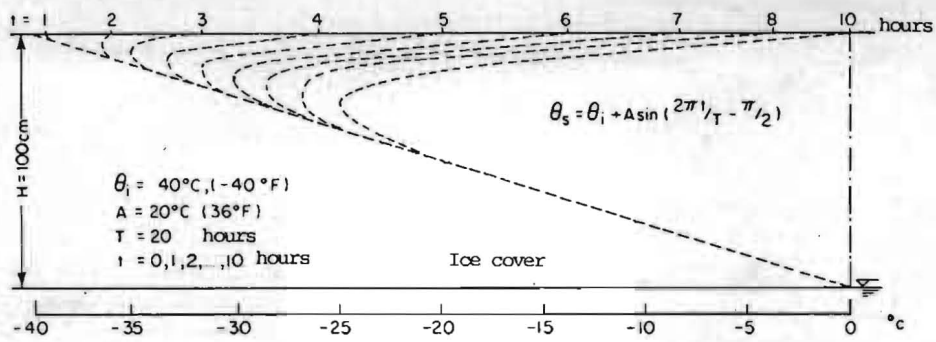


FIGURE 3- TEMPERATURE AND THERMAL PRESSURE DISTRIBUTIONS IN A COLUMNAR ICE COVER WITH VERTICAL C-AXIS FOR A SINUSOIDALLY RISING TEMPERATURE OF THE SURFACE FROM $-40^\circ\text{C} (-\frac{\pi}{2})$ TO $0^\circ\text{C} (+\frac{\pi}{2})$ IN 10 HOURS.

a- Temperature distribution



b- Pressure distribution in a cross section of the ice cover (one direction restraint)

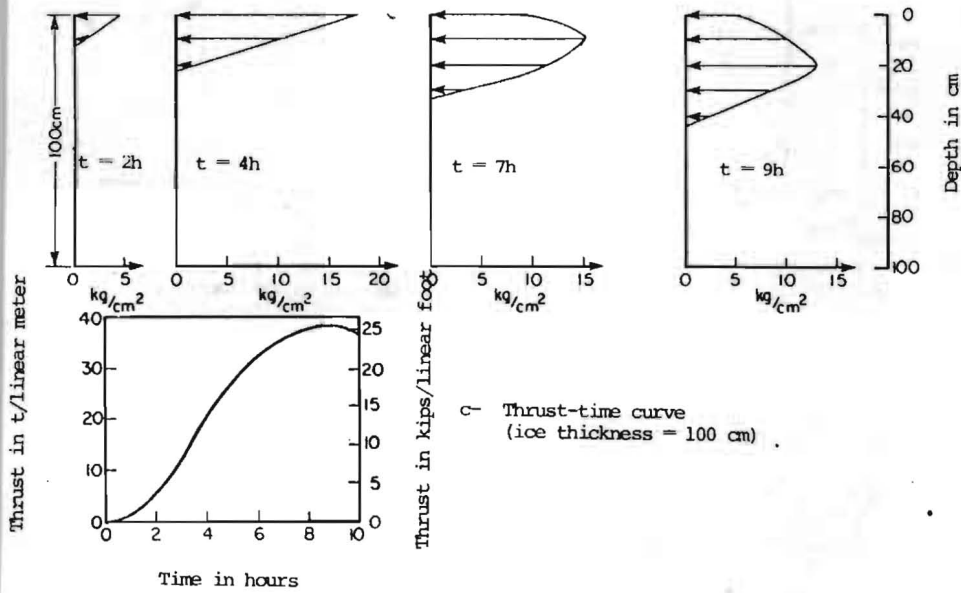


FIGURE 4- TEMPERATURE AND THERMAL PRESSURE DISTRIBUTIONS IN A SNOW ICE COVER FOR A SINUSOIDALLY RISING TEMPERATURE OF THE SURFACE FROM $-40^\circ\text{C} (-\frac{\pi}{2})$ TO $0^\circ\text{C} (+\frac{\pi}{2})$ IN 10 HOURS.



HYDRAULIC CRITERION FOR SUBMERGENCE OF
ICE BLOCKS

M.S. Uzuner, Graduate Research Associate,	Iowa Institute of Hydraulic Research,	Iowa U.S.A.
John F. Kennedy, Director	the University of Iowa,	
	Iowa City;	

SYNOPSIS

The conditions at which buoyant blocks on a stream become unstable and are swept under the downstream floating cover are investigated analytically and experimentally. The theoretical model is based on a one-dimensional analysis of the flow passing under the floating cover and moment equilibrium of the floe. Laboratory experiments to verify the analysis were conducted in a flume using individual blocks with three different specific gravities and ranges of length and thickness. Values for the moment coefficient arising in the analysis were determined from the laboratory data. Satisfactory agreement was found between the analytical model and laboratory and field data.

RESUME

Les auteurs présentent une étude théorique et expérimentale des conditions dans lesquelles des blocs de glace flottant sur un courant d'eau deviennent instables et s'enfoncent en aval sous la couche de glace recouvrant la rivière. Le modèle théorique est basé sur une analyse unidimensionnelle de l'écoulement sous la couche de glace et de l'équation des moments appliquée au bloc de glace flottant en amont. Afin de vérifier l'analyse, des expériences de laboratoire ont été effectuées dans un canal en utilisant des blocs de bois de trois densités différentes et de diverses longueurs et épaisseurs. Les valeurs du coefficient de moment introduit dans l'analyse sont déterminées à partir des mesures effectuées en laboratoire. Les résultats expérimentaux obtenus en laboratoire et in situ concordent d'une manière satisfaisante avec les prédictions théoriques.

INTRODUCTORY REMARKS. Ice blocks which have been transported along a river to the upstream end of a floating ice cover may either come to rest against the cover, causing upstream propagation of the leading end of the fragmented cover, or be submerged by the stream and swept under the cover. In the latter case the floes generally come to rest beneath the floating ice, and an accumulation of many blocks can produce an ice jam which may block the channel sufficiently to cause flooding. Hence it is of interest to ascertain the conditions for incipient submergence of floes arrested against a floating cover by a free-surface flow. The following sections develop an analytical model for incipient submergence of floes, describe laboratory experiments conducted to verify the analysis, and present a comparison of the analytical results with laboratory and field data.

ANALYSIS. In the laboratory investigation, described in the following section, it was observed that right parallelepiped blocks generally are submerged by rotating about the lower, downstream edge, as shown in figure 1, until the stagnation water-surface elevation equals that of the upstream top edge of the block. Thereupon the block becomes unstable and submerges by rotation about point D (see figure 1), a process herein termed underturning.

It is necessary at the outset to find the equilibrium flow depth, $h_d = \bar{h}H$, beneath a cover of thickness t and density ρ' which is at an elevation of vertical-force equilibrium on a flowing stream. The continuity and Bernoulli equations for sections 1 and 3 are, respectively,

$$V_u H = \bar{V}_d h_d \quad (1)$$

and

$$V_u^2/2g + H = \bar{V}_d^2/2g + h_d + (\rho'/\rho)t \quad (2)$$

from which there results

$$\bar{h}^3 + [(\rho'/\rho)(t/H) - F_2^2 - 1] \bar{h}^2 + F_2^2 = 0 \quad (3)$$

where $F_2^2 = V_u^2/2gH$.

The moment balance about point D will now be examined. The pressure, $p(x)$, at any point under the block after it has rotated about D through an angle δ is obtained from the continuity and Bernoulli equations between sections 1 and 2:

$$V_d(x) \cdot h(x) = V_u H \quad (4)$$

and

$$V_u^2/2g + H = V_d^2/2g + (H\bar{h} - x \sin \delta) + p(x)/\rho g \quad (5)$$

The corresponding moment, M_p , about D is given by

$$\frac{M_p}{\rho g H^3} = \frac{1}{\rho g H^3} \int_0^L x \cdot p(x) dx = \frac{L^2}{2H^2} (F_2^2 - \bar{h} + 1) - \frac{F_2^2}{\sin^2 \delta} \left[\ln \frac{\bar{h} - \frac{L}{H} \sin \delta}{\bar{h}} + \frac{\bar{h}}{\bar{h} - \frac{L}{H} \sin \delta} - 1 \right] + \frac{L^3}{3H^3} \sin \delta \quad (6)$$

The moment, M_h , resulting from the increased pressure (due to the lower velocity) along AB and the reduced pressure in the separation zone, BC, will be expressed as

$$M_h / \rho g H^3 = C_m (L^2/H^2) F_2^2 \quad (7)$$

where the coefficient C_m is a function of ρ'/ρ , t/L , and t/H . The final moment to be considered is that due to the weight of the block, M_w , which is given by

$$M_w / \rho g H^3 = (1/2)(\rho'/\rho)(t/H)(L/H)^2(\cos \delta + t/L \sin \delta) \quad (8)$$

At the critical condition for submergence, depicted in figure 1,

$$L \sin \delta_c = t(1 - \rho'/\rho) - (H - t\rho'/\rho - \bar{h}H) - C_s v_u^2/2g \quad (9)$$

where $\sqrt{C_s}$ is the ratio of the maximum (surface) velocity to the mean velocity.

The equation to be solved is

$$M_p - M_h - M_w = 0 \quad (10)$$

where M_p , M_h , and M_w are given by (6), (7), and (8), respectively, \bar{h} is the largest real positive root of (3), and $\delta = \delta_c$ is given by (9). The solution was accomplished on an electronic computer.

EXPERIMENTS. The experiments were conducted in a laboratory flume that is one foot wide, twelve feet long, and two feet deep. Right parallelepiped blocks of three different specific gravities (0.50, 0.67, and 0.87) and two different thicknesses (1.25 in. and 3.81 in.) were used to cover the desired ranges of ρ'/ρ , t/H , and t/L . In each experiment the discharge was increased, with the depth held constant by progressively opening the downstream gate, until the block became unstable and submerged by underturning. Depth, discharge, etc., were measured by standard laboratory techniques.

In the course of the experiments it was found that all blocks, except very short and very long ones, submerged in the manner described above. Determination of incipient instability was dependent to some extent, of course, on the judgment of the experimenter. Most experiments were repeated one or more times, and the reproducibility of the data found to be satisfactory.

RESULTS. Figure 3 presents a typical set of experimental results, together with the corresponding analytical curves. A value of $C_s = 1.3$ was adopted on the basis of float measurements in the flume. For each t/L , the value of C_m selected was that which gives the best overall correspondence between theoretical and experimental results for the whole range of t/H . The agreement between predicted and measured values of F_2 is, on the whole, quite satisfactory. It can be improved by taking into account the dependence of C_m on t/H , and finding the C_m for each t/L , ρ'/ρ , and t/H which gives best experimental-theoretical concurrence. Some tests were also conducted with blocks with lower upstream corners shaped to be a quarter circle with radius equal to block thickness; these experiments were performed to illustrate the importance of the pressure distribution around the upstream end of the block on submergence.

Figure 3 shows the relation between C_m , ρ'/ρ , and t/L determined from figure 2 and similar plots for ρ'/ρ of 0.50 and 0.67. The data were extended by visual extrapolation to $\rho'/\rho = 0.92$, the value for fresh-water ice. As was noted above, for values of t/L less than about 0.1 or greater than about 0.8, submergence was not generally by the overturning mode described by the analysis, but by vertical sinking, sometimes accompanied by rotation.

Figure 4 shows a comparison of field data reported by Pariset, Hausser, and Gagnon [1] and by Mathieu (taken from a publication by Michel [2]) with analytical curves for limiting values of t/L and C_m . The predicted relations are seen neatly to bracket the data, giving further corroboration to the analytical model. The analytical relation of Pariset *et al* [1], also shown in figure 4, is based on a vertical-sinking mode of submergence. It is seen to be nearly coincident with the analytical relation based on overturning for long blocks, which have a relatively small value of δ_c , and hence a submergence mode not too dissimilar from the vertical-sinking mode treated by Pariset *et al* [1].

REFERENCES.

1. Pariset, E., Hausser, R., and Gagnon, A., 1966 "Formation of Ice Covers and Ice Jams in Rivers," *Proc. ASCE, Jour. of Hydr. Div.*, 92, HY6.
2. Michel, B., 1966 "Ice Covers in Rivers," *National Research Council of Canada, Technical Memorandum 92, App. IV(c)*.

ACKNOWLEDGEMENTS. The research reported herein was sponsored by the Army Corps of Engineers, Rock Island Division, under Contract No. DACW25-72-C-00012.

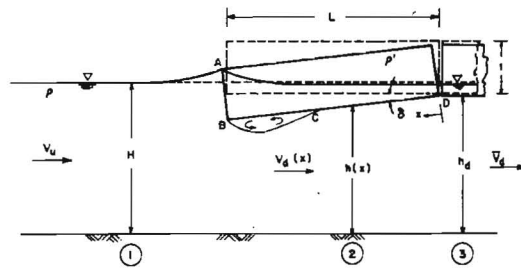


Figure 1 Definition sketch for analysis
Figure explicatrice

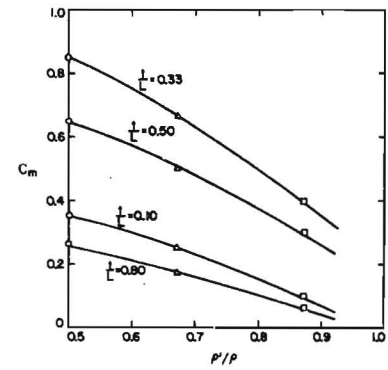


Figure 3 Variation of C_m with ρ'/ρ and t/L
Variation de C_m avec ρ'/ρ et t/L

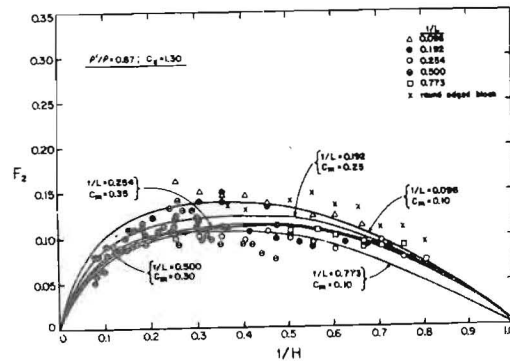


Figure 2 Summary of typical experimental results
Résultats expérimentaux typiques

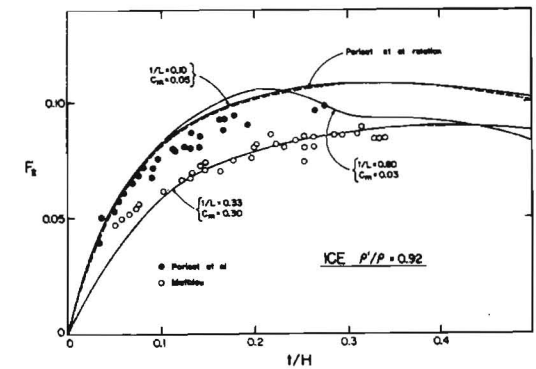


Figure 4 Comparison of analysis and field data
Comparaison des résultats théoriques et en situ



ICE SYMPOSIUM 1972
LENINGRAD

BEHAVIOUR OF WATER-STAGE IN THE RIVER
CLOSED WITH THE ICE COVER

Shin-etsu Kamada

Civil Engineering Research
Institute,
Hokkaido Development Bureau

Sapporo, Hokkaido,
Japan

SYNOPSIS

In this paper, the first discussion is in relation to vertical displacement of an ice layer with which a water surface of the streamflow is wholly covered. The ice layer was assumed to be an elastic plate. Then, it was discussed that the displacement of the ice layer is due to changes of water-stage, snow weight accumulated on the layer, the discharge, thickness of the ice layer, etc. On the other hand, a relation between the discharge and cross section of the streamflow under conditions of whole frozen surface was obtained from the data in the ISHIKARI river. Consequently, a practical formula about a relation between the discharge, the water-stage and the snow weight was led forth. The formula gives many qualitative informations about the water-stage in the river under ice condition, although the formula would be restricted greatly in applications to the actual river. Especially, the water-stage of the river in heavy snow area in winter is changeable even when the discharge is constant.

1. Introduction

Almost every river in winter of a cold climate freezes at the surface near the sides and sometimes on the bottom due to intense radiation from the river bed upward. The surface ice fasted at the side grows towards a center of the river and an ice layer becomes to cover wholly the water surface. A streamflow in such river is loaded with frazil ice, floating ice, such as a pancake ice, and slush. These circumstances make changes of the conditions of the streamflow from them in the same river without ice. Water-stage in a river without ice is connected closely to the discharge. However, even a definition of water-stage in the river covered wholly the water surface with the ice layer is not so clear as in an open channel. When the water-stage in the river covered wholly is defined as water level in a hole of ice layer drilled for measurements, it is considered that the water-stage in the river under conditions of ice would be changed by the discharge, thickness of the ice layer, snow weight accumulated on the ice layer, etc. It is the first step of hydraulic researches for the river in winter of a cold climate that the behaviour of the water-stage are thrown light on. Data used in this paper are obtained in the ISHIKARI river which the river width is 200 meter and the discharge in winter is about 100 - 150 m³/s at the observation site.

2. Vertical Displacement of the Ice Layer

A primary discussion for vertical displacement of the ice layer is to taking into consideration only an equilibrium between buoyancy of the ice layer due to the water-stage, weight of the ice layer and weight of snow accumulated on it. It is necessary for the discussion in further detail to treat the ice layer as an elastic plate. In the following discussions, it will be assumed that the streamflow is covered wholly with the ice layer. Under these conditions, a formula for the displacement of the ice layer was led forth as follows:

$$y = (S - S_0 + \frac{H}{2} - Hd - w) \left\{ A \cos \frac{nx}{\sqrt{2}} \cosh \frac{nx}{\sqrt{2}} + D \sin \frac{nx}{\sqrt{2}} \sinh \frac{nx}{\sqrt{2}} - 1 \right\}$$

$$\text{for } S_0 - S - \frac{H}{2} \leq y \leq S_0 - S + \frac{H}{2} \quad (1)$$

$$\text{where } n = \left[\frac{1 - \nu^2}{EI} \right]^{1/4}$$

y is vertical displacement of a neutral layer of the ice layer,
 x is abscissa which a center of the river width is defined as zero,
 d is density of ice,
 w is snow weight accumulated on the ice layer,
 s_0 is altitude of y at $x=L/2$,
 s is altitude of water-stage,
 L is river width,
 H is thickness of the ice layer,
 E is Young's modulus,
 I is moment of inertia of a cross section of the ice layer,
 ν is Poisson's ratio of ice,
 and A, D are constant determined from n, L and boundary conditions at sides.

A numerical analysis by the Milne method for differential equations may give more valid solutions free from the condition, $s_0 - s - l/2 \leq y \leq s_0 - s + H/2$.

It is indicated by (1) that the displacement except in the vicinity of the sides is nearly independent on elasticities of the ice layer, if a width of the river under consideration is sufficiently large. Therefore, the primary discussion mentioned above is sufficient for investigations of the displacement except in the vicinity of the sides. Then, for a great part of x , (1) becomes as follows:

$$y = Hd + S_0 + W - \beta - \frac{H}{2} \quad (4')$$

In (4'), it is indicated that cross section of the streamflow under the ice layer is controlled by the water-stage, thickness of the ice layer and snow weight accumulated on it. Fig. 1 shows the observed displacements of the ice layer in the ISHIKARI river, Hokkaido, Japan. In fig. 1, values of y on 28 Jan. are taken as temporal zero. Fig. 2 shows precipitation in snow height during the observation. It is seen in fig. 1 that the ice layer displaces downward due to depression of the water-stage and solid precipitation on the ice layer. As the ice layer displaces downward, stresses in the ice layer increase and cracks occur in the vicinity of the sides. These cracks were sometimes observed in the ISHIKARI river. After occurrence of the cracks, A , D and s_0 in (1) will be changed to new values. Fig. 3 shows changes of the cross section, in the same case, which are made by not only the water-stage but solid precipitation on the ice layer. It is easy to be recognized that deviations of observed data from a linear line in fig. 3 are due to the solid precipitation.

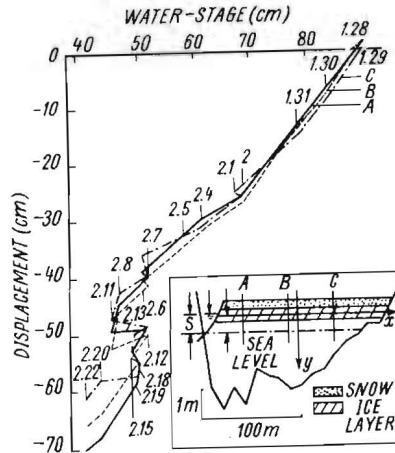


FIGURE 1. DISPLACEMENT OF ICE LAYER IN THE ISHIKARI RIVER, '68'

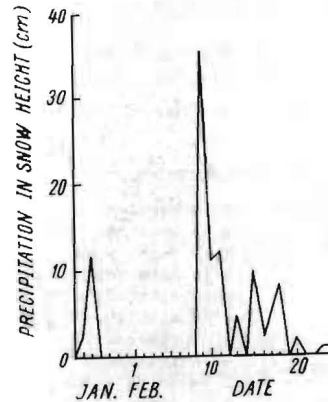


FIGURE 2. PRECIPITATION DURING THE OBSERVATIONS

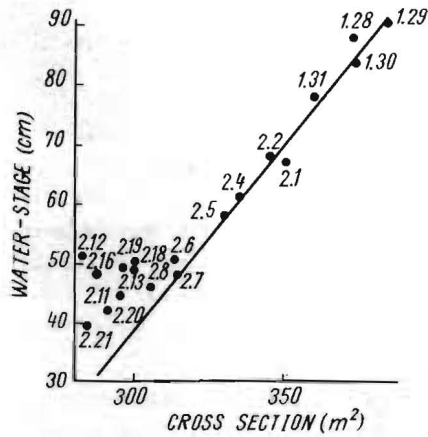


FIGURE 3. WATER-STAGE AND CROSS SECTION IN THE ISHIKARI RIVER, '68

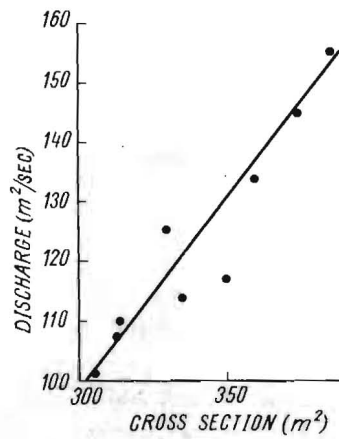


FIGURE 4. DISCHARGE AND CROSS SECTION IN THE ISHIKARI RIVER, '68

3. Discharge and Water-Stage in the River closed with the Ice Cover

A relation between the cross section and the discharge will be discussed before investigations for a relation between the discharge and the water-stage. In strict sense, the relation between the cross section and the discharge is considered not to be linear and depends on hydraulic roughness of the ice surface, hydraulic gradient, frazil ice loaded in the streamflow, boundary conditions of the ice layer at the sides, shape of the cross section, etc. However, since change of discharge of a river in winter of a cold area is small generally, this relation may be regarded as to be linear at a given site of the river with practical accuracy. Fig. 4 shows a relation between the discharge and the cross section in the ISHIKARI river. Data in fig. 4 exhibit a good linearity. Thus, the following formula is obtained:

$$\Delta A \propto \Delta Q \quad (2)$$

where Q is discharge and A is cross section of the streamflow.

And, with (1'),

$$\Delta \left(y - \frac{H}{2} \right) \propto \Delta Q \quad (3)$$

$$\Delta W - \Delta \beta + \Delta H \cdot d = F \cdot \Delta Q \quad (4)$$

F in (4) is dependent usually on hydraulic roughness of the ice surface, hydraulic gradient, frazil ice in the streamflow, shape of the cross section, etc, but not on H. In practical applications, it may be assumed for a short period that F is constant. After all, the water-stage of the river closed wholly with the ice layer is controlled by the snow weight, thickness of the ice layer and the discharge even with an assumption $F = \text{const.}$. The water-stage in the river with the ice cover is changeable due to the snow weight and thickness of the ice layer under condition of $Q = \text{const.}$ A more usefull relation between the water-stage, the snow weight, the discharge and thickness of the ice layer are obtained by integrating (4), but the integration of (4) for an actual river would be impossible.

4. Conclusions

The formula led forth above in relation to the discharge, the water-stage, the snow weight on the ice layer and thickness of the ice layer would be restricted greatly in applications to an actual river under conditions of ice. In suite of this circumstance, it gives many qualitative informations about the water-stage of the river in winter of a cold area. Especially, it should be noticed that the water-stage of river in heavy snow area in winter is changeable under the condition of $Q = \text{const.}$ and the water-stage of the river with the ice cover is distinguished in physical meanings from it in an open channel.



ICE SYMPOSIUM 1972
LENINGRAD

SPECIFIC FEATURES OF ICE JAM FORMATION
AT THE END OF THE BACKWATER CURVE.
SOME QUANTITATIVE REGULARITIES.

V.I. Sinotin, M. Sc. (Eng.) River and Reservoir Winter Leningrad, U.S.S.R.
Regime Laboratory, Head,
the B.E. Vedenev All-Union
Research Institute of Hyd-
raulic Engineering

SYNOPSIS

The problem is considered of ice jam formation at the end of the reservoir backwater curve due to submergence of ice floes under the edge of the stationary ice cover. Proceeding from a previously established law of ice floe submergence and experimental data, the feasibility is substantiated of studying the above phenomena using wind-tunnel models. Experimental findings are presented resulting in a quantitative evaluation-to a first approximation - of ice jam formation mechanism.

RESUME

On analyse le processus de la formation des embâcles dans la zone d'affleurement de la courbe de remous des retenues, ces embâcles étant imputables aux glaçons plongeant sous le bord de la glace continue. C'est sur la base de la loi du mouvement des glaçons plongeants établie auparavant et des résultats expérimentaux que l'auteur justifie la possibilité d'étudier ce phénomène sur les modèles aérodynamiques. Les résultats des expériences qui en première approximation permettent d'évaluer quantitativement le processus de la formation des embâcles sont donnés.

Ice jam formation in rivers is due to a combination of certain factors, the most important being presence of large ice masses during the break-up, and obstructions preventing them from moving downstream. As most representative examples of such conditions can be cited those to be encountered at locations with abrupt changes in river bottom slope, e.g. at the end of the backwater curve or at the river mouth where the river falls either into the sea, or a lake.

Experimental research into ice jams is known to be hampered by insurmountable obstacles involved in modelling them accurately. The absolute majority of studies in this field is devoted to analysing the hydraulic conditions of movement of ice and its impact against an obstruction. However, even these simplified investigations failed to produce quantitative relationships to be used in practice, which can be attributed to the necessity of conducting labour consuming experiments for a wide range of parameter variation.

Our previous hydraulic model studies^{1/} showed the ice floe submergence conditions to be described by the relationship

$$V_{cr} = \sqrt{0.035 g l} \quad (1)$$

correlating the submergence velocity and the ice floe length. The reservoir can hold only a definite quantity of ice due to reservoir storage, the approximately similar dimensions of ice floes, and a steady velocity at the end of the backwater curve. Evaluation of the ice accumulating capacity of the reservoir is of interest in ice jam control.

By analysing the peculiarities of ice jam simulation on hydraulic models (neglecting ice strength and temperature effects) a conclusion can be drawn on the feasibility of applying wind-tunnel models, which presents certain advantages in widening the investigation scope. Such models are known to have been successfully utilized in studying sediment movement, flow under an ice cover, etc. The application of a wind-tunnel model to the case in hand is connected with using the force of gravity instead of the Archimede's buoyant force which necessitates rotating the river reach model considered by 180° along the longitudinal axis. The volume weight of the material simulating the ice floes is independent of the model scale, the movement of ice floes made of materials characterized by different volume weight γ depending on the choice of a corresponding speed, with an identical relative variation at each cross-section.

^{1/} Sinotin V.I., Guenkin Z.A., Etude de plongement des glaçons sous un obstacle. - IAHR Symposium Ice and its Action on Hydraulic Structures, Reykjavik, Iceland, 1970.

The validity of such models for studying the phenomena in question is proved by a definite relationship $V_{cr} = f(l)$ holding true for the motion of plates made of the same material but of different dimensions. When scaled up according to the laws of similitude described in Ref. 2 the experimental data display a fair agreement with prototype velocities.

The experimental rig is a 5.00 m long, 0.65 m wide wind-tunnel with a horizontal bottom representing the free surface, the channel depth being 0.10 m, with a smooth expansion starting 2.5 m from the intake at an angle 12° .

At the section with an abrupt change in the river bottom slope, a bottom projection simulates the ice cover. The wind-tunnel equipment and instrumentation are those commonly used in aerodynamic experiments. Foam plastics with $\gamma_1 = 3.0 \text{ kg/m}^3$ and $\gamma_2 = 11 \text{ kg/m}^3$ are employed to model ice floes. $5 \times 5 \times 1 \text{ cm}$ plates with γ_1 are used in the main test runs.

The experimental findings substantiate the assumption that ice floes of given dimensions form a corresponding ice jam body described by constant parameters W_{cr}, l_{cr}, h_{cr} (Fig. 1, 2) (W_{cr} takes into account that the plates are loosely compacted) for $V_0 = V_{cr}$. Definite relations may be obtained of W_{cr}, l_{cr}, h_{cr} as a function of V_{cr} . After stabilization of the ice jam body the foam plastics plates fed into the wind-tunnel fall beyond its limits. For the prototype this corresponds to the moment when the water stage rises above the ice jam elevation, and the decreasing velocities make for the growth of the ice jam in the upstream direction.

In case the velocity in the control cross-section (at an abrupt change in river bottom slope) exceeds the critical, the ice jam parameters are experimentally shown to differ from the critical ones (certain parameter values corresponding to $V > V_{cr}$) and to grow with the velocity. The relations illustrated in Fig. 3 may be obtained if the critical parameters are taken as initial ones and their relative increase is plotted against the relative velocity increase. The curves are drawn from the test run data with $l/h_0 = 0.50$, and $\gamma = 3$ or 11 kg/m^3 , the latter circumstance, as stated, previously, does not affect the general experimental results.

Using the above relations one can determine the total volume of the ice jam body in the reservoir, and its volume at different jam formation stages. The limit length of submerged ice floes can be established knowing the velocity at the end of the backwater curve. The ice jam body volume corresponding to a given ice floe length can be determined from Fig. 2. Ice floes of larger dimensions will be arrested forming a one-layer jam. A particular velocity usually

^{2/} Averkiev A.G., Research methods for studying open surface flows on pressure models. - Gosenergoizdat, Leningrad, 1957.

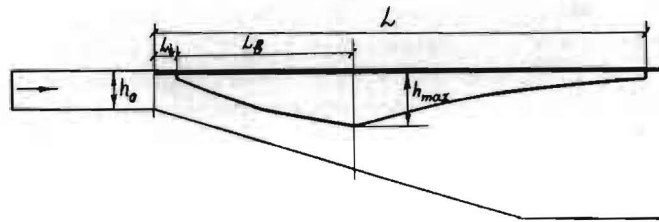


Fig. 1.

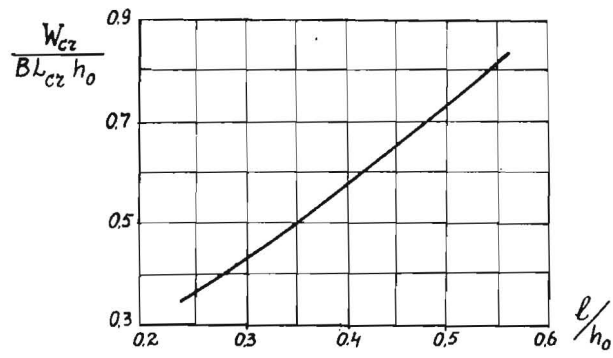


Fig. 2.

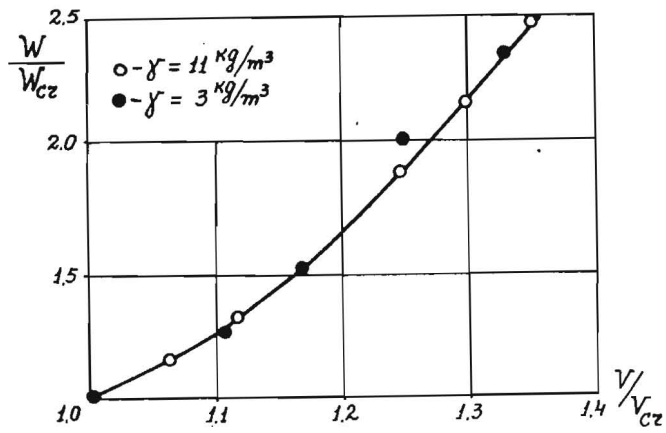


Fig. 3.

prevailing along a reach, submergence conditions will remain practically stable, the larger ice floes will eventually break due to ice pressure and adhere to the ice jam.

V_{cr} can be evaluated from Eqn (1), W_{cr} from the curve in Fig. 2, given the predominant ice floe dimensions ^{3/}. Then, from V/V_{cr} and Fig. 3, W/W_{cr} can be found, i.e. W (model ice compaction being different from that of the prototype, the net ice volume is to be determined by introducing the natural porosity coefficient).

Based on the studies conducted, relations were obtained between different parameters permitting their evaluation during ice jam formation provided a time history graph of ice motion towards the jam is available. The method for determining the parameters of such ice jams is undoubtedly approximate. Nevertheless it yields quite definite characteristics, and may be used in the first approximation for the evaluation of ice jam formation mechanisms.

^{3/} Koren'kov V.U., Prototype observation data on ice passage through the structures of the Krasnoyarsk power plant. - Gidrotekhnicheskoye stroitel'stvo, N 7, 1970.



ICE SYMPOSIUM 1972
LENINGRAD

ON WIND DRIFT OF ICE FLOES

Korzavin K.N., Head of Chair	The Institute of Railroad	Novosibirsk
D. Sc. (Eng.)	Transportation Engineers	U.S.S.R.

SYNOPSIS

When estimating ice pressure against hydraulic structures the action of large ice floes drifting in the reservoir should be taken into account. The drift velocity is known to be generally proportional to the calculated wind velocity but the wind factor is not yet evaluated exactly.

The paper analyses the conditions of ice floe motion in the reservoir and describes the technique of drift velocity prediction using the data on the roughness of the ice surface and on the percentage of the ice-covered surface of the reservoir.

RESUME

En évaluant la valeur de la pression de glace sur l'ouvrage il faut tenir compte de l'action d'un grand champ de glace en dérive dans la retenue. Il est bien connu que la vitesse de dérive est proportionnelle à la vitesse calculée du vent, mais la valeur du facteur de vent n'est pas encore bien déterminée.

Le rapport analyse les conditions du mouvement d'un champ de glace dans l'écoulement et décrit une méthode qui permet de prévoir la vitesse de dérive en fonction des conditions locales - le pourcentage de la surface de retenue couverte de glace et la rugosité de celle-ci.

STATE OF THE PROBLEM

When estimating the ice pressure against bridge piers or hydraulic structures the action of large ice floes drifting in the reservoir should be taken into consideration.

According to the published data available [1,2] the steady motion velocity of ice floes (V) is generally proportional to the calculated wind velocity (W) and described by the formula

$$V = \alpha W \quad (1)$$

in which α is the so-called wind factor.

The investigations carried out by Shuleikin, Zubov, Gordienko, Vlasov et al. for both sea and river conditions yielded widely varying values of the wind factor (i.e. from 0,02 to 0,10) depending on the roughness of ice floes, character of hummocks, reservoir depth and the percentage of ice-covered surface of the reservoir. A possible explanation to the fact may be that many investigators seem to proceed from separate field observations and do not analyse the physics of the phenomenon adequately.

STRUCTURE OF THE CALCULATING FORMULA

The wind factor may be determined by the analysis of the physics of the phenomenon under study.

Consider an ice floe drifting in a lake or a reservoir in which the currents may be neglected. The wind acting on a rough surface of an ice floe can impart some velocity to it. This velocity is constant when the force transmitted from the wind to the floe is equal to the force of the water flow resistance to the ice motion.

It is known that the wind force transmitted to the ice floe is determined by the formula

$$P = C_w \rho_w W^2 \Omega \quad (2)$$

where C_w is the resistance coefficient, ρ_w = the air density, Ω = the surface area of a floe and W = the wind velocity.

On the other hand, the resistance force is equal to

$$R = f \Omega V^2 \quad (3)$$

with f designating the coefficient of the total resistance of water to the ice floe motion.

For the case of uniform steady motion

$$P = R, \quad (4)$$

hence

$$V = \sqrt{\frac{C_w \rho_w}{f}} W \quad (5)$$

and

$$Q = \sqrt{\frac{C_w \rho_w}{f}} \quad (6)$$

Thus the wind factor is dependent upon the correlation between the wind flow friction across a rough floe surface and resistance of water to ice drift.

PRACTICAL CONCLUSIONS

As the first approximation the drift velocity of an ice floe can be obtained from Eq.(5) on the basis of the following assumptions:

1. According to the considerations reported in [3,4] the coefficient of total water resistance (f) to the ice floe drift is approximated by the equation

$$f = \frac{\rho}{2} \left[1.89 + 1.65 \lg \left(\frac{x}{\epsilon} \right) \right]^{-2.5} + \frac{0.045 h}{x} \quad (7)$$

where x, h = ice floe length and thickness, respectively; ϵ = height parameter of roughness.

2. The product ($C_w \rho_w$) is taken equal to $2 \cdot 10^{-6} \text{ t sec}^2/\text{m}^4$

3. Compacted ice is expected to drift at a lower velocity, therefore the calculating formula is to involve the factor (z), whose value is less than unity. Then Eq.(5) becomes

$$V = z \sqrt{\frac{C_w \rho_w}{f}} W \quad (8)$$

4. According to Soviet experience the recommended value of the factor (z) is 0.50-0.70 with the 75-50% ice-covered surface of the reservoir.

In conclusion it is of importance to note a need for more field observations.

REFERENCES

1. N.N. Lubov, Arctic ice M., Glávsevmorput', 1945.
2. K.N. Korzhavin, A.D. Reshta, On wind drift of ice floes. Trudy Instituta Inzhenerov Zheleznodozhnogo Transporta, vyp.124, Novosibirsk, 1971.
3. K.N. Korzhavin, Ice action on engineering structures, Izd. AN SSSR, Novosibirsk, 1962.
4. G. Shlikhting, The Theory of the Boundary Layer, Moscow, 1956.



OBSERVATIONS ON THERMAL CRACKS IN LAKE ICE

S. S. Lazier, Professor of Civil Engineering, Queen's University at Kingston,
Ontario, Canada

M. Metge, Research Assistant, Queen's University at Kingston, Ontario, Canada

SYNOPSIS

Three main types of cracks due to thermal contraction in lake ice are defined: wide cracks, narrow wet cracks, narrow dry cracks. The formation and behaviour of these various cracks is described. Wide cracks have been observed to produce a violent impact when they close and this could be a hazard to structures which are sensitive to impact loading.

RESUME

On définit trois principaux types de fissures dues à la contraction thermique de la glace de lac: Fissures larges, fissures étroites mouillées, fissures étroites sèches. On décrit la formation et le comportement de ces différentes fissures.

On a observé que les fissures larges produisent un impact violent quand elles se ferment et cela pourrait être un danger pour des constructions sensibles à l'impact.

1. INTRODUCTION

The static thrust which an ice sheet may exert on hydraulic and extended structures due to changes in the temperature of the sheet is a hazard for which reliable and realistic design figures are not yet available.

The occurrence of thermal thrust is explained by most experts as follows: tension cracks form in the ice sheet during a cold period, these cracks fill up with water which freezes, thus increasing the dimensions of the sheet; a subsequent rise in temperature causes the ice to expand and exert a thrust at its boundaries. This paper reports the authors' investigation of this process and their field observations of the formation and behaviour of thermal cracks in a fresh water ice sheet.

Over the past three winters visual observations of thermal cracks have been made in Kingston harbour, Ontario, Canada. As well the movements across the cracks and across thermally induced pressure ridges have been recorded, along with other pertinent parameters such as temperature, solar radiation, etc. Samples of typical cracks were cut from the ice sheet and thin sections were examined under polarized light. The frequency of crack formation was studied by implanting geophones into the ice.

2. TYPES OF THERMAL CRACKS

Close examination of individual cracks revealed that different kinds of cracks exist and each one behaves quite differently. The authors propose to divide them into three main types:

- i) Wide cracks: more than 10 cm in width, extending to the bottom of the ice sheet
- ii) Narrow dry cracks: less than 2 cm in width, empty
- iii) Narrow wet cracks: less than 10 cm in width, filled with water or fine grained ice.

2.1 WIDE CRACKS

Wide cracks occur when the amount of contraction of the ice cover is very large, i.e. during very cold nights if there is no snow cover on the ice. At first many narrow cracks form, but with a succeeding drop in temperature some of these cracks open to the bottom and become lines of weakness in the sheet. Further contraction is concentrated at these cracks and the authors have observed such cracks to be as wide as 20 cm. The large volume of water in this type of crack cannot freeze completely during the night and as a result by morning a typical wide crack has taken the shape shown in figure 1. Several cracks of this type were observed during the winter of 1972.

If, during the next day, the ice temperature rises, the thin bridge

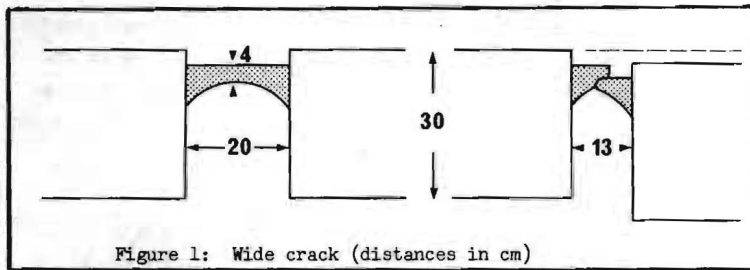


Figure 1: Wide crack (distances in cm)

of ice across the crack is put in compression and suddenly fails. The closure of these cracks produces a loud noise and a violent impact. Indeed, in one case the shock was sufficiently violent to shift the field office, a trailer, mounted on a rubble mound breakwater, several centimeters. This experience agrees with observations elsewhere as reported by (1) and (2) who recorded shocks at seismic stations located near frozen lakes, which could only be attributed to cracking of ice.

Figure 2 shows typical experimental results associated with wide cracks. The frequency of cracking, movement across the crack and air temperature are plotted against time for a fifteen hour period, and a sample of the geophone output is shown.

It will be noted that maximum cracking activity occurred while the temperature was rising and the ice sheet was expanding. There were two sudden shifts, one at about 0930 hours and the other at about 1130. The event at 0930 hours corresponds to a large signal on the geophone trace which indicated a substantial impact. This type of occurrence could be a hazard to structures which are sensitive to impact loading, such as lightly constructed

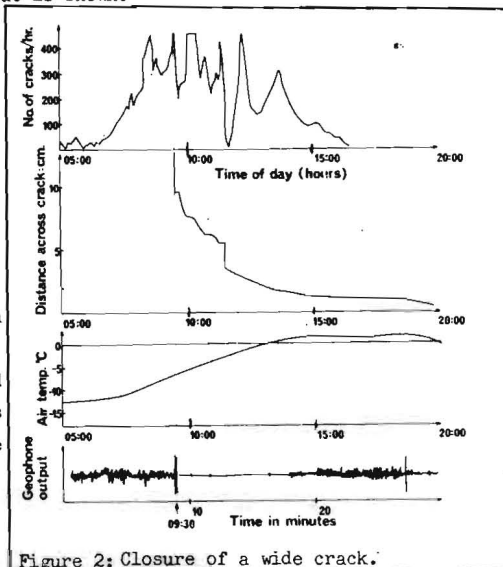


Figure 2: Closure of a wide crack.

extended structures or even arch dams. To the authors' knowledge such a hazard has not been recognized before.

As noted in (2) wide cracks remain as lines of weakness even after they have closed and may develop into pressure ridges if the ice is not too thick. The authors feel that this process starts when the two faces of the crack become misaligned, after failure, as shown in figure 1. Subsequently, expansion may force one side of the crack to push under the other, thus creating a pressure ridge.

Figure 3 shows the large movements which occurred across a pressure ridge at the authors' field station in 1971.

2.2. NARROW CRACKS

The theory of the formation of narrow cracks by bending, due to differential heating of the ice cover, has been investigated (3). This theory may be summarized as follows: During a cold night, the top of the ice cools, while the bottom remains at 0°C . This causes the ice cover to curve upwards (like a bimetallic strip) until the moment due to the weight of the edges is so large that the sheet cracks.

Part of this theory allows the spacing of narrow cracks and their width to be calculated; knowing the surface temperature and the thickness of the ice. An example given in (3) shows that for an ice thickness of 30 cm and a surface temperature of -9°C , the spacing of the cracks should be 22 metres and at -3.5°C the spacing should be 25 metres, whilst the crack width should be about 0.6 cm. The authors observed, in 1972, narrow cracks which formed at intervals of about 25 to 30 metres when the ice was about 35 cm thick and at about the same temperature range as above. The average crack width was observed to be about 0.5 cm. It is interesting to note that a theory which assumes ice to be perfectly elastic gives such a good description of the cracking process.

2.2.a NARROW DRY CRACKS

Cracks formed in the manner described above often do not fill with water because the crack is not propagated to the bottom of the ice sheet. Figure 4 shows the appearance of such a crack taken from field observation in 1972. The presence of the shear planes at the bottom indicates that the under-

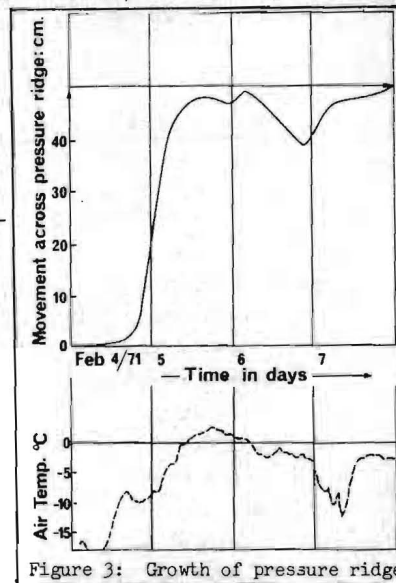


Figure 3: Growth of pressure ridge

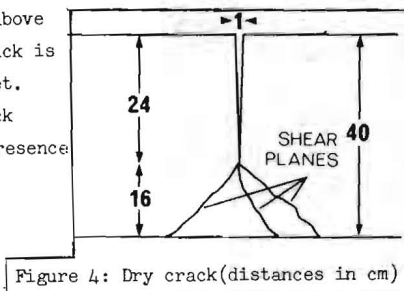


Figure 4: Dry crack (distances in cm)

side of the ice sheet must have been in compression at some time. This may explain the curious phenomenon reported by several observers that ice seems to push toward shore during a drop in temperature. In figure 3 it may be seen that at midnight on 5 February and again on 6 February, while the air temperature was falling, the two sides of the ridge were pushing towards each other. This is an example of "ice push" during a drop in temperature. Providing that the crack stays dry, it will close up when the temperature rises and little thrust will be exerted. Figure 5 shows the history of such a crack and it may be seen that the crack opened and closed in a series of small steps, not instantaneously.

2.2.b. NARROW WET CRACKS

If a narrow crack fills up with water either because the sheet contracts further or because there are no constraints at its boundaries, a narrow wet crack is formed. The water that enters the crack freezes very quickly, losing its heat to the surrounding ice. Figure 6 shows a thin section of such a crack seen through crossed polarisers.

It seems that because of its crystalline structure, this ice wedge withstands the compression due to a rise in temperature during the next day. However it fails in tension during the next night. In this way the ice sheet is progressively lengthened in the classical manner. In the Kingston area, narrow wet cracks seem to occur

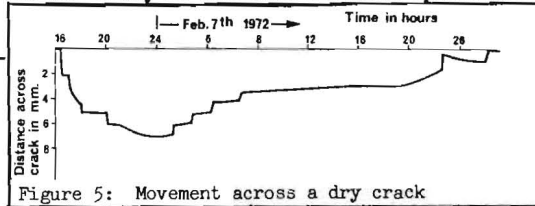


Figure 5: Movement across a dry crack



Figure 6: Thin section of a narrow wet crack

only when the ice is relatively thin, i.e. less than 30 cm.

3. THERMAL CRACKS AND PRESSURE RIDGES

Detailed observations of the movements across thermally induced pressure ridges were made during the winters of 1971 and 1972, and these exhibited the same pattern. Pressure ridges started to form immediately after freeze-up, and at the same time narrow wet cracks were observed everywhere. The movement across the ridges was substantial, up to 50 cm in 12 hours, as shown in figure 3. Then during a thaw, the pressure ridges strengthened and "healed", and, after that, little movement was recorded. The only cracks that were observed to form after the "healing" of the pressure ridges were narrow dry cracks.

It could be postulated that narrow wet cracks and pressure ridges are interdependent phenomena. Pressure ridges relieve the restraint of the ice sheet and thus allow numerous wet cracks to form; in turn, this causes considerable lateral expansion of the sheet and consequently the pressure ridges grow. However, if there are no pressure ridges the ice sheet is constrained and the narrow cracks do not fill up with water and there is little lateral expansion.

Perhaps the interdependence of narrow wet cracks and pressure ridges, as observed by the authors, is a special case. However, if the hypothesis is correct, generally, it would mean that in thick ice sheets where pressure ridges cannot form, the lateral expansion of the sheet may not be great enough to cause significant forces.

4. CONCLUSIONS

The authors' observations and some analysis of past work lead to the following conclusions:

1. The sudden failure at a wide crack during a rise in temperature may produce a large impact load on hydraulic and extended structures.
2. Pressure ridges start to form at wide cracks due to misalignment after closure.
3. The maximum potential for lateral expansion is likely to occur when the ice sheet is relatively thin and free from snow, such that narrow wet thermal cracks form.
4. Narrow wet thermal cracks and pressure ridges appear to be interdependent phenomena.
5. It would appear that "ice push" can occur when the air temperature is dropping.

The authors wish to acknowledge the encouragement of Dr. L. W. Gold and Dr. R. O. Ramseier and the support of the National Research Council of Canada for this work.

REFERENCES

- (1) "Observations about Ice-Shocks on Lake Saaksjarvi"
U-Luosto and P. Saastamoinen, *Geophysica* 9:1, Helsinki 1964.
- (2) "Ice Tremors Generated in the Floating Lake Ice"
By S. Omote, Y. Yamazaki, N. Kobayashi and S. Murauchi.
Bulletin of the Earthquake Research Institute - Vol. 33, pp. 663-679, 1955.
- (3) "A Study of Ice on Inland Lake"
By J. T. Wilson, J. H. Zumberge, E. W. Marshall.
Sipre report No. 5 - part I - 1954.



ICE-DAM STUDIES ON MODELS

Prof. B.V. Proskuryakov State Hydrological Leningrad
V.P. Berdennikov Institute U.S.S.R.

SYNOPSIS

The report considers the modelling of the most typical for rivers of the U.S.S.R. ice-dams, which are formed during the destruction of ice-cover and while ice-reefing and ice push create accumulation of ice on river banks and in river channels. Indicators of mechanical similarity are proposed that enable modelling of ice-dams of this type. Main requirements to materials for ice-dam modelling are formulated and an example of application of this material (ice substitute) is given. In particular, one of the initial problems of ice-dam studies, i.e. evaluation of strength of ice in ice-dams under natural conditions, is solved.

RESUME

Dans le rapport sont exposées les études sur les modèles d'un type d'embâcle de glace le plus fréquent sur les rivières U.R.S.S. qui est formé pendant la destruction de la couverture de glace, quand les crêtes de compression de glace créent l'accumulation des masses de glace sur les rives et le lit de la rivière. On propose une série des indicateurs de la similitude mécanique, qui fait possible les études des embâcles de ce type sur les modèles. Les exigences principaux pour les matériaux des modèles sont formulées et l'application de ces matériaux le substitut de glace - est exposée. En particulier le problème initial de la recherche du phénomène d'embâcle, c'est-à-dire l'évaluation de la stabilité d'embâcle dans les conditions naturelles est posée.

Ice-dams in rivers are formed sometimes by drifting of separate ice floes under the ice cover and their accumulation there. In other cases they are formed during the destruction of the whole ice cover when ice-reefing and ice push contribute to the accumulation of ice masses at some stretch of the river. The first type of ice-dams has been studied in models by B. Michel, E. Pariset, H. Kivisild and others. The present report deals with the problems of modelling of the second type of ice-dams, which are called hummock ice-dams.

The initial principle for establishment of mechanical similarity is that the ratio of temporary material resistance of the model and that of the modelled object must be equal to the ratio of geometrical dimensions of both, as well as equal to the ratio of the elastic moduli of materials of the model and of the object *). In accordance with this principle, for the modelling of the destruction of ice cover on a large river it would be necessary to have either a model of a very large scale, or a very soft ice, which is unfeasible.

In one of the previous papers **) the following additional indicator of mechanical similarity was stated:

$$\frac{m_g \cdot m_h}{m_e^2 \cdot m_\gamma} = 1 \quad (1)$$

where m_g is the scale coefficient of temporary resistance, m_h - scale coefficient of vertical dimensions, m_e - is the same of horizontal dimensions and m_γ is the same of volumetric weight of the underlying medium.

The use of equation (1) greatly facilitates the development of a model with the scale acceptable within a laboratory. Nevertheless, one should bear in mind that the ratio of temporary resistances of the model and of the object must be 1:1000 or 1:100. The above-mentioned paper solves the problem of selection of the required model material.

The examination of force conditions of the hummock ice-dams leads to the separation of two subtypes, characterized by the absence or presence of contact between ice masses and river banks. In the first case, for the increase of tension of ice-dam ($d\sigma$) at the length (X), the following equation is valid.

$$d\sigma = \frac{\alpha \gamma^2}{h} \cdot dx \quad (2)$$

*) Lavrov V.V. Deformatsia i prochnost lda (Deformation and strength of ice). Gidrometeoizdat, Leningrad, 1969.

**) Proskuryakov B.V., Berdennikov V.P. Metody modelnogo issledovaniya rasrusheniya ledianogo pokrova. (Methods for the studying of ice-cover destruction on models) Trudy G.G.I., v.192, 1971.

In the second case the equation is as follows:

$$d\sigma = \left(\frac{\alpha v^2}{h} - 2 \frac{\sigma \xi \lambda}{B} \right) dx \quad (3)$$

Where α is the coefficient of ice-water friction, v - stream velocity, h - thickness of ice-dam, B - river width, ξ - coefficient of lateral pressure, λ - coefficient of friction of ice along the banks.

On the basis of equations (2) and (3) it is easy to derive indicators of similarity for both subtypes of ice-dams:

$$\frac{m_\sigma \cdot m_h}{m_\alpha \cdot m_v^2 \cdot m_e} = 1 \quad (4)$$

$$\frac{m_\sigma \cdot m_h \cdot m_\xi \cdot m_\lambda}{m_\alpha \cdot m_v^2 \cdot m_e} = 1 \quad (5)$$

Where m_α is the scale coefficient of friction at the "ice-water" boundary, m_v - the scale coefficient of stream velocity, m_ξ - the scale coefficient of lateral pressure and λ is the scale coefficient of friction of ice against river banks.

The study of hummock ice-dams on models becomes practicable when the scale coefficients (all but one) are known for one of the similarity indicators (1), (4), (5). Among them m_e is most difficult for determination. Therefore, to solve the problem of strength characteristics of ice, it is necessary to use the complex method, combining studies on models and field studies.

In field conditions, when an ice floe is piled up along the river bank it usually crushes all along the bank line. The authors determined the distance (l_n) between the crack plane and the river bank, and ice thickness (h_n) as well on the Sukhona river at the beginning of ice-dam formation in 1970. Experiments of destruction of ice floe made of model material (substitute of ice), were carried out and the values of distance (l_m) and thickness (h_m) were obtained.

Thus, the scale coefficients $m_e = \frac{l_m}{l_n}$ and $m_h = \frac{h_m}{h_n}$ were also determined from these measurements. The scale coefficient for field conditions and for modelling is the same and equals $m_y = 1$.

Substituting the known values of scale coefficients in equation (1), the authors determined M_G .

It should be noted that temporary resistance of model material (σ_m) is easily determined by experiment and, consequently, according to $M_G = \sigma_m / \sigma_n$ the temporary resistance σ_n for field conditions may be found. At the beginning of ice-dam formation on the Sukhona river in 1970 the obtained value of σ_n was equal to 13 ton/m².

C o n c l u s i o n s

1. The possibility of studies of hummock ice-dams on models has been demonstrated and preliminary experiments carried out.
2. Similarity indicator for two subtypes of hummock ice-dams was proposed: for the case of the absence of contact of ice with river-banks (2) and for the case of contact of ice with river-banks (3).
3. An example of studies on models for the determination of temporary resistance of ice during ice-dam formation is demonstrated. For the ice on Sukhona river was found to be equal to 13 ton/m².



ICE FLOES VELOCITIES IN THE ST.LAWRENCE
RIVER FROM OBLIQUE PICTURES

Marc Drouin, Research Associate	Université Laval	Québec, Canada
Laurent Simard, Engineer	St.Lawrence Ship Channel	Montréal, Canada
Bernard Michel, Dr. Eng. Professor of Ice Mechanics	Université Laval	Québec, Canada

SYNOPSIS

For several years, the St.Lawrence Ship Channel has been conducting ice observations on the St.Lawrence River, the purpose of which, in the early years, was to alleviate the dangers of inundations, always a menace in the periods of thaw. In the last few years, in a burst of energy, further aroused by the promotion of winter navigation, the same organization, with the collaboration of the Ice Mechanics Laboratory personnel of Laval University has carried out a number of studies purposely designed to better understand the principles governing the formation and regime of the St.Lawrence River ice as well as its physical properties. Studies started in 1970 on the movements of ice floes in tidal reaches. Furthermore, a new programme to determine the ice regime of the St.Lawrence River, between Trois-Rivieres and Quebec City was originated in 1972. This paper is intended to elaborate on the technique used to measure ice floe velocities from the Pierre Laporte and Laviolette bridges, respectively located in Quebec City and Trois-Rivieres. Figure 1

RESUME

Depuis plusieurs années, le Chenal Maritime du Saint-Laurent procède à des relevés concernant l'état de la glace du Saint-Laurent dont le but premier était, initialement, de prévenir les dangers d'inondations. Au cours des ans, ce programme fut sensiblement élargi du fait de l'augmentation considérable de la navigation d'hiver. Avec la collaboration du personnel du Laboratoire de Mécanique des Glaces de l'Université Laval, une étude systématique fut alors entreprise sur la formation le régime et les propriétés mécaniques de la glace du Saint-Laurent. Les mesures ayant trait au mouvement des glaçons dans la zone de marée comprise entre Trois-Rivières et l'Île d'Orléans ont débuté en 1970. Ce programme est maintenant poursuivi par des relevés dont le but est de déterminer le régime des glaces du Saint-Laurent entre Trois-Rivières et Québec. Le texte présente les grandes lignes de la méthode utilisée pour mesurer les vitesses des glaçons observés depuis les ponts Pierre Laporte et Laviolette respectivement situés à Québec et Trois-Rivières. Figure 1

INTRODUCTION

Evacuation rate of drifting ice could be obtained in several different ways, of which some are: by transits conveniently located on the shore, from aerial photographs taken from a helicopter or an airplane and from a camera fixed on a bridge from which two oblique photographs can be taken at a known interval of time. For this study, the latter method has been selected for obvious reasons, of which, practically, reliability and economy were given most important consideration. Furthermore, this method is extremely accurate as the stations are fixed throughout the winter and the interpretation is made on as many ice floes as desired because the survey can be done without frequent interruptions due to bad weather.

INSTALLATION AND PROCEDURE

Permanent steel plates were fastened horizontally to the bridge structure by means of U-bolts (figure 2a). A wooden cover fixed to the steel plate can swing around its hinges, thus keeping the working surface free of ice and snow. A 35 mm Nikon camera was fixed permanently on a portable support of steel construction, the base of which could perfectly mate the horizontal steel plate secured to the bridge structure (figure 2b). Accurate mating of both plates was assured by dowel pins. The shooting angle of the camera was pre-adjusted with the aid of a simple rotating plate hinged to the portable support, and locked in place with wing nuts. The operating methods was as follows: after walking to each station (three on the Pierre Laporte bridge and two on the Laviolette bridge, refer to figure 3) the cameraman only had to replace the wooden cover of that particular station by his camera assembly and secure it in place with speed nuts. Two photographs were then taken, recording the time interval (figures 2c and 2d). The ice coverage on the river at that particular instant was also recorded, either in writing or with a carefully oriented snapshot, thus completing the cycle which was repeated at regular intervals during the day.

FLOE DISPLACEMENT COMPUTATION

A profile view of both bridges of interest is shown in figure 3. The field of view of the negative is limited by the lengths XX' and YY' in figures 3 and 4. The distance travelled by an ice floe is obtained from simple mathematical relationships deduced from figure 4a and the design characteristics of the photographic equipment. The final result is:

$$L = \frac{H\ell \sec^2 \alpha}{f(1 - \frac{a}{f} \tan \alpha)(1 - \frac{a'}{f} \tan \alpha)} \quad (1)$$

where L is the distance travelled by the ice floe, H is the height of the camera lens above the water level, α is the shooting angle of the camera, f is the focal length, a and a' are the distances travelled by the ice floe at times t_1 and t_2 as scaled from XX' (refer to figure 4b), a and a' being positive or negative according to whether they are measured downstream or upstream of the bisector XX', and ℓ is the scaled distance travelled by the ice floe between times t_1 and t_2 .

The method by equation (1) is laborious as each negative has to be printed following a sequence which allows each photograph to be chronologically identified. It is therefore extremely advantageous to project the negatives on a screen enlarged to a convenient size. Figure 5 shows a schematic of the screen enlarged 28.2 times and calibrated in feet along the YY' axis. This graduated screen directly gives the distance travelled by a drifting ice floe. The calibration is obtained from elementary mathematical manipulation, using equation 1 and the enlargement ratio h_s/h_n , where h_s and h_n are respectively the heights YY' of the screen and of the negative.

The final result is:

$$y_s = \frac{\pm Lf h_s/h_n}{H + H \tan^2 \alpha \pm L \tan \alpha} \quad (2)$$

where y_s is a measured distance along the YY' axis of the screen. L is positive or negative according to whether it is taken above or below XX'.

DISCHARGE OF MOVING ICE

The total discharge I of floating ice can be obtained from a formula of the type:

$$I = \sum_{i=0}^m n_i v_i h \Delta B_i$$

where n_i is the coverage percentage of ice considered in a strip of width ΔB_i (figure 3), v_i and h are the average velocities and thicknesses of the drifting ice floes of that strip. For this study, the river width has been divided into 3 strips at the Pierre Laporte bridge and into 2 strips at the Laviolette bridge (figure 3). Photographs is taken every two hours at Trois-Rivières and each hour at the Québec site where tidal motion exists.

CONCLUSION

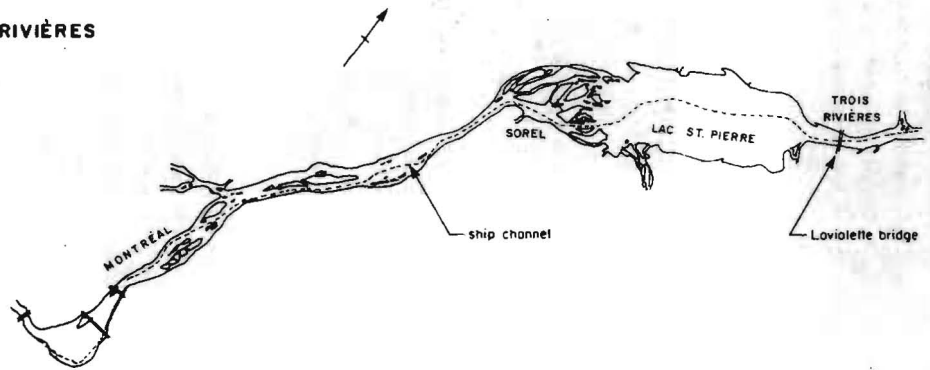
The technique described to determine the ice floe velocities in the St. Lawrence River from oblique pictures taken from bridges has been used successfully during the winter 1972. The cost of such an installation is less than \$1,000.00 and there is no need to print the negatives as they are directly projected on a screen. The data obtained from such a survey can be used for many purposes such as the formation of ice jams, the ice discharge of a river and the calibration of a hydraulic model taking into account the ice movement during tides.

REFERENCES

- 1- Kuznetsov, A.I. (1955)- "Method of measuring the amount of ice passing a given point (text in Russian) Meteorologiya i Gidrologiya, No. 2, pp. 42-44.
- 2- Michel, B. (1971)- "Winter regime of rivers and lakes". Corps of Engineers, U.S. Army, Hanover, New Hampshire, AD 724 121, pp. 12-14.

MONTREAL - TROIS RIVIÈRES

0 50,000'



TROIS RIVIÈRES - QUÉBEC

0 50,000'

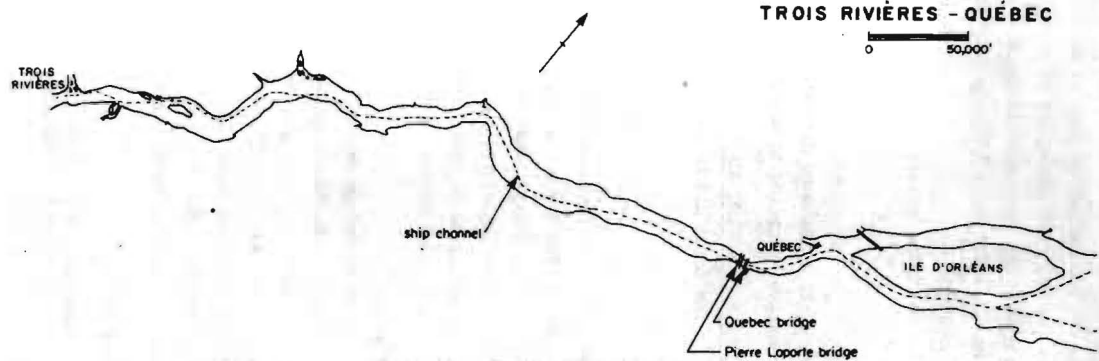
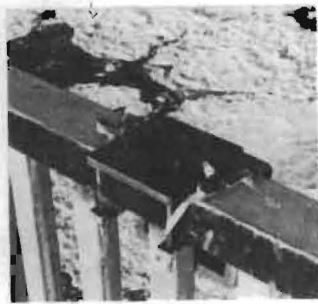


FIGURE 1 — THE ST.-LAWRENCE RIVER



(a)



(b)

FIGURE 2a- A view of the permanent steel plate fixed on the bridge side-walk arm.

FIGURE 2b- A view of the camera fixed on the support.

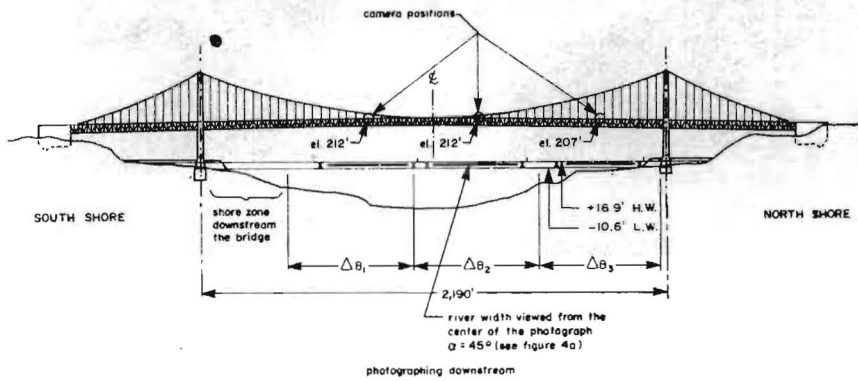


(c)

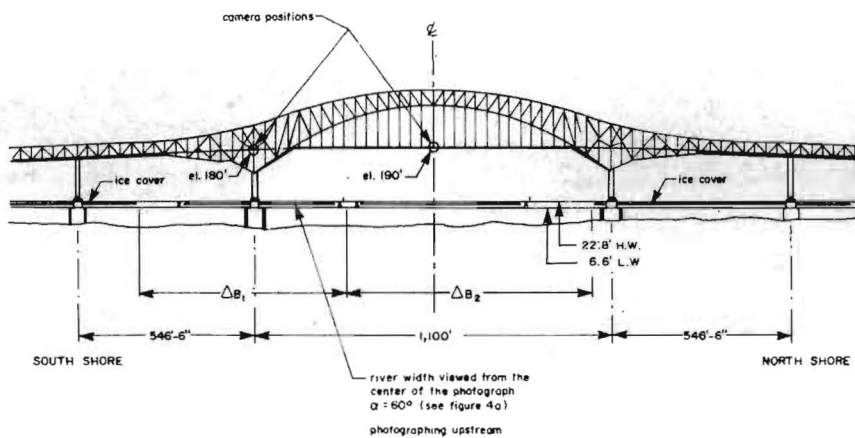


(d)

FIGURES 2c AND 2d- Pictures taken from the Pierre Laporte bridge at an interval of 33 seconds.



a - THE PIERRE LAPORTE BRIDGE.



b - THE LAVIOLETTE BRIDGE

FIGURE 3

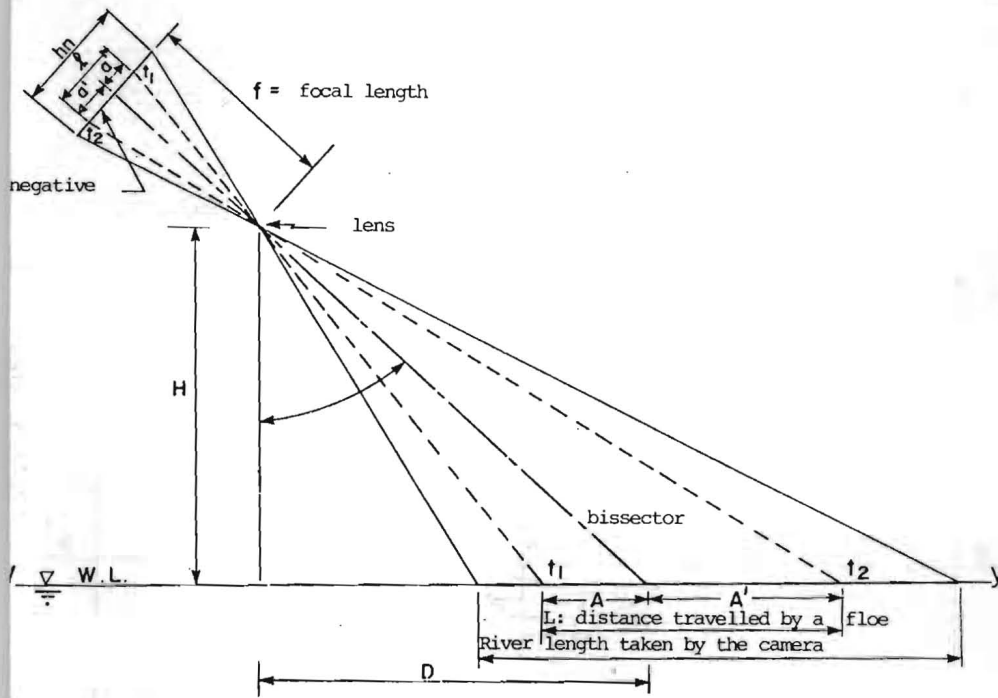


FIGURE 4a- ICE FLOE POSITIONS AS SEEN BY THE CAMERA AT TIMES t_1 AND t_2 .

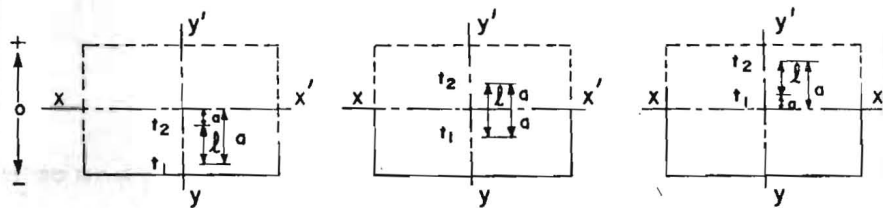


FIGURE 4b- CASES OF ICE FLOE POSITION AT TIME t_1 AND t_2 ON TWO SUPERIMPOSED NEGATIVES.

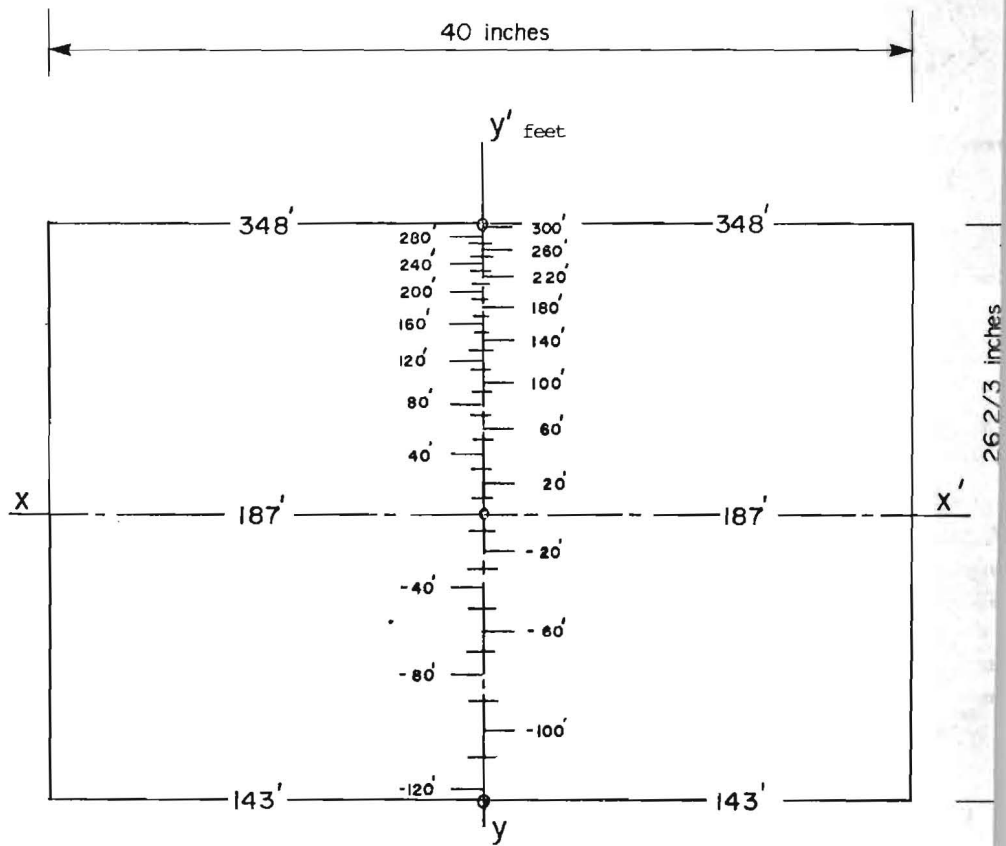


FIGURE 5- EXAMPLE OF A CALIBRATED SCREEN GIVING THE ICE FLOE DISPLACEMENT ALONG THE YY' AXIS ($\alpha = 45^\circ$, $H = 210'$, $f = 28.6$ mm, negative dimensions 24 x 36 mm).

Water power development on most rivers in the U.S.S.R. has to take into account the problems of ice passage.

Ice phenomena being very complicated, the process of ice passage through hydraulic structures has not been yet described by a system of equations while laboratory investigations also present many difficulties. Under such conditions summarizing field observation data acquires a vital significance. Of particular importance are the observation results on passing ice through the structures of hydro power plants under construction and in operation on the Siberian rivers, which are notorious for massive movement of ice during spring break-ups./1,2/.

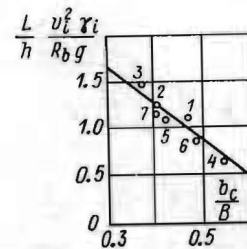
Field observation can be considered as a kind of modelling which does not interfere with the process under study. Observation data are to be treated with the help of dimensionless criteria of similarity. In the paper the quantity and the structure of the similarity criteria characteristic to the process of ice passage was established using dimensional analysis. /3/.

Determination of a restricted river channel width (b_r) with the passage of ice fields taken into account. When an ice field greater in width than the restricted channel approaches the restriction it will either pass or stop at the entrance to the restriction. The field observation data on temporary stops of ice fields (Fig. 1) are treated with the aid of the following similarity equation

$$\frac{b_r}{B} = f \left(\frac{L}{h} \cdot \frac{V_i^2 \gamma_i}{R_b g} \right) \quad (1)$$

Fig. 1. Field observation data on stops of ice fields at the entrance to river channel restrictions:

- 1-4 - the Krasnoyarsk power plant dam, 1961-1965;
- 5 - State Regional Power Plant-2 dam, 1969;
- 6 - the Ust-Khantaika power plant dam, 1969;
- 7 - the Sayano-Shushenskaya power plant dam, 1970.



- /1/ Sokolnikoff N.M., Passing ice through the structures of hydro power plants under construction in Siberia. Ice Symposium 1970, Reykjavik.
- /2/ Koren'kov V.A., Field observation results on passage of ice through the structures of the Krasnoyarsk power plant. Gidrotekhnicheskoye Stroitel'stvo 1970, N 7.
- /3/ Venikov W.A., Application of the theory of similitude and modelling to the problems of power development. Izd. Vysshaya shkola, Moskva, 1966.

With b_r/B varying from 0.3 to 0.6 Eq.(1) has the form:

$$\frac{b_r}{B} = 0.72 B \left(1 - 0.35 \frac{L}{h} \cdot \frac{V_i^2 \cdot \gamma_i}{R_i g}\right) \quad (2)$$

where V_i - velocity of ice floes approaching the restriction; B - width of river channel upstream from the restriction; L - width of ice fields approaching the restriction; g - acceleration of gravity; h - ice thickness; R_i - cross-breaking strength of ice determined on cantilever ice specimens of $h \times h$ cross-section and $3h$ length tested under a downward destructive force; γ_i - volume weight of ice.

In our research R_i was established by field investigations performed by the moment of ice passage. When these data are not available R_i was calculated from the prognostic equations [4].

The straight line divides Figure 1 into two areas: the upper area corresponds to the conditions of successful passage of ice, while the lower one to the conditions of long stops of ice fields before restriction entrances.

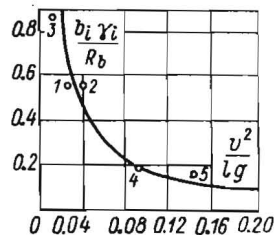
Determination of the width of ice control facility spans (b_r) with broken sheet ice passage taken into account. When an ice floe of width l greater than the span but less than two spans approaches an ice control facility it will either pass or stop in front of the span depending on certain conditions.

The field observation data on short-term stops of ice floes (Fig. 2) are treated with the aid of the following similarity equation:

$$\frac{b_i \cdot \gamma_i}{R_i} = f\left(\frac{V_i^2}{gl}\right) \quad (3)$$

Fig. 2. Field observation data on stops of ice floes before the ice control facility spans.

- 1 - the Bratsk power plant, 1960;
- 2 - the Krasnoyarsk power plant, (15 m span), 1963;
- 3-5 - the Krasnoyarsk power plant, 1964-1966.



[4] Koren'kov V.A. Experimental research findings on decrease of river ice strength in spring. Ice Symposium, 1970, Reykjavik.

The curve in Fig. 2 makes it possible to derive the equation for b_i :

$$b_i = \frac{0.017 R_i \cdot l \cdot g}{V_i^2 \cdot \gamma_i} \quad (4)$$

The upper part of Fig. 2 is the area of reliable b_i values. Equation (4) is valid under the following single-valued conditions: the ice floes approaching the spans are 0.5-1.2 m thick, almost square in plan and $b_i < l < 2 b_i$; the ice floes start moving under the impact of other floes; the drop-down curve before the piers is insufficient for breaking ice; the pier heads 10 m wide are streamlined.

Determination of mean flow velocities (V_m), at which the ice can be stopped in front of ice control facilities. During the spring break-up at certain mean flow velocities ice accumulates in the vicinity of ice control facilities.

Field observation data on temporary stops of ice floes (Fig. 3) calculated from the following equation of similitude:

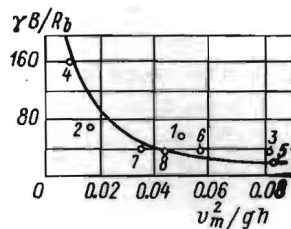
$$\left(\frac{V_m^2}{gh}\right) = f\left(\frac{\gamma_i \cdot B}{R_i}\right) \quad (5)$$

enabled V_m to be found as

$$V_m = 1.3 \sqrt{\frac{h \cdot R_i \cdot g}{\gamma_i \cdot B}} \quad (6)$$

Fig. 3. Field observation data on temporary stops of ice floes in front of structures.

- 1-4 - the Krasnoyarsk power plant, 1964-1967;
- 5 - the Vilyui power plant, 1965;
- 6 - the Novosibirsk power plant, 1957;
- 7-8 - the Bratsk power plant, 1960-1961.



Eq.(6) is valid for the conditions when one-layered ice floes not connected with the banks and commensurable to the river channel in width approach the dam along a straight reach of $(10-15)B$. Ice floes may exert pressure on structures or banks. The relationship of the ice thickness versus the water depth before the dam varies within the range of 0,015-0,10.

Ice floes can be stopped at values of V_m lower than those found from Eq.(6).

Determination of the minimum head (H_{min}) for ice passage over spillway gates. In some cases the ice is passed over the gates closing spillway spans.

Laboratory and field investigation data (Fig. 4) treated with the aid of the relation

$$\frac{H_{min}}{h} = f\left(\frac{c}{h}\right) \quad (7)$$

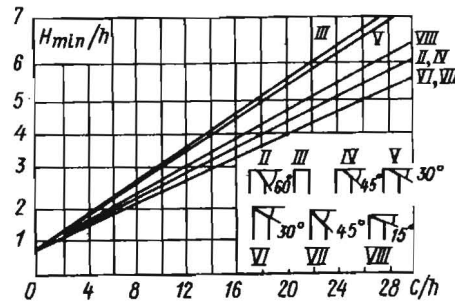
yield the formula which allows to calculate the minimum water head on the gates ensuring the impact-free passage of ice.

It acquires the following form:

$$H_{min} = 0,9h + k \cdot c$$

where K = dimensionless coefficient whose values for the vertical-lift gate are tabulated below; C = length of ice floes passing through the spillway spans.

Fig. 4. Generalized diagram for the choice of K -values.



Table

Values of K -coefficient for various shapes of gate head

Shape of gate head	K -values
Rectangular	0,224
Triangular with angle of 15°	0,178
30°	0,155
45°	0,152
Trapezoidal with angle of 30°	0,211
45°	0,172
60°	0,172

The data obtained by the author are in close agreement with those received in Poland for gates with Krieger heads [5].

[5] Manthey Tadeusz, *Bodanie warunkow przepuszczania kry lodowej ponad zasuwa jazowa*. Rozpr. hydrotechn., 1964, N 15.



ICE SYMPOSIUM 1972
LENINGRAD

FIELD IMPLICATIONS OF THE FORMATION OF
ICE RIPPLES

George D. Ashton,
Hydrologist

U.S. Army Cold Regions Research and
Engineering Laboratory,

Hanover,
New Hamp-
shire, U.S.A.

SYNOPSIS

The results of a recent experimental and analytical study are used to predict the conditions under which ice ripples form on the underside of river ice covers. A relationship between the wavelength of the ripples and the flow velocity is proposed and compared with existing field data. The effect of flow depths on the wavelength - velocity relationship is examined and found to be small.

INTRODUCTION

The results of a recent¹ experimental and analytical study of ice ripples which form on the underside of river ice covers provide a basis for evaluating certain effects resulting from their formation. The purpose of this paper is to provide the means by which the occurrence of ice ripples may be predicted from knowledge of thermal and hydraulic characteristics of a river. Attention is centered on the behavior of the ice cover in the absence of frazil in the flow. Implications with regard to the initial appearance of ice ripples, their wavelengths, effects of air and water temperatures, and heat transfer characteristics are discussed.

THEORETICAL BASIS

The appearance of ice ripples on the underside of river ice covers is a quite common occurrence although there have been but few detailed studies of their occurrence and behavior. The most detailed of these have been the studies reported by Carey^{2,3,4}, by Larsen^{5,6}, and by Ashton and Kennedy^{1,7}. The latter¹ recently presented an analytical model for the initial onset and development of ice ripples which results in a stability criterion for an initially plane interface of the form

$$-\frac{\bar{q}_w \bar{\eta}}{\bar{q}_i L} B_1 \cos \theta = \begin{array}{l} > +1 \text{ unstable} \\ = +1 \text{ neutrally stable} \\ < +1 \text{ stable} \end{array} \quad (1)$$

wherein \bar{q}_w is the mean heat transfer rate to a plane ice-water interface, \bar{q}_i is the mean heat transfer rate into the ice at the interface, $\bar{\eta}$ is the mean thickness of the ice cover, L is the wavelength of the ripple features, B_1 is a local amplification coefficient and θ is an angular phase shift of \bar{q}_w relative to a sinusoidal interface. Over a range of flow temperatures and velocities (and wavelengths since L depends upon the flow velocity) the product $B_1 \cos \theta$ was found to have a value of about -13.5.

FIELD EVALUATION OF THE STABILITY CRITERION

Direct application to field situations of the stability criterion requires a

- ¹ Ashton, G. D., and Kennedy, J. F., 1971, Ice Ripples on the Underside of River Ice Covers, submitted to ASCE Jl. Hydraulics Division.
- ² Carey, K. L., 1966, Observed Configuration and Computed Roughness of the Underside of River Ice, St. Croix River, Wisconsin, U. S. Geological Survey Prof. Paper 550-B, pp. B192-B198.
- ³ Carey, K. L., 1967a, Analytical Approaches to Computation of Discharge of an Ice-Covered Stream, U. S. Geological Survey Prof. Paper 575-C, pp. C200-C207.
- ⁴ Carey, K. L., 1967b, The Underside of River Ice, St. Croix River, Wisconsin, U. S. Geological Survey Prof. Paper 575-C, pp. C198-C199.
- ⁵ Larsen, P. A., 1969, Head Losses Caused by an Ice Cover on Open Channels, Jl. Boston Society Civil Engineers, Vol. 56, No. 1, pp. 45-67.
- ⁶ Larsen, P. A., 1971, On Hydraulic Roughness of Ice Covers, paper presented at 19th Annual Hydraulics Division Specialty Conference, Iowa City, Iowa, August 1971.
- ⁷ Ashton, G. D., and Kennedy, J. F., 1970, Temperature and Flow Conditions During the Formation of River Ice, IAHR Ice Symposium, Reykjavik, paper 1.2.

knowledge of the component quantities \bar{q}_w , $\bar{\eta}$, \bar{q}_i , and L . By means of certain approximations an equivalent stability criterion may be derived in terms of the air temperature T_a , the water temperature T_∞ , the mean velocity U and depth D of the flow, the thickness of the ice cover and properties of water and ice.

The heat transfer \bar{q}_w to the ice from the flow may be estimated using one of the empirical relationships developed for pipe flow. One such relationship⁸ is of the form

$$Nu = -C_1 Re^{0.8} Pr^{0.4} \quad (2)$$

wherein $Nu = \bar{q}_w R / [(T_\infty - T_m)k_w]$ is the Nusselt number, $Re = UR\rho/\mu$ is the Reynolds number, and $Pr = \mu C_p/k_w$ is the Prandtl number of the flow. Herein μ is the dynamic viscosity, C_p is the specific heat, ρ is the water density, k_w is the thermal conductivity, T_m is the melting point of ice and R is the hydraulic radius. The constant C_1 is approximately 0.017, and for water near the freezing point $Pr = 13.6$.

The heat transfer \bar{q}_i into the ice at the ice-water interface may be estimated on the basis of steady-state heat conduction through a two-layered media (ice and snow) by

$$\bar{q}_i = \frac{-(T_m - T_a)}{\frac{\bar{\eta}_i}{k_i} + \frac{\bar{\eta}_s}{k_s}} \quad (3)$$

where $\bar{\eta}_i$ and $\bar{\eta}_s$ are the ice and snow thicknesses, respectively, and k_i and k_s are the ice and snow thermal conductivities, respectively. For pure ice, $k_i = 2.24 \text{ W m}^{-1} \text{ deg}^{-1}$ while for dry snow k_s depends largely upon the density. A summary of a number of investigations of the relationship between k_s and snow density is presented by Mellor⁹.

The thickness $\bar{\eta}$ may be obtained by measurement, by empirical formulas for prediction of the ice thickness such as those described by Michel¹⁰, or by comparison with previous records for the same site.

The characteristic wavelength L of ice ripples was related to the velocity of the flow by an empirical expression of the form¹

$$L = 0.09 + 0.29/U \quad (\text{m - sec units}) \quad (4)$$

and to be consistent with field observations. Equation 4 does not take into account flow depth effects which, while thought to be small, are expected to be present. In an attempt to evaluate depth effects as well as determine a non-dimensional relationship between L , R , and U , the laboratory data of Ashton and Kennedy¹ together with all available field data are plotted in Figure 1 in the

⁸Rohsenow, W. M., and Choi, H. Y., 1961, Heat, Mass and Momentum Transfer, Prentice-Hall, New Jersey, pp. 192-196.

⁹Mellor, M., 1964, Properties of Snow, USACRREL Monograph III-A1.

¹⁰Michel, B., 1971, Winter Regime of Rivers and Lakes, USACRREL Monograph III-B1a.

¹op. cit.

form $L/R = f(UL/v)$ and in Figure 2 in the form $L/R = f(UR/v)$. The hydraulic radius R was taken as the depth of flow in the open-channel laboratory experiments, as one-half the local effective flow depth for field data when local values of U and depth were available, and otherwise as the cross section R . These latter points are plotted as "open" points (St. Croix River, Kilforsen and Alvkarleby Canals). In Figure 1 the data are reasonably represented by

$$\frac{L}{R} = C_2 \left(\frac{UL}{v} \right)^\zeta \quad (5)$$

where the line drawn corresponds to $C_2 = 4 \times 10^{19}$ and $\zeta = -4$. In Figure 2 the data are reasonably represented by

$$\frac{L}{R} = C_3 \left(\frac{UR}{v} \right)^\alpha \quad (6)$$

and the line corresponds to $C_3 = 8400$ and $\alpha = -0.8$. In both cases the scatter of the data prevents accurate determination of the exponents in (5) and (6). Features similar in appearance to ice ripples have been observed to form at ablating plaster-water and limestone-water interfaces, and at air-ice interfaces. For these features it has been suggested on the basis of dimensional analysis that the length Reynolds number (UL/v) is a universal constant (Curl¹¹, Blumberg¹²) with a value of about 2.5×10^4 . For ice-water interfaces the length Reynolds number is somewhat larger (see Fig. 1) and there appears to be some influence of the depth. The effect of depth, in either case, is small and estimated to be about $L \propto D^{0.2}$. Similarly the effect of velocity may be estimated to be about $L \propto U^{-0.8}$. These particular values are similar to the effect of depth on heat and mass transfer rates although the data exhibit too much scatter to offer more than a suggestion of the trend of depth effects. Additional measurements on deep fast-flowing canals such as reported by Larsen⁵ would aid in defining this trend.

As the $\bar{\eta}$ term in the numerator of (1) arises from an analysis in which only a single layer of ice was considered in the heat conduction model the criterion should be modified for the case of a snow cover. This may be done by defining an "equivalent ice thickness", η_e , which represents the thermal resistance of the combined snow and ice cover. This equivalent ice thickness is then given by

$$\eta_e = \bar{\eta}_i + \frac{k_i}{k_s} \bar{\eta}_s \quad (7)$$

Substitution of (7) for $\bar{\eta}$, (3) for \bar{q}_i , use of (2) to evaluate \bar{q}_w , and (6) to evaluate L , results in the following alternate form of the stability criterion given by (1):

¹¹Curl, R. L., 1966, Scallops and Flutes, Trans. Cave Res. Group of Great Britain, Vol. 7, No. 2, pp. 121-160.

¹²Blumberg, P. N., 1970, Flutes: A Study of Stable, Periodic Dissolution Profiles Resulting from the Interaction of a Soluble Surface and an Adjacent Turbulent Flow, Ph. D. thesis, University of Michigan, Ann Arbor, Michigan.

⁵op. cit.

$$\beta = \frac{-C_1}{C_3} Pr^{0.4} B_1 \cos \phi \frac{k_w (T_\infty - T_m) \eta_e^2}{k_i (T_m - T_a) R^2} \left(\frac{UR}{v}\right)^{0.8} - \alpha \begin{matrix} > +1 \text{ unstable} \\ = +1 \text{ neutral} \\ < +1 \text{ stable} \end{matrix} \quad (8)$$

In application of (8) it is noted that when T_a is greater than 0°C there is no flux of heat through the ice cover and the parameter $(T_m - T_a)$ should be taken as zero; correspondingly β becomes infinite, i.e., in this case the undersurface of the ice cover is inherently unstable if there is a finite rate of heat transfer to the ice-water interface. Similarly, if the flow temperature is at or below 0°C the parameter $(T_\infty - T_m)$ should be taken as zero and corresponds to an inherently stable ice-water interface since the instability requires a finite (although small) heat transfer to the ice-water interface.

As a practical matter even very small water temperatures yield values of β greater than unity. Equation (8) may be written in more compact form by substitution of the following constants:

$$\begin{aligned} Pr &= 13.6 & C_1 &= 0.017 & C_3 &= 8400 & B_1 \cos \phi &= -13.5 & \alpha &= -0.8 \\ k_i &= 2.24 \text{ W m}^{-1} \text{ deg}^{-1} & & & & & & & & \text{(pure ice)} \\ k_w &= 0.54 \text{ W m}^{-1} \text{ deg}^{-1} & & & & & & & & \text{(water at } 0^\circ\text{C)} \end{aligned}$$

Equation (8) becomes:

$$\beta = 1.87 \times 10^{-5} \frac{T_\infty}{-T_a} \frac{\eta_e^2}{R^2} \left(\frac{UR}{v}\right)^{1.6} \begin{matrix} > +1 \text{ unstable} \\ = +1 \text{ neutral} \\ < +1 \text{ stable} \end{matrix} \quad (9)$$

We choose as example conditions:

$$\begin{aligned} \bar{\eta} &= \eta_i = 0.20 \text{ m (snow free cover assumed)} \\ U &= 0.30 \text{ m s}^{-1} & T_a &= -10^\circ\text{C} \\ R &= 0.50 \text{ m (total flow depth = 1 m)} \end{aligned}$$

For these conditions the temperature corresponding to neutral stability is calculated, using Eq. 8, to be $T_\infty = 0.04^\circ\text{C}$. For a thicker ice cover the "critical" T_∞ will be reduced proportionately to the thickness squared.

Of even more significance is the effect of even a small thickness of snow cover. As an example, a 50mm snow cover of density 0.3 kg m^{-3} , with a corresponding estimated $k_s = 0.29 \text{ W m}^{-1} \text{ deg}^{-1}$, increases the equivalent ice thickness to 0.58 m and results in a "critical" water temperature, for the above conditions, of 0.005°C . While the calculations presented above are based on very simplified heat transfer models they do indicate the very small above-freezing water temperatures which may result in the formation of a wavy relief pattern on the underside of a river ice cover.

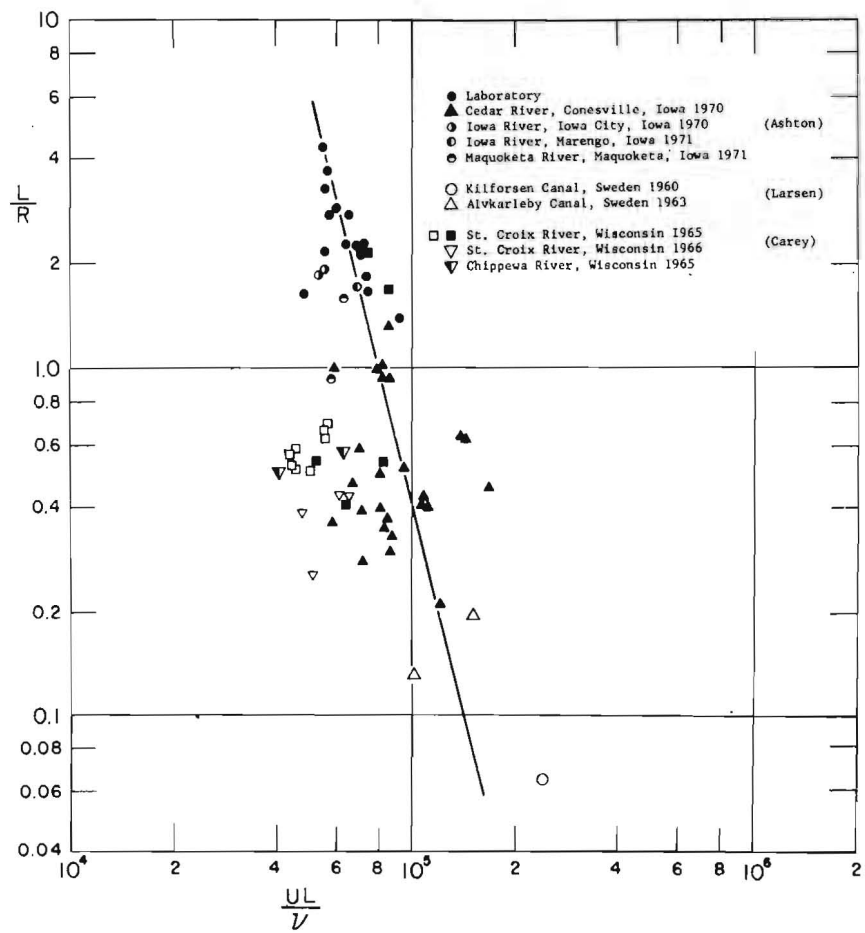
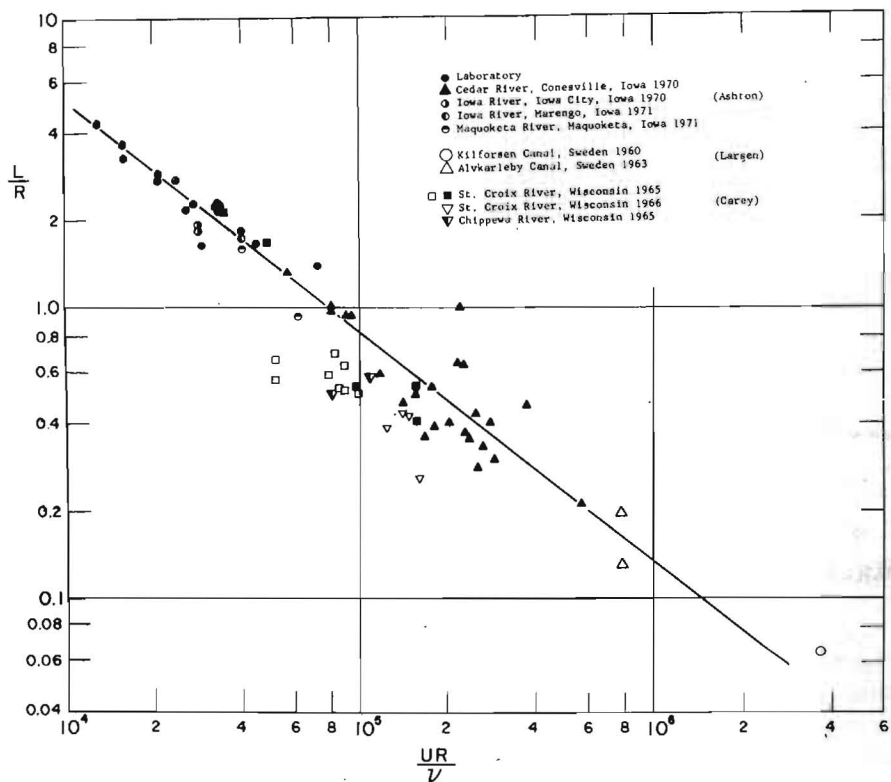


Figure 1.



• Figure 2.



TOP AND BOTTOM ROUGHNESS OF A MULTI-
YEAR ICE FLOE

W.D. Hibler, III, Research Physicist	USACRREL	Hanover, NH, U.S.A.
S. Ackley, Research Physicist	USACRREL	Hanover, NH, U.S.A.
W.F. Weeks, Research Glaciologist	USACRREL	Hanover, NH, U.S.A.
A. Kovacs, Research Civil Engineer	USACRREL	Hanover, NH, U.S.A.

SYNOPSIS

A spectral study of the snow and ice topography on a multi-year ice floe has shown that the snow cover, although attenuating the roughness amplitude of the ice surface, does not cover it completely. In general the snow surface variance is lower by a factor of $1/3$ to $1/4$ as compared to the ice surface variance. The correlation between snow and ice surface roughness is highly significant for long wavelengths (> 8 m), but fails to be significant for short wavelengths (< 4 m). These results agree with what might be expected intuitively in that long wavelength variations are not masked appreciably while short wavelength variations are well hidden. Although the ice sheet as a whole is in free-floating, isostatic equilibrium, pronounced local deviations from isostatic equilibrium are common. The trend is for ice drafts to deviate more than expected from isostasy for thin ice and less than expected for thick ice. Estimates are also made of the number of ice thickness measurements required to obtain the mean thickness of the multi-year floe to any specified accuracy.

INTRODUCTION

Little work has been done on the correlation between the roughness of the upper and lower ice surfaces of sea ice. At first thought this might appear rather surprising inasmuch as the surface roughness is important in controlling the wind and the water drag exerted on the ice. However, there is still no indirect method of determining the thickness of sea ice, much less a method of doing this remotely as a continuous profile. Drilling is, of course, time consuming and tiring, but is virtually the only means of determining freeboard and draft at a point. Present observations on ridging in first year ice suggest that although lack of local isostatic equilibrium is common, a good overall correlation between top and bottom roughness is to be expected. Whether this is generally true for multi-year ice has not been previously studied.

The following is a preliminary look at the freeboard to draft correlation problem in multi-year ice. In addition a study of the relation between the snow surface and the true ice surface of the multi-year floe was completed. This is of interest because remote sensing techniques using laser profilometry record the elevation of the snow surface and not the true ice surface.

The study site was part of a multi-year floe approximately 5 km² in area, located in the Beaufort Sea at the site of the 1971 AIDJEX pilot study about 550 km north of Tuktoyaktuk, N.W.T. The exact study area is shown in Figure 1, an aerial photograph taken by NASA on 11 March 1971. At the time when this picture was taken the ice surface was effectively scoured free of the snow that is shown in Figure 2. The structure of the large multi-year pressure ridge on the right portion of the figure was also studied and is the subject of another paper¹. The differences in roughness between first- and multi-year ice are quite evident from the "freckled" appearance of the multi-year ice as shown in the figure compared to the smooth first-year ice whose surface is marked only by snowdrift features.

Figure 2 shows cross-sectional views of the five elevation profiles that were studied. The snow depth and the ice elevation above sea level were determined at 1 meter intervals along each profile by leveling. In addition ice thicknesses were determined by drilling at 31 locations. The figure clearly shows the undulating topography characteristic of multi-year floes.

RESULTS

Snow Surface - Ice Surface Correlations

In much remote sensing data, in particular in laser profiles and digitized roughness plots made from aerial photographs, the surface of the snow is "seen" rather than the true ice surface. It was apparent by observation at the study site that after a storm, snow drifting could change the effective surface sampled by remote sensing. From a visual examination of the profiles shown in

¹Kovacs, A., Weeks, W. F., Ackley, S. and Hibler, W. D. (1972). A study of a multi-year pressure ridge in the Beaufort Sea. AIDJEX Bulletin 12, 17-28.

Figure 2 it initially appears that the snow covers up much of the interesting roughness. A more detailed examination of the surface roughness indicates that this may not be the case. Figure 3 shows both snow and ice spectra along all profiles. The spectra were calculated using a Hamming spectral window and a maximum wave number of 50. The confidence limits are indicated. Computational detail and a discussion of the particular interpretation of the power spectra of sea ice can be found in Blackman and Tukey (1958)² and Hibler and LeSchack (1972)³ respectively. For our analysis here, the spectra may be considered a plot of the amount of variance or roughness versus the frequency or wavelength of the roughness. The plots shown in Figure 4 are normalized to the total variance so that the area under the spectral curve in any given frequency band gives the total variance or mean square roughness in that region.

From Figure 3 we see that as expected the spectral components for the snow surface are generally all smaller by a factor of 1/3 to 1/4 than the spectral components of the ice surface. This means that the roughness has been smoothed out and consequently wind stress measurements⁴ might be expected to change as the snow cover shifts. Taking the square root of the variance to be some measure of the mean roughness height we see that a factor of 2 variation in the mean roughness height can easily be caused by shifts in the snow cover.

The other point obvious from Figure 3 is that the general shapes of the snow surface and ice surface spectra are much the same for the same profile, with many of the same spectral peaks occurring in the snow surface spectrum as in the ice surface spectrum. These peaks indicate that the snow cover, although attenuating the amplitude of the ice surface, does so in such a way that the dominant spectral components, especially at low frequencies, are still observable.

To obtain a more quantitative analysis of how well the snow surface correlates with the ice surface at different frequencies, we passed three band pass filters over the parallel snow and ice profiles A'-A', B'-B' and C'-C', and plotted up the results. This procedure has the advantage of indicating at what position correlation takes place. We also calculated the correlation coefficient between snow and ice profiles for each band passed result. When determining the degrees of freedom for calculating the significance of the correlation coefficient for a band pass filtered profile, the total number of data points is multiplied by the fraction of the spectrum filtered. The frequency response of the filters (less than 1% side lobe errors in all cases) together with the average correlation coefficient for each frequency band is given in Figure 4. The 10% significance

²Blackman, R. B. and Tukey, J. W. (1958). The Measurement of Power Spectra. Dover Publications, New York, 190 pp.

³Hibler, W. D. and LeSchack, L. (1972). Power Spectrum analysis of undersea and surface sea ice ridge profiles. Journal Glaciology (in press).

⁴Banke, E. G. and Smith, S. D. (1971). Wind stress over ice and over water in the Beaufort Sea. Journ. Geophys. Research 76 (30), 7368-7374.

level for the correlation coefficient (using 16 degrees of freedom) is given by the dotted line. The plot clearly indicates the stronger correlation for wavelengths longer than 8 m. In fact the average correlation coefficient for the lowest frequency band is .80 which is greater than the average total correlation coefficient (for all frequencies) of .72.

The filtered profiles for each of the three pass bands together with the unfiltered results are given in Figure 5. These plots qualitatively give the same results indicated by the correlation coefficients, namely that wavelengths longer than about 8 meters are well correlated whereas shorter wavelengths have a poorer correlation. In summary the quantitative results suggest that as a rule of thumb 8 m is the demarcation wavelength with shorter wavelength variation in the ice surface being masked by the snow cover while the longer wavelength components are not strongly affected.

Both before and after these measurements were made, high winds blew away much of the snow cover. Consequently, the resulting surface roughness spectrum changed to one more nearly approaching the true ice surface. The spectra plotted in this paper give some indication of the limits of the surface roughness spectrum expected due to such changing conditions.

The spectra of the true ice surface also indicated a dominant low frequency spectral peak at a wavelength of about 30 m which persisted on parallel profiles. We feel this peak is representative of melt hummock spacings for the region analyzed. The low frequency peak did shift as the profile direction was changed indicating lineation³ in the surface approximately parallel to the nearby pressure ridge shown in Figure 1. It should be noted here that the profiles analyzed do not include the pressure ridge, so that we are discussing here only the "flat" part of a multi-year floe.

Freeboard - Ice Thickness Correlations

To study the correlation between surface roughness and thickness and the bottom topography we calculated a correlation coefficient of .60 for the correlation of freeboard to draft and a coefficient of .79 for the correlation of freeboard to thickness. Both these numbers indicate a linear correlation significant at better than the 1% level by an analysis of variance test.

To determine the ice draft and/or the ice thickness from the freeboard, we can calculate the regression line between these variables. The resulting equations are $d = 1.337f + 2.80$ and $t = 2.32f + 2.80$ where d and t are the ice draft and the thickness respectively and f is the freeboard (all in units of m). Using these relations, the root mean square error between the predicted and the observed values of draft and thickness were in both cases 0.36 m. These numbers indicate the improvement that can be made in draft or thickness estimates by having information on the local freeboard available (the standard error of the

³op. cit.

estimate of 0.36 m obtained by using the regression line is significantly less than the standard errors of the estimate on draft (0.46 m) and thickness (0.60 m) see Table I.

Table I. Summary of Statistical Results (31 Holes)

mean ice draft	3.24 m
ice draft standard deviation	.46 m
mean ice thickness	3.57 m
thickness standard deviation	.60 m
mean freeboard	.33 m
freeboard standard deviation	.20 m
mean snow depth	.16 m
snow depth standard deviation	.13 m
Correlation Coefficients	
depth to freeboard	.60
thickness to freeboard	.79

Both linear regression lines deviate significantly from the result expected if the ice is in isostatic balance. In particular the isostatic balance result would be of the form $t = \alpha d$ where $\alpha = (\text{density of sea water})/(\text{ice density})$. Assuming a sea ice density of 0.91 g/cm^3 (estimated from the ice cores) and a sea water density of 1.03 g/cm^3 , we would obtain ratios for d/f and t/f of 7.58 and 8.58 respectively.

The trend of the deviations from isostatic balance is indicated very clearly in Figure 6 where we have plotted the (freeboard/draft) ratio vs. thickness. The isostatic balance line with the snow cover neglected and an effective isostatic balance line considering both the density of the ice and the depression of the ice sheet by the snow cover are indicated. In calculating the effective line a mean snow thickness of 0.16 m and a snow density of 0.45 g/cm^3 were used based on snow measurements at the site. Also shown is the regression line of (f/d) on t . The trend is clearly for the ice draft to be greater than expected from isostatic balance for thin ice and the inverse for thick ice. Therefore, on a point to point basis, the assumption of isostatic balance breaks down.

However, as might be expected since the ice sheet is clearly free-floating, if cross-sectional areas rather than individual points are used for comparison with the assumption of isostatic balance, the results are quite good. To illustrate this we note that the mean thickness and mean draft are proportional to the total cross-sectional area and cross-sectional area below the water level respectively of the ice floe. If a depression of 0.07 m due to 0.16 m of snow cover is included we find that the average draft of 3.24 m and the average ice thickness of 3.57 m imply a mean ice density of 0.915 g/cm^3 for isostatic balance. This is in agreement with the findings of Kovacs *et al.* (1972)¹ and is a very

¹op. cit.

reasonable value since cores taken in this region of the floe indicated densities between 0.90 and 0.92 g/cm³. The mean thickness we obtained also compares well with the mean value for Beaufort Sea "unhummocked" multi-year ice (3.47 m) obtained by Koerner (1971).⁵

The fact that individual points deviate significantly from isostatic balance while on the average the overall ice sheet is in isostatic balance is similar to the situation observed in pressure ridges^{6,7}. The form of the deviations suggest that a model similar to the Wittmann-Makaroff pressure ridge model⁸ may well also apply to the small melt hummocks that develop on a multi-year floe. In this model the underside of the hummock has a greater horizontal extent than the sail. This would yield deviations of the type observed; i.e. deep hummocks are less deep than would be expected on the basis of isostasy. The actual balance would be between the volume of the hummock below water as compared to the volume above water.

Estimating the Average Ice Thickness

One interesting application of the thickness data is to estimate, using sampling theory, the number of holes needed to obtain the mean ice thickness of the multi-year floe with a specified accuracy. Based on the 31 measurements, the mean and standard deviation of the ice thickness are 3.57 ± 0.60 m respectively. The frequency distribution of the ice thicknesses is shown in Figure 7 and is to a good approximation normal. The 90% confidence limits on the true mean are 3.39 and 3.75 m. If we now assume⁹ that the value of the standard deviation is independent of the sample size (N), a t distribution may be used to estimate the number of holes required to estimate the ice thickness to a given accuracy. Figure 8 shows the 90% confidence limits on the mean calculated using this procedure plotted against N. To obtain the mean thickness of the unridged portion of the multi-year floe accurate to better than 0.5 m, with a 90% certainty, only 6 holes are necessary. On the other hand, for an accuracy of 0.1 m with the same certainty, 100 holes would be required.

⁵Koerner, R. M. (1971). Ice balance in the Arctic Ocean. AIDJEX Bulletin 6, 11-26.

⁶Fukutomi, T. and Kusunoki, K. (1951). On the form and formation of hummocky ice ranges. Low Temperature Science 8, 59-88.

⁷Weeks, W. F., Kovacs, A. and Hibler W. D. (1972). Pressure ridge characteristics in the Arctic coastal environment. In "Proceedings First International Conference on Port and Ocean Engineering under Arctic conditions, 23-30 August 1971", Tech. University of Norway, 32 pp.

⁸Wittmann, W. and Schule, J. J. (1966). Comments on the mass budget of Arctic pack ice. In "Proceedings Symposium on the Arctic Heat Budget and Atmospheric Circulation (J. O. Fletcher, ed.), pp. 217-246. The Rand Corporation (RM-5233-NSF).

⁹Griffiths, J. C. (1967). Scientific Method in Analysis of Sediments, McGraw-Hill, New York, 303-310.

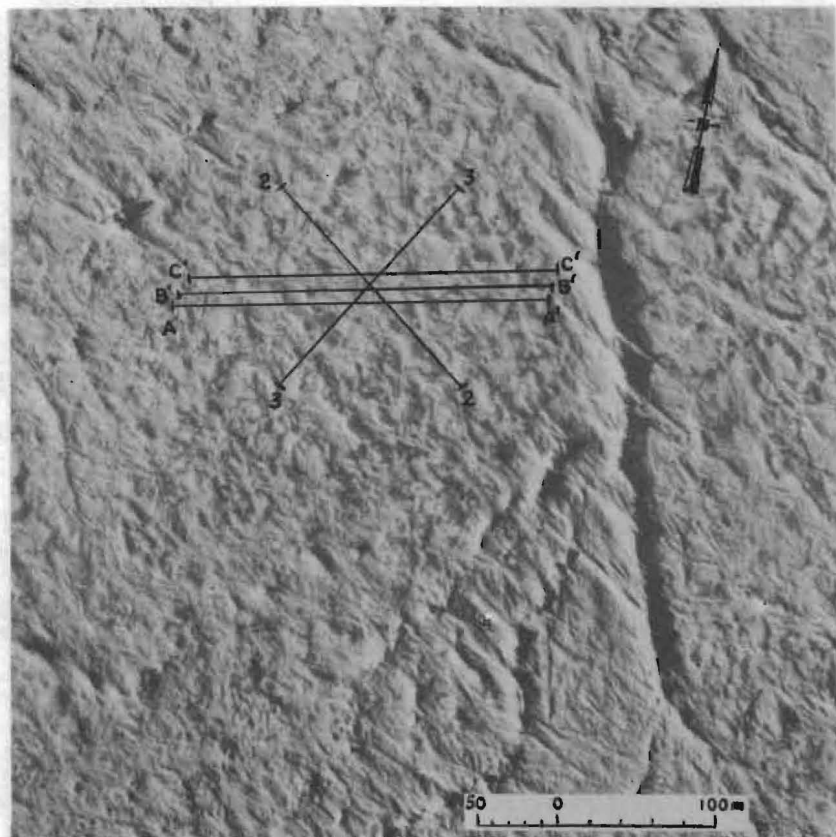


Figure 1. Aerial view of the multi-year floe that was studied. The locations of the profile lines along which snow and ice elevations and random thickness measurements were taken are marked.

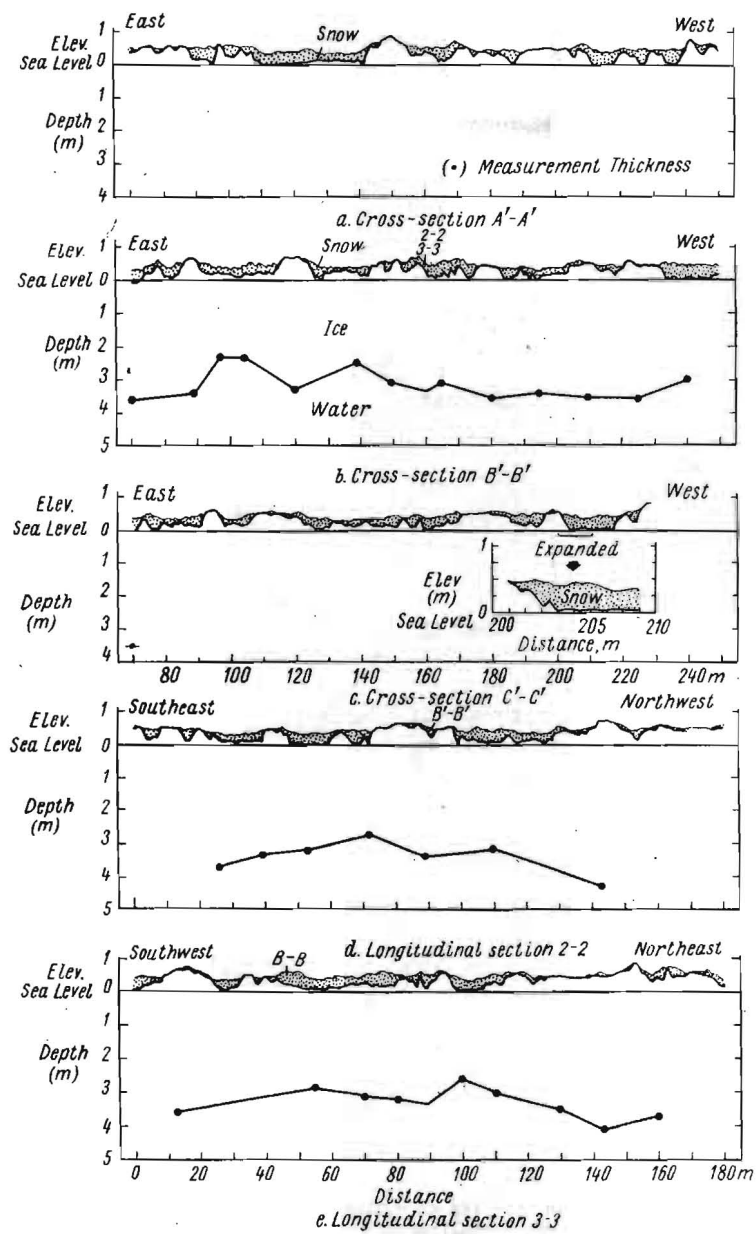


FIGURE 2.

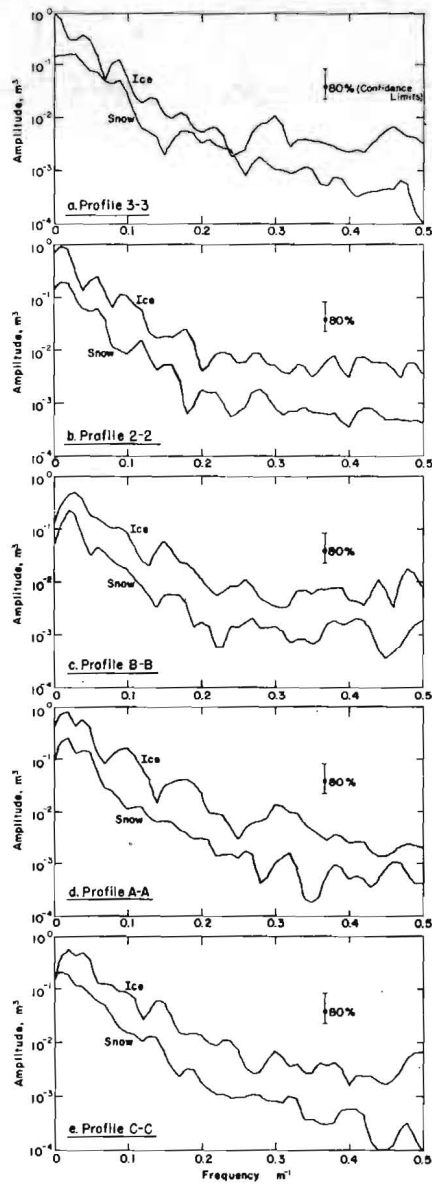


Figure 3. Snow elevation and ice elevation power spectra along five profiles. The spectra are normalized so that the total area under the spectral curves equals the total variance for any given profile. The y-axis amplitude represents the variance per frequency interval. The 80% confidence limits are as indicated.

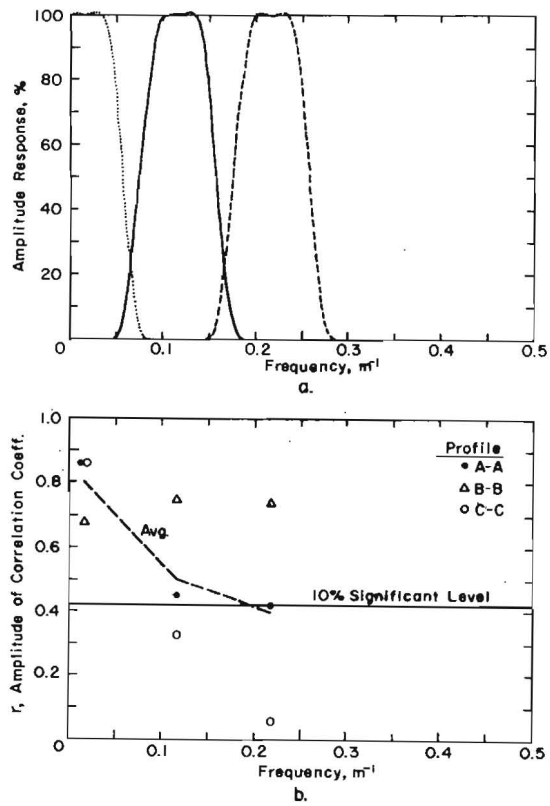


Figure 4. a) Frequency response of convolution filter weights and
 b) correlation coefficient amplitudes for each filtered profile. The line connects the average correlation coefficient result in each pass band. The 10% confidence level represents the value which would be exceeded 10% of the time by the correlation coefficient obtained from 18 random samples of uncorrelated normal variates.

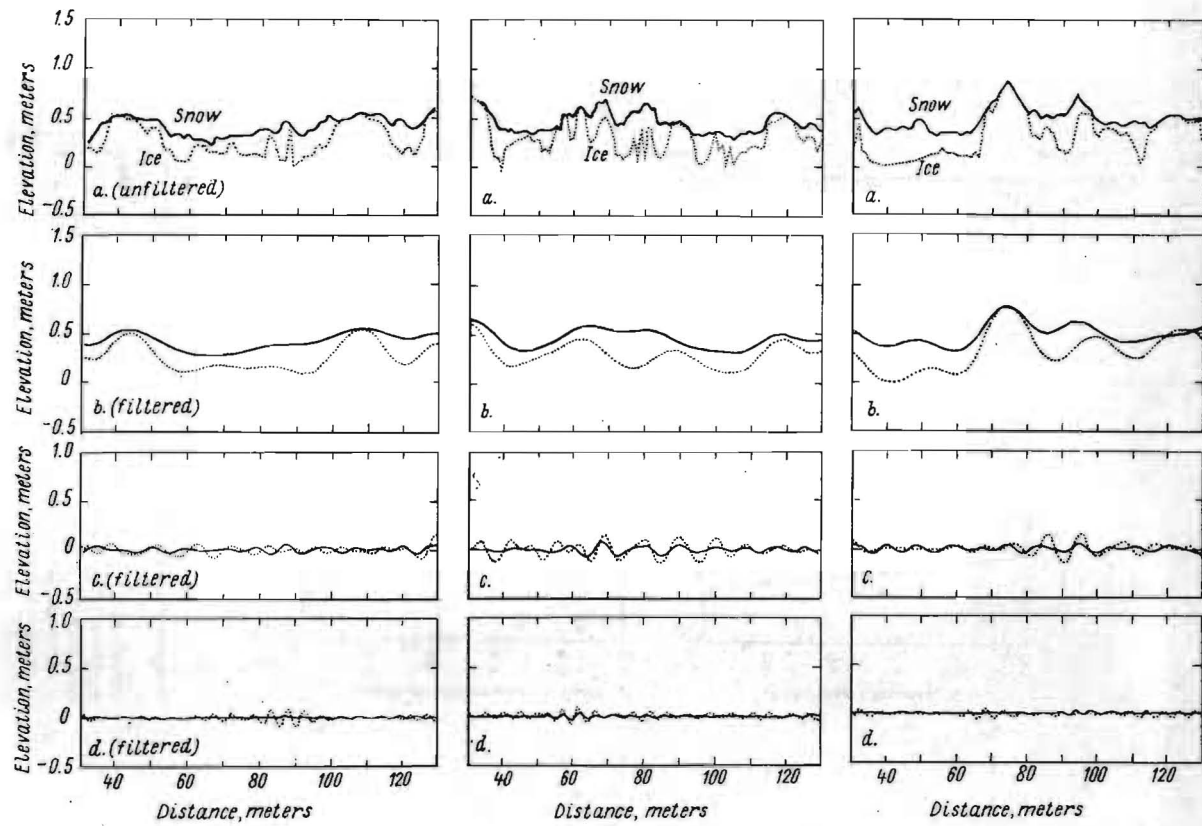


FIGURE 5.

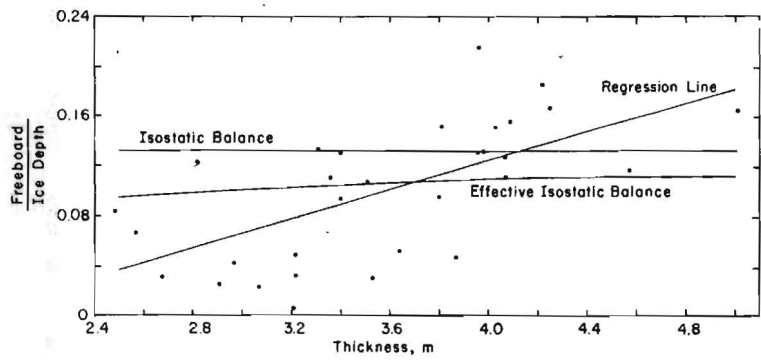


Figure 6. Ice freeboard/ice depth ratio (f/d) versus ice thickness (t). The isostatic balance line was calculated assuming ice and sea water densities of 0.91 and 1.03 gm/cm³. In the effective isostatic balance the weight of the snow was also included.

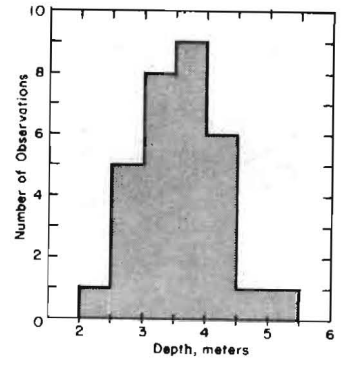


Figure 7. Distribution of ice thickness measurements.

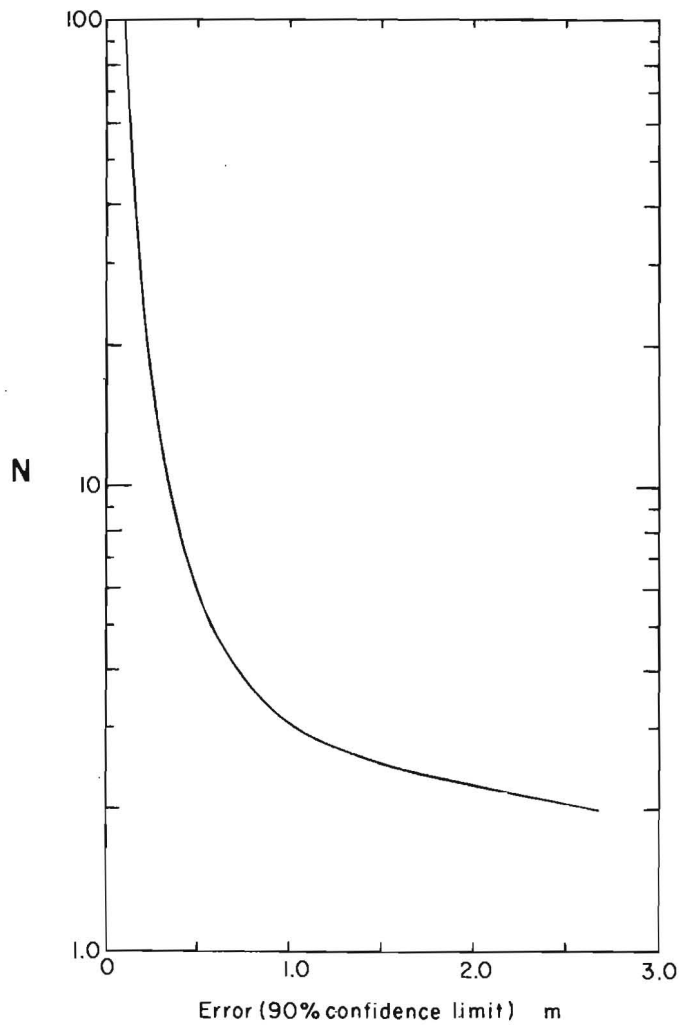


Figure 8. Estimated error (90% confidence limits) of the mean ice thickness as a function of the number of holes used in making the estimate.



A NEW APPROACH TO FIELD AND LABORATORY
TESTS OF TENSILE, COMPRESSIVE, AND FLEXURAL
STRENGTH OF POLYCRYSTALLINE, FRESH WATER
ICE

René O. Ramseier, Research Scientist Department of the Environ- Ottawa,
David F. Dickins, Physical Scientist ment, Inland Waters Branch Ontario,
Canada

SYNOPSIS

Field tests of the strain and the resulting stress calculations for ice shelves gave values which agreed well with the results of laboratory tests of tension and compression under uniaxial conditions. A hyperbolic sine function

$$\dot{\epsilon}/D = A [\sinh \alpha \sigma/E]^n$$

is proposed, where $\dot{\epsilon}$ is the strain rate, D is the self-diffusion coefficient, σ is the stress, E is the apparent elastic modulus, and A , α and n are constants. The equation applies within the range $2 \times 10^2 < \dot{\epsilon}/D \leq 2 \times 10^{13} \text{ m}^{-2}$. It is shown that the uniaxial tension results, from laboratory studies, are directly related to the flexural strength values, reported with beam studies.

RESUME

Les calculs de contrainte obtenus expérimentalement sur le terrain concernant la déformation relative de la calotte glaciaire concordent bien avec les résultats des essais de laboratoire qui ont été effectués sous des conditions uniaxiales sur la tension et la compression. Il est proposé dans ce rapport, une fonction sinusoidale hyperbolique telle que:

$$\dot{\epsilon}/D = A [\sinh \alpha \sigma/E]^n$$

ou $\dot{\epsilon}$ est le taux de déformation relative, D le coefficient d'auto-diffusion, σ la contrainte, E le coefficient apparent d'élasticité et A , α et n sont des constantes. L'équation s'applique dans les limites $2 \times 10^2 < \dot{\epsilon}/D \leq 2 \times 10^{13} \text{ m}^{-2}$. Il est démontré aussi que les résultats de laboratoire obtenus pour la tension uniaxiale, sont directement liés aux valeurs de la contrainte de flexion obtenues à partir des études de déformation de poutres.

Only a few countries have been acquainted with the navigational problems in ice-infested, inland waters and thus have researched them in past years.¹⁻³ Both the results of oil exploration in ice-infested waters and the extension of the navigable season in the St. Lawrence Seaway and the Great Lakes intensified the recognition of scale effect in testing ice under field and laboratory conditions. For example, a more accurate forecast is greatly needed of the behaviour of fresh-water ice types during the break-up in order to schedule the shipment of material and goods in inland waters which are associated with the use of fresh-water ice breakers and the water level of rivers and reservoirs.⁴

TENSILE AND COMPRESSIVE STRENGTH OF POLYCRYSTALLINE ICE

Recently small-scale laboratory tests^{5,6} of the low - stress behaviour of equiaxed polycrystalline ice gave values which apparently agree with values from large-scale field experiments^{7,8}. The laboratory tests with the use of cylindrical samples were conducted under compression and tension.⁶ The cylinder had a diameter of 0.025 m and a ratio of length to diameter equal to 3:1. The material was fine - grained with random crystallographic orientation.

The lines in Figure 1 represent the field results of ice shelves obtained by Thomas⁷ and Holdsworth⁸ and the extrapolated values for laboratory tests by Barnes et al.,⁵ and Ramseier.^{6,9} As can be seen, the agreement is good even though no

1. Butiagin, I.P. (1966). Strength of ice and ice cover. Izdatel'stvo "Nauka" Sibirskoe Otdeleniye, Novosibirsk, pp. 154.
2. Peschanskiy, I.S. (1967). Ice science and technology. Ledovedeniye i ledotekhnika, Gidrometeorologicheskoye Izdatel'stvo, Leningrad.
3. Lavrov, V.V. (1969). Deformation and strength of ice. Deformatsiya i prochnost' l'da. Gidrometeorologicheskoye Izdatel'stvo, Leningrad, pp. 164.
4. Balanim, V.V. Personal communication.
5. Barnes, P., Tabor, D., and Walker, J.C.F. (1971). The friction and creep of polycrystalline ice. Proc. Roy. Soc. Lond. A. 324, 127-155.
6. Ramseier, R.O. (1972). Growth and mechanical properties of river and lake ice. D.Sc. Thesis, Laval University, Québec, Province of Québec, Canada, pp. 26.
7. Thomas, R.H. (1971). Flow law for Antarctic ice shelves. Nat. Phys. Sci. 232, 85-87.
8. Holdsworth, G. (1972). Erebus Glacier tongue McMurdo Sound, Antarctica. Paper in preparation.
9. Ramseier, R.O. Mechanical properties of snow ice. Proc. Int. Conf. Port and Ocean Engineering Under Arctic Conditions, Trondheim, 17 p.

allowance has been made for the differences in grain sizes of the ice. The very low values for stress from field measurements could not be duplicated practically in the laboratory because similar tests in a laboratory would have to be of extremely long duration.¹⁰

Based on the obtained results the following law is proposed for the range $2 \times 10^2 < \dot{\epsilon}/D \leq 2 \times 10^{13} \text{ m}^{-2}$,

$$\dot{\epsilon}/D = A' [\sinh \alpha \sigma/E]^n \quad (1)$$

where $\dot{\epsilon}$ is the strain rate, D is the self - diffusion coefficient¹¹, σ is the applied normal stress, E is the apparent elastic modulus which takes into account the grain boundary effects $E = (5150 - 66\theta)\text{MNm}^{-2}$ ($\theta = \text{temperature } ^\circ\text{C}$) and the constants $A' = 1.76 \times 10^{10} \text{ m}^{-2}$, $\alpha = 1.31 \times 10^3$, and $n = 3.56$. In summary, a good correlation between small scale laboratory tests in compression and tension and field tests of low stress has been obtained in the ductile region without the use of a scale factor. We hope that further data may be available from the U.S.S.R. and the U.S.A. ice islands to verify the proposed law at even lower stresses.

FLEXURAL STRENGTH OF POLYCRYSTALLINE ICE

Although the testing methods have been greatly improved,^{1,3,12-15} important variables which affect the end results have been ignored in many cases. Among them the effect of strain rate or stress rate, correction for buoyancy, and ice type are probably the key parameters which were not investigated thoroughly. Based on the work of Carter^{16,17} and Ramseier^{6,9} it was shown¹⁴, by using the results of beam tests, that an apparent stress increase could account for as much as

10. Weertman, J. (1969). The stress dependence of the secondary creep rate at low stresses. *J. Glaciology*, 8, 494-495.
11. Ramseier, R.O. (1967). Self - diffusion of tritium in natural and synthetic ice monocrystals. *J. Appl. Phys.*, 38, 2553-2556.
12. Palosuo, E. Personal communication.
13. Dykins, J.E. (1971). Ice engineering - material properties of saline ice for a limited range of conditions. Naval Civil Engineering Laboratory, Port Hueneme, California. Technical Report R 720, pp. 96.
14. Lafleur, P. (1970). Propriétés mécaniques de la glace de neige en flexion. M.Sc. Thesis, Université Laval, Québec, Province de Québec, Canada, pp.81.
15. Ramseier, R.O. and Dickins, D.F. (in preparation). Cantilever beam tests in the St. Lawrence Seaway.
16. Carter, D. (1971). Lois et mécanismes de l'apparente fracture fragile de la glace de rivière et de lac. D.Sc. Thesis, Université Laval, Québec, Province de Québec, Canada, pp. 392.
17. Carter, D. (1970). Brittle fracture of snow ice. Intern. Assoc. Hydraulic Research Symposium on ice and its action on hydraulic structures, Reykjavik, Iceland. 5.2.1-5.2.8.

50 per cent of the failure stress under flexure. The results for tension and compression, presented in Figure 2, show that the behaviour of ice is distinguished by two regions: ductile region (I) and brittle region (II). Region I has no-crack formation zone, Ia, and crack formation zone, Ib; region II has ductile - brittle transition zone, IIa, and the quasi-brittle zone, IIb. The results of the flexure tests fall into zones Ia, Ib, and IIa. The transition zone for flexure encompasses Ib and IIa.

The stress which is required to nucleate a crack σ_n has to be equal to the plastic stress σ_p at the no-crack to crack formation zone, and equal to the elastic stress σ_e at the transition to the quasi-brittle zone. It follows then that the equations for stress, in terms of the bending moments M_e and M_p , for the elastic and plastic case, respectively, can be set equal to

$$\sigma_n = \sigma_p = M_p/Z = M_e/S = \sigma_e \quad (2)$$

where Z is the plastic modulus and S is the section modulus. The value for factor K was obtained¹⁴ from

$$K = Z/S = \frac{2(h/4)(bh/2)}{(bh^3/12)/(h/2)} = 1.5 \quad (3)$$

where h and b are the height and the width of the beam respectively. Consequently the apparent stresses will be up to 1.5 times greater than the real stress going from the no-crack to crack transition to the quasi-brittle zone. Applying this correction to the flexure strength results, a 1:1 relationship was obtained¹⁴ between the flexural strength of beams and the direct tension test of Carter¹⁷ and Ramseier⁹ for snow ice.

Therefore, the no-crack zone in flexure is identical to the proposed law (equation 1) for the range $2 \times 10^2 < \dot{\epsilon}/D \leq 1 \times 10^9 \text{ m}^{-2}$. The flexural strength becomes equal to the ultimate tensile strength which is independent of $\dot{\epsilon}$ ¹⁶ in the crack-formation zone as illustrated in Figure 2 for $\dot{\epsilon}/D > 1 \times 10^9 \text{ m}^{-2}$.

With the above presented material we have been able to relate some of the basic laboratory tests, such as pure tension and compression, to the deformation of large floating ice masses and the flexural strength of beams.

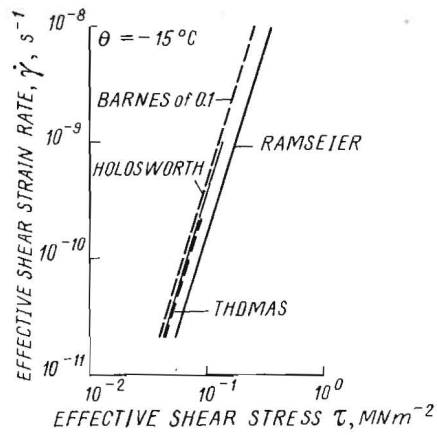


Fig. 1. Low stress-strain rate lines from extrapolated laboratory results and field measurements.

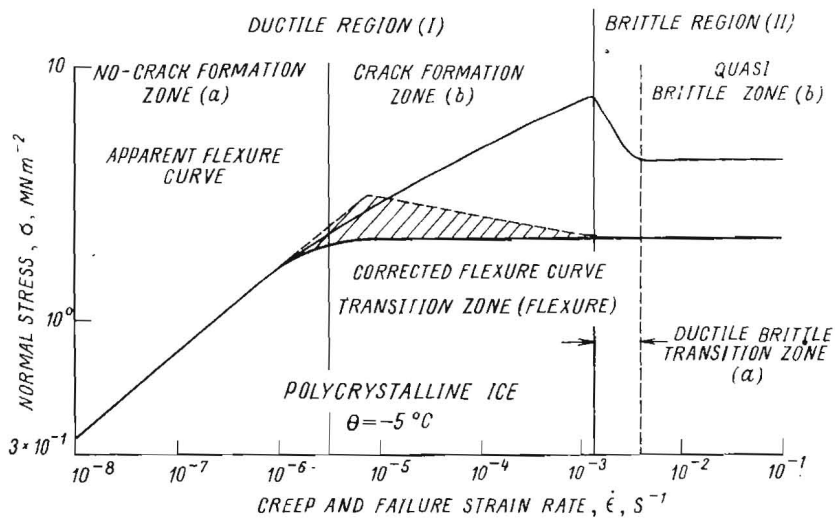


Fig. 2. Stress-strain rate for uniaxial tension and compression and flexural strength.



STEADY MOTION OF PACKED FINE-FRAGMENT-
ED ICE MASSES IN A STRAIGHT RIVER REACH

D.F. Panfilov, M. Sc. (Eng.), the Gorki Institute of Civil Engineering, Gorki, U.S.S.R.
Associate Professor,

SYNOPSIS

The steady motion of ice compacted by the flow is considered in a straight reach of a wide rectangular channel, with the flow velocities across the river width assumed to be equal and ice accumulations to obey the laws of mechanics of non-cohesive media. The river is supposed to be blocked at the downstream end of the reach either by a natural obstruction (e.g. ice cover, or ice jam) or an artificial one (e.g. a dyke to hold the river ice, or bridge piers) which does not lead to a considerable rise in the water stage, and so does not materially affect the upstream flow conditions. Analysis resulted in the evaluation of the mean ice drift velocity, and the maximum ice pressures. Conditions are established governing ice movement in a river channel free of obstructions.

RESUME

On étudie le mouvement permanent des masses de glace compactées par l'écoulement dans un tronçon droit d'un large chenal rectangulaire. On envisage que les vitesses d'écoulement de l'eau sont égales sur toute la largeur de la rivière et que les accumulations de glace obéissent aux lois de la mécanique d'un milieu non-cohérent. A l'aval du tronçon considéré la rivière est supposée d'être rétrécie par des obstacles naturels (couverture de glace, empilement de glace) ou artificiel (mur de retenue de la glace, piles de pont) qui ne conduisent pas à une remontée considérable du plan d'eau et, donc, n'ont pas de l'influence sensible sur le régime d'écoulement en amont de ceux-ci. A la suite de l'analyse on a déterminé la vitesse moyenne du mouvement et la pression maximale des masses de glace, les conditions de mouvement de celles-ci dans une rivière sans obstacles étant établies.

The ice cover L long, B wide and of average thickness h is subjected (Fig. 1) to the action of:
hydrodynamic pressure

$$F_0 = \frac{\gamma_0}{2g} B h (V_0 - V_1)^2 \quad (1)$$

gravity force component in the direction of the flow

$$F_1 = \gamma_1 h L B J (1 - \varepsilon) \quad (2)$$

flow friction across the underside of the ice cover

$$F_2 = \gamma_0 H_2 L B J (1 - \theta) \quad (3)$$

air friction across the upper side of the ice cover

$$F_3 = \lambda L B (V_2 - V_1)^2 \quad (4)$$

ice mass friction against the river banks

$$F_4 = 2h \int_0^L \tau_x dx \quad (5)$$

and the frontal resistance of the obstruction, F_c (determined with particular reference to its type, configuration and dimensions)

In these formulae $\theta_1 = \frac{V_1}{V_0}$; $V = \Psi V_*$; $V_* = \sqrt{g H J}$;

$$\Psi = 2.8 \left[1 + \frac{1}{2\alpha_1} - \exp\left(2 - \frac{1}{2\alpha_1}\right) \right]; \quad \alpha_1 = \frac{\sqrt{2g} \Pi_1}{H^{\eta_0}};$$

$$H_2 = \eta_2 H; \quad \eta_2 = \frac{\alpha^{6/5}}{1 + \alpha^{6/5}}; \quad \alpha = \frac{\Pi_2}{\Pi_1};$$

where V_1 and V_0 = ice mass and surface water layer motion velocities, respectively; V_2 = wind velocity; γ_1 and γ_0 = unit weights of ice and water, respectively; ε = porosity of ice accumulations; J = hydraulic gradient; H = depth of flow under the ice cover; Π_1 and Π_2 = roughness coefficients of the channel and ice cover underside; λ = friction coefficient across the air-water boundary. (See the scheme in Fig.)

Pariset and Hausser [1] used the Yansen silo theory while Michel and Ouellet [2] applied that of Caquot to determine shearing stresses along the contact between the ice mass and the bank. However, these theories are yet insufficiently accurate, viz. they neglect the considerable initial adhesion of the ice masses.

[1] Pariset E., Hausser R., Formation and evolution of ice cover in rivers. Trans., E.I.C., Vol.5, No 1, p.11, 1961.

[2] Michel B., Ouellet Y., Pousseed'un champ de glaces morcelees sur ouvrage. AIRH, Onzieme Congres, Vol.V, seminaires, Leningrad, 1965.

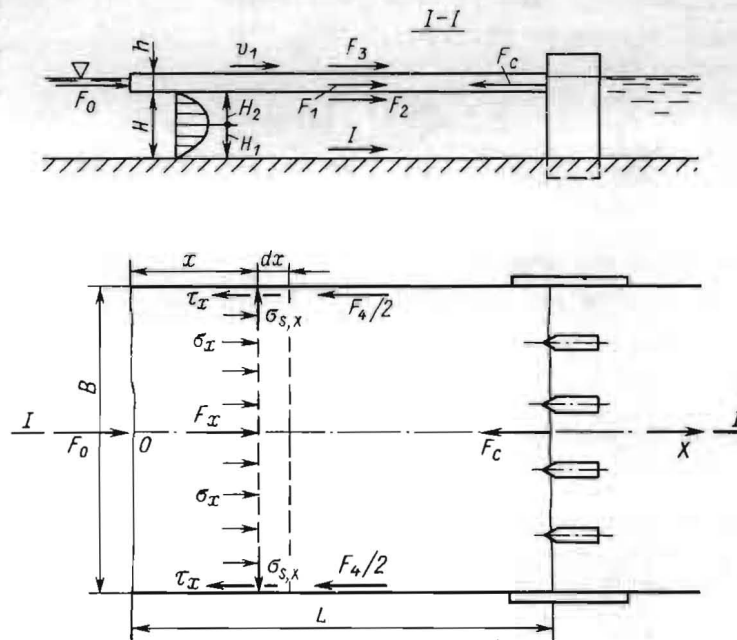


Fig. Diagram of forces acting on the ice cover.

Therefore, we make use of other, more general theories of non-cohesive media.

Thus, borrowing the relation for the lateral thrust coefficient established by G.I. Pokrovsky [3], one can write

$$\tau_x = \xi (\sigma_x + k \zeta) \quad (6)$$

where

$$\xi = (1 - 0.74 \operatorname{tg} \beta) \operatorname{tg} \delta; \quad \zeta = \frac{1 - 1.52 \operatorname{tg} \delta}{(1 - 0.74 \operatorname{tg} \beta) \operatorname{tg} \delta}; \quad \sigma_x = \frac{F_x}{Bh};$$

F_x = total ice pressure in the direction of the flow at the distance x from the upstream edge of the ice cover; k = adhesion coefficient; β = internal friction angle of the ice mass; δ = friction angle of the ice mass against the river banks (in many cases δ may be taken equal to β).

[3] Klein G.K., Structural mechanics of non-cohesive bodies, Moscow, 1956.

According to V.V. Sokolovsky's theory of limit equilibrium of a non-cohesive medium [1] we have

$$\tau_x = \xi (\sigma_x + kctg\rho) \quad (7)$$

where

$$\xi = \frac{\sin\delta}{1 + \sin\rho} (\cos\delta - \sqrt{\sin^2\rho - \sin^2\delta}) \exp\left[\left(\delta - \arcsin \frac{\sin\delta}{\sin\rho}\right)tg\rho\right]$$

The total pressure F_x can be found by solving the differential equation

$$\frac{dF_x}{dx} + 2 \frac{\xi}{B} (F_x + F_k) - \gamma_0 H_2 B J (\theta - \theta_1) = 0 \quad (8)$$

obtained for equilibrium conditions of an ice cover element with the dx dimension along the flow, and expressed by

$$F_x = F_0 \eta_x - (1 - \eta_x) [F_k - A(\theta - \theta_1)] \quad (9)$$

where

$$A = \frac{\gamma_0 H_2 J B^2}{2\xi}; \quad \theta = 1 + \frac{\gamma_1 h}{\gamma_0 H_2} (1 - \varepsilon) \pm \frac{\lambda V_2^2}{\gamma_0 J H_2}; \quad \eta_x = \exp\left(-2\xi \frac{x}{B}\right)$$

$$F_k = \begin{cases} Bhk\xi & \text{for Eqn (6)} \\ Bhkctg\rho & \text{for Eqn (7),} \end{cases}$$

each of them yielding its own value of the ξ coefficient for the stress τ_x .

A positive wind pressure term is used with a following wind, and a negative one with a head one.

By integrating Eqn (5) taking account of (9) the value of the force becomes

$$F_x = \gamma_0 H_2 L B J (\theta - \theta_1) + (1 - \eta_x) [F_0 + F_k - A(\theta - \theta_1)] \quad (10)$$

Steady ice mass movement at velocity, V , appears to be possible under the condition

$$F_0 + F_1 + F_2 \pm F_3 - F_4 - F_c = 0 \quad (11)$$

The formula of mean velocity of ice motion in the reach above the obstruction may be obtained by substituting the expression for the forces into the condition

$$\frac{V_1}{V_0} = \theta - \frac{F_c - F_0 \eta_x + F_k (1 - \eta_x)}{A (1 - \eta_x)} \quad (12)$$

[1] Sokolovsky V.V., Statics of a cohesionless medium.

With large ratios of $\frac{L}{B}$ the function $\eta_L \rightarrow 0$ and Eqn (12) assumes the form

$$\frac{V_1}{V_0} = \theta - \frac{F_c + F_k}{A} \quad (13)$$

With $F_c = 0$, Eqn (13) can be used to evaluate the ice accumulation movement velocity in an obstructionfree channel.

The formulae derived permit to solve certain engineering problems, other than determining ice motion velocity affecting the water stage. Thus, the maximum ice pressure against ice-retaining structures may be obtained, given

$V_1 = 0$ and $\eta_x = 0$ in Eqn (9), i.e.

$$F = A \left[1 + \frac{\gamma_i h}{\gamma_0 H_2} (1 - \varepsilon) + \frac{\lambda V_2^2}{\gamma_0 H_2 J} \right] - F_k \quad (14)$$

The conditions for ice mass movement upstream from the obstruction without ice jam formation may be formulated as:

$$F_c + F_k \leq A \left[1 + \frac{\gamma_i h}{\gamma_0 H_2} (1 - \varepsilon) - \frac{\lambda V_2^2}{\gamma_0 H_2 J} \right] \quad (15)$$

With $F_c = 0$ the latter inequality expresses the conditions for ice mass movement in an open channel without ice jam formation.



ISRAEL RIVER ICE JAM

G. Frankenstein, Research Engineer	U.S. Army Cold Regions	Hanover
A. Assur, Chief Scientist	Research and Engineer-	New Hamp-
	ing Laboratory	shire,
		U.S.A.

SYNOPSIS

In December of 1967 Northern New England experienced an extended period of mild weather. Ice in the Israel River broke up and formed a jam near Lancaster, NH. without serious flooding. Subsequent severe weather led to the production of frazil ice and solidification of the ice jam. Ice observations and recommendations were made to prevent flood damage. Rapid thawing with rain in March produced a new ice jam with catastrophic flooding and damage in the neighborhood of 0.5 million dollars. Several reasons are advanced for susceptibility of sites to ice jamming. Two criteria are derived which show critical numbers for ice clogging when the surface cannot accommodate the ice discharge and ice jamming when the channel cannot transport the ice. Model tests for verification are planned.

RESUME

Pendant une période assez étendue en décembre, 1967, il faisait doux dans le nord de la Nouvelle-Angleterre, aux Etats Unis. La glace du fleuve Israel s'est rompue et a formé un embâcle près de Lancaster, N.H., sans débordement sérieux. Le temps rigoureux qui a suivi a produit de la glace du type frazil et l'embâcle s'est solidifié. On a fait des observations et des recommandations pour éviter des dommages causés par un débordement. On n'a pas suivi ces recommandations. Une fonte rapide des neiges à cause des pluies en mars a produit un nouvel embâcle avec un débordement catastrophique et des dommages d'environ 0.5 millions de dollars. On suggère plusieurs raisons pour lesquels les endroits soient susceptibles à des embâcles. On dérive deux critères qui montrent des nombres critiques pour l'obstruction d'un fleuve quand la superficie du fleuve ne peut pas porter la charge de glace et pour la formation des embacles quand le lit du fleuve ne peut pas transporter la glace. On projéte des essais avec des modèles pour vérifier.

ICE JAM OBSERVATIONS

Cold weather came early to New England during the 1967/68 winter. Unusual amounts of ice formed in smaller rivers and lakes. Lancaster, N.H. had early production of ice on the Israel River which flows through the center of town and is heavily constrained by structures.

In mid-December temperatures climbed above freezing. This combined with rain caused the Israel River ice to break up and move down the stream. The ice pieces were 15 to 20 cm in diameter and 10-15 cm thick.

The moving ice jammed up at Pt. 2, Figure 1, and piled up to Pt. 3.

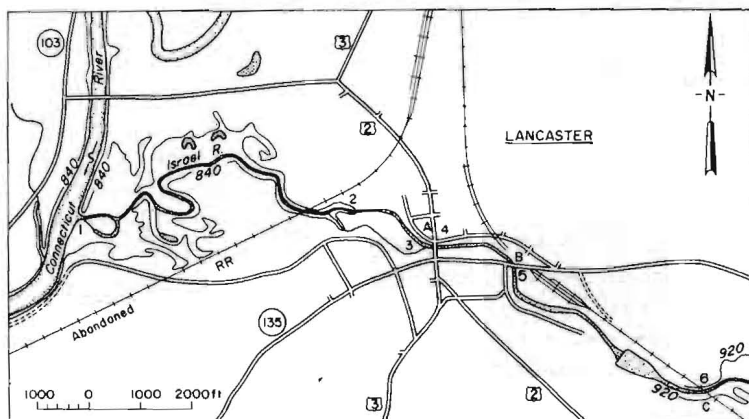


Figure 1. Ice jams in Israel River, N.H., 1967/68.

Much of this ice was in contact with the river bed which typically was covered with boulders and gravel. There was some minor flooding. The water soon cut a channel through and over this jammed up ice.

The temperatures soon dropped and the open reaches of the river soon froze over again. However, much frazil ice was produced before the shallow open water areas froze. This frazil ice moved into the jammed ice which contributed to further blocking of the channel.

Due to these conditions it was felt that the chances for a major spring ice jam were very high. A careful survey was made of the river and ice conditions to find ways to lessen the chances of a major flood. The following measures were recommended:

- 1) Construct a temporary earth dyke just above Pt. 6 (Fig. 1). The dyke would hold the upper river ice and allow it to melt in place as well as hold back much of the newly formed frazil ice. The construction of such a dyke was by far the best solution to the prevention of a major flood.
- 2) Dust the trouble area below the jam in the spring with dark material and therefore hasten the breakup.

3) Remove the formed ice by explosives.

Dr. B. Michel participated in the survey and recommendations.

For reasons unknown to the authors no preventive measures were taken assuming that a normal breakup would occur.

Ice thicknesses were measured weekly in January and February. By mid-February much of the river from the covered bridge, Pt. 5, to the toe of the ice jam was frozen to the bottom. These surveys gave no indications that the chances of having a major spring flood had lessened. The observations were similar to those reported by Frankenstein (1971)¹⁾ on the White River, Hartford, Vt.

On 16th March intense thawing started. Soon the ice in the upper reaches of the river broke up. The moving ice stopped at the jam formed in December and proceeded to form a new and bigger jam. The ice pieces averaged about a meter in diameter. Some were frozen 1 m thick. Figure 2 shows the



Figure 2. View of ice jam at bridge.

ice conditions at the Main Street bridge just up from the toe of the new jam.

The water level continued to rise to such an extent that flooding increased to major proportion. The water had to find its way around the constriction through the streets. The town hall was completely under water. The water rose as fast as 1.8 m in 20 minutes. Flooding started on 19 March and continued until the evening of 23 March.

The total flood and ice damage was estimated to exceed \$500,000. Damage cost was far in excess of a temporary dyke.

To avoid future floods due to ice some channel improvements were made subsequently between Pt. 2 - 3 (Fig. 1). A dam is proposed at Pt. 6. The local topography is almost ideal for an ice wasting pool since extensive meadows lie above Pt. 6.

- 1) Frankenstein, G. (1971): The modification of a river to prevent ice jams, ASCE, Speciality Hydraulics Conference, Iowa City.

ICE JAM CRITERIA

The discussed site has the following characteristics, all conducive to ice jamming:

- 1) Located near the White Mountains the tributaries have high slopes leading to rapid increase in discharge including the necessity to discharge ice.
- 2) Located near the Atlantic Ocean in a maritime province sudden thawing weather is not unusual.
- 3) The bed is rough, as not unusual for a mountain river with boulder and rock ledges, as well as vegetation hindering the discharge of ice.
- 4) Past construction measures narrowed the available width especially for flood stages so that the ice carrying capacity is sharply reduced.
- 5) Relatively thin ice in its early stages breaks up. With limited width clogging occurs even at that stage.
- 6) The river is shallow which severely increases the probability of jamming.
- 7) A sudden transition to small slopes due to backwater from the Connecticut River (power stations) is probably the main cause for the formation of the foot of the ice jam.

This and many similar occasions invite the formulation of criteria for ice jamming depending upon morphological factors so that an orderly analysis of sites subject to frequent ice jams can be made as well as a prediction how channel modifications affect the probability of ice jams. Such criteria were proposed by Assur (1961)²⁾ in an unpublished note.

The ice discharge Q_i [m^2/sec] for floating ice pieces is

$$Q_i = b v_o p_2 h_i \quad (1)$$

b - width of water surface, v_o - average velocity of moving ice, h_i - thickness of ice, p_2 - coverage of surface with ice (0→1).

After ice pieces clog and pile up but the whole layer of broken ice still moves the ice discharge is

$$Q_i = b v_o p_3 h \quad (2)$$

p_3 - solidity of ice mass, h - overall thickness of broken up ice layer.

The water discharge Q_w without ice corresponds to an average water depth H which is increased by

$$\Delta H = p_2 \gamma_i h_i \quad (3)$$

due to ice volume alone (γ_i - ice density).

The ice velocity v_o can be related to average velocity by $v_o = \psi v$, where v can be calculated from the modern version of Chezy's equation

$$v = \sqrt{\frac{8g}{f} RS} \quad (4)$$

g - acceleration of gravity, f - dimensionless friction constant, R - hydraulic radius, S - slope where

$$V \sqrt{\frac{g}{f}} = c \left(\frac{R}{N} \right)^{1/6} \quad (5)$$

with c and $n = N^{1/6}$ the Manning coefficients as a simplified representation (N - friction height).

In assuming that ice clogging and piling up begins with close packing of broken surface ice we derive

$$P_2 = G_2 \frac{Q_i}{b h_i R^{2/3} S^{1/2}} \quad (6)$$

when P reaches a critical value, say 0.70(?).

$$G_2 = \frac{N^{1/6}}{D C} \quad (7)$$

However, ice can continue to move in a multiple broken up layer until it fills a sufficient part of the available channel to come to a standstill and form an ice jam. This critical condition is characterized by

$$P_3 = G_3 \frac{Q_i}{b H^{2/3} S^{1/2}} \quad (8)$$

with

$$G_3 = \frac{N^{1/6}}{D C \gamma [\beta (1 + P_3 \gamma) \gamma']^{2/3}} \quad (9)$$

$\gamma = h/H$ critical ratio of thickness of broken ice layer to available water depth. P_3 is somewhat less than P_2 . $\beta = \beta P_w$; P_w - wetted perimeter.

These relationships are helpful in designing channel modifications to handle the discharge of ice without difficulties. It is planned to test the validity of these criteria in model experiments.

LOCATION AND GEOGRAPHY

Lancaster, N.H. is located on the Israel River in Northern New England. It is approximately 2.4 km from its confluence with the Connecticut River and slightly above 300 km north of Boston, Mass.; 75% of its 3200 inhabitants live in the central area subject to flooding.

The Israel River is a tributary of the Connecticut River with a length of 34 km and a drainage area of 344 km². The watershed area is generally steep above the ice jam location and flat below. The slope is 0.0049 from the Main Street bridge to Pt. 2 (Fig. 1) and 0.00095 below Pt. 2 to the mouth.

- 2) Assur, A. (1961): Criteria for ice jamming, USACRREL Technical Note 61-II-26.



CALCULATION OF THAWING ICE COVER STRENGTH
AND FREEZE-UP AND BREAK-UP PERIODS IN
RESERVOIRS

S.N. Bulatov, D.Sc.(Eng.), Head of the Lab. The U.S.S.R. Hydro- Moscow,
 meteorologic Centre U.S.S.R.
B.M. Ginzburg, Sr Res. Offr,
I.V. Balashova, Sr Res. Offr

SYNOPSIS

The method of estimating the strength of thawing ice cover on rivers and reservoirs depending on solar radiation absorbed by ice and its application both for calculating the beginning of the wind drift of ice on reservoirs with the account of wind velocity and for determining the ice disappearing date for the reservoir is discussed. The method of calculation of the equation parameters for the frequency curves of freeze-up and ice disappearing dates for the reservoirs from the climatic data is described. The frequency curves are approximated by the Pearson type III equation. The evaluation of changing the ice phenomena dates and the ice-free season duration as a result of reservoir establishing on large rivers is given.

RESUME

On expose la méthode de l'évaluation de la solidité du manteau glacial en fonte des rivières et des réservoirs selon le rayonnement absorbé par la glace et l'utilisation de cette méthode pour calculer le commencement de la dérive de vent de la glace dans les réservoirs tenant compte la vitesse du vent aussi que pour déterminer la période de la délivrance des réservoirs de la glace. On décrit la méthode de calcul des paramètres des équations des courbes de fréquence des délais de prise en glace et de la délivrance des réservoirs d'après les données climatologiques. On décrit approximativement les courbes de fréquence à l'aide de l'équation de Pearson du type III. On donne l'évaluation des changements des délais des processus glaciaux et de la durée de la période sans glace grâce à la création des réservoirs sur de grandes fleuves.

The economy of water carriage defines the striving for increasing the duration of sailing on inland waterways. The beginning of transit sailing on rivers in the spring is prevented by the delay of ice clearance of the reservoirs as compared to the rivers on which these reservoirs exist. The up-to-date river boats, however, can navigate not only before the last ice date but even before the beginning of ice drift, if the ice cover strength does not exceed the fixed limits.

The evaluation of strength of the thawing ice cover is of great value for the designing and operation of hydrotechnical constructions, autoroutes on ice, ice river crossing, etc.

The strength of thawing ice cover depends mainly on the absorption of solar radiation by ice and the accumulation of liquid phase in it.

On the basis of field observations and laboratory experiments on the thawing ice the equation is obtained which combines the relative flexural breaking stress φ for the disappearing ice and the content of melt water in ice:

$$\varphi = (1 - \sqrt{S/S_0})^2 \quad (1)$$

In this equation $\varphi = \sigma/\sigma_0$, where σ is the flexural breaking stress of the disappearing ice (ultimate resistance), σ_0 is the same for the ice at 0°C, which was not influenced by the solar radiation, S is the content of melt water, expressed by the heat amount of solar radiation absorbed by the unit volume of ice,

S_0 is the amount of solar radiation after the absorption of which the ice-cover loses its strength completely. From the experiments on the ice specimens of different structure the value S_0 equals 27 cal/cm³ for fine crystal ice, 35 cal/cm³ for frazil ice and 55 cal/cm³ for snow ice.

The mean value of S_0 for the ice cover of the rivers and reservoirs equals 44 cal/cm³. It is determined by the strength of ice specimens, taken at a moment close to the complete loss of strength by the ice cover. The method of determining S_0 and the calculation technique (from the meteorological elements) of decreasing the content of melt water in ice as well as decreasing the ice strength when melting, are given in the monograph¹⁾.

1) S.N. Bulatov (1970). Rastchet prochnosti tajushego ledjanogo pokrova i natchala vetrovogo dreifa lda. Trudi Gidromet-sentra, vyp. 74, 117 str.

The wind is a main factor which determines the beginning of the ice drift on the reservoirs. The vertical component of wind velocity in certain conditions produces the pressure to the ice cover sufficient for its breaking.

The breaking pressure q produced by the loading P which is distributed over the area πr_0^2 is calculated by the equation obtained in accordance with the elasticity theory:

$$q = \frac{P}{\pi r_0^2} = \frac{\sigma h^2}{3(1+n)\ell^2 C_2(\alpha)} \quad (2)$$

where h is the ice thickness, σ is the breaking flexural stress, n is the Poisson coefficient, $C_2(\alpha)$ is the ratio function r_0/ℓ , $\ell = \sqrt[4]{D/\gamma}$ is the characteristic of ice cover, where D is a cylindrical stiffness of the slab and γ is the coefficient of elastic base.

The breaking pressure q becomes minimum if the loading is distributed over the area with the radius of 4,7-15,5 m. In this case equation (2) can be transformed as follows:

$$q_{min} = C \varphi h^{1/2} \quad (3)$$

where C is some dimensional coefficient, which may be considered constant, if by the beginning of ice drift the ice thickness is in the limits of 20-60 cm.

Equation (3) defines the condition of ice cover breaking due to the wind loading. This condition can be written in the following way:

$$\varphi h^{1/2} = m w^2 \quad (4)$$

where w is the wind velocity which is the greatest one of four observations made for 24 hours by the nearest meteorological station and m is the empirical coefficient. $m = 0,018$ if h is expressed in cm and w in m/sec. This coefficient is gained from the observations made on the Bratsk and Novosibirsk reservoirs.

The duration of ice drift, i.e. the date of ice clearance of the reservoir is calculated on the basis of heat balance from the meteorological data depending on the amount of ice (per unit area of the reservoir) remained by the date of ice drift.

For the calculation of the reservoir freezing Prof. Shuljakovsky's well known method¹⁾ is used.

By means of discussed methods the annual dates of freezing and ice clearance for all large reservoirs of the U.S.S.R. rivers were calculated. For the purpose of hydrotechnical design, however, such detailed calculations are unreasonable. It is sufficient to calculate the frequency curves of ice phenomena. These curves are approximated by the Pearson type III equation. It is suggested to calculate the parameters of this equation by the empirical formulae²⁾. The mean freeze-up and last ice dates for the reservoir are determined by accumulating the necessary sum of negative ($\Sigma\theta_-$) or positive ($\Sigma\theta_+$) daily mean air temperatures (C° by the climatic data).

$$|\Sigma\theta_-| = 10h + 37e^{-0.4h} + 175v + 2,7\theta' - 27 \quad (5)$$

where h is the mean depth of the reach (in meters; from 2 to 20);

v is the mean flow velocity (in m/sec);

θ' is the air temperature for the day of accumulation of the necessary $\Sigma\theta_-$.

$$\Sigma\theta_+ = 2,5|\Sigma\theta_-| - 0,2e^{0,062|\Sigma\theta_-|} - 53lg\left(1 + \frac{w}{W}\right) - 0,16Q' + 95 \quad (6)$$

where $\Sigma\theta_-$ is the sum of negative monthly mean air temperatures for the winter season (in C° 10 to 85°), w is the volume of water, flowing through the reservoir during two last decades of ice melting (in km^3), W is the volume of the reservoir in the end of winter decrease (in km^3), Q' is the daily mean heat influx from the solar radiation during two last decades of ice melting (in cal/cm^2 per 24 hours).

The other two parameters of the Pearson equation, that is the standard deviation from the mean date and the skewness coefficient of distribution, are determined for the reservoir by means of found relation with the same parameters for the particular river reach in natural conditions.

1) Shuljakovsky L.G. Pojavlenie lda i nachalo ledostava na rekah, ozerah i vodohranilishah. Raschety dlja tchelej prognozov. Gidrometeoizdat, M., 1960, 215 str.

2) Ginzburg B.M. O verojatnostnyh karakteristikah reshima samerzaniya i otchicheniya oto lda vodohranilish. Trudy Gidrometsentra S.S.S.R., vyp. 55, L., 1969, str. 102-115.

The duration of ice free period which defines the sailing period is calculated as the difference between the dates of first and last ice. These dates are independent values from the statistical point of view, therefore the parameters of the equation for the frequency curve can be obtained from the known formulae for the composition of two initial distributions.

The alteration of ice regime resulting from the reservoir establishment is determined both by the geographical conditions and hydrological regime of the river and by the peculiarities of established reservoir and flow control system. The change in the freeze-up dates compared to the same river reach depends on the ratio between the depth increasing and the decreasing of flow velocity. The freeze-up formation in the area of backwater wedge on the individual reservoirs occurs in times close to the dates of the ice appearing on the river. If the reservoir is situated in the cascade of hydropower plants the zone of freeze-up beginning displaces downstream and its dates approach to the dates of river freezing. The deep reaches of the reservoir near the dams freeze later than before the dam construction.

The dates of ice disappearing change depending on the direction of river flow, the duration of spring ice movement on it, and on the reservoir size and flowage. On rivers where the ice is broken mainly due to melting in situ the establishment of the reservoir does not delay ice disappearing. On rivers particularly those flowing from the South to the North, where the mechanical debacle by the spring flood wave is prevailing, the ice disappearing after the construction of hydropower plants occurs later as compared to the natural conditions. In the backwater wedge areas of the individual reservoirs on the rivers like that the dangerous ice dams are frequent.

The study of changes in the duration of ice free period showed that the favourable conditions for its increasing appear after the establishment of the reservoirs on large rivers especially those which flow from the north to the south. The sailing duration, all other conditions being equal, is always longer on deep and flowing reservoirs, especially those which are in the cascade of hydropower plants.



STATIC GROWTH OF BLACK ICE IN COLD REGIONS

Berhard Michel, Dr. Eng.
Professor of Ice
Mechanics

Université Laval

Quebec, Canada

SYNOPSIS

Many empirical formulas have been used to express the growth of black ice in Arctic regions. These formulas of the exponential type, take into account the number of degree-days of frost since the beginning of ice formation. They do not consider the thermal properties of the ice cover and this makes them very hard to use for particular applications, out of their broad context. Along lines used by Bilello (1), it is shown that the straightforward heat exchange formula with only one adjusted parameter gives a very good fit for ice formation in the McKenzie river and in the Beaufort sea for a period of six years from 1960 to 1966.

RESUME

Il existe de nombreuses formules empiriques pour exprimer la croissance de la glace noire dans les régions Arctiques. Ces formules, de type exponentiel, prennent en compte le nombre de degrés-jours de froid depuis le début de la formation de la glace. Il ne considèrent pas les propriétés thermiques de la glace, ce qui les rend difficiles d'utilisation dans les applications particulières, hors de ce contexte général. Suivant une méthode semblable à celle de Bilello (1), nous montrons que la formule directe d'échange thermique conduit à d'excellents résultats avec un seul paramètre ajusté et ce pour la formation de la glace dans la rivière McKenzie et la mer de Beaufort pour une période de six ans de 1960 à 1966.

INTRODUCTION

Up to now many global empirical formulas have been used to represent the average growth of ice in the Arctic regions. We note two of them:

The Lebedev formula² for the U.S.S.R. Arctic:

$$H = 1.245 S^{0.62} H_s^{-0.15} \quad (1)$$

where H and H_s are the ice and snow thicknesses in cm, and

$$S = \left| \int_{t_0}^t T_A dt \right| \quad (2)$$

S is the number of degree-days of frost since the beginning of ice formation at time t_0 , where t and t_0 are in days and T_A is the air temperature in $^{\circ}\text{C}$.

The Zubov formula³ also for the Kara and Chukhotsk seas:

$$H^2 + 50 H = 8 S \quad (3)$$

These formulas contain empirical coefficients that are adjusted for a best fit with the measured data, irrespective of varying ice thermal properties and of other important parameters. They are unyieldy in engineering applications where particular variables have to be varied.

BASIC HEAT TRANSFER FORMULA

The expression for the growth of a solid continuous ice cover from heat exchange with the atmosphere, under permanent conditions, in the case of black ice formation only with snow cover, has been known for a long time³ and its basic formulation is (Figure 1):

$$\gamma_i L \Delta H = \frac{K_i (T_c - T_s)}{H} \Delta t = \frac{K_s (T_s - T_a)}{H_s} \Delta t \quad (4)$$

where γ_i is specific weight of ice, L : latent heat of fusion of ice, t : time, T_a , T_s , T_c : temperature of the air, temperature at the snow-ice interface and at the water-ice interface which can be taken as 0°C , K_i , K_s : coefficient of thermal conductivity of ice and snow.

When there is no snow, equation (4) leads to the Stefan⁴ formula:

$$H = \sqrt{\frac{2K_i}{\gamma_i L}} S \quad (5)$$

A workable engineering formula for (5) is given by^{5, 6}:

$$H = \alpha \sqrt{\frac{2K_i}{\gamma_i L}} S \quad (6)$$

where α is a coefficient always smaller than one that takes into account the boundary layer at the air-ice interface which reduces the temperature of the ice surface, the absorption of radiation inside the ice, the effect of the inclusion of air in the ice, that of the difference between air temperature at site of ice thickness measurements and that of the meteo station and finally, non-permanent phenomena.

With basic expression (4) and a coefficient α of the same type as that from (6) which will take into account these small and unaccountable factors we

get, in finite differences:

$$\Delta H = \frac{\alpha^2 K_i \Delta S}{\gamma_i L \left[H_M + \frac{K_i}{K_S} H_S \right]} \quad (7)$$

where ΔS is the number of degree-days of frost for the considered interval of time (one day), H_M and H_S the average ice and snow thicknesses during that day.

In the case where H_S would be a constant during the whole period of ice growth, we would get:

$$H = \sqrt{\left(\frac{K_i}{K_S} H_S\right)^2 + \frac{2\alpha^2 K_i S}{\gamma_i L}} - \frac{K_i}{K_S} H_S \quad (8)$$

USE OF MATHEMATICAL MODEL

A mathematical model⁷ was developed to use formula (7) for six years of ice thicknesses measurements at Inuvik in the McKenzie river and at Sachs Harbour in the Beaufort sea.

The essential objective of the model was to find a best fit value of the coefficient α that would adjust to the measurements at Inuvik and Sachs Harbour in any one year. Another unknown was the time of beginning of ice formation at each site which was recomputed starting from an arbitrary chosen origin when the ice thickness was around 25 cm. All programs were written in A.P.L./360 language except the computation of degree-days of frost which were made in FORTRAN directly from punched cards of climatological data obtained from the Meteorological Branch, Department of Transport, Canada.

The final value of α was obtained by an iterative process to reduce the standard deviation between the computed and measured thickness to a minimum. This process is too long to describe here.

The following values of the physical parameters were used in the computation:

Fresh water in the McKenzie river

γ_i : 0.92 gr/cm³

K_i : 18 cal/hr. cm. °C

L: 80 cal/gr.

K_S : 2.3 cal/hr. cm. °C for snow of density 0.3

Sea ice in the Beaufort sea

γ_i : 0.90 gr/cm³

K_i : 17 cal/hr. cm. °C.

L: 70 cal/gr.

K_S : 3.4 cal/hr. cm. °C for dense snow ice (0.4)

RESULTS AND CONCLUSIONS

This mathematical model for ice growth in natural conditions gives us the following information:

- 1- The value of α of the model

- 2- The value of the initial degree-days of frost and the time of beginning of ice formation
- 3- Degree-days of frost for each winter in function of time
- 4- The computed ice thicknesses day by day in comparison with the measured ones
- 5- The standard deviation each year for the model

The overall results are shown graphically on Figure 2 and 3 and summarized on tables 1 and 2.

The mathematical model that is proposed for ice growth in the Beaufort sea is strongly related to the basic physical processes of ice growth in the presence of a snow cover. It can be seen that this model is perfectly valid to compute the growth of ice in this area and the standard deviation between measured and computed value is about 5 cm on the average for 12 years of measurements where the growth of ice, each year, gave a maximum of the order of 1.25 m at Inuvik and 2.05 m at Sachs Harbour.

It is very difficult to measure the thicknesses in a consistent manner in nature. For instance at Inuvik in 1964-65 we find successive values of ice thickness between weekly intervals of 1.54, 1.48 and 1.64 m when weather was always below freezing point. In the same year we find 1.69, 1.48, 1.77 and 1.66 m of ice in successive measurements at Sachs Harbour. The decrease of ice thickness is not logical with an increase of degree-days of frost. One possible explanation is that the measurements in nature might have been taken at different places. In this year of 1964-65 the standard deviation of our model is abnormally high as could be expected.

It may be observed that the Beaufort sea and the Mackenzie delta are areas of very efficient heat exchange between the atmosphere and the ice cover. The coefficient α should theoretically be 1 for perfect heat transmission when the air temperature is exactly the same at the surface of the ice cover and in the atmosphere. It is on the average for six years 0.87 at Inuvik and 0.90 at Sachs Harbour. It is most logical that it should be higher in this last location more exposed to high winds.

In conclusion this theoretical model should be used with a high degree of confidence to compute ice growth in Arctic areas and eventually around engineering structures. In the open Beaufort sea in the presence of sea ice, equation (7) should be used with an α coefficient of 0.9.

REFERENCES

- Bilello, M.A. (1961)- "Formation, Growth and Decay of Sea Ice". Arctic, Vol. 14, No. 1, p. 3-25.
- Lebedev, V.V. (1938)- Rost l'da v arkticheskikh rekakh i moriakh v zavisimosti ot otritsatel'nykh temperatur vozdukha. Problemy arktiki 5-6: 9-25.
- Zubov, N.N. (1945)- L'dy arktiki. Moskva: Izd-vo. Glavsevmorputi. 360 pages.
- Stefan, J. (1889)- Uber die theorien des Eisbildung insbesondere uber die eisbildung in Polarmeere. Wien Sitzungsber. Akad. Wiss., ser. A., Vol. 42, p. t.2, p. 965-983.
- Assur, A. (1956)- Airfields on floating ice sheets. U.S. Army Snow, Ice and Permafrost Research Establishments (USA SIPRE) Technical Report 36.
- Michel, B. (1971)- "Winter regime of rivers and lakes". Cold Regions Science and Engineering. Monograph III-B1a, U.S. Army Corps of Engineers. 130 p.
- Michel, B. (1971)- "Ice Management at Marine Terminal, Herschel Island"- Report Dept. of Public Works, Canada. 212 pages.

Year	Degree- days max.	Ice thickness maximum		α	Standard deviation B
		comp.	mes.		
60-61	4532.2	125.2	124.5	0.845	4.242
61-62	4346.3	138.2	142.2	0.997	4.191
62-63	3964.4	89.2	104.1	0.789	5.131
63-64	4948.4	107.2	111.8	0.744	2.997
64-65	4175.7	142.0	162.6	0.952	9.474
65-66	4875.2	166.4	170.2	0.902	4.724
Mean value	4473.7	126.0	135.9	0.872	5.127

TABLE I: Summary of results for natural ice growth on the MacKenzie Delta at INUVIK Station

Year	Degree- days max.	Ice thickness maximum		α	Standard deviation B
		comp.	mes.		
60-61	4887.1	214.9	228.6	0.971	6.934
61-62	4800.7	181.4	185.4	0.858	3.150
62-63	4141.4	196.9	207.0	0.992	5.639
63-64	5405.3	205.0	215.9	0.890	4.140
64-65	4747.4	178.6	188.0	0.812	8.458
65-66	4739.6	184.7	195.6	0.880	5.715
Mean value	4786.9	193.5	203.4	0.900	5.673

TABLE II: Summary of results of natural ice growth in the Beaufort Sea at SACHS HARBOUR Station

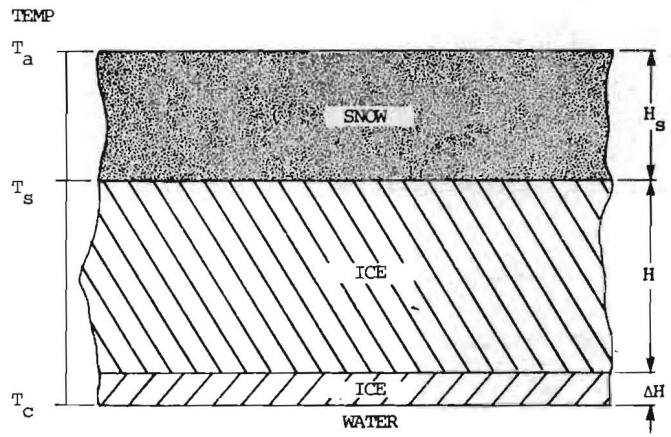
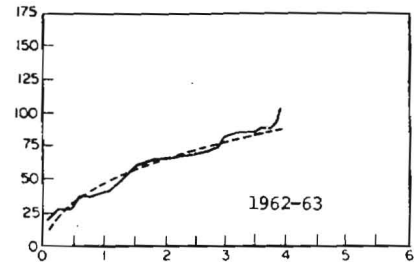
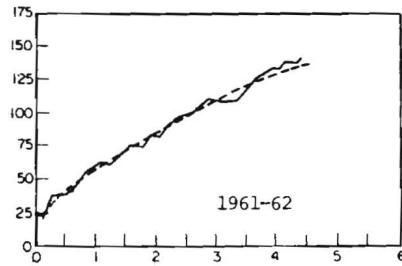
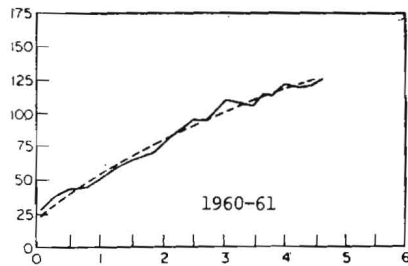


FIG. 1- NATURAL BLACK ICE GROWTH

Thickness
cm



Degree-days of frost $^{\circ}\text{C} \times 10^{-3}$

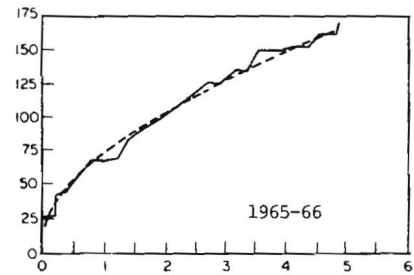
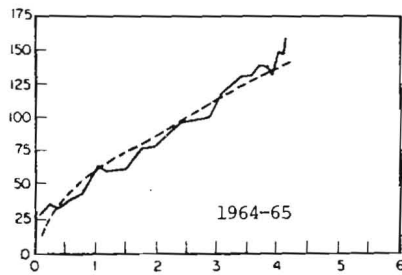
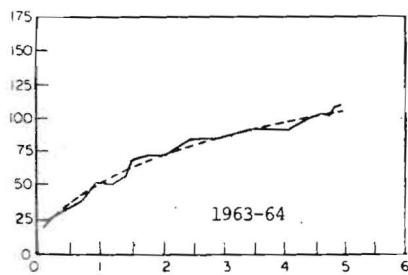


FIGURE 2- ICE THICKNESSES AT INUVIK

Measured values - Computed values

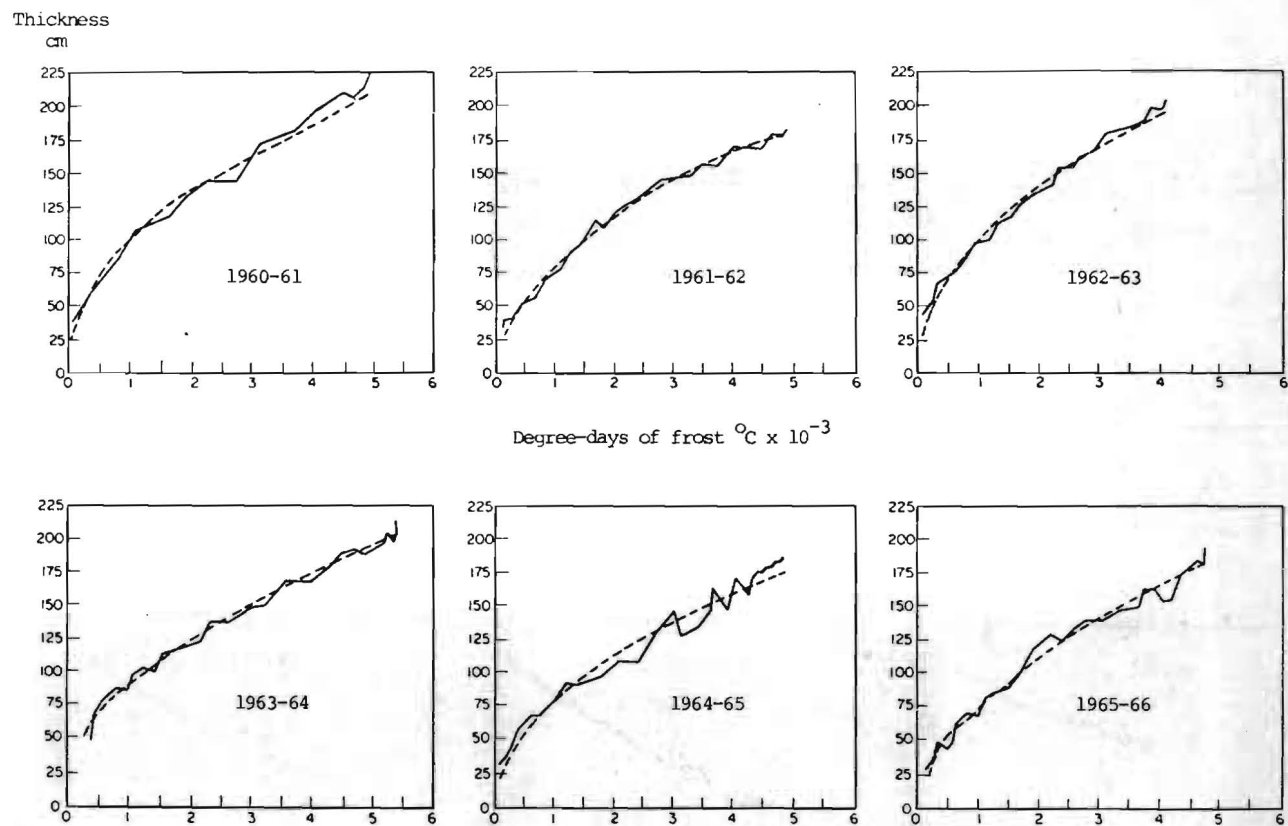


FIGURE 3- ICE THICKNESSES AT SACHS HARBOUR
 Measured values - Computed values



ICE SYMPOSIUM 1972
LENINGRAD

PROBLEMS WITH SLUDGE ICE CONNECTED WITH
THE PLANNING AND UTILIZATION OF WATER
POWER IN NORWAY

Edvigs V. Kanavin, Head of the Ice Water Resources and Elec- Norway
Office tricity Board

SYNOPSIS

In this paper, properties of SLUDGE ICE and problems created by sludge ice in the planning and utilization of water power plants, are discussed. Our investigations show that sludge ice contains properties comparable to those of clay. This makes it imperative for the engineer to reduce the sludge formation, transportation, pack-ice accumulation, and especially the formation of ice-bridges and ice jams.

RESUME

Dans cette publication sont discutées les propriétés du fraizil-glace et les difficultés dues à la présence du fraizil qui doivent être prises en compte dans les projets et lors de l'exploitation des usines hydro-électriques. Nos investigations indiquent que certaines propriétés du fraizil sont comparables avec celles de l'argile. C'est pourquoi il est indispensable de réduire les processus de formation du fraizil, de son accumulation et transport, et surtout de formation des embâcles de glace et de fraizil.

A number of problems of various kinds are connected with the ice, creating trouble at power-plants, especially in rapid rivers. In Journal IAHR Vol 2, no 1, by Dr. Phil. Olaf Devik: "Present experience on ice problems at the Norwegian power plants", is presented [1]. In the following paper a supplement will be given on the basis of recent investigations in nature, and in the laboratories.

1. STATIC AND DYNAMIC ICE PRODUCTION

It is generally known that the formation of an ice cover a lake will start with the supercooling of a thin surface film where ice crystals will grow from nuclei suspended in the water. The growth of the ice sheet will be a slow continuous procedure, which may be called *static ice production*.

Running water will contain floating aggregates of growing ice sponges called *frazil ice* and the ice of the river bottom - "*bottom ice*" ("*anchor ice*", "*tapped ice*"). In this case heat of crystallization is lost in the water masses, which may generally be called *dynamic ice production* - production of *underwater ice* (germ. "Tiefeneis", russ. "podwodnij l'jod").

In Norway and northern countries generally, the beginning of winter frost will very often be followed by the formation of this type of ice in the rivers.

The formation of peculiar "ice bridges" of compressed floating frazil ice, called "*sludge*" (russ. "schuga", norw. "sarr", polsk. "sryz") is shown on Fig.1.



Fig. 1.
Formation of "Ice-Bridge"
in the Forra river
(Water velocity 0.7 m/sec)

2. ACTIVE AND PASSIVE SLUDGE. EVOLUTION OF SLUDGE ICE IN A RIVER

In turbulent water, "ice needles" may be carried with the water stream at any depth of the river. This combination of frazil ice floating in slightly supercooled water with incessantly new formed supercooled water film elements whirling down and gradually "dying", represents a most potent factor in the ice formation in rapid rivers. It may be called "active sludge", in contrast to sludge in water which is not supercooled and might be classified as "passive sludge".

Ice accumulation and formation of ice bridges is a combined effect of supercooling, crystal growth, sludge drift, dynamic compression and refreezing.

Sludge clusters floating downstream in the surface layer of a river have a very loose structure. However, when we fetch a portion of such sludge, we can easily squeeze it to an ice ball which is quite similar to a snowball, such as we make from wetish snow - "slush" (norw "sørpe").

Evolution of sludge ice in a river is illustrated in sketch Fig. 2.

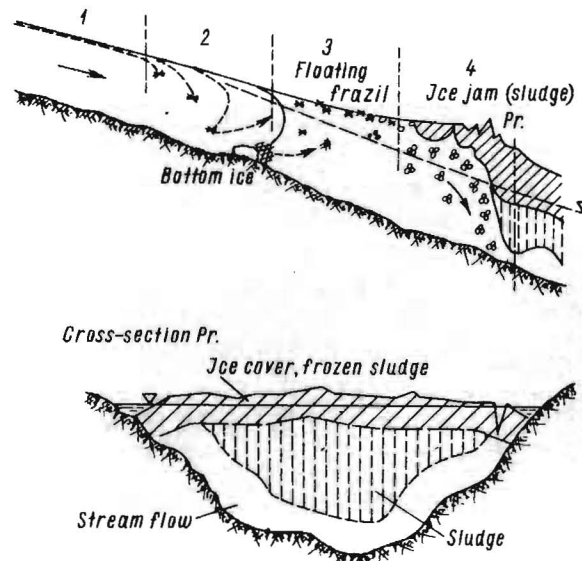


Fig. 2. Evolution of sludge ice in a river.

- Zone 1: Supercooling of water surface
- Zone 2: Formation of "active" sludge ice and bottom ice
- Zone 3: Sludge ice and loosened bottom ice drift up in flocks (Ice flows)
- Zone 4: Progressive deposit of pack ice downstream

When the water transport is illustrated by stream-lines the following consequences will appear for the relation between surface areas covered by clusters of sludge ice and open areas in between:

- a. Where stream-lines are diverging, open surface areas will be increased. In such places, e.g. where the river expands, just in front or behind an obstacle etc, the supercooling will produce conditions for bottom ice formation.
- b. Where streamlines are converging, for instance near an obstacle, the open areas will be reduced. As long as the velocity of the water is below, the critical value mentioned above, the chance for bottom ice production will also be reduced. If the convergence should increase the velocity above the critical value, the sludge would be immersed in the water, leaving the surface open to the production of a supercooled water film, the elements of which would follow the converging water stream which would then be sweeping along the obstacle on its way, leaving the supercooled water elements at the back of the obstacle.

3. COMPRESSION AND SOLIDIFICATION OF SLUDGE ICE SHEAR STRENGTH OF ACCUMULATED PACK ICE

The formation of ice bridges and pack-ice, gives a type of ice which has a shear strength comparable to that of a substance like clay.

The fact that an ice layer has a vertical face, height H , demonstrates that the acting forces, weight and actual stress, are in a stable equilibrium in the ice volume adjacent to the side wall as illustrated in Fig. 3.

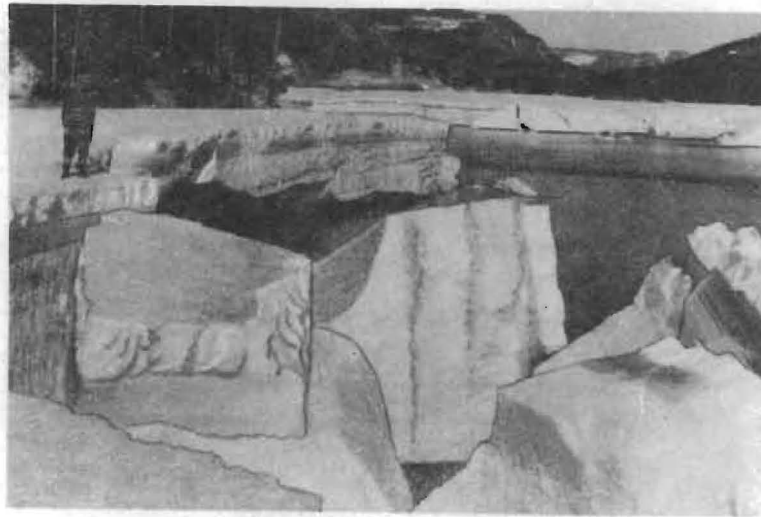


Fig. 3. Accumulated pack-ice in the Hallingdal river

The stability is characterised by the shear stress (s) in the plane along which a rupture will take place when the critical breaking stress (s_k) is reached. As long as the safety factor $F = s_k/s > 1$, the ice wall will be stable. The shear stress (s), which will correspond to a given height (H) and a given density (d) of the ice layer, may be calculated by applying the classical theory for earth pressure against a vertical wall, with the simplification that the horizontal component in this case is zero. This gives the formula (2): $S = 0.5 F \cdot d \cdot H$. When $F > 1$, the shear strength will be greater than $0.5 d \cdot H$. In an ice layer with mean density $d = 8 \text{ ton/m}^3$, the shear strength will then be greater than $0.4 h$ (measured in ton/m^3).

We thus find that the observed ice layers producing ice walls of a height from 2 m to 5 m, will have a shear strength exceeding 0.8 ton/m^3 , resp. 2 ton/m^3 . In the same order of magnitude is the shear strength of such materials as ordinary clay.

It is important to emphasize that compressed sludge ice is a substance quite different from floating sludge of loose structure and from clear ice [3].

The respective properties of frozen sludge ice and clear ice can to a large extent, be shown by compression tests. The results of such investigations are shown graphically on Fig. 4.

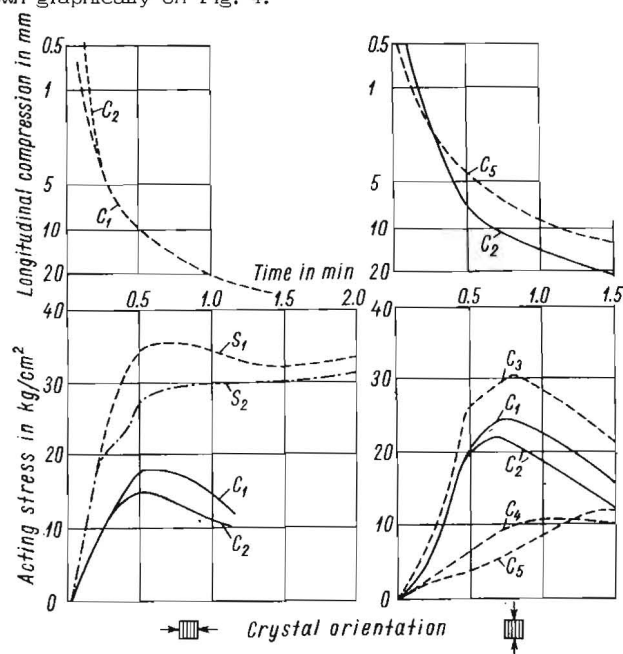


Fig. 4. Summary of determinations of the limit of brittle stages

- C - clear ice (lake ice)
- S - sludge ice (river ice) (Testing done on 20 cm cubicles)
- C_1 and C_2 - tested straight from normal conditions
- C_4 and C_5 - after 4 hrs placed in sunlight
- C_3 - after 24 hrs submerged in water
- S_1 and S_2 - sludge ice from river rapids. No cracks appeared during testing

Also the absorption properties of radiation in clear ice and sludge ice are very different, as can be seen on Fig. 5.

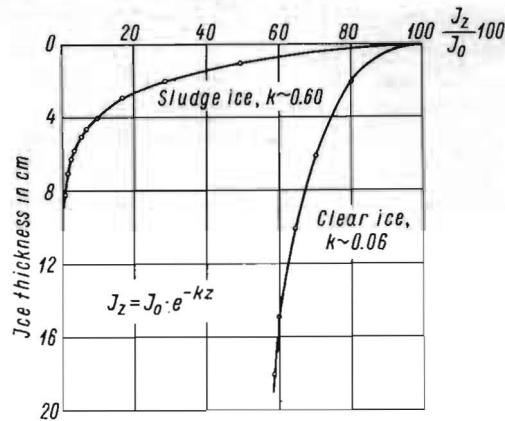


Fig. 5.

If we take the compression strength as an indication of the consistency of the ice, the investigations in the out-door laboratory show that with an ice cover of 45 cm thickness, the compression strength decreased 1 kg/cm^2 for every degree increase in the mean day temperature of $+5^\circ\text{C}$. Large blocks of sludge ice, however, lay on the river banks and took a long time to melt. These properties are characterized on Fig. 6.

Sludge ice contains a good deal of sand, gravel and stones and floats therefore rather low in the water. This creates difficulties when large sludge-ice blocks pass through the ice - sluice, and one often has to, under great risk, lead them over the regulating - dam.

When the ice masses in a river are broken up by a winter flood carrying the masses downwards, a mixture of all type of ice, sludge ice, loosened bottom ice, broken land ice, small and great pack-ice blocks, will float downstream towards the power-plants.

4. CONCLUSIONS AND RECOMMENDATIONS

The fundamental importance of the supercooling associated with the formation of sludge ice, has emphasized the necessity of avoiding supercooled water and active sludge near the constructions of a plant. Formation of an ice cover on an intake reservoir must be promoted.

The formation of "ice bridges", associated with the accumulation of pack-ice masses produces a type of ice having a shear strength which may cause much greater practical difficulties than previously assumed.

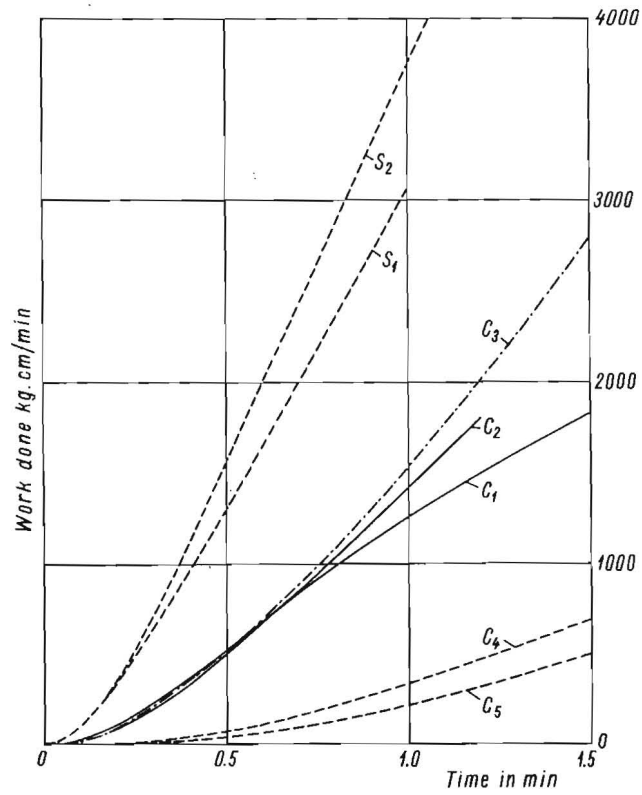


Fig. 6. Work done in longitudinal compression during pressure-tests with ice-cubes

C - clear ice (lake ice)
 S - sludge ice (river ice)

C₁ and C₂ - tested straight from normal conditions

C₃ - after 24 hrs submerged in water

C₄ and C₅ - after 4 hrs placed in sunlight

S₁ and S₂ - sludge ice from river rapids.

The analysis of the different ice problems given in this paper is pointing to the possibilities which exist to reduce the sludge ice production. The possibilities are:

1. To reduce effectively the open areas.
2. To establish reservoirs which can store sludge ice, prevent step bursts and prevent the formation of ice bridges at critical places.
3. To secure slow water flow and promote the formation of an ice cover at the intake of a power plant.

The Norwegian rivers are troublesome sludge ice producers of great dimensions /3 and 4/. The problems which the planners of power plants encounter, will, however, not only arise from the magnitude of moving ice masses, but far more from the changes of physical qualities which accompany the different stages of ice production, sludge transportation and pack-ice accumulation.

REFERENCES

1. Devik, O., Present Experience on Ice Problems connected with the Utilization of Water Power in Norway, I.A.H.R. Vol. 2, no 1, 1964.
2. Devik, O. and Kanavin, E.V., Final Report on Analysis and Consideration of the Ice Conditions in the Hvítá and Thórsá River Systems, Southern Iceland, Oslo, 1965.
3. Kanavin, E.V., Problems with Underwater Ice in Rivers Reprintes from Journal "Teknosk Ukeblad" Oslo, 1951.
4. Devik, O. and Kanavin, E.V., Ice Problems in Norwegian Lakes and Rivers, Oslo 1963.



FRAZIL ICE DURING SPRING BREAK-UP

G.P. Williams, Division of Building Research, National Research Ottawa,
Council of Canada Canada

SYNOPSIS

Frazil ice caused the complete blockage of a large industrial water intake twice in about forty years. Both cases occurred during spring break-up when the river was essentially open, with water temperatures close to 32°F (0°C). Weather conditions were similar in both cases with wind speeds averaging 20 mph (9 metres/sec) or greater, air temperatures about 20°F (-7°C), and extremely low dew-point temperatures of 1°F (-17°C). These cases illustrate the need to be aware of potential frazil problems at sites where frazil is not a common occurrence.

RESUMÉ

Les glaces de fond ont occasionné l'obstruction totale d'un important bassin industriel d'approvisionnement d'eau à deux reprises durant les quarante dernières années. Ces deux incidences se sont produites durant le dégel printanier alors que la rivière était essentiellement ouverte et que la température de l'eau approchait les 32°F (0°C). Les conditions atmosphériques étaient semblables dans les deux cas: la vitesse du vent était d'une moyenne de 20 m/h (9 mètres/seconde) ou plus, la température de l'air à peu près 20°F (-7°C) et la température extrêmement basse du point de rosée à 1°F (-17°C). Ces cas démontrent le besoin d'être conscients des problèmes éventuels des glaces de fond dans les endroits où elles ne se présentent pas tellement souvent.

INTRODUCTION

This paper describes an unusual case of frazil ice formation at a large industrial plant water intake located on the Ottawa River near Ottawa, Ontario, Canada. The site is several kilometres downstream from hydro plants where frazil is a common occurrence (1). Frazil caused complete blockage of the intake and a costly plant shutdown twice in about forty years of operation. Both these shutdowns happened during the spring break-up period and relatively mild air temperatures, when frazil would not normally be expected to occur. Frazil has also been reported, during the early winter but was not sufficient to cause plant shutdowns.

THE CONDITIONS UNDER WHICH FRAZIL OCCURRED

Weather records were obtained from weather stations located a few kilometres from the site for the two dates (5 April, 1963 and 11 April, 1967) on which the intakes were blocked. Figure 1 shows the air temperatures, dew-point temperatures, and wind speeds and directions for the 24-hour periods during which the frazil formed. Conditions were remarkably similar during the two periods. In both cases morning fog occurred on the previous day, and high flows indicated that the river was essentially open. Strong north to west winds averaging 20 to 30 mph (9 to 13.5 metres/sec) persisted for about 24 hours before the ice occurred. Night temperatures went down to about 20°F (-7°C). Exceedingly low dew-point temperatures were reported; in the early hours of the morning on the day that frazil formed, the dew-point temperature in both cases was about 1°F (-17°C). Clear sky conditions prevailed on both occasions.

The weather data were used to calculate the hourly average rate of surface heat loss from open water for the period 1200 h April 4 to 1200 h April 5, 1963 (Figure 2). This heat loss not only determines the rate at which the water cools prior to frazil formation but also the subsequent rate of frazil production. Surface heat losses were obtained by calculating the components of atmospheric heat exchange: net short-wave radiation, net long-wave radiation, evaporation and convection. Net short-wave radiation was determined from measured values for incoming short-wave radiation obtained from the National Research Council meteorological station. Long-wave radiation, convection and evaporation losses

(1) Williams, G.P. A Case History of Forecasting Frazil Ice - A paper prepared for publication in symposia on the role of snow and ice in hydrology, International Hydrological Decade, Banff, Alberta, Canada, 6-20 Sept. 1972.

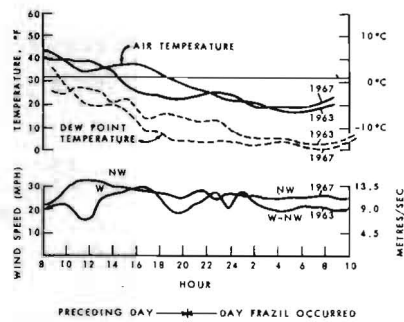


FIGURE 1
COMPARISON OF WEATHER CONDITIONS APRIL 4-5/63,
APRIL 10-11/67

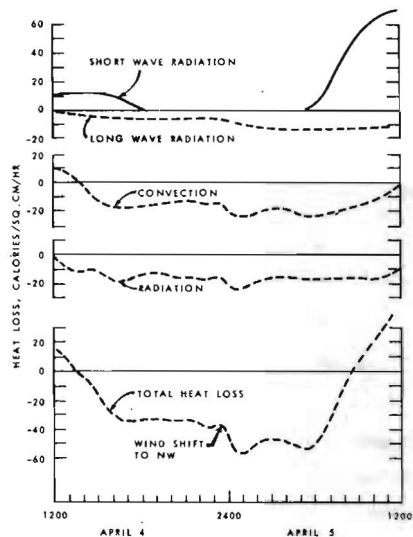


FIGURE 2
SURFACE HEAT EXCHANGE COMPONENTS FROM OPEN WATER,
OTTAWA RIVER, 1963

were calculated using the formulas proposed by Michel (2). These formulas compare reasonably well with formulae proposed by other authors.

The calculations showed the relative contribution of radiation, evaporation and convection to the total rate of heat loss. The heat loss by evaporation, caused by the high winds and low dew-point temperatures, was especially significant. There was a marked increase in heat loss at about 2300 h, April 4, when the wind shifted from west to northwest and dew-point temperatures continued to fall. It was only after this increase that the rate of heat loss was probably sufficient to cause a severe frazil problem at the site. A study of heat loss during frazil production at a nearby section of the river (1) indicated that severe frazil will occur only if the rate of heat loss is greater than about 50 cal/sq cm/h. Once the sun rose the heat loss decreased rapidly because of incoming solar radiation.

(2) Michel, B. (1971) Winter Regime of Rivers and Lakes. Cold Regions Science and Engineering Monograph 111-Bla, Hanover, N.H.

The conditions under which severe frazil will occur at this site can be summarized as follows:-

- (1) The wind speed must average at least 20 mph (9 metres/sec) or greater for several hours, sufficient to mix the water to considerable depth and prevent a stable ice cover from forming.
- (2) The rate of heat loss from an open water surface must be greater than about 50 cal/sq cm/h for several hours.
- (3) The section of river upstream from the intake must be essentially open, with water temperatures close to 32°F (0°C).

The third requirement is met only for a few days during the spring break-up. In 1968, a year when accurate water temperatures were available, this period with open water and water temperatures close to the freezing point lasted from about March 30 to April 3 (Figure 3). The duration of this critical period is probably even shorter during freeze-up, as a stable ice cover usually forms rather quickly upstream from the site once water temperatures are close to 32°F (0°C). The probability of weather conditions conducive to severe frazil occurring within this critical period must not be very great, as severe frazil has occurred at this site only twice in about forty years. Now that frazil is recognized as a hazard, advance warning of severe attacks can be made because the weather conditions under which it occurs are such that they can be predicted a few hours in advance.

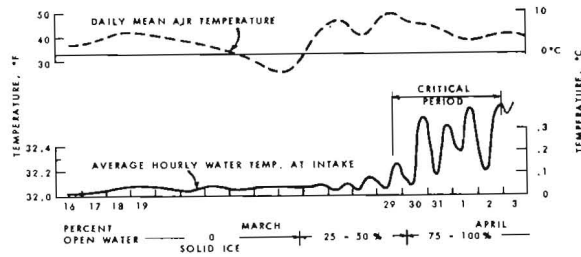


FIGURE 3 WATER AND AIR TEMPERATURES OTTAWA RIVER, 1968

CONCLUDING REMARKS

Designers and operators of water intake structures should be aware of potential frazil problems for intakes located near frazil-producing rapids (or at shallow depths in large lakes and reservoirs) where stable ice covers normally form and frazil is not a common occurrence. All that is needed for frazil to occur at these sites are strong winds combined with low dew-point temperatures when an ice cover is just starting to form at freeze-up or at break-up when water temperatures are close to the freezing point. Frazil occurring under these circumstances often causes the complete blockage of intakes because plant operators are unprepared to combat it.

This paper is a contribution from the Division of Building Research, National Research Council of Canada, and is published with the approval of the Director of the Division.



ICE SYMPOSIUM 1972
LENINGRAD

ON FRAZIL ICE MEASUREMENTS IN THE KEMI
RIVER

M.V. Kuuskoski
Director IVO Hydraulic Laboratory

Imatran Voima Osakeyhtiö

Helsinki,
Finland

SYNOPSIS

Frazil Ice is accumulated in huge amounts in the Taivalkoski area in early winter before the Kemi River has got its ice cover. 9,5 millions of cubic metres of frazil ice was measured in the area in December 1971.

RESUME

Les glaces fraziles s'accumulent en grandes quantités dans la région de Taivalkoski au début de l'hiver, avant que le fleuve de Kemi ait reçu sa couche de glace. En décembre 1971, le volume des glaces fraziles dans cette région a été mesuré à 9,5 millions de mètres cubes.

ON FRAZIL ICE MEASUREMENTS IN THE KEMI RIVER

The development of the main course of the Kemi River, which is located in North Finland, for generating water power has almost been completed. In fall 1972 the construction work will be started on the Taivalkoski power plant (Fig. 1, object 2). The river channel has to be reduced by means of coffer dams. For choosing their heights the water levels of the river in the different seasons of the year must be known.

In the lower part of the river water is already rather cooled. Furthermore there is a large open water area in Taivalkoski through all the winter (Fig. 2), where much heat from the flow is conveyed to the atmosphere. As a consequence of that the flow is supercooled and formation of frazil ice will start. The Taivalkoski area is located about 80 km from the Arctic circle to the south and the average temperature in February is -12°C . The lowest measured temperature has been -44°C .

The forming of frazil slush begins concurrently with the ice cover formation in tranquil zones. The frazil slush drifts with the stream in very large quantities and it is often clearly visible. Below the rapids, where the flow velocity is sufficiently retarded, frazil ice gets anchored to the under side of the ice cover. The layer of frazil ice often fills up the whole channel depth from the under side of the ice cover to the bed bottom so that the flow can utilize only narrow tunnels. When formation of frazil ice thus reduces the channel, the flow velocity is increased and frazil ice can not adhere to the ice cover but will move downstreams, where the flow velocity is low enough so that the accumulation of frazil can take place. Thus frazil ice can be accumulated on a distance of many kilometres and its total volume can be millions of cubic metres. Owing to the very little cross sectional area which is freely available for the flow, a rising of the water level above the reduced section occurs. The height of rising may be many metres.

The highest raise in the water level in the ice forming period has been measured in winter 1917-18 (Fig. 3) when water level at the end of November rose in a couple of days by 4 metres. The greatest damming up of 4,6 metres occurred at Christmas time and even at the end of the winter the height of damming up was 3 metres.

The time of the break-up of ice brings up additional risks of its own. When the river channel below the rapids is filled up by millions of cubic metres of frazil ice on a distance of several kilometres, it takes a long time, before the ice masses are weakened. During this time the rising flood has made the ice above stir. With the stream the ice blocks move downstreams and when they stop against the strong ice zone below the rapids, they form an ice jam, which may cause a raise of nearly 10 metres in the water level in a few hours. The attached photographs, which have been taken on May 4, 1965, when the peak of the flood has already passed indicate, how high the water level has been and how huge ice masses are involved. The peak of the flood was attained on April 30, 1965. Below the rapids, it exceeded the elevation of + 20 metres from the sea level and it was 8 metres above the mean water level (Fig. 2).

In winter 1970-71 ice measurements in 7 different cross sections on the area of Taivalkoski were started (see the map in Fig. 2). The measurements were continued in winter 1971-72 when the early winter was especially cold and plenty of frazil ice was formed.

Fig. 4 shows the results of ice measurements in cross section 1 during the period between November 26, 1970 - April 4, 1971. In Fig. 5 fluctuations of temperature and flows have been presented. The shares in percentage of the cross sectional area occupied by frazil ice, solid ice and water have also been calculated. It can be seen that the early winter was mild. Temperatures below -20°C were scarce and many periods of

above 0°C temperatures were between them. On December 10, 1970 50 % of cross sectional area was in possession of frazil ice, which was the maximum value in that year. Since then the volume of frazil ice reduced though even temperatures of -30°C appeared later.

Figures 6 and 7 show corresponding results during the period from December 9, 1971 to February 9, 1972. It was very cold in November and therefore 94 % of cross sectional area was in possession of frazil ice on December 9, 1971. Still on February 9, 1972 the share of frazil ice was 64 %, though January was rather mild. Further it can be seen that the water level was staying about one metre above that in previous year, though the flow quantities were approximately of the same size.

On December 10, 1970 frazil ice could be found below Taivalkoski on a distance of about 5 km, in total 3,5 million cubic metres. On December 9, 1971 frazil ice was found on a distance of about 7 km, in total about 9,5 million cubic metres.

The results of the executed measurements lead to the assumption that the height of floods caused by break-up of ice depends on the volume of accumulated frazil ice, which in its turn is determined by the weather conditions in early winter. When writing this (on February 20, 1972) we have a good reason to predict that in spring 1972 the break-up of ice will be severe. In the fall of this year, when this article is published, we shall know the accuracy of the prediction.

POWER PLANTS IN THE RIVER KEMI

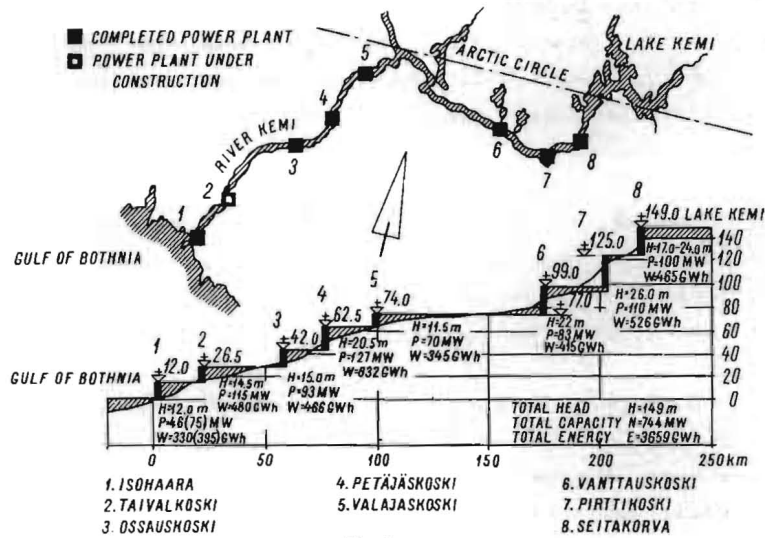


Fig.1

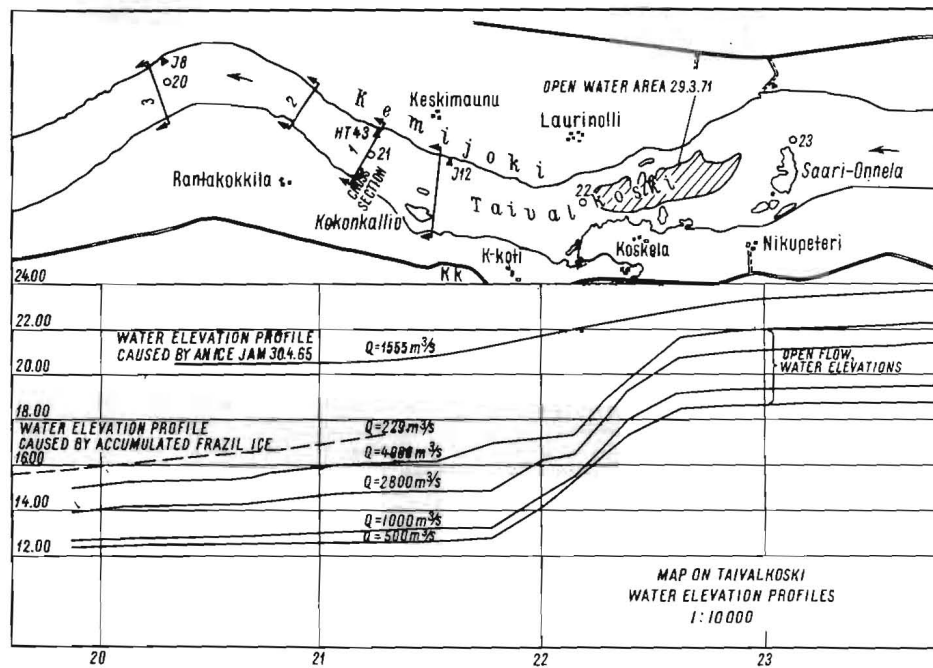


Fig. 2

DAMMING-UP CAUSED BY ICE IN THE WINTER 1917-18
IN CROSS SECTION 1

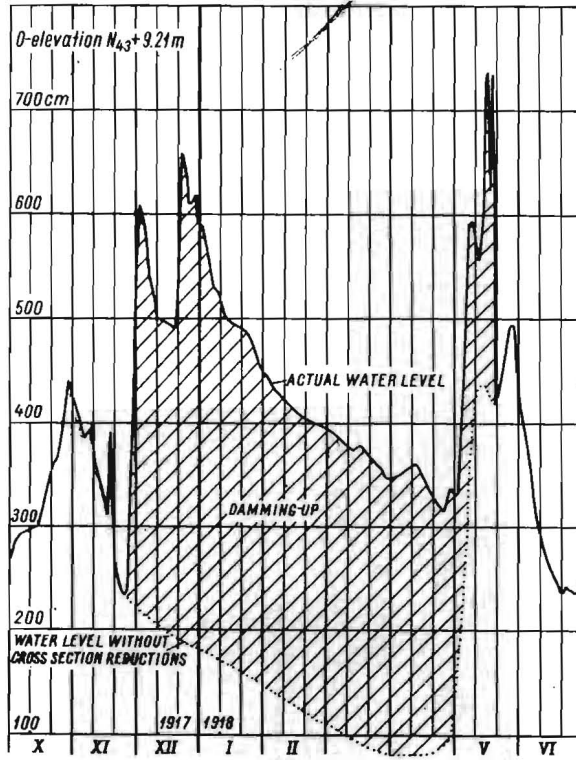


Fig.3

THE DEVELOPMENT OF ICE CONDITIONS
IN THE WINTER 1970-71

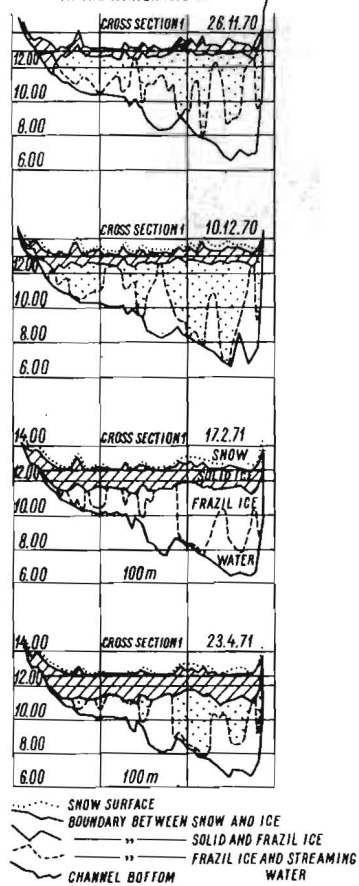


Fig.4

TEMPERATURE, FLOW, WATER LEVEL AND ICE
DATA IN THE WINTER 1970-71, CROSS SECTION 1

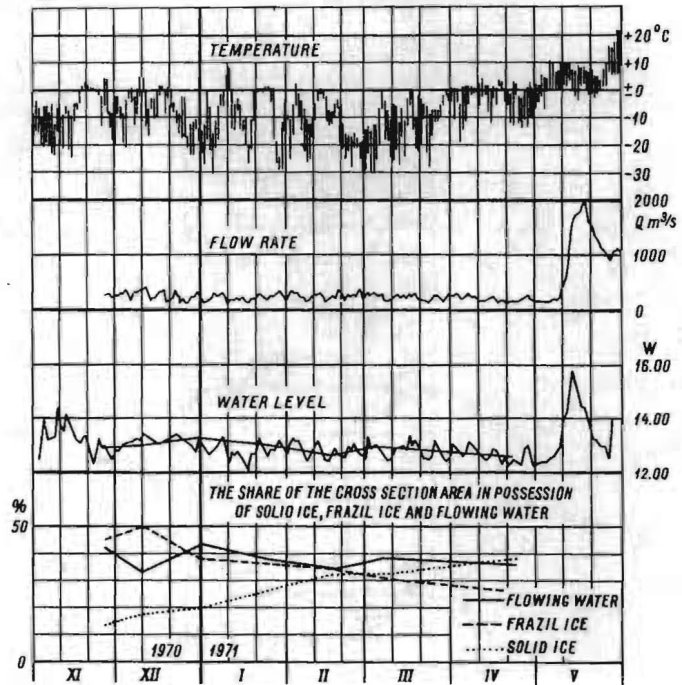


Fig. 5

THE DEVELOPMENT OF ICE CONDITIONS
IN THE WINTER 1971-72

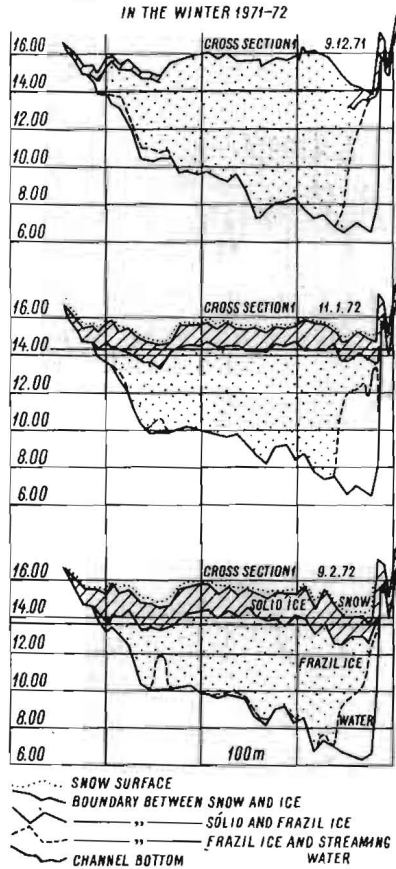
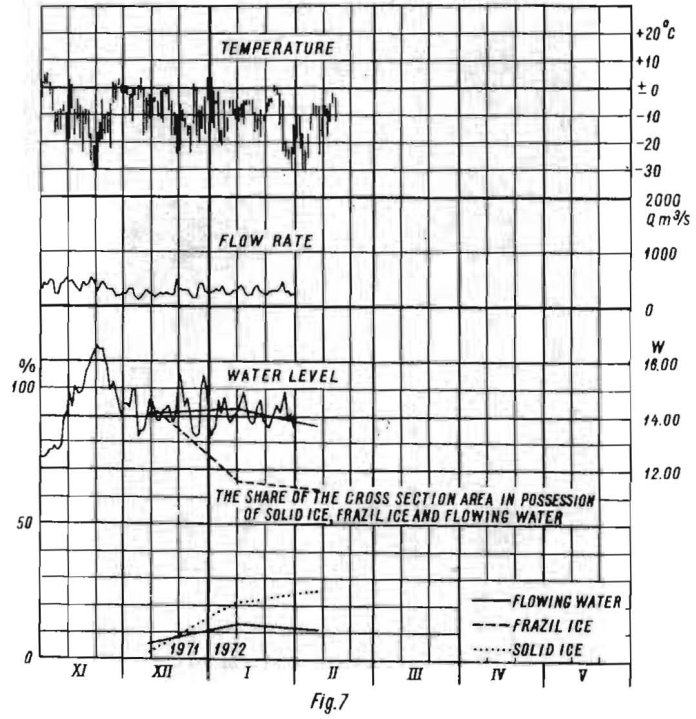


Fig. 6

TEMPERATURE, FLOW, WATER LEVEL AND ICE
DATA IN THE WINTER 1971-72, CROSS SECTION 1







ICE SYMPOSIUM 1972
LENINGRAD

UTILIZATION OF A WATER RESERVOIR TO
CONTROL WINTER PHENOMENA ON A RIVER

Václav Matoušek,
Head of department

Ohře River Basin Chomutov, Czechoslovakia

SYNOPSIS

By controlling the discharge from a reservoir in relation to the meteorological situation it is possible to attain a substantial limitation of winter phenomena on the river below the reservoir and thus to avoid the formation of ice jams and barriers and difficulties on intake structures. The method of solution and its results are reported, using an actual example from the lower reaches of the river Ohře with the completed water reservoir of Nechranice.

RESUME

Par la régularisation de l'écoulement d'un barrage suivant la situation météorologique on peut atteindre la restriction des phénomènes d'hiver sur la rivière au-dessous du barrage; ainsi on peut éliminer les cas de la formation des barrières des glaçons et éviter les problèmes sur les installations de pompage. Mode de la direction des travaux et les succès sont présentés sur le barrage Nechranice (Basse - Ohře) qui sert d'exemple.

During the winter season, flood situations are encountered every year on the lower reaches of the river Ohře. In this sector of the river great quantities of in water ice are produced which in places of solid ice cover and in sharp bends create jams and barriers. The frozen river with ice jams does not permit the preliminary emptying of the Nechranice Reservoir and retaining of the flood. Difficulties arise also in throughflow hydroelectric power plants and intake facilities. During ice movement, hydraulic structures are endangered, too, especially the old weir at Terezín which is combined with a bridge of great traffic importance.

To eliminate these difficulties an attempt was made to utilize the Nechranice Reservoir on the river Ohře, which was completed in 1969.

By discharging sufficient quantities of warm water from the bottom layers of the reservoir, it is possible to affect significantly the whole winter regime on the river downstreams of the reservoir. The reservoir is situated at km 103 of the river stationing. Its total volume is 287 mil. cu.m with a useful space of 269 mil. cu. m. The reservoir dam is 3280 m long at the ground and 48 m high. The water discharge from the bottom layers is achieved by two bottom outlets with a total capacity of 110 cu.m per sec. and two turbines of 18.0 cu.m/sec. of absorption capacity each. The maximum water quantity discharged from the reservoir is, however, given by a safety condition, which permits a maximum daily water level decrease in the reservoir of 28 cm. During normal winter inflow of 12 - 20 cu.m/sec. into the reservoir, the maximum discharged quantity can then be 47 - 55 cu. m/ sec.

For the control of the winter regime in the river downstream of the reservoir, it is essential to know:

1. the temperature of the water discharged from the reservoir
2. the method of calculating the water temperatures on the longitudinal profile and the movement of the ice drift
3. the meteorological forecast
4. harmless discharge of ice drift.

In connection of the lower reaches of the river Ohře these questions are solved as follows:

- Ad 1) According to measurements carried out, it is possible to discharge from the Nechranice Reservoir water of about 6°C at the beginning of the winter season. Towards the end of the season the water temperature drops to 3°C .
- Ad 2) The computation of the longitudinal profile of water temperature and movement of ice drift is based on the thermal balance equation of the river. The equation used is derived from measurements on the canal from the river Ohře to the river Bělina (1). The balance equation and the relation for the computation of water temperature and ice drift movement is shown in the appendix. The necessary river parameters, such as advance times, channel width, gradient, magnitude of tributaries, etc., were determined by measurement. The computation of the longitudinal temperature profile and ice drift movement was verified by direct measurements. On the river there were established seven gauging stations. Also frequent river surveys were carried out to obtain the necessary data on ice drift transport. In 37 calculated longitudinal temperature profiles, there were only two instances of $0,5^{\circ}\text{C}$ differences between the calculated and measured water temperature and that in a distance of 100.5 km from the reservoir at a discharge of 40 cu.m/sec. In all other cases the differences were smaller. The comparison carried out confirms the applicability of this method of computation. Also verified was the computation of the ice drift motion and determination of the starting point of the ice drift formation. Also these calculations show a very close agreement with the values obtained by measurement. The starting point of ice drift formation has been determined with a difference not exceeding 2.0 km.
- Ad 3) For the control of the discharge from the reservoir in relation to the meteorological situation, a satisfactory meteorological forecast is essential. In our case, the length of the affected river is 103 km and the advance time of the current in this river length amounts to 64 hours at a discharge of 20 cu.m/sec. and 39.5 hours at a discharge of 55 cu.m/sec., respectively.

(1) Matoušek, V.: Thermal balance of open supply canals,
Práce a Studie 3, Povodí Ohře Chomutov, 1971

Meteorological forecasts are carried out by the Hydrometeorological Institute in Prague. To make the forecast more precise, information on the actual meteorological situation prevailing at the river gauging stations is passed on to this Institute. However, inspite of that the forecast is not always in good agreement with the real weather development. Not precise is mainly the prognosis for the third day. Difficulties also arise with sudden changes in the weather. This has to be borne in mind and the discharge from the reservoir must be chosen with a certain safety degree.

- Ad 4) As harmless ice drift motion we understand such a flow in which no ice jams are produced; it is dependent on the river and structures on it and on the total discharge. Such a harmless ice drift can be determined only experimentally. Following the ice drift transport, two dangerous profiles for the creation of ice jams were found, and that at km 14.3 and km 47.9. Ice jams occur when the discharge of ice drift is greater than 3.5 cu.m/sec. and 1.5 cu.m/sec., respectively. These data apply for water discharges of 40.0 cu.m/sec.

Conclusion :

Measurements and observations on the river have shown that the reservoir can be used with advantage to eliminate winter defects on the river. At the same time it has been also proved that the procedure for solving this problem and the calculating the longitudinal water temperature profile and ice drift movement is correct. By discharging the permissible quantity of 55 cu.m/sec., it can be achieved that 40 km of the river will be free of all ice phenomena during the whole winter season and 63 km will encounter only harmless winter phenomena.

For the winter season of 1971/72 regular water temperature and ice drift movement forecasting has been started. Forecasts are prepared for the most important profiles. This permits to continue with building operations on the river longer and also into the winter season the optimal protection of the weirs at Terežín.

A p p e n d i x

Thermal balance equation of the river :

$$\begin{aligned}
 s = & (12.7 + 1.8 w) [0.46 (t_{vz} - t_v) + (e - e_o)] + \\
 & + 4.95 \cdot 10^{-8} \cdot T_{vz}^4 [0.613 (1 + c_o + c_1 n) + \\
 & + 0.013 e (1 - c_2 n)] - 4.75 \cdot 10^{-8} T_v^4 + \dot{s}_4 \left(\frac{\tau}{100} + \right. \\
 & + 0.0655 \sec Z) (1 - n) k_o + 0.936 k_1 n] + 6 + \\
 & + 8430 \cdot l \cdot \frac{Q}{B} + 0.15 \left(\frac{1}{2} t_{vz} - 80 - t_v \right) A_{bn} + \\
 & + \frac{3.6 \cdot 10^6 \cdot Q_p (t_p - t_v)}{F} \quad [kcal/m^2h] \quad (1)
 \end{aligned}$$

Relation for water temperature calculation :

$$t_{v2} = t_{v1} + \frac{s \cdot B \cdot L}{3.6 \cdot 10^6 Q} \quad [^\circ C] \quad (2)$$

Relation for ice drift movement calculation :

$$Q S = \frac{1}{\gamma \cdot r} s \cdot B \cdot L \quad [m^3 / h] \quad (3)$$

s = total heat loss (kcal/m²h)

w = wind velocity 2.0 m above water level (m/s)

t_{vz} = air temperature 2.0m above water level (°C)

t_v = water temperature (°C)

e = real vapour tension 2.0 m above water level (mm Hg)

e_o = vapour tension at saturation and water temperature (mm Hg)

T_v = absolute water temperature

T_{vz} = absolute air temperature

n = cloudiness in fraction of one (0 - 1) ;
 clear sky $n = 0$

c_0, c_1, c_2 = coefficients dependent on cloudiness,
 density of clouds and visibility

\bar{s}_4 = direct solar irradiation from clear sky

η = percentage of direct solar irradiation absorption

Z = zenit distance of sun in degrees

k_0, k_1 = coefficients dependent on cloudiness, cloud density
 and visibility

i = level gradient

Q = water discharge (m^3/s)

B = water surface width (m)

Δ_{sn} = thickness of atmospheric precipitation layer (mm/h)

Q_p = rate of inflow (m^3/s)

t_p = temperature of inflowing water

F = area of water surface (m^2)

t_{v2}, t_{v1} = water temperature in station 1 and 2 , respectively ($^{\circ}C$)

L = distance between two stations (m)



ICE SYMPOSIUM 1972
LENINGRAD

ICE PROBLEMS IN WINTER OPERATION -
BUREAU OF RECLAMATION EXPERIENCE

Philip H. Burgi, Hydraulic
Engineer

Bureau of Reclamation

Denver, Colorado,
U.S.A.

SYNOPSIS

Ice formation on reservoirs, rivers, canals, and associated structures hinders and, at times, prevents winter operation on a number of Bureau of Reclamation projects. Ice difficulties as they occur on rivers, water conveyance systems, and hydraulic structures are briefly described in this paper. Although the ice difficulties do not have simple solutions, several planning, design, and operational considerations are proposed to reduce the detrimental effect of ice formation. Environmental limitations to some of the river ice control problems are also discussed.

INTRODUCTION

A number of Bureau of Reclamation projects are handicapped during winter operation by ice formation (1). To establish a research program related to alleviation of ice problems, the project offices experiencing ice difficulties were asked to describe ice jams occurring in natural channels, and damage, safety hazards, and inconvenience that have resulted from ice formation in canals and in entrances to powerplants, spillways, outlet works, and other hydraulic structures. Information of any corrective or preventive measures that had been undertaken to alleviate the problems was also requested. It was difficult to put a monetary value on the extent of damages or operational losses caused by ice formation. The problems ranged from extensive flood damage resulting from river ice jams to cumbersome problems such as manually clearing ice from trashracks.

NATURAL CHANNELS

Ice formation which results in the most extensive physical damage lies in the area of ice jams on rivers. The formation, growth, and decay sequence of a river ice cover may occur several times during one winter, depending on climatic conditions. Although ice jams may form during any phase of the ice cover sequence, they are usually more frequent and severe in the decay phase.

One of the most common areas for ice jam formation is where a river enters the backwater of a reservoir. The quiet water of the reservoir develops an ice cover earlier in the winter season than the turbulent water of the river. When ice develops in the river, it floats down to the backwater of the reservoir where it accumulates against the lake ice. The resulting river ice cover may progress upstream from the reservoir while water flows underneath the ice cover. In high velocity zones the ice cover thickens when floating frazil ice plunges under the leading edge of the ice cover, resulting in an ice jam. This obstruction creates a rise in the water level immediately upstream of the jam. The added water pressure will either break the jam or the river water will continue to rise until it finds another route around the jam, flooding adjacent lowlands. Figure 1 illustrates the severity of the problem.

The Yellowstone River presents another unique ice jam formation problem. It flows northeasterly to its confluence with the Missouri River, and therefore it is not uncommon for the upper reaches of the river to experience a warming trend before the lower reaches. If a chinook wind develops, the runoff will greatly increase, resulting in severe ice jamming in the lower reaches of the river. Figure 2 illustrates the degree of flooding which can occur when the river channel is choked with ice.



Figure 1. - Aerial view of flooding in Montour, Idaho, immediately upstream of the Black Canyon Reservoir (looking downstream)



Figure 2. - Aerial view looking upstream on the Yellowstone River. Note flooding on both sides of the river channel.

There are no general solutions for ice jam formation in natural channels. However, the following are some measures tried on Bureau of Reclamation projects to alleviate ice jam formation in river channels:

1. Improve the channel by dredging, removing debris, and eliminating sharp bends
2. Construct levees to contain the river and/or ice flow
3. Construct ice boom control structures where feasible to trigger an ice cover earlier in the winter season
4. Where river control is possible, maintain river discharge as constant as possible to eliminate ice cover breakup
5. Maintain winter releases from reservoirs close to the native riverflow
6. Utilize the warmer releases from outlet works and/or powerplants rather than spillway releases whenever practicable

Many of these measures used to alleviate river ice jams also affect the river environment. For example, Peters (2) and Gebhardt (3) have conducted studies indicating a decrease in fish population of 80 percent for fully channelized streams, 50 percent if basic stream cross sections and meanders are retained, and 25 percent if there is replanting of bank vegetation on basic cross sections and meanders. Variations in temperature and discharge may also adversely affect the river fish populations.

WATER CONVEYANCE SYSTEMS

Winter operation of water conveyance systems in cold regions has been accompanied by problems of such magnitude and complexity as to preclude year-round operation in some areas. Some project offices, however, due to years of experience and persistent efforts of their operating personnel, have been able to maintain winter operation. Indeed, the feasibility of some projects is contingent upon a 12-month operation period.

Some operating canals experience complete blockage of flow. A canal operating with an ice cover can become blocked by a large volume of frazil ice taken into the canal from a river diversion. A canal operating without an ice cover may produce a large volume of frazil and/or anchor ice which blocks the flow of water. A canal which has been shut down for the winter, if operated too early in the spring, may become blocked by ice which has accumulated in the canal prism during the winter. Such blockage can result in a "washout" of the canal or in the case of a power canal, the shutdown of the powerplant with loss of power revenue.

Several methods are used to divert relatively ice-free water from a river. However, all of these methods require excess water to carry the ice away from the diversion entrance. This excess water is not always available. Most schemes

utilize ice-shearing booms to divert floating ice down the river and allow water which is more or less ice free to flow through the headgates. A similar result can be accomplished where an ice cover develops at the area of diversion by cutting a channel through the ice cover surface. Use of outboard motors or electric motor-driven propellers will increase the flow through the narrow ice channel and the slush ice can be diverted into a wasteway (Figure 3).

HYDRAULIC STRUCTURES

Hydraulic structures operated during periods of extended cold weather are subject to operational difficulties resulting from ice formation, which affects intakes, outlets, and spillways by choking or restricting normal operation and by limiting or preventing emergency operations.

Intake trashracks may become clogged with collections of frazil ice on the bars or they may be choked off with chunks of floating surface ice. In either situation, delivery of water or production of power, or both, may be interrupted. Trashracks should have adequate submergence when possible to prevent surface ice accumulation against the racks. Placing trashracks on a flat slope will minimize ice jamming against them if proper submergence is not available. Racks should be heated if there is a possibility of frazil ice accumulation on the bars.

Ice formation on outlet works or spillways is usually a direct result of leakage or spray (Figure 4). Such accumulation may prevent emergency usage of gates and delay or interfere with early spring water deliveries. Ice formation resulting from spray or leakage also provides serious safety hazards to operating personnel and maintenance crews. Maintenance schedules during winter months may be delayed or prevented.

Heat tapes should be installed in drains, in air vents, around control piping, behind wall plates and under sill plates of outlet and spillway gates where winter operation is normal or where emergency operation may be required.

Air bubbler systems have been very effective in eliminating intake structure ice problems in deep reservoirs. Air injected into the bottom of the reservoir rises to the surface and creates convection currents that circulate warmer water from the lower levels of the reservoir to the surface.

SUMMARY

As a result of the review of ice problems, the Bureau of Reclamation has established an Ice Research Management Committee to coordinate and direct a research program with the objectives of eliminating or alleviating the ice difficulties mentioned in this paper. Many of these ice difficulties are not easily resolved. The efforts of the committee will be directed toward:



Figure 3. - View looking at channel cut in the ice at the Wind River Diversion Dam. Outboard motors are used to divert slush ice away from the power canal entrance .



Figure 4. - View of ice accumulation on Morrow Point Dam outlet gate house due to spray and spillway gate leakage (spillway located above outlet works).

1. Design, laboratory, and field studies to develop solutions for specific problems which later may be applicable to more general problem areas
2. Establishing more coordination between the Bureau of Reclamation and other organizations involved in similar research

REFERENCES

1. Burgi, P.H., and Johnson, P.L., "Ice Foramlion - a Review of the Literature and Bureau of Reclamation Experience", REC-ERC-71-8, U.S. Bureau of Reclamation, Denver, Colorado, September 1971
2. Peters, J.C., "Operations sice 1963 under Montana's Stream Preservation Law", Transactions of the Thirty-fifth North American Wildlife and Natural Resources Conference, March 7-10, 1970
3. Gebhardt, J., "The Vanishing Stream", Idaho Wildlife Review, Vol. 22, No. 5, March-April 1970



ICE SYMPOSIUM 1972
LENINGRAD

WINTER OPERATION OF HEATING SYSTEMS OF
HYDROMECHANICAL EQUIPMENT OF HYDRAULIC
STRUCTURES

S.M. Aleinikov, Head of Group,	the B.E. Vedeneev VNIIG,	Leningrad, USSR
R.A. Gutkin, Chief Design Engr,	Design Bureau, Lengidro-	Leningrad, USSR
	stal'	
V.M. Chesnokov, Chief Engr,	Design Bureau, Lengidro-	Leningrad, USSR
	stal'	

SYNOPSIS

Problems are considered pertaining to winter operation of hydromechanical equipment of hydroelectric power plants. Emphasis is placed on heating which appears to be the most effective means of combatting ice troubles. A description is presented of induction-heating, a most advanced heating technique. Studies of winter operation experience permitted to formulate the general principles of proper design for heating systems.

RESUME

On analyse un nombre de problèmes relatifs aux particularités de l'exploitation hivernale de l'équipement hydromécanique des usines hydro-électriques. C'est le chauffage qui donne la possibilité de surmonter les difficultés dues à la glace. Le procédé le plus progressif du chauffage - le chauffage par induction - est décrit. On démontre que l'étude de l'expérience acquise lors de l'exploitation hivernale des usines hydro-électriques permet de formuler les règles principales d'élaboration des projets pour les systèmes de chauffage.

In view of propagation of hydroelectric construction in the U.S.S.R. to regions with a rigorous climate, problems relevant to combatting ice troubles in operating hydromechanical equipment of power plants have become most urgent.

Heating is at present the most extensively used anti-icing technique to ensure reliable service. A wide variety of heating system designs is available in operation practice, choice of a suitable design being determined both by winter service conditions and by design features.

The most common arrangements are those based on circulation and non-circulation oil heating, bar-heating (supplying current directly to the metal members), ohmic furnace heating, warm-air heating, induction-heating. Each of these methods possesses certain merits and disadvantages, though induction-heating appears to be the most efficient one and the most extensively used one at present. The main advantages of the method are as follows: liberation of 80 to 85% of heat energy within the metal to be heated (dispensing with a heat-transfer agent), absence of external current-carrying details, possibility of standard voltage application, feasibility of differential heat liberation in the structural members in which it is needed.

Induction-heating is based on utilizing a well-known physical phenomenon, viz. generation of eddy currents when ferromagnetic bodies are crossed by an electromagnetic field. The magnitude of the currents depends on the electromagnetic field, the dielectric constant and the magnetic permeability of the material and the field frequency variation. When using industrial frequency voltage, current intensity control and, hence, that of the magnitude of energy release may be effected in practice by varying the electromagnetic field intensity. Field intensity being proportional to the number of ampere-turns, one can obtain practically any value of energy release in the metal by varying the impressed voltage and the number of turns in the inducing winding. To get high energy parameters when applying induction-heating an inductor with a magnetic circuit is utilized, such an electromagnetic scheme permitting the use of a simple inductance coil. Both laboratory and field tests of the above inductance-heating schemes revealed that their electrical efficiency may be about 0,85-0,90 and the power coefficient 0,75-0,85. The service life of an induction heater is assessed at 25-30 years.

Induction schemes are mainly used to heat the embedded parts of gates and trash racks at hydroelectric power plants.

In recent years the B.E. Vedenev VNIIG and the Design Bureau of the Leningrostal' conducted extensive joint investigations to gain a better insight into and generalize winter service experience of hydroelectric power plants. The research results indicate that ice troubles may occur during winter operation of hydroelectric power plants almost in every region in this country. The main difficulties encountered in winter operation of hydromechanical equipment are: icing of service and emergency-maintenance gates and embedded parts of spillways,

those of turbine emergency closing valves, of gate operating gear, freezing-over and ice clogging of water intake and turbine trash racks and concrete surfaces adjacent to trash racks, gates and gate guide ways, static action of the ice cover against the gates.

The heating arrangements for hydromechanical equipment of hydroelectric power plants have proved to be sufficiently effective in ensuring normal winter operation of hydro power plants against ice and frazil-ice troubles. The design of heating systems is based on calculation procedures substantiated theoretically whose main principles are presented in a code of practice*.

It should be stressed, however, that the proper design of heating arrangements is inseparable from specially designed hydromechanical equipment elements to be heated considering service conditions under which ice troubles may occur.

Let us examine the problem in greater detail with regard to trash racks and gates.

A study of the operation of an experimental trash rack with induction-heating at the Matkozhenskaya hydro power plant demonstrated that the trash rack turned out to be almost completely clogged with frazil at a high frazil-ice run rate, which resulted in a significant reduction in the power unit load, though the temperature of the heated members (i.e. of the frontal parts of the bars and cross beams) was above the freezing point and fully conformed to thermal design. Trash rack clogging was caused by the presence of unheated structural members on which frazil crystallization commenced. Later the process was greatly intensified embracing the heated members of the trash rack.

It stands to reason that trouble-free operation of the heated trash rack, with the water supercooled and frazilization proceeding at a great rate, may be ensured only in case all the structural elements of the trash rack can be heated.

Experimental laboratory studies at the VNIIG and the Leningradskiy Design Bureau resulted in working out by the latter of an original trash rack design meeting the requirement; the first trash racks of this type being installed at the Vygostrovskaya, Byelomorskaya and Poduzhenskaya hydro power plants. The drop-shaped trash rack bars reduced to a minimum head losses at the trash rack and facilitated induction-heating at high power parameters.

The unusual design features of the trash rack permitted to practically eliminate unheated members providing for effective control of frazil ice troubles at the hydro power plants.

A survey undertaken in October 1970 disclosed that, on the whole, the new design of trash racks at the Vygostrovskaya and Byelomorskaya power

* Recommendations on the Design of Heating Arrangements for Hydromechanical Equipment Elements of Hydroelectric Power Plants, VSN 029-70 Minenergo U.S.S.R., Energia, 1971.

plants makes for normal operation of power units during frazil ice passage. The authors would like to emphasize that it was not only the application of induction-heating, but also the efficient design of the trash rack structure which easily lent itself to the heating arrangement were conducive to finding the proper solution to the problem. It is worthy of note that no matter how efficient the design of the trash rack or how high the heating intensity may be, the great masses of frazil cannot be melted. The frazil mass will pass through the heated trash rack provided the frazil lump diameter is smaller than the spacing between the trash rack bars. Hence, heating of trash racks must go hand in hand with effective measures contributing to speedy stabilization of ice cover, special arrangements for partial detention of frazil in the forebay, or frazil passage through the structure.

Significant modifications facilitating frazil-ice control have been lately introduced in the design of trash racks where frazil is likely to occur, but the design features of gates used for winter service have remained essentially unaltered due to a number of reasons, though problems pertaining to gate operation in winter are in every respect as pressing as frazil ice passage through the trash racks.

Almost in every case when gates have to be manoeuvred in winter, the operating staff are confronted by troubles due to icing of the gate structures and their freezing either to the concrete or to the embedded members, though heating is provided.

Severe troubles in winter operation of gates are caused not so much by the disadvantages of the gate heating arrangements as by the gate design being badly adapted to operation under ice regimes.

The unheated skin plates and sealing ribs protruding upstream lead to ice bridge formation between the gate and the concrete. The arm of a tainter gate and its side plating freeze to the concrete, particularly, at partial gate openings. Ice in the guide rails of slide gates tightly bonds the ribs, the stiffening plates and supports to the concrete of the guide slot.

Considerable ice mounds form around bogies disrupting normal operation, manual removal of the ice being impossible due to confined slot space. No heating system is capable of melting an ice layer thicker than 1.5-2.0 mm and is manifestly unable to remove ice from the protruding parts of the structure.

Hence, in our opinion, gates adapted to winter service should be free of outward elements strongly projecting upstream in the neighbourhood of the slot, or into the slot. Radial gate arms should be covered with smooth skin plates and be heated. Slide gate bogies must be located within the gate chamber which must accommodate a heating arrangement.

Tentative attempts towards achieving such a gate design were made at the Leningrad Design Bureau. A fixed roller gate was designed for the Voro-

nezh reservoir, with the roller path, the side frame of the gate, the bogies inside the gate chamber, i.e. within the heated zone. The gate design avoids elements projecting upstream or into the gate slot. The gate is expected to operate more efficiently under ice conditions as against conventional gates. Thus, specially adapted gate designs coupled with suitable heating systems must promote favourable winter service conditions.

In conclusion it should be strongly emphasized that combatting icing of hydraulic structure elements assumes an ever growing importance because of extensive water power development in the north-eastern regions of the Soviet Union, i.e. regions with a severe climate. Under these conditions effective operation of heating systems requires a considerable heightening of the unit capacity of heating arrangements which leads to great energy expenditure.

Hence, a quest for new effective means to control the freezing-over of metal and concrete surfaces has come to be eminently urgent.

Application of various polymeric materials with very low adhesion to ice appears to be very promising in this respect. An adequate solution to the problem may be the formation over the surfaces liable to freeze either of a strong permanent covering, or of one to be periodically renewed, which would do away with power consumption and ensure good protection against freezing over. However, in spite of some encouraging results already obtained there do not seem to be as yet available any coverings of such a type.

New vistas are opened by using electroconductive polymeric materials to combat icing. Beside being highly water repellent, they permit to supply power directly to the surface layer. Such a combination of characteristics permits to reduce unit capacities versus those applied in a conventional heating arrangements that ensure steady ice-free operation.



ICE SYMPOSIUM 1972
LENINGRAD

NAVIGATION LOCK EQUIPMENT FOR OPERATION
AT NEGATIVE AIR TEMPERATURES AND LOCK
CLASSIFICATION

Balanin V., Head, Chair, Mr. Sc. (Eng.)	Leningrad	
Dytman A., Head, Dept., Mr. Sc. (Eng.)	Water	Leningrad
Zhidkikh M., Senior Engineer	Transport	Moscow
Zugrova E., Senior Engineer	Institute	U.S.S.R.
Bykov L., Chief Engineer, Mr. Sc. (Eng.)		

SYNOPSIS

The paper deals with the classification of navigation locks concerning their operation at negative air temperatures. A typical layout of lock equipment for these conditions as well as some design relationships for the equipment of navigation locks are given too.

The problems considered are: velocity of the upward water flow preventing ice formation on the plating of the gates, and design loads on the ice boom in front of the lower mitre gate to protect the gate chamber from ice penetration.

RESUME

Dans ce rapport on donne la classification des écluses navigables pendant leur fonctionnement aux températures négatives de l'eau, le schéma typique de l'équipement de l'écluse dans les conditions mentionnées et les dépendances de calcul pour le projet de cet équipement.

On a envisagé les questions suivantes: la vitesse du courant ascendant de l'eau près de la porte, prévenant la formation de la glace sur le revêtement de la vanne et la charge de calcul devant la porte aval à deux vantaux pour la protection de sa chambre contre la pénétration de la glace.

As the freight traffic capacity of rivers must be increased and scheduled navigation terms ensured, the operation of navigation structures at negative air temperatures is imperative. Due to the above considerations a necessity arises of changing the structure maintenance regime, supplying them with special additional equipment and adapting the existing equipment to operation in new conditions.

The variety of navigation structure designs used on the waterways of our country, and different conditions they are to work in call for a new classification of those structures in order to outline typical layouts of lock equipment and typical model design schemes.

The above structures may be classified as follows:

a) Type of arrangement - a channel or a flood-plain arrangement with an outer harbour. In the latter case there is a considerable vertical temperature stratification in the outer harbour. This temperature stratification makes it possible to use the bottom water heat to maintain an unfrozen navigable channel.

b) Upstream and downstream level conditions are stable, e.g. in navigable channels, or fluctuate, either slowly or rapidly, as for instance in the upstream pools of hydroprojects with considerable winter drawdown, and the downstream pools with power stations operating to meet peak loads. The above regime determines the conditions of icing and ice cornice formation on vertical lock-chamber surfaces, on lock-chamber equipment (gates), and on guide and mooring devices at the approaches. Besides, water level conditions govern the type of equipment ensuring trouble-free operation of the lower gates.

c) Navigation lock-chamber location above or below the dam. To optimize the conditions of lock operation at negative temperatures it is important to maintain the upstream pool level in the lock. Favourable conditions for keeping such a water level are created in locks extending into the upstream pool beyond the dam, as the work of keys becomes easier.

d) The type of filling and emptying system - with controlled or uncontrolled flow during filling and emptying of the lock chamber. Locks of the first group are those in which separate chamber sections are fed from individual culverts. During emptying of locks with such supply systems it is possible to create a flow towards the upper lock head, thereby ensuring more favourable operation conditions of the lower (usually mitre) gates and minimizing the necessary additional equipment. The locks of the second group include those with a head-filling system as well as locks with simple distributing and equi-inertial filling systems.

Taking into account the fact that with the extension of the navigation period the traffic intensity decreases and, hence, a certain increase of locking

time is permissible, it is possible to get the required water flow direction in the chambers of locks with distribution filling systems incorporating not less than two culverts by quite simple means. Some culverts are used for filling and the others for emptying. In the latter, part of the orifices nearest to the lower head (1/3 or 1/2) are closed with simple dampers, say, iron sheets. These sheets are to be provided with simple locking devices, as during the emptying of the lock they will be pressed against the bottom or wall surface by hydrostatic pressure.

e) Gate design - mitre, rolling, tainter with a vertical axis of rotation, flap gates, vertical-lift gates, tainter gates with a horizontal axis of rotation, etc. Operation of the first four types presents the greatest difficulties. Figure 1 shows the typical layout of a lock operating at negative air temperatures.

While designing navigation lock equipment, it becomes necessary to determine some parameters. These are: air or water discharges from pneumatic installations and flow-forming devices of the lower gate used to maintain the water area of the chamber free from ice. These calculations may be carried out using dependences given elsewhere*. Icing of the lower gates may be prevented by insulating the downstream skin plates as well as by heating the interplating space or by intensifying upward water currents along the plating using pneumatic installations. Proceeding from thermal balance equation and assuming the factor of heat transfer from water to ice surface $\alpha_1 = 300 + 1800 \sqrt{V}$ kcal/m² hr °C (V = the velocity of upward current, m/sec), and heat transfer factor from the metal of plating to the air $\alpha_2 = 6.47 V_a^{0.78}$ kcal/m² hr °C (V_a = the velocity of air motion, m/sec), the following velocity value preventing ice formation on the plating surface of more than prescribed thickness δ_i will be received

$$V = \left[\frac{-t_a}{t \left(\frac{\delta_i}{\lambda_i} + \frac{\delta_0}{\lambda_0} + \frac{1}{\alpha_2} \right) 1800} - 0.167 \right]^2 \quad (1)$$

where t_a and t = air and water temperatures, °C, respectively; δ_0 and λ_c = thickness and plating heat conductivity factor, respectively.

When neglecting icing of the plating, in Equation (1) $\delta_i = 0$ should be adapted. The required air discharge for ensuring the velocity, V, in the upward current is determined from the paper cited above.

Calculation of the ice boom in front of the lower gates is done for three types of loads.

* Balanin V. Effect of ice on water intakes including the design of ice-free channels. LAHR Symposium, Ice and its action on hydraulic structures, Reykjavik 1970.

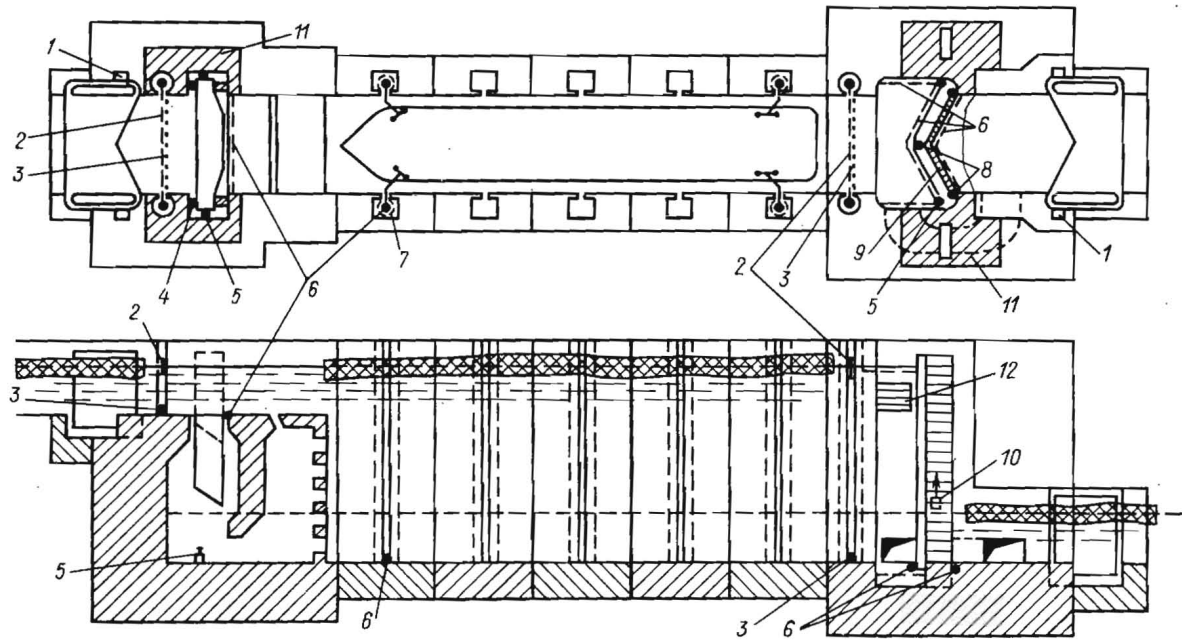


Fig. 1. Typical layout of a lock operating at negative air temperatures:

1 - recess for flow-forming device; 2 - ice boom; 3 - perforated airline with nozzles; 4 - heating of the upper part of the gate sealing; 5 - air nozzle; 6 - perforated airline; 7 - heated floating mooring ring; 8 - heating of the saddle beam and mitre sealing; 9 - insulation plating; 10 - heating of interplating gate space; 11 - heated rooms; 12 - heaters of supplied water.

The dynamic pressure of a separate block of ice, P_1 , derived from the kinetic energy equation, considering the ice boom deformation, is determined according to

$$P_1 = 2 \cos \alpha \sqrt{\frac{ES}{B} \left(\frac{h \Omega \gamma_i V_i^2}{2g} - P_1 f \right)} \quad (2)$$

where α = angle between the end of the ice boom and the longitudinal lock axis due to ice impact; E = rope elasticity modulus; S = area of rope cross-section; B = chamber width; h = thickness of ice block; Ω = area of ice block; γ_i = ice volume weight; V_i = ice block velocity; g = acceleration of gravity; P_1 = linear metre weight of ice boom; and f = original sag of ice boom.

The pressure of broken ice on the ice boom during chamber emptying is due to hydrodynamic pressure on the end ice block surface and to flow friction against its lower surface. Per linear metre of the ice boom it equals

$$P_2 = (\alpha \gamma h + 1.72 \beta \gamma B) \frac{V_s^2}{2g} \quad (3)$$

where α = factor depending on the shape and streamlining of the ice block (varying from 1 to 2); γ = volume weight of water; β = factor varying as a function of the ratio of ice thickness to the depth of flow, H , ($\beta = 0.05$ when $\frac{h}{H} = 0.1$ and $\beta = 0.2$ when $\frac{h}{H} = 0.45$); V_s = surface flow velocity in the lock chamber. The velocity V_s may be defined by the electrodynamic analogy method on a space model.

Pressure on a linear metre of the ice boom, P_3 , during the ship movement arises if the latter approaches the ice boom closer than $3B$

$$P_3 = \frac{R \left(1 - \frac{f}{3B \psi} \right)}{B} \quad (4)$$

where R = propeller thrust; f = factor of ice friction against concrete; and ψ = angle of the ship bow.

Optimal stress in the boom rope causes pressure, P_3 . When it is possible to moor a ship at a distance of $> 3B$ in a lock 30 m wide the limiting load is P_2 , and in a lock 18 m wide, the limiting load is P_1 .



ON THE APPLICABILITY OF DIFFERENT ELECTRI-
CALLY-CONDUCTIVE POLYMERIC COMPOSITIONS
IN LOW-TEMPERATURE HEATERS

K.A. Andrianov, Acad.	The M.V. Lomonosov	Moscow,
L.M. Khananashvili, M. Sc. (Chem.)	MITKHT	U.S.S.R.
G.I. Chogovadze, Director	GrusNIEGS	Tbilisi,
D.G. Pagava, Jr Res. Offr		U.S.S.R.
M.I. Topchiashvili, Head of Lab.		
A.G. Zelentsov, Jr Res. Offr		

SYNOPSIS

Presented are results of investigations carried out at the Georgian Research Institute of Power Engineering and Hydraulic Structures (GrusNIEGS) to obtain low-temperature heating elements characterized by a high conductivity, a stable performance, and a wide operating temperature range (with the upper limit of 70 to 80°C).

The applicability of conductive polymeric materials as anti-icers is considered.

RESUME

Le rapport contient les résultats des recherches sur l'obtention des éléments chauffants à basse température, effectuées à l'Institut des Recherches de l'Energétique et des Ouvrages Hydrauliques à Tbilissi. Ces éléments sont caractérisés par une haute conductivité électrique, par la stabilité de fonctionnement et par une large intervalle de température (limite supérieure 70-80°C).

On considère la possibilité d'utiliser les matériaux polymères conductifs pour la lutte contre la glaciation.

From a great body of published data on electroconductive polymeric materials [1-5] it is known that many research institutes in this country and abroad have been developing and studying semiconductive plastics.

By their electric resistivity ($\rho = 10^{-2}$ to 10^7 ohms/cm) polymer-based conductive materials are classed with semiconductors.

Conductive materials can be obtained by introducing substances of low electric resistance (metals, salts, conductive black or graphite) into conventional organic dielectrics (both monomers and polymers).

As reported elsewhere [6], polymeric semiconductors containing the above-mentioned fillers possess n -type conductivity. In contrast to common conductors, conductive polymers have the following advantages: high corrosion resistance, ease of manufacturing of complex-shaped parts, low specific weight, and high plasticity (low modulus of elasticity).

The GrusNIEGS has succeeded in developing conductive polymeric compositions, homogeneous over the sheet, with a wide modulus of elasticity range and a resistivity varying within 1 to 10^6 ohms/cm.

At present, for aircraft and ship deicing use is made of various conductive polymers which have proved effective under the most rigorous conditions. In connection with recent hydropower development in cold regions in the USSR and other countries, much emphasis has been placed on the research into anti-icing precautions for hydraulic structures.

The studies on new conductive polymeric compositions carried out at the GrusNIEGS resulted in obtaining different polymers of high conductivity, which provided a basis for considering the possibility of using these materials as low-temperature heaters.

It should be noted that Soviet investigators have already done some work on the development of polymeric heaters which have found application in various branches of national economy [7].

The polymeric compositions developed at the GrusNIEGS on the basis of chlorinated polyvinylchloride, with silicoorganic compounds used as modifiers, and different types of rubbers with resistivities of 0.8 to 2.0 ohms/cm were employed in low-temperature heating elements.

The stable performance of a heating element to be operated under high-humidity low-temperature ambient conditions and exposed to repeated heating-cooling cycles, is of paramount practical importance.

Testing of conductive compositions under repeated heating-cooling indicated that their high electric conductivity permits to obtain heaters with capacities of 0.3 to 0.8 W/cm², which meets the low-temperature operation requirements.

The optimum thickness of a heating element is governed by specified operating conditions and may vary from 0.5 to 10 mm.

It should be emphasized that for practical use of polymeric heaters their adequate adhesion to protected (heated) surfaces is of great significance. In-

vestigations of the available conductive silicoorganic compositions demonstrate their high adhesion to metals and concrete, the employment of special glues and glueing techniques ensuring ease in treating heated surfaces of intricate shape.

One of the major criteria of stable performance of a heating element is the temperature resistance coefficient of the conductive material.

For approximate evaluation of the temperature resistance coefficient within a narrow range of temperatures, the well-known formula may be used:

$$\alpha = \frac{R_2 - R_1}{R_1(t_2 - t_1)} \quad (1)$$

in which R_1 and R_2 are the initial and the final resistances of the element; t_1 and t_2 are the initial and the final temperatures of the element; and α is the temperature resistance coefficient of the element.

To ensure stable performance of a heating element within a given temperature range it is essential that a positive temperature resistance coefficient in the same range be provided. A negative temperature resistance would be conducive, (with the terminal voltage held constant) to a monotonic increase in the heat output of the element, which would eventually disturb the structure of the material and cause its failure.

As found from the results of a 40-day test on a heating element of chlorinated polyvinylchloride modified with silicoorganic compounds under the conditions of a diurnal heating-cooling cycle, the resistance of the conductive material and its temperature resistance coefficient vary with time as shown in Fig. 1. Throughout the experiment a constant voltage of 6 V A.C. was maintained at the element tested.

Figure 1 shows the following curves:

1. The time-dependent variations in the resistance of the heating element when switched off (steady-state conditions, cooling cycle, ambient temperature of 20°C).
2. The time-dependent variations in the resistance of the heating element when switched on (steady-state conditions, heating cycle, ambient temperature of 50 to 60°C).
3. The time-dependent variations in the temperature resistance coefficient of the heating element.

As evident from Fig. 1, during the first days of the test the resistance of the heating element decreases to a certain level, whereupon it will rise with heating and drop with cooling, tending to stabilize with time under the steady-state heating conditions, provided the voltage at the element terminals remains constant. The increase in the temperature resistance coefficient of the heater with time is due to the opposite signs of the second derivative of curves 1 and 2, which shortens the duration of the transient process, the increase in the absolute value

of resistance under the steady-state heating conditions being insignificant.

An investigation of the transient process seems to be of interest and is expected to give more complete information on the changes in the resistance of a given conductive material under different operating conditions.

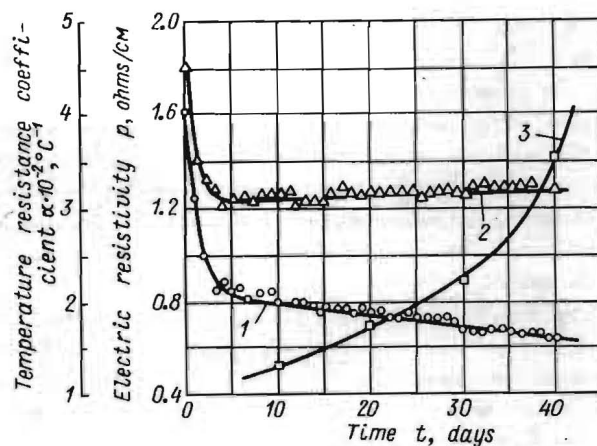


Fig. 1.

- 1 - temperature resistance coefficient α , $^\circ\text{C}^{-1}$
- 2 - electric resistivity ρ , ohms/cm
- 3 - time t (days)

Recent investigations conducted at the GrusNIEGS resulted in the development of heating elements displaying a stable performance in the temperature range of 80 to 100 $^\circ\text{C}$, which encourages their ever growing application as anti-freezing means and opens up a wide field of other uses in various domains of science and engineering.

The conductive polymeric materials used in heating elements have an extremely homogeneous structure preventing nonuniform heating or local overheating.

Heating elements can be designed for voltages ranging from a few to hundreds of volts, direct or alternating current, as may be required.

In conclusion it may be pointed out, that using adequate techniques, the available conductive polymeric compositions can be applied for deicing of apparatus and structures of most intricate shape.

The anti-icing effectiveness of conductive heating elements and coatings using different types of rubbers or compositions based on chlorinated polyvinylchloride modified with silicoorganic compounds needs to be corroborated by field tests under different operating conditions, including such factors as humidity, minimum temperature, mechanical loads and impacts on the surface, vibration, etc.

REFERENCES

1. Organic semiconductors. Edited by V.A. Kargin, Akademia Nauk SSSR, 1968.
2. Galperin, B.S., Wireless resistors. Energia, 1968.
3. Conductive resins. Otechestvennaya i inostrannaya knizhnaya, zhurnalnaya i patentnaya literatura (1955-1960), Sibirskoye otdelenie Akademii Nauk SSSR, N 20747, 1960.
4. Electroconductive polymeric materials, their properties and application. Edited by V.E. Gulia, ZTI, Moskva, 1961.
5. Boguslavski, L.I., and Vannikov, A.V., Organic semiconductors and biopolymers. Nauka, 1968.
6. Sazhin, B.I., Electric conductivity of polymers. Khimia, 1965.
7. Gull, V.E., et al., Electroconductive polymeric materials. Khimia, 1968.



SPECIFIC FEATURES OF ICE CONDITIONS IN
RIVERS AND RESERVOIRS OF CENTRAL ASIA

V.P. Zakharov, Acad., the Kazakh SSR Acad. of Sci.	The Kazakh NIIE,	Alma-Ata, USSR
M.M. Beilinson, M. Sc. (Eng.)	The Kazakh State Pe- dagogical Institute nam- ed for Abai	Alma-Ata, USSR
I.N. Shatalina, M. Sc. (Eng.)	The B.E. Vedeneev VNIIG	Leningrad, USSR

SYNOPSIS

Considered is the character of ice production (frazil ice, shore ice), frazil ice cover formation and progression, frazil ice jamming in rivers and reservoirs of Central Asia. Ice troubles in hydraulic structure operation fall into two main categories: one is related to supercooling of water, and the other to the rise of the water level due to ice jams. Means for eliminating such troubles are indicated.

Discussed is forecasting of hazardous ice phenomena, freeze-up dates, the amount of ice and the dynamic behaviour of frazil in the flow.

RESUME

On considère le caractère de formation de glace (sorbet, glace le long des rives), de formation et de progression du couverci de sorbet, de l'embâcle dans les rivières et réservoirs de l'Asie Centrale. Les troubles créés par la glace dans les ouvrages hydrauliques en service sont divisés en deux catégories principales: la première est liée à la surfusion de l'eau et l'autre à la remontée du plan d'eau due à la formation des embâcles. On indique les moyens pour éliminer ces troubles.

On examine les problèmes de la prévision des phénomènes de glace dangereux, de la date de prise en glace, de la quantité de glace et du comportement dynamique du sorbet dans un écoulement.

Ice Production in Rivers and Reservoirs of Central Asia

The region in question has a continental climate. The character of ice production, viz. formation of narrow bands of shore ice, underwater ice - both frazil and bottom ice - due to supercooling of the flow, is conditioned by relatively high channel slopes.

Shore ice which forms most intensively in tranquil zones is a more stable ice formation and is incompletely destroyed with a periodic onset of higher temperatures. The shore ice bands increase gradually constricting the open water area of the river. Drifting frazil accumulations (frazil covers) and bottom ice in suspension freeze to the shore ice contributing to its growth. At the narrowest section the frazil comes to a standstill and gets frozen forming an ice dam. Part of the ice material adheres to the dam, and the rest is carried under it forming frazil accumulations underneath the ice cover. On the Ili river frazil accumulation under the ice cover is estimated at 3 m thick, while on smaller rivers it is 1.5 m. Freeze-up on frazil-producing rivers occurs as an ice jam progressing upstream, which sets up rising of the water level, retards frazil cover movement and accelerates ice cover formation.

The earliest ice jams in rivers are commonly observed in the upper zones of reservoirs. Flow velocity retardation is conducive to frazil packing, decreasing of frazil cover movement and ice jamming, which frequently leads to flooding of the surrounding area.

On the freezing rivers of Kazakhstan the mean duration of frazil ice run in autumn ranges from 12 to 64 days, the maximum duration being within 38-114 days. On large rivers (the middle course of the Ili river) the frazil cover thickness is assessed at 25-40 cm, while on small rivers it is 8-10 cm. The volume of frazil ice on the Ili river may reach 40-50 million of cubic metres which may cause serious ice troubles.

Ice Troubles in Hydraulic Structures

Troubles in hydraulic structure operation due to ice production in autumn and winter fall into two main categories: one is related to supercooling of water, and the other to rising in the water level due to ice jams.

Rational preventive measures against supercooling comprise heating of metal and concrete constructions of hydraulic structures, frazil ice passage through spillways and special ice chutes of hydropower and pumping stations, or local heating of watercourses.

As regards the second group, it may be of advantage to remove projects located in the flood zone beyond the jam backwater area or to protect them by temporary earth dykes. Recommended are also channel improvement and use of explosives, the latter being not always efficient in ice jam removal.

Ice Forecasts

Of essential importance in establishing a means of combatting ice and frazil ice troubles is adequate ice forecast for watercourses submitted to supercooling.

Heat balance estimates from hydrometeorological data, which are commonly used in engineering practice, allow to determine the total quantity of ice material ^{1/}. Provided hydrologic observation data are not available, meteorological and synoptic data are employed in forecasting ice phenomena ^{2/}. The amount of frazil ice and its behaviour in the flow may be evaluated based on the physics of ice production in supercooled water ^{3/}.

Freeze-up Date Forecasts

In case hydrologic data are not available, methods for predicting the freeze up date are based on the dependence of ice phenomena on the foregoing synoptic situation over the reservoir surface.

The investigations indicated that the onset of ice production is strongly affected by the west ridge of the Siberian anticyclone and anticyclones from the North forming over the territory of Kazakhstan. The predominant direction of air masses in the troposphere is established using the index of atmospheric circulation, J , and atmospheric pressure, P . Proceeding from the analysis of the data, a prognostic relationship for determining the freeze-up date beginning from November 1 is proposed

$$T = aJ_{IX} + b \Delta P_{VM \rightarrow IX} + C \quad (1)$$

Formula (1) predicts well in advance the penetration of a meridional flow of cold air masses from the North. However, in the southern regions of Kazakhstan cold waves are generally of short duration not always sufficient for freezing of a reservoir. In order to enhance the reliability of long range forecasts

^{1/}Shulyakovski L.G., Ice production and freeze-up date in rivers, lakes and reservoirs (Estimates for forecast purposes). - Gidrometeoizdat, Moscow, 1960.

^{2/}Beilinson M.M., Use of meteorological and synoptic data for short and long range forecasts of freeze-up dates in lakes and reservoirs of Kazakhstan in the absence of hydrologic data. - Trudy Kazakhskogo nauchno-issledovatel'skogo gidrometeorologicheskogo instituta, 1966, vyp. 25.

^{3/}Pekhovitch A.I., Shatalina I.N., Experimental evaluation of the crystallization rate of supercooled aqueous solutions. - Izvestia VNIIG, vol. 90.

reservoir heat reserves on the forecast day should be considered, and the heat balance resultant, \mathcal{G} , included in (1). Hence, the prognostic relationship for the freeze-up date assumes the form

$$T = f(J, \Delta P, \mathcal{G}) \quad (2)$$

Dynamic Behaviour of Frazil Ice in the Flow

Frazil production starts with the growth of ice crystals in supercooled water. As the growth of ice crystals proceeds, they are distributed and gradually become buoyant in the flow depending on crystal size and turbulence of the flow. Ice crystals will be floated if the fall velocity of the frazil ice exceeds the mean vertical fluctuating flow velocity. The fall velocity of frazil ice, v (cm/sec), may be represented as ^{4/}

$$v = 167 \sqrt{d}^{0.69} \quad (3)$$

and the mean vertical fluctuating velocity may be written as ^{5/}

$$W_m = \frac{\sqrt{g} V_m}{\sqrt{MC}} \quad (4)$$

in which $M = 0.7 C + 6$, C being Chezy's coefficient. Hence, the condition of frazil ice buoyancy may be expressed as

$$V_m \leq \frac{167 \sqrt{d}^{0.69} \sqrt{MC}}{\sqrt{g}} \quad (5)$$

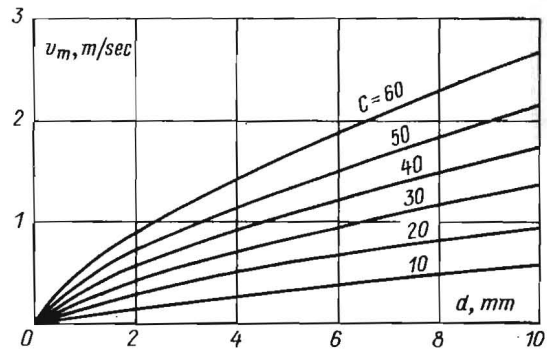
i.e. if the flow velocity is lower than V_m , frazil ice crystals of the diameter, d , will become buoyant in the flow under given channel characteristics, C . The smaller Chezy's coefficient, the lower velocities condition frazil ice floating. At $C = 10 \text{ m}^{1/2}/\text{sec}$ the frazil ice cover forms at velocities lower than 0.5 m/sec (Fig. 1), this value recommended for ice control in situ ^{6/}. In channels with larger Chezy's coefficients a frazil ice cover occurs at higher velocities as well.

The calculations performed enable ice regimes in regulated rivers to be modified thus preventing frazil ice jamming and associated rises in the water level.

^{4/} Bibikov D.N., On the fall velocity of frazil ice.-Gidrotekhnicheskoye stroitel'stvo, 1952, N 3.

^{5/} Kamushev A.V., Problems of dynamic behaviour of water streams.-Gidrometeorologiya, 1960.

^{6/} Yestifeev A.M., Control of frazil ice flows in hydropower plants.-Gosenergoizdat, Moscow-Leningrad, 1958.





ICE SYMPOSIUM 1972
LENINGRAD

EFFECT OF ICE FORCES ON SOME ISOLATED
STRUCTURES IN THE ST. LAWRENCE RIVER

J.V. Danys	Ministry of Transport	Ottawa
Superintendent	Marine Services	Canada
of Civil Engineering	Operations Branch	

SYNOPSIS

The St. Lawrence River is one of Canada's most important waterways. A great number of large and small offshore lightpiers have been built to accommodate the navigational aids. The winters are rather severe and the main force on such isolated structures has been the ice thrust. Still it is difficult to correlate the theoretical analysis with a practical design; therefore, in this paper, the actual ice forces on some small lightpiers which have caused some structural deformations are calculated and compared with previous and contemporary design values. Only the river reach between Montreal and Lake Ontario is considered. Two large hydro plants at Beauharnois and Cornwall control the flow and levels to a great extent, thus reducing the potential ice forces.

SOMMAIRE

Le fleuve Saint-Laurent est l'une des voies navigables les plus importantes du Canada. Un grand nombre de phares, de toutes dimensions (reposant sur le lit du fleuve), ont été construits pour fin d'aides à la navigation. Les hivers étant très rigoureux, la force dominante sur les charpentes construites est facilement la poussée des glaces. Toutefois, on se trouve en difficultés quand il s'agit d'établir une corrélation entre l'analyse théorique et la pratique; à cette fin, et par cette présentation, nous avons tenté d'établir une comparaison entre les forces attribuables à la glace ayant causé des déformations à certaines des fondations de phares telles que calculées, d'une part, et comparaison avec les valeurs utilisées soit dans le passé ou couramment, d'autre part. Seule la partie du fleuve située entre Montréal et le Lac Ontario est considérée. Deux importantes centrales hydro-électriques situées à Beauharnois et à Cornwall permettent de contrôler le débit et le niveau des eaux dans une large mesure, réduisant ainsi l'effet possible des forces en jeu attribuables à la glace.

The off-shore lightpiers in Canada have been built for more than one hundred years, and the most popular type of sub-structure, almost to the last decade, has been a timber cribwork filled with stones founded on the timber piles or directly on rock or some other hard foundation. Although it was always acknowledged that the ice thrust was the main force to be resisted by a lightpier, the size of the ice force was unknown, and the design of the new structure was based on experience of the previously built ones. In the last decade a considerable amount of research has been done about the properties of the ice, but so far not too much correlation has been made with the practical experience. In this paper the calculated ice forces which caused structural damages or partial failure of the structures will be compared with some design values.

LAKE ST. FRANCIS AND LAKE ST. LOUIS

The glacial till deposits are in many areas covered with very soft marine clays reaching thicknesses of approximately 110 feet. The glacial tills are very firm foundations, approaching a hardpan in their properties and contrarily, the clays of the marine deposit are a very weak foundation for any structures.

In 1958 a number of lightpiers were built in Lake St. Francis and four of them were of the type shown in Fig. 1, built in 3, 6 and 10 feet depth of water. Traditional construction methods were followed for these small lightpiers and the main part of the substructure was a timber cribwork filled with stones and capped with a concrete slab. Where a soft foundation was encountered, eight timber poles were driven 40 feet deep or to refusal which was 15 and 25 feet. Three of these lightpiers sustained various structural damages, such as tilting or some displacement. Some repairs and modifications of the concrete cap and pile foundation were carried out in 1964 but the tilting has still occurred.

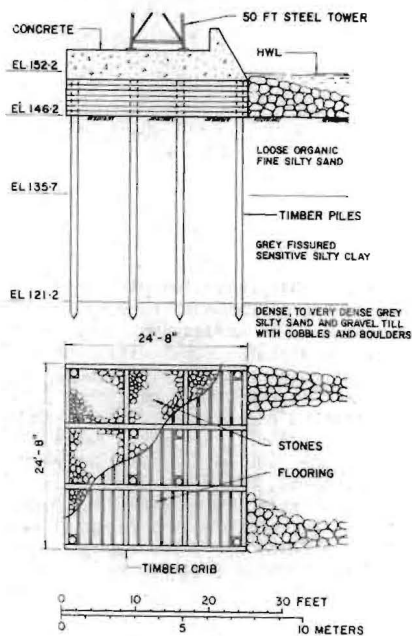


Fig. 1 Lake St. Francis-Substructure for Lightpier L.I. 124

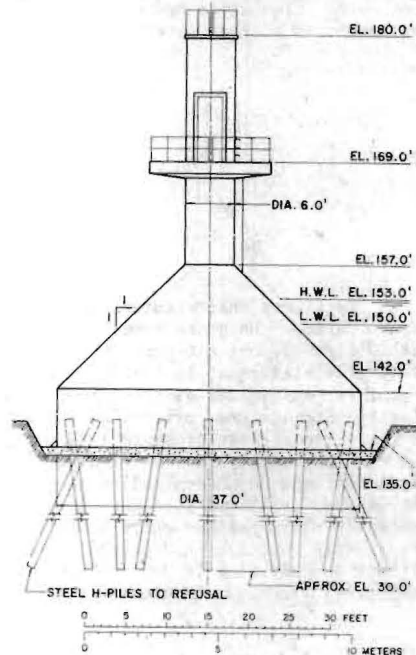


Fig. 2 Lake St. Francis-Lightpier at McKies Point

In 1966 five lightpiers of the type shown in Fig. 2 were built in Lake St. Francis in the locations where the depth of the soft marine clay was from 70 to 110 feet deep. The main part of the substructure of the lightpier was designed as a cone as such a shape more effectively breaks the floating ice and permits the building of a structure of smaller dimensions and so reduces construction costs. ¹ In 1967 in Lake St. Louis four lightpiers were built of the same type except that they were founded on the firm glacial till not requiring any piles. These nine piers have not suffered any damage or deformation. The design data of the assumed ice forces is summarized in Table 1.

Fig. 3 shows ice breaking against one of these lightpiers of the conical shape which has been widely used for Canadian lightpiers in the last decade. Fig. 4 illustrates in more detail the inter-action between the floating ice and the conical shape of the lightpier in Lake St. Peter.



Fig. 3 Lake St. Louis-Ice against conical substructure



Fig. 4 Lake St. Peter-Breaking of ice floe by conical substructure

ST. LAWRENCE RIVER INTERNATIONAL RAPIDS SECTION

Six of these concrete lightpiers were of the type shown in Fig. 5 built in 15 to 28 feet depths of water on firm glacial till. Their longitudinal axes are located in the direction of the flow, and the upper part exposed to the ice pressure is made of the minimum dimensions required for the placing of the small light towers. The stability of these piers in the direction of the current is much larger, roughly about four times as much, than in the lateral direction. After 12 years one of these lightpiers was overturned by the lateral ice thrust. At this particular location the channel is exposed to open water one mile in width. Under exceptional conditions the southerly winds may propagate large ice floes against the long side of the lightpier which introduce impact force on the ice floes. The calculated ultimate ice forces for these six piers are summarized in Table 1.

1. Danys, J.V. (1971) - "Effect of Cone-shaped Structures on Impact Forces of Ice Floes", 1st Intern. Conf. on Port and Ocean Engineering under Arctic Conditions, Abstracts p. 128-135

TABLE 1 - DESIGN AND CALCULATED ICE FORCES AT FAILURE

Designation of Structure	DESIGN FAILURE PRESSURES		Sustained Damage to Structure	CALCULATED FAILURE PRESSURES			
	lb/sq.in - (kg/sq.cm)			1000 lb	1000 kg	lb	kg
	XX-axis	YY-axis		lin.ft.	lin.m	sq.in	sq.cm
LAKE ST. FRANCIS - CRIBWORK SUBSTRUCTURES (1958)							
LL124	38 (2.6)		yes	11	16.5	38	2.6
LL127	32 (2.2)		yes	9	13.5	32	2.2
LL126	38 (2.6)		no	-	-	-	-
LL130	38 (2.6)		yes	11	16.5	38	2.6
LAKE ST. FRANCIS - MODIFIED CRIBWORK SUBSTRUCTURES (1964)							
LL124	90 (6.3)		yes	26	39	90	6.3
LL127	108 (7.6)		yes	31	46	108	7.6
LL130	70 (4.9)		yes	20	30	70	4.9
LAKE ST. FRANCIS - FIVE CONICAL CONCRETE SUBSTRUCTURES (1966)							
LL99 & 114	300 (21)	300 (21)	no	-	-	-	-
LAKE ST. LOUIS - FOUR CONICAL CONCRETE SUBSTRUCTURES (1967-8)							
LL 14 & 16	300 (21)	300 (21)	no	-	-	-	-
ST. LAWRENCE RIVER INTERNATIONAL RAPIDS SECTION - CONCRETE PIERS (1958)							
LL237	335 (24)	76 (5.3)	no	-	-	-	-
LL238	330 (23)	72 (5.1)	no	-	-	-	-
LL242	420 (30)	84 (5.9)	yes	24	36	84	5.9
LL248	295 (21)	63 (4.5)	no	-	-	-	-
LL249	430 (30)	84 (5.9)	no	-	-	-	-
LL259	430 (30)	84 (5.9)	no	-	-	-	-

TABLE 2 - PROPOSED THERMAL ICE THRUST

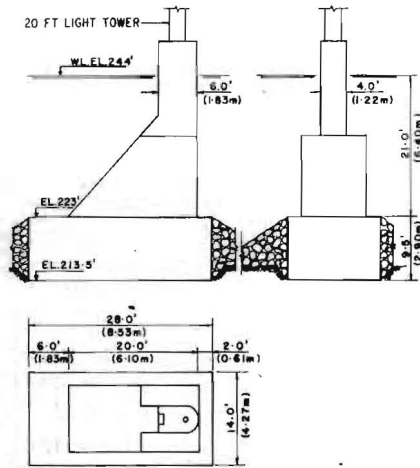
Author	1000 lb / lin.ft.		1000 kg / lin. m	
	Ice Thickness			
	17.6 in	35.2 in	45 cm	90 cm
Rose (1947)	3.2	5.9	4.8	8.8
From Monfore's values (1953)	15.2	15.8	22.6	23.6
CN-76-59, U.R.S.S.	8.7	17.4	13.0	26.0

TABLE 3 - APPLIED DESIGN VALUES FOR ICE FORCES

Type of Structure	Static or Impact Force	1000 lb lin.ft.	1000 kg lin. m	lb sq.in	kg sq. cm
Concrete dams	static	10	15		
Small lightpiers in lake	static	25	38		
Lightpiers built 1960-70	impact			120-400	8-28
Lightpiers, contemporary design	impact			200-250	14-18
Bridge piers (as per Code)	impact			400	28

PROPOSED AND APPLIED DESIGN VALUES FOR ICE FORCES

Table 2 shows the thermal ice thrust calculated from the experimental data or theoretical formulae. ² The field observations and measurements of the static ice thrust in Canada was made about 20 years ago by Ontario Hydro-Electric Commission. ³ The proposed design values for the concrete dams were 10,000 lb/lin.ft. This value has been used for the design of many Canadian dams by the various governmental authorities and consulting engineers, for example, for the Power Dam at Barnhart Island and the Long Sault and Iroquois dams of 2,200,000 hp power project at Cornwall, Ontario, on the St. Lawrence River built in 1954-58, which are in the same river reach as the discussed lightpiers.



For the lighthouse design, a value of 25,000 lb/lin.ft for thermal thrust has been used because the offshore lightpiers generally are small and isolated structures.

Generally, the impact force of the floating ice governs the design. In Canadian Marine Services the calculation of this force is based on the crushing strength of the ice. The design values have varied from 120 lb/sq.in to 400 lb/sq.in depending on the importance of the lighthouse and the severity of the expected conditions. For the contemporary design 200-250 lb/sq.in are used. The design thickness of the ice varies from 2 to 4 ft. and is based on measurements and observations. In Canada the design values of ice forces are not as yet standardized. Some applied design values are shown in Table 3.

Fig. 5 St. Lawrence River Lightpier 12

ACKNOWLEDGEMENT

The permission granted by Mr. J.N. Ballinger, P.Eng., Director, Operations, to present this paper, is gratefully acknowledged.

2. Drouin, M. (1970) - "State of Research on Ice Thermal Thrust" I.A.H.R. Symposium 1970 Proceedings 5.6, 11p.
3. Hogg, A.D. (1952) - "Ice Pressure against Dams: Some Investigations in Canada", A.S.C.E. Proc. vol. 78, separate no. 161



ICE SYMPOSIUM 1972
LENINGRAD

TWO LIGHTHOUSES DAMAGED BY ICE

Lars Bergdahl
Research engineer

Division of Hydraulics
Chalmers University of
Technology

Göteborg
Sweden

SYNOPSIS

Two cases of damage to lighthouses in the Baltic are reported. The maximum ice pressure is estimated from the mode of failure of the lighthouses. The calculations give a horizontal load of 1.1 to 1.7×10^6 N per meter width of structure.

RESUME

Deux cas de dommage à phare dans la mer Baltique sont rapportés. La poussée maximale est estimée par le mode de défaut des phares. Le calcul donne une poussée horizontale de 1.1 à 1.7×10^6 N/m.

ICE PRESSURE AGAINST LIGHTHOUSES [1]

Lighthouses, mooring and other isolated structures in the arctic and temperate seas are exposed to moving ice fields and pack ice. Dimensional criteria and rules for the design has long been needed.

In the Baltic isolated lighthouses have been built in areas with severe ice conditions since the thirties in spite of the fact that little was known about the forces from the ice. Some experiments with wood instead of pack ice was made by Frost [2] in 1941.

Only two of these lighthouses have been damaged by the ice so far. Thus, the other lighthouses seem to be pretty safe, but the probability of damage is very difficult to estimate.

DAMAGED LIGHTHOUSES

Two cases of damage to lighthouses, due to the ice, are known in the Baltic. One is Tainio lighthouse outside Helsinki in the Gulf of Finland and the other is the lighthouse of Nygrån outside Luleå in the Bay of Bothnia.

The lighthouse of Tainio. - Tainio lighthouse consists of a caisson which was sunk on a leveled macadam bed at nine meters depth in the summer of 1966. The lighthouse was finished in october except for the injections of the macadam bed. This work was postponed to the next summer.

At one occasion in the winter 1966-67 the lighthouse was pushed 14 m in the ESE-direction. The surrounding ice cover had an estimated thickness of 0.3 to 0.5 m. At the lighthouse, however, the ice was packed up to approximately 4 m thickness against the weatherside and 1 m against the leeside. The sea level was slowly rising and winds were strong.

The caisson was placed in position on radially arranged steel rails. At first these rails could have lessened the friction but in the final stage the lighthouse stopped against some protruding rocks.

[1] Bergdahl, Lars: Ice Pressure against Lighthouses. Report nr 59, Division of Hydraulics, Chalmers University of Technology, Göteborg 1971

2 Frost, Rikard: Uppförandet av fem bottenfasta fyrar invid djuprännan i Kalmar sund. Betong, Arg:26, pp 215-256, Stockholm 1941.

Hence, Löfquist and Palosuo [3] made the following estimation. The friction factor must have been between 0.3 and 0.7 until the lighthouse stopped against the rocks. The weight in water was $8 \cdot 10^6$ N which gives the ice pressure $4 \cdot 10^6$ à $5.6 \cdot 10^6$ N. Divided by the diameter, 3.5, of the circular cylinder this gives $1.2 \cdot 10^6$ à $1.6 \cdot 10^6$ N/m. ← from Mo Tests

The Lighthouse of Nygrån. - In late April 1969 the lighthouse of Nygrån was broken down by the ice. The type of rupture has been classified as pure bending after inspection by divers. According to Ernstsons and Kjellgren [4] there was no evidence indicating that the lighthouse had moved out of position. See figure 1.



Figure 1 The lighthouse of Nygran in June 1969.
Photo: Swedish Board of Shipping and Navigation 1

[3] Löfquist, Bertil: Istryck vid Ölandsbron. Statens Vägverk, PTB 102, Stockholm 1967

[4] Ernstsons, E. and Kjellgren, G.: Estimation of ice pressure and the bending moment at rupture of the light-house tower Nygrån. Swedish Board of Shipping and Navigation, Stockholm 1969.

Ernstsons has estimated the bending moment at rupture to $8.1 \cdot 10^6$ Nm from the appearance of the fracture. The surface of rupture was one meter under the sea level. So if the force acted at sea level it must have been $8.1 \cdot 10^6$ N. But the tensile crack formations on the tower indicate that the point of action was between one and two meter above sea level. That is the ice pressure could have been as low as $2.7 \cdot 10^6$ N.

The lighthouse was built on sand with a friction factor of 0.60 à 0.75. The weight was $7 \cdot 10^6$ N. This gives a highest probable load of $4.2 \cdot 10^6$ N. That is the resultant force from the ice must have attacked at least 1 m above sea level. The conclusion from the tensile crack formation is thus supported.

The lighthouse had a diameter of 2.5 m. See figure 3. The ice pressure would then be between $1.1 \cdot 10^6$ and $1.7 \cdot 10^6$ N/m.

What actually happened when the lighthouse broke down is not known. But the pack ice must have built up to at least one meter above sea level so that the forces from the surrounding ice fields could act at that elevation. See figure 3.

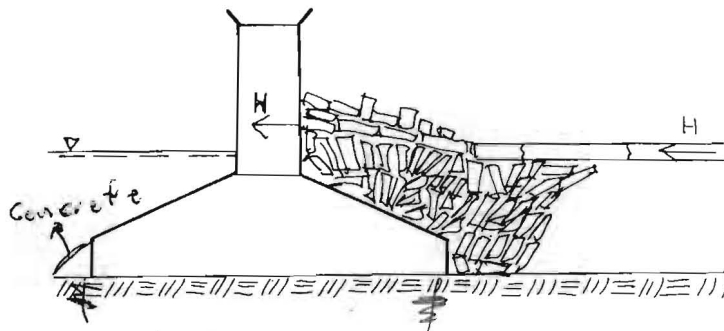


Figure 2 Scheme for the action of the ice

The lighthouse has been replaced by a new one on the same foundation caisson. The new tower is designed to withstand an ice load of $2.2 \cdot 10^6$ N/m at 2 m above sea level.

According to the maritime office of the Swedish meteorological and hydrological institute (SMHI, Larsson) the ice cover in the area most winters

reaches a maximum thickness of 0.70 m in late March or early April. The thickest smooth ice cover ever reported in the area is 0.90 m. Salinity in the water is 4.5 to 5 ‰. No regular observations of the ice have been carried out before the winter 1969/70.

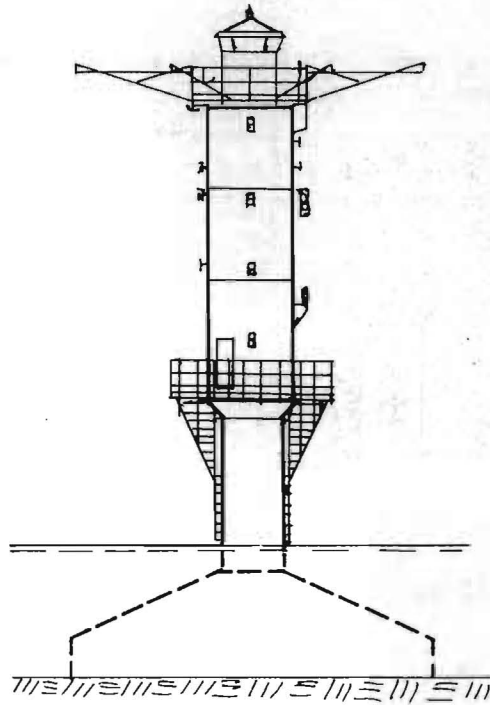


Fig. 3 Nygrån 1956.
From Ernstsons and Kjellgren [1]



ICE SYMPOSIUM 1972
LENINGRAD

THERMAL CALCULATIONS IN PREDICTION OF
ICE ACTION ON HYDRAULIC STRUCTURES

A.I. Pekhovich, M. Sc. (Eng.) The B.E. Vedenov All-Union Leningrad,
Sr Res. Offr Research Institute of Hydraulic U.S.S.R.
Engineering (VNIIG)

SYNOPSIS

Thermal calculations are indispensable in prediction of ice action on hydraulic structures and development of ice control measures. An analytical method based on the principles of superposition, equivalence and reciprocity is suggested for solving thermal problems. Presented are solutions to the problem on the ice cover thermal behaviour under variable air temperature and to that on the surface heating of concrete blocks with different layouts of heaters; formulae are given for evaluating the power required for heating trash racks.

RESUME

Les calculs thermiques font partie des prévisions de l'action de glace sur les ouvrages hydrauliques et de l'élaboration des mesures de lutte contre les difficultés dues à la glace. Pour la solution des problèmes thermiques on recommande d'utiliser une méthode analytique qui se base sur les principes de superposition, d'équivalence et de réciprocité.

On donne les solutions des problèmes concernant le régime thermique de la couverture de glace à la température d'air variable et le chauffage de la surface des blocs de béton pour différents schémas de disposition de réchauffeurs; on propose des formules de calcul de la puissance nécessaire du chauffage des grilles.

Once ice engineering was merely a complex of already existing branches of science. Now it consists of a number of new independent sciences, viz. ice physics, ice hydraulics, and ice thermal engineering, the latter being the subject of the present study. The aim of the paper is to show the place of thermal calculations among the problems associated with ice action on hydraulic structures, and to outline ways of solving the thermal problems encountered.

Ice has a profound effect on the construction and operation of hydraulic structures in winter.

Ice is known to act both mechanically, causing ice loads, and hydraulically, bringing about variations in water discharges, levels and heads due to the formation of ice cover, ice jams and ice dams. Ice forming on trash racks, dam and lock gates, or other elements of hydraulic structures may upset their normal operation. Among other things, ice conditions govern the navigation period, etc.

It can be easily seen that, nearly always, thermal calculations are indispensable when predicting ice effects on hydraulic structures, or developing adequate ice control methods and precautions against hazardous after-effects of ice troubles.

Such a wide scope of ice problems involves an equally wide scope of relevant thermal calculations. Thermal problems are solved with the aid of physical models, the electric and hydraulic analogy methods, or the net method, with nets being either plotted geometrically or calculated numerically, sometimes using electronic computers.

In every case the sequence of the formulation and solution of a thermal problem is as follows:

1. Definition of the calculation purpose.
2. Selection of basic data.
3. Physical and mathematical formulation of the problem.
4. Selection of a method for the solution of the problem.
5. General solution of the problem.
6. Calculation procedure.
7. Analysis of calculated data.

Analytical methods have recently found extensive use in solving thermal problems, which is largely explained by the progress of the theory of heat conductivity [1].

As applied to ice engineering thermal problems, a method has been developed based on general physical principles of superposition, equivalence, and reciprocity [2,3]. The inculcation of this method into engineering practice is favoured by the availability of a series of calculation graphs for elementary problems, which permits to solve problems with complicated initial and boundary conditions.

Some schematized solutions are given below.

CALCULATION OF SURFACE HEATING OF A CONCRETE BLOCK

The purpose is to heat point A to a given temperature to prevent icing (Fig. 1). With a constant linear heat source, q , the solutions are as follows: for steady-state conditions

$$\theta = \frac{1}{2\pi} \ln \sqrt{\frac{\eta^2 + (1 + 2/Bi)^2}{\eta^2 + 1}}$$

and for non-steady conditions

$$\theta = \frac{1}{4\pi} \left\{ \text{Ei} \left[-\frac{\eta^2 + (1 + 2/Bi)^2}{4Fo} \right] - \text{Ei} \left[-\frac{\eta^2 + 1}{4Fo} \right] \right\}$$

where $\theta = \frac{\lambda(t_s - \vartheta)}{q}$, $\eta = \frac{x}{b}$, $Bi = \frac{\alpha b}{\lambda}$, $Fo = \frac{a\tau}{b^2}$, and $\text{Ei}(-x) = \int_{-\infty}^{-x} \frac{e^z}{z} dz$

Here λ , and a are the thermal conductivity and thermal diffusivity coefficients of the concrete block, respectively, α is the coefficient of heat-transfer to the environment with the temperature ϑ , and τ is time.

If a flat heater of S_1 -intensity is located on the surface of a concrete block $-\infty \leq y \leq 0$, the surface temperature in the absence of heat transfer to the environment is determined from the equation

$$\theta = \frac{1}{\sqrt{\pi}} \left[\text{erfc} \frac{1}{2\sqrt{Fo}} + \frac{1}{2\sqrt{\pi Fo}} \text{Ei} \left(-\frac{1}{4Fo} \right) \right]$$

in which $\theta = \frac{\lambda(t - t_0)}{S_1 \sqrt{a\tau}}$, $Fo = \frac{a\tau}{y^2}$, t_0 being the initial temperature.

The above problem whose calculation graph is given in Fig. 2 can serve as a basis for solving more complicated problems. Some schemes using the superposition principle are shown in Fig. 3. It should be noted that with a uniform heating the block surface temperature will be $\theta = \frac{\sqrt{Fo}}{\pi}$. The analytical solutions to the problem presented in Fig. 3b and Fig. 3c have the form

$$\theta = \sqrt{\frac{Fo}{\pi}} \left[\text{erfc} \frac{1-\eta}{2\sqrt{Fo}} + \text{erfc} \frac{1+\eta}{2\sqrt{Fo}} - \frac{1-\eta}{2\sqrt{\pi Fo}} \text{Ei} \left(-\frac{(1-\eta)^2}{4Fo} \right) - \frac{1+\eta}{2\sqrt{\pi Fo}} \text{Ei} \left(-\frac{(1+\eta)^2}{4Fo} \right) \right]$$

and

$$\theta = \sqrt{\frac{Fo_n}{\pi}} \left[2 - \text{erfc} \frac{1+\eta}{2\sqrt{Fo_n}} + \text{erfc} \frac{1-\eta}{2\sqrt{Fo_n}} - \frac{1-\eta}{2\sqrt{\pi Fo_n}} \text{Ei} \left(-\frac{(1-\eta)^2}{4Fo_n} \right) + \frac{1+\eta}{2\sqrt{\pi Fo_n}} \text{Ei} \left(-\frac{(1+\eta)^2}{4Fo_n} \right) \right]$$

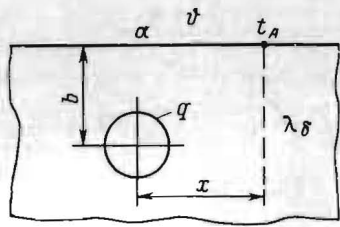


Fig. 1.

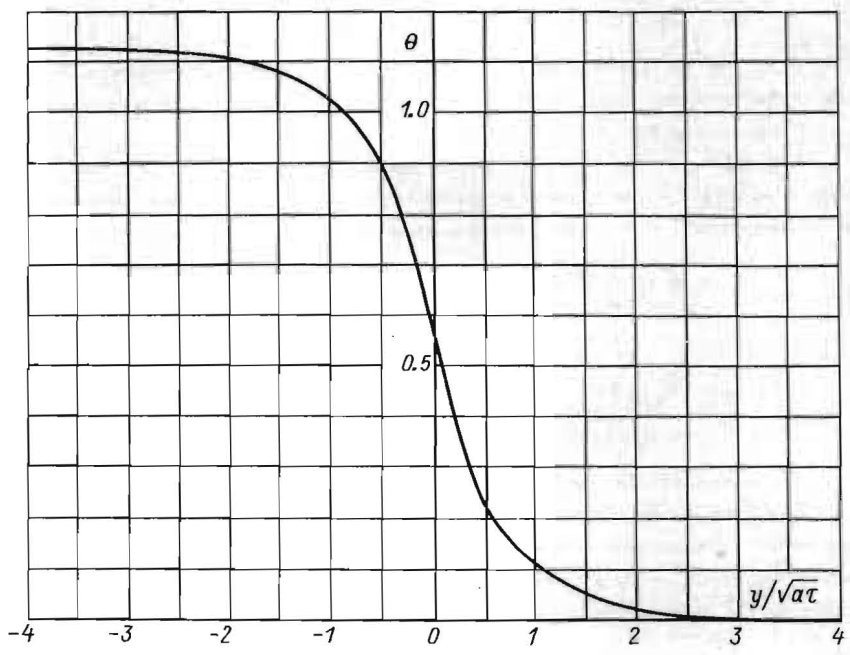


Fig. 2

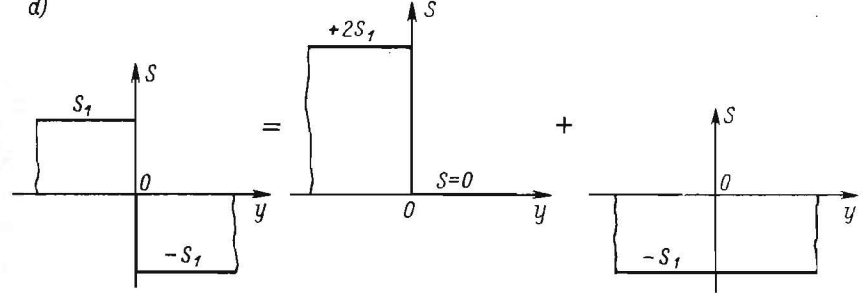
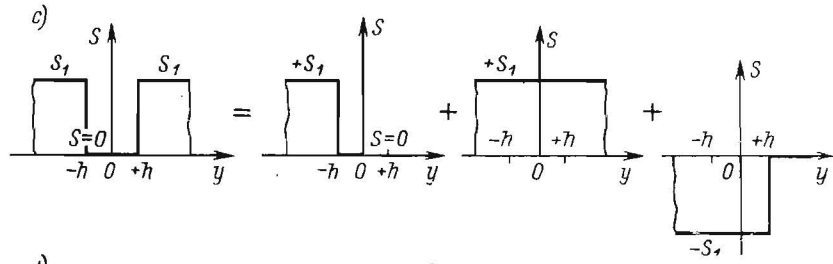
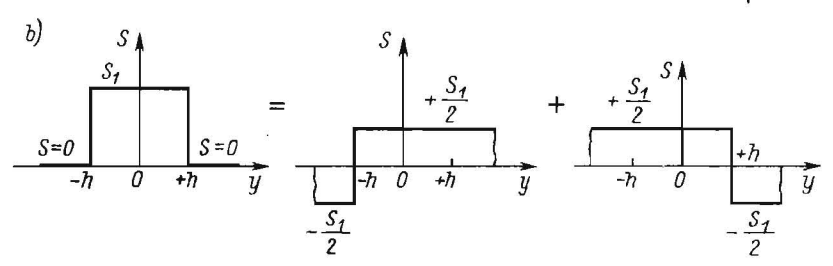
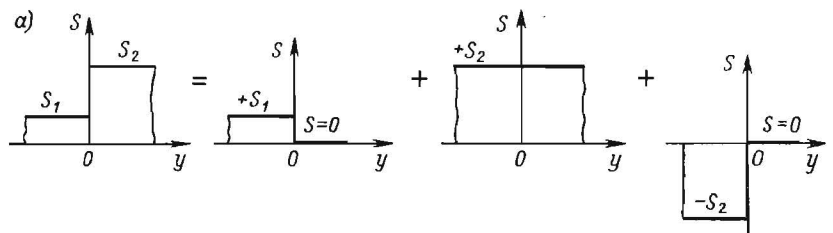


Fig. 3

in which $\theta = \frac{\lambda(t-t_0)}{S_1 h}$, $Ro = \frac{a\tau}{h^2}$, and $\eta = \frac{y}{h}$.

To take an approximate account of the effect of heat transfer to the environment it is necessary to find $S_x = \int_{-\infty}^{+\infty} (t - \vartheta) dy$ and to substitute $S_1 - S_x$ for S_1 in all the computations.

THERMAL CALCULATION OF ICE COVER FOR LINEAR VARIATIONS IN THE AIR TEMPERATURE

Given that for $\tau = 0$ $t = \eta \vartheta_0$, where $\eta = \frac{x}{h}$; for $0 < \tau < \tau_1$
 $\vartheta = \vartheta_0 + b_1 \tau$; and for $\tau_1 < \tau < \tau_2$, $\vartheta = \vartheta_0 + b_1 \tau_1 + b_2 (\tau - \tau_1)$
 define $t = f(\tau, x)$ with $\tau > \tau_1$.

A solution for $t = f(\tau, x)$ is sought through algebraic addition of the solutions of the two problems: $t = t_1 + t_2$ where $t_1 = f(Ro_1, \eta)$ for
 $Ro_1 = \frac{a\tau}{h^2}$ and $\vartheta = \vartheta_0 + b_1 \tau$, and $t_2 = f(Ro_2, \eta)$ for
 $Ro_2 = \frac{a(\tau - \tau_1)}{h^2}$ and $\vartheta = (b_2 - b_1)(\tau - \tau_1)$.

The knowledge of the ice cover temperature is essential for the evaluation of the ice cover growth and melt rate. The ice cover temperature determines the main physical properties of ice, including its strength and rheological properties. The latter data are required for solving problems on dynamic loads, static pressure, ice passage through hydraulic structures, etc.

ICE PROTECTION OF TRASH RACKS

To avoid the crystallization of supercooled water and adherence of frazil ice to trash racks, the surface temperature of the trash rack must be at least somewhat above zero, $t_s \geq 0.01^\circ\text{C}$.

Uniform heating is usually applied, thus ensuring a uniform intensity of the heat flux, q , all over the surface of the trash rack rods. The heat transfer coefficient, α , varying from section to section of the rack, the surface temperature of the rods varies as

$$t_s = \frac{q}{\alpha} + t_w$$

where t_w is the temperature of supercooled water.

It is common practice to specify power required for heating of the trash rack surface on the basis of the area characterized by the maximum value of α , which results in all the other points of the surface being overheated. Therefore it seems more reasonable to supply heat differentially, ensuring a uniform temperature, t_s , over the entire surface. Thus, for heating of round rods the rated power per unit area (kW/m^2) is

$$P = K \frac{v^{0.6}}{d^{0.4}} (t_s - t_w)$$

where v is the flow velocity, m/sec; d is the rod diameter, m; $K = 2$ for uniform heating, and $K = 1.1$ for differential heating.

REFERENCES

1. Lykov, A.B., Theory of thermal conductivity. Vysshaya shkola, 1967.
2. Pekhovich, A.I., Zhidkikh, V.M., Calculation of thermal behaviour of solid bodies. Energiya, 1968.
3. Pekhovich, A.I., The application of the reciprocity principle to the solution of thermal conductivity problems. Izvestia VNIG, v. 91, 1969.



THERMAL REGIME OF DEEP RESERVOIRS IN
SIBERIA AND INVESTIGATION OF THEIR THER-
MAL CHARACTERISTICS

Ya.L. Gotlib, M.Sc.(Eng.),	the S.Ya.Zhuk Gidroprojekt,	Moscow, U.S.S.R.
F.F.Razzorenov, Head, Dept.	the S.Ya.Zhuk Gidroprojekt,	Moscow, U.S.S.R.
N.M.Sokolnikov, Head, Sectn,	the Leningrad Branch of	Leningrad, U.S.S.R.
	the S.Ya.Zhuk Gidroprojekt	
V.M.Zhidkikh, M.Sc.(Eng.),	the B.E.Vedeneev VNIIG,	Leningrad, U.S.S.R.
Sen. Res. Off.		

SUMMARY

The characteristic features of the thermal behaviour of the deep reservoirs in Siberia, namely, Bratsk and Krasnoyarsk Reservoirs, are considered. A thermal classification of impoundments according to their depth is outlined and a procedure for hydrothermal calculations is suggested. Data are given on the coefficients of both turbulent and free-convection (equivalent) heat conductivity of water derived from the observations of Bratsk Reservoir.

RESUME

On examine les particularités du régime thermique des retenues profondes de la Sibérie, celles de Bratsk et de Krasnoïarsk. Une classification thermique des retenues selon la profondeur et les méthodes des calculs hydrothermiques sont brièvement décrites. Le rapport traite les données relatives aux coefficients de la conductivité thermique de l'eau tant turbulente qu'à convection naturelle (équivalente) calculés selon les résultats des observations in situ effectuées sur la retenue de Bratsk.

In connection with the construction of large deep reservoirs under the rigorous climatic conditions of Siberia, hydrothermal engineering was faced with new problems in studying the thermal regime of such impoundments and refining the existing calculation procedures. Significant contribution to the relevant research was made by the S.Ya. Zhuk Gidroprojekt Institute and the B.E. Vedenev VNIIG.

Field observations of Bratsk [1, 2] and, later, of Krasnoyarsk Reservoirs were important steps in the investigations undertaken.

By way of example, Fig. 1a shows water temperature changes in the vicinity of the Bratsk Dam recorded in 1969. An analysis of the field data indicates that the entire water body may be divided into two layers: the upper layer about 40 m deep which is liable to considerable annual temperature variations, and the lower one characterized by stable temperatures.

As seen from Fig. 2a, the amplitude of the annual water temperature variations near the reservoir surface is about 18 to 20°C, decreasing down to 1.5-2°C in the bottom layers of water. The maximum water temperatures are observed towards the end of July or the beginning of August. For lower layers of water, the date of the maximum temperatures is delayed. Thus, for instance, the maximum of the bottom temperatures is recorded late in October or in November.

During most of the year significant vertical temperature gradients occur. Only during the homothermal periods in the spring and autumn months, when free-convection mixing takes place, the temperatures become more uniform across the depth. The homothermal period lasts half-a-month in spring and one to one-and-a-half month in autumn.

It should be emphasized that freeze-up of the reservoir occurs at relatively high mean water temperatures (up to 2-2.5°C), the temperatures in the bottom layers occasionally reaching 3 to 3.5°C.

In winter the thermal regime of the reservoir is stable throughout the whole depth up to the bottom. This infers that in deep impoundments heat exchange with the bottom has practically no influence on the thermal regime of water.

Krasnoyarsk Reservoir, the same as Bratsk Reservoir, ranks among very deep impoundments and is located in a zone with similar climatic conditions. Therefore the thermal regimes of both reservoirs possess much in common. Some characteristic features of the thermal processes in Krasnoyarsk Reservoir are associated with its large through-flow.

An intensive dynamic mixing of the water mass results in an increasing depth of the upper active layer up to 50 m. The amplitude of the annual water temperature variations also reaches 22°C near the reservoir surface and 4 to 6°C in the bottom layer, as shown in Figs 1b and 2b.

The above observational data were used as a basis for thermal classification of reservoirs according to their depth [3] (Table 1) which is to facilitate

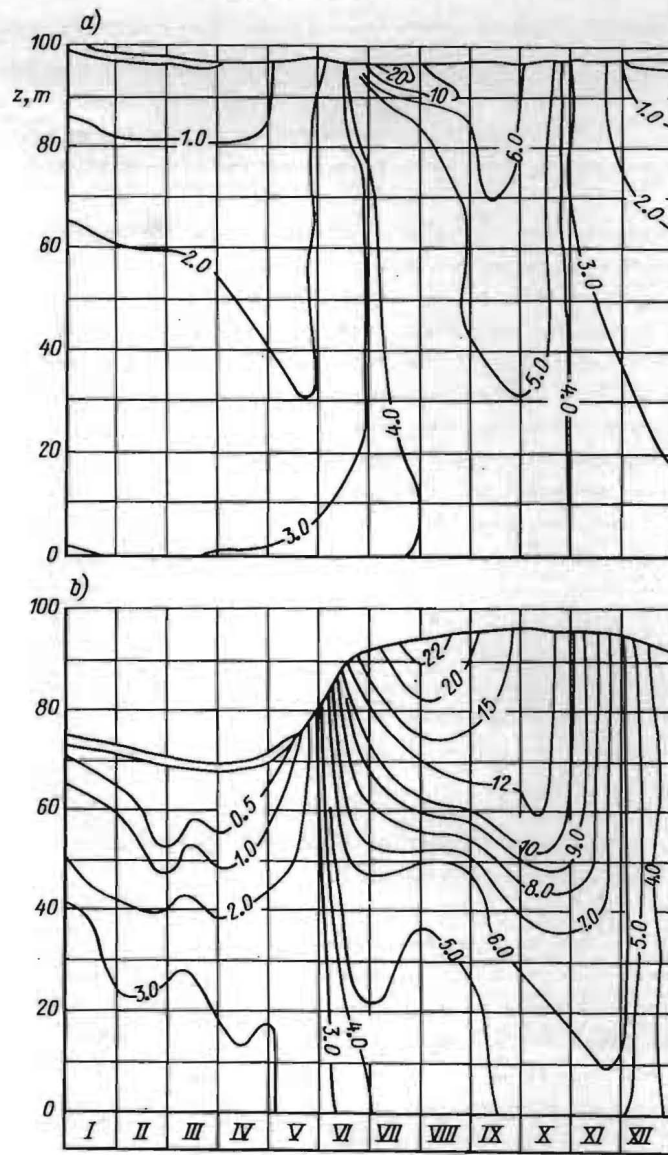


Fig. 1. Water temperature profiles in Bratsk and Krasnoyarsk Reservoirs, 1969

- a) Bratsk Reservoir
- b) Krasnoyarsk Reservoir

the calculation of the thermal regime of impoundments.

Table 1

Thermal classification of reservoirs according to their depth

Reservoir type	The ice-covered season		The non-freezing season					
	Indications		Criteria	Indications		Criteria		
	Bottom temperature variation	Heat transfer from the bottom		Temperature drop over the depth	Bottom temperature variation			
Shallow	$t_{bot} = \text{var}$	$S_{bot} \neq 0$	$Fo > 1$	$Fo \gg 0.15$	$t \approx 0$	$t_{bot} = \text{var}$	$Bi \leq 0.2$	-
Deep	$t_{bot} = \text{var}$	$S_{bot} = 0$	$Fo < 1$	$Fo \gg 0.15$	$t \neq 0$	$t_{bot} = \text{var}$	$Bi > 0.2$	$Fo \gg 0.3$
Very deep	$t_{bot} = \text{const}$	$S_{bot} = 0$	$Fo < 1$	$Fo < 0.15$	$t \neq 0$	$t_{bot} = \text{const}$	$Bi > 0.2$	$Fo < 0.3$

The thermal behaviour of the first two types of reservoirs is governed by the heat fluxes both at the surface and at the bottom. Such impoundments may be referred to as "finite-depth reservoirs". In extremely deep reservoirs there are no heat sources at the bottom, and here the term of a "semi-confined body" is applicable. In practice the reservoir type is defined by the Fourier (Fo) and the Biot (Bi) criteria.

The procedure for prediction of water temperatures is based on the superposition principle [4] permitting to solve a thermal problem involving complicated conditions as a sum of more simple problems for which graphs in dimensionless coordinates are available. The procedure allows to compute the time-dependent variations in the water temperatures over the length and the depth of the reservoir, taking into account the flow through the reservoir, the time-dependent variations of the boundary conditions and the heat conductivity coefficient, the initial temperature varying with depth, etc.

In selecting the basic data for thermal calculations major difficulties are involved in the evaluation of the coefficients of turbulent, λ_t , and free-convection (equivalent), λ_c , heat conductivity.

There are several well-known methods (of Schmidt, Stockmann, and others) for the determination of the λ -coefficients based either on the heat conduction equation itself, or on a given solution to this equation. The λ_t -coefficient can be easily obtained from the formula $\lambda_t = c\rho \frac{\Delta t}{\Delta \tau} \left(\frac{\Delta^2 t}{\Delta z^2} \right)$ which results directly from the Fourier equation expressed in terms of finite differences. This formula is, however, not valid for λ_c because it fails to give an accurate value of $\frac{\Delta^2 t}{\Delta z^2}$ under the homothermal conditions. In this case the formula

$\lambda_c = Sh / (2\Delta t)$ is available, where S is the heat transfer at the reservoir surface; h is the water depth; and Δt is the temperature drop across the depth. The above formula is based on the theory of a regular regime of the second kind.

The formulae given above were employed to evaluate λ_t and λ_c for Bratsk Reservoir. The calculation results are presented in Table 2 and Fig. 3, where Nu is the Nusselt number, and Ra is the Rayleigh number.

Table 2
Calculated values of coefficient $\lambda_t \cdot 10^{-3}$ Cal/m²hr⁰C

Month Year	I	II	III	IV	V	VI	VII	VIII	IX	X	XI	XII
	1964	0.98	2.02	-	-	-	0.80	0.80	0.06	0.02	11.00	-
1965	0.04	0.41	1.13	0.25	0.28	0.21	0.04	0.08	0.85	17.50	-	2.02
1966	0.33	-	1.40	1.80	-	-	1.15	0.58	0.52	-	-	-
1967	0.86	0.16	0.29	0.60	-	1.35	0.45	0.54	-	4.52	12.50	0.97
1968	0.54	0.15	0.10	0.95	2.08	1.20	0.12	0.17	1.52	-	-	0.15
1969	0.86	0.23	0.21	1.26	-	0.76	0.34	0.43	-	10.10	-	0.35

The calculation procedure briefly discussed herein is used for predicting the hydrothermal regime of deep impoundments. Fair agreement has been obtained between the calculated and measured data.

References

- /1/ Gollib Ya.L., Razzorenov F.F., Thermal regime upstream and downstream from the Bratsk Dam during the initial filling of the reservoir. *Gidrotekhnicheskoye stroitel'stvo*, N 11, 1965.
- /2/ Razzorenov F.F., Thermal regime of Bratsk Reservoir in the vicinity of the dam. *Gidrotekhnicheskoye stroitel'stvo*, N 7, 1968.
- /3/ Recommendations on thermal calculation of reservoirs, BCH 18-68. Minenergo S.S.S.R.
- /4/ Pekhovich A.I., Zhidkikh V.M., Calculation of thermal regime of solid bodies. *Energia*, 1968.

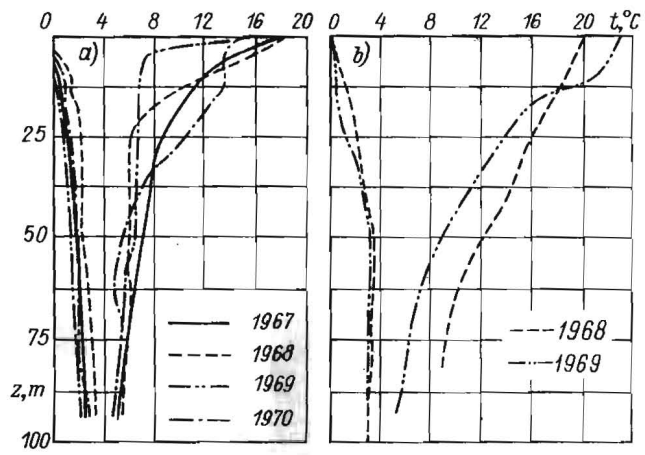


Fig. 2. Maximum and minimum water temperatures
 a) Bratsk Reservoir
 b) Krasnoyarsk Reservoir

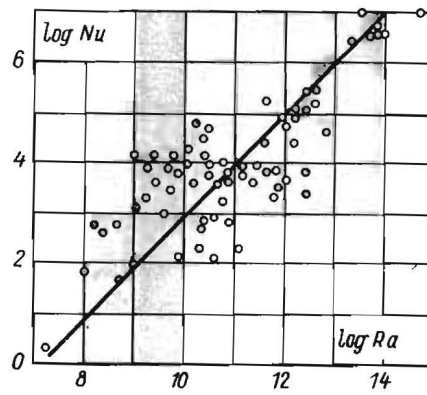


Fig. 3. Nu versus $f(Ra)$ relationship



ICE SYMPOSIUM 1972
LENINGRAD

PRESSURE CONDUIT ICING STUDIES AND
ANTI-ICING TECHNIQUES

V.M. Zhidkikh, M. Sc. (Eng.), the B.E.Vedeneev VNIIG, Leningrad, U.S.S.R.
Sr Res. Offr,
Yu.A. Popov, M. Sc. (Eng.), the Siberian TsNIIS, Novosibirsk, U.S.S.R.
Sr Res. Offr,

SYNOPSIS

Considered are procedures for calculating pressure conduit icing and anti-icing techniques. Dimensionless numbers are derived permitting to simplify calculations, facilitate the analysis of the phenomenon and elaborate modelling techniques. Analyzed are thermal, hydraulic and technological conditions ensuring stable operation of a pump - ice-coated conduit system.

RESUME

Le rapport analyse les méthodes de calcul de la glaciation des conduites d'eau en charge et les moyens de la lutte contre celle-ci. On introduit les nombres sans dimension qui permettent de simplifier les calculs, de faciliter l'analyse du phénomène et d'élaborer les procédés de la représentation en similitude. Les conditions thermiques, hydrauliques et technologiques assurant le fonctionnement stable du système pompe-conduite congelée sont examinées.

In operation of pressure conduits incorporated in hydraulic structures and hydraulic transport systems, troubles are frequently experienced due to ice formation on the internal conduit surfaces.

For calculating the ice layer thickness and developing anti-icing techniques a set of three equations is employed, viz. the heat balance equation for a conduit with running water, the heat balance equation for conduit walls, and the equation for water pressure in a conduit.^{1/} The solution of the set of equations involves serious difficulties of methodological and computational nature.

In case the above equations are used for defining the dimensionless numbers, the calculation methods may be considerably simplified. As a result, the number of independent variables is reduced, the analysis of the phenomenon is facilitated, and there arises an opportunity for devising modelling techniques for pressure conduit icing.

Utilizing the similarity theory methods, the following dimensionless numbers may be obtained from the above equations

$$\theta \equiv \frac{\vartheta \lambda \varepsilon^{4/2}}{c \gamma \beta i_c C R^2}; \quad Q \equiv \frac{q \varepsilon^{4/2}}{C R^2}; \quad L \equiv \frac{a \alpha \varepsilon^{1/2}}{c \gamma C^{1/4} R^{3/4}}; \quad (1)$$

$$T \equiv \frac{c \beta i_c C \tau}{\rho \varepsilon^{1/2}}; \quad \eta \equiv \frac{r}{R}$$

in which r = radius of an ice-coated conduit cross-section; R = reduced radius of a conduit; τ = time; α = coordinate coinciding with the longitudinal axis of a conduit; ϑ = air temperature; λ = thermal conductivity coefficient of ice; C = thermal capacity of ice; γ = specific weight of ice; ρ = latent heat of ice formation; i_c = conduit slope; q = water discharge; C - Chezy's coefficient; a = magnitude proportional to the heat transfer coefficient from water surface to ice; β = coefficient including the effect of pressure on the freezing temperature; ε = mechanical heat equivalent; $\beta' = \frac{1}{\varepsilon} - c\beta$; $\varepsilon = \beta' / c\beta i_c R$.

The differential equation describing icing of pressure conduits with due regard for (1) has the form

$$\frac{\theta Q^{4/3} (\frac{3}{4} \ln \eta - 1)}{\eta^{4/3} \ln^2 \eta} \frac{\partial \eta}{\partial L} + 2\pi m \eta \frac{\partial \eta}{\partial T} + \frac{7}{4} m Q \frac{\partial \eta}{\partial L} \frac{\partial \eta}{\partial T} + m Q^{4/3} \eta^{7/3} \frac{\partial^2 \eta}{\partial L \partial T} = (2)$$

$$= Q + \frac{2Q^3}{\pi^2 \eta^5} + \frac{2\pi \theta}{\ln \eta},$$

^{1/} Bogoslovski P.A., Ice regime of hydropower plant conduits. - Gosenergoizdat, Moscow-Leningrad, 1955.

where $m = \gamma/\gamma_w$; γ_w = specific weight of water.

In continuous operation of a conduit there comes a point where the loss of heat to the atmosphere is compensated by heat liberation induced by the internal friction forces. Such a kind of icing is called ultimate. An equation for ultimate icing is derived from Eq.(2) if $\frac{\partial \eta}{\partial L} = 0$ and $\frac{\partial \eta}{\partial T} = 0$. The plot presented in Fig. 1 is used for practical calculations of the thickness of an ice layer formed. Given the arguments θ and Q , it is easy to find η by the plot and calculate $r = \eta R$ ^{2/}

The hydraulic conditions of a pump - ice-coated conduit system are characterized by the equation

$$H(q) = \int_l J(x) dx + \bar{z}, \quad (3)$$

where $H(q)$ = pump head at the discharge q ; $J(x)$ = hydraulic slope;
 l = distance from the conduit entrance up to the given cross-section including a length free of ice and lengths liable to conic and cylindrical icing; \bar{z} = static head.

The discharge capacity of a conduit under given icing conditions may be determined from Eq.(3), (Fig. 2). The head is related to the water discharge through a function $H = f_1(q)$ which is a technical characteristic of a pump. The right-hand side of Eq.(3) is a hydraulic characteristic of a conduit

$H = f_2(q)$ which may be plotted according to P.A. Bogoslovsky ^{1/}

It is seen from Fig. 2 that the curves $f_1(q)$ and $f_2(q)$ intersect at the two points A and B. The basic difference in conduit operation at those points is that the heat balance is unsteady at the point A, while it is steady at the point B. This conclusion can be easily proved by analyzing the heat balance equation and comparing thermal and hydraulic inertia of a conduit.

Actually, the operational conditions of a conduit are nonstationary. Therefore, the working point B may be displaced along the length B'B' depending on the air temperature and other factors. B'B' is termed the working zone of the system. It is of great practical importance to know the minimum discharge capacity of a conduit (the position of the point B') and the length of the working zone (the length B'B'). Both may be found from Eq.(3) under given meteorological conditions. Measures for the control over the thermal regime and icing of conduits are chosen by comparison of the minimum water discharge

^{2/} Zhidkikh V.M., Calculation of ultimate freezing-over of conduits. - Izvestia VNIIG, 1970, v.92.

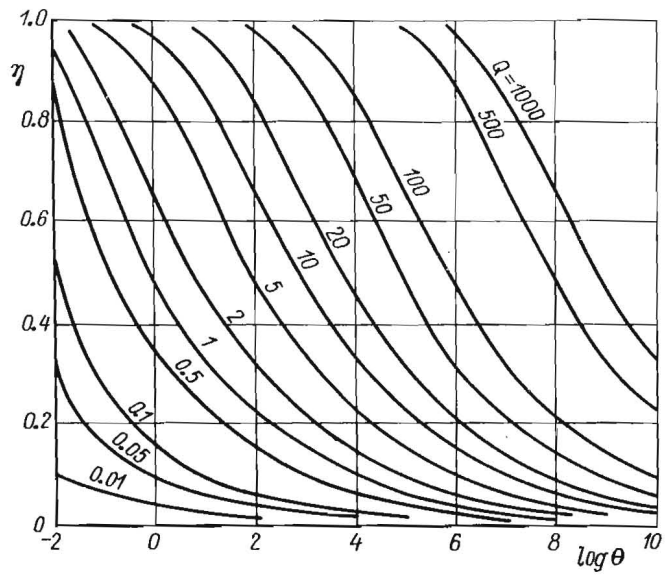


Fig. 1

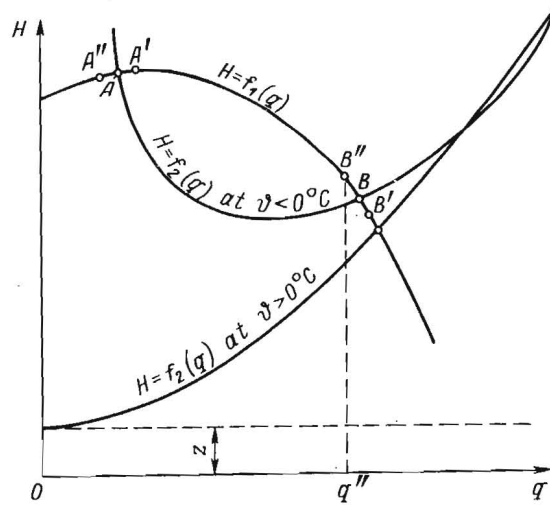


Fig. 2

q^* corresponding to the point B^* , with the minimum permissible discharge $q_{min}^{3/}$.

When designing conditions for a non-operating conduit a significant practical problem is to determine the minimum allowable radius of the conduit which may be found proceeding from the thermal, hydraulic and technological conditions formulated as follows:

the thermal condition $W_1 + W_2 > W_3$;

the hydraulic condition $q_0 > q_{min}$;

the technological condition $\tau < \tau_{perm}$;

where W_1 = variation in heat content of water; W_2 = heat liberated in conversion of the mechanical energy of the flow into the thermal energy; and

W_3 = heat losses to the atmosphere; q_0 = initial water discharge; τ and τ_{perm} = actual and permissible time of ice melting, respectively.

It is expedient to present the calculation data as technological graphs which may be effectively employed for the control of conduit operational conditions.

^{3/} Popov Yu.A., Thermal design of pressure conduits for winter conditions. - Sbornik trudov TsNIIS, 1968, vyp.24.



ICE SYMPOSIUM 1972
LENINGRAD

THE APPLICATION OF HEAT-TRANSFER
RELATIONSHIPS TO WATERCOURSES

Ö. Štarosolszky, Dr. Engr,	Department for Design and	Budapest,
C. Sc. (Techn.)	Research,	HUNGARY
Head Dept	National Water Authority	

SYNOPSIS

Thermodynamics has solved heat-transfer problems for mechanical and chemical engineering both in the case of laminar and turbulent flow in closed conduits and in boundary layers, - by simultaneously applying continuity, movement and energy equations. Some difficulties emerge in the course of its application in hydraulic engineering, because velocity-distribution and boundary conditions are irregular, and also, because the changes in the turbulent diffusion-factor must be taken into account. The main fields in the hydraulic engineering application are the flow in closed conduits or between two plates and solutions for turbulent flow and heat transfer in boundary layers under certain assumptions, which whether fulfilled or not, must be judged for each particular problem. The study makes a comparison of the natural and ideal state and tries to point out the possible applications of the heat-transfer relationships.

RESUME

Pour suppléer aux exigences des ingénieurs mécaniciens et des chimistes, la thermodynamique a trouvé des solutions aux problèmes concernant la transmission de chaleur dans un écoulement laminaire, ou turbulent, dans des conduites fermées et dans les couches limites par l'application simultanée des équations de la continuité et énergétique. L'application des résultats dans la pratique de l'hydraulicien se heurte aux difficultés que causent la répartition inégale des vitesses et les irrégularités dans les conditions aux limites, ainsi qu'à celles dues à la manière avec laquelle on doit tenir compte de la variabilité du facteur de diffusion turbulente. Ce sont en premier lieu les solutions concernant la transmission de chaleur dans les courants turbulents en conduite fermée ou entre deux plaques, et dans les couches limites, qui peuvent entrer en ligne de compte en relation avec les constructions hydrauliques, sous la réserve de certaines conditions, dont la validité doit être néanmoins examinée dans chaque cas particulier. L'étude met en confrontation l'état idéal et l'état naturel, et signale les possibilités d'application des relations concernant la transmission de chaleur.

Thermodynamics has solved problems - first of all for mechanical and chemical engineering - of heat-transfer in the case of laminar and turbulent flow /1, 2, 3, 4, 5/.

The basic starting point consists of the simultaneous application of the continuity, motion and energy equations, which are valid for heat-transfer processes in flowing water, in their principles and differential-equation forms. The solutions - almost without exception - are worked out for steady state flow, and initial and boundary conditions are determined for this flow as well. The practical solutions refer first of all to closed conduits, - mainly circular pipes - and laminar and turbulent boundary layers with ideal velocity distribution. A great part of the experiments was carried out with water (or air) and the experimental factors were generally determined in the usual range of the Reynolds and Prandtl-numbers occurring in hydraulic engineering practice.

Some difficulties emerge from the facts that the velocity-distribution is non-regular, consequently it cannot be described by equations, and the boundary-conditions are irregular. An exact determination of the velocity-distribution is a difficult problem even in the case of a regular trapezoidal section - let alone in the completely irregular beds of the natural watercourses. As a result the turbulent diffusion-factor may significantly differ from that calculated with an assumption of theoretically regular velocity-distribution. The application in the field of hydraulic engineering depends on a better knowledge about turbulent diffusion.

Solutions have been worked out in the terms of thermodynamics for three ideal situations /8/ (Fig. 1; a, b, and b_2 cases):

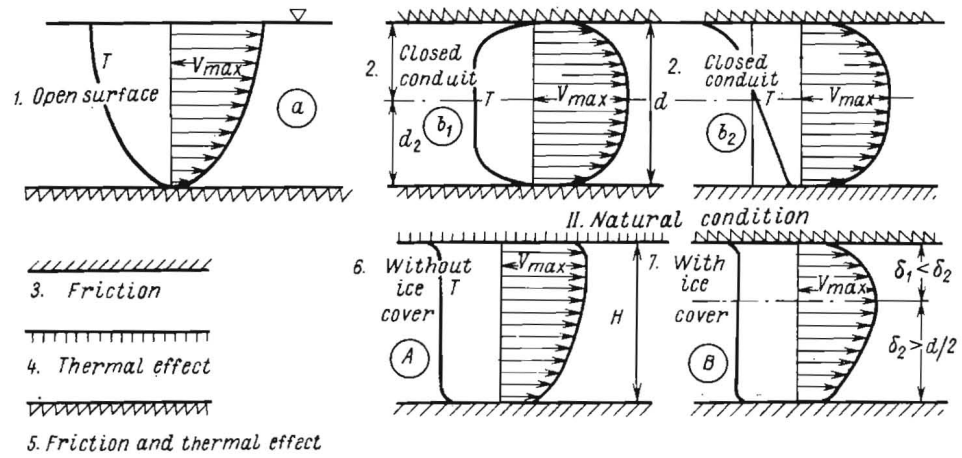
- a) boundary layer on a flat plate, where friction and heat-transfer both act on the lower plate;
- b) closed conduit, where the velocity graph is symmetrical and b_1) heat transfer is symmetrical, or b_2) heat transfer is asymmetrical, i.e. heat transfer acts only on one side of the fluid.

In watercourses, however, there are two basic natural states (Fig. 1, A and B cases).

A) Open-surface flow. The dynamic boundary layer is close to the surface, but maximum velocity is not on the surface, which fact indicates that there is also a boundary layer present. This can be observed especially in the case of winds of opposite direction. The heat acts on the surface of the flowing water and as a function of the turbulence a thermal boundary layer may also exist.

B) Closed-surface flow in the case of ice-cover /8/. Maximum velocity is not along the banks or at the middle, but somewhere in the upper part and it depends on the ratio of ice and boundary roughness. (According to observations in Canada these are similar and in this case the phenomenon is close to that of b_2). The heat acts on the water through the ice, and a thermal boundary layer may exist in the upper part, which is however, much more thinner

I. Ideal condition



than that in case \underline{A} , as a result of the insulation effect of the ice.

There is a difference between the ideal and natural state with respect to both dynamic and thermal boundary conditions.

Cases \underline{B} and b_2 show the closest similarity. In the case of significant turbulence and if the surface of the ice is too smooth, the thermodynamic solution may be regarded as completely valid for prismatic beds, and may be applied in the case of irregular beds, as well, for calculating longitudinal temperature-changes.

The effect of the difference between cases \underline{A} and \underline{a} is significant if the turbulence is small, if the velocity distribution over the cross-section is rather uniform and there is no significant wind (i.e. convection), and if the heat action on the surface is predominant as compared to the friction-heat, then, the longitudinal changes in the mean temperatures of the sections are not significantly affected by the facts that the friction acts upwards and the temperature changes downwards, and that the place of the maximum velocity is not completely on the surface. So case \underline{a} may be regarded as an extreme value of case \underline{A} , which represents the slowest change in temperature along the longitudinal section. In this concept it represents the most favourable case for slush ice and over-cooling and the most unfavourable situation with cooling processes (heat-pollution).

For informatory calculations, in the case of open surface the turbulent boundary layer (\underline{a} case), and in the case of closed section the flow between two asymmetrically heated (cooled) plates may be taken into account. The author has derived relationships for temperature changes under the ice cover, by using thermodynamical relationships and experimental factors $/\beta/$. According to his studies relative temperature change depends exponentially on the Reynolds number (i.e. turbulence) and on a relative distance related to the water depth, and on experimental factors depending on the Reynolds number. In the case of wide prismatic river-beds the calculated values are certainly quite close to reality. In the case of frequently changing beds the local changes of the diffusion factor, which is heavily influenced by side-effects and helical flow, may have such a strong effect that even the validity of the relationships may be endangered.

In the above case the problem may be solved by measuring the local diffusion factor and by converting the basic differential equations into difference-equations.

The turbulent diffusion factor can be only greater than that assumed for regular sections, which again leads to the conclusion that the slowest process is described by using these thermodynamic relationships for the determination of temperature changes, i.e. they give extreme values.

*

* *

The validity of the thermodynamic relationships in artificial channels has been checked by many research workers, but establishing a clear-cut application for natural watercourses is the task of future research.

REFERENCES

1. Kay, I.M.: An introduction to fluid mechanics and heat transfer. Cambridge, University Press, Second Edition, 1963.
2. Grober-Eik-Grigell: Die Grundsätze der Wärmeübertragung. Springer Verlag, Berlin, 1963, 3. Ausgabe.
3. Kays, W.M.: Convective heat and mass transfer. MacGraw Hill, New York, 1963.
4. Eckert, E.R.G. - Gross, J.F.: Heat and mass transfer. MacGraw Hill, New York, 1963.
5. Kreith, F.: Principles of heat transfer. (Second Edition) International Textbook Company, Schauton, Penns., 1967.
6. Štarošolszky, Ö.: Ice in hydraulic engineering (in Hungarian). VITUKI Tanulmányok és kutatási eredmények, 1970.
7. Štarošolszky, Ö.: Diffusion and dispersion in technical hydraulic. (in Hungarian) Műszaki Tudomány, 1970/3.
8. Štarošolszky, Ö.: An application of heat transfer relationships in watercourses. (in Hungarian). Hidrológiai Közlemény, 1970/11.



ON THE TIME DEPENDENT TEMPERATURE
VARIATION WITHIN ICE SHEETS

Joachim Schwarz, Dr. Ing.*
Visiting Research Engineer,
Touvia Miloh, Dr.
Research Engineer

Institute of Hydraulic Research Iowa City,
The University of Iowa Iowa
U.S.A.

SYNOPSIS

Large ice blocks frequently are deposited on the dry tidal flats during the low tide, where they may remain for an extended period. The distribution of ice temperature throughout the whole ice thickness can then be assumed to be uniform and equal to the air temperature. At high water stages (high tides or wind floods) the floes will again be floated and be carried away by the current. The temperature versus time variation (local and mean temperature) is calculated for pure ice and for sea ice of several salinities after the floes are again floated. The exact one-dimensional heat diffusion equation with a variable diffusivity is solved numerically by a finite difference method. The variation of the temperature distribution within the ice sheet is given as a function of time.

RESUME

Lors des marées basses des grandes blocs de glace se déposent fréquemment sur les étendues de sable découvertes par la marée, où ils peuvent rester pendant une période de temps prolongée. On peut supposer que la distribution de la température à l'intérieur du bloc de glace est uniforme et égale à la température de l'air. Lors des hautes eaux (marées hautes et inondations dues au vent) les blocs de glace peuvent flotter à nouveau et être transportés par le courant. Dans ce cas la variation de la température (locale et moyenne) par rapport au temps, pour des blocs de glace pure et pour des blocs de glace avec différentes salinités est calculée. L'équation exacte et unidimensionnelle de la diffusion de la chaleur est résolue numériquement, avec un coefficient de diffusion variable, au moyen de la méthode de différences finies. La variation de la distribution de la température à l'intérieur de la couche de glace est donnée en fonction du temps.

* On leave from the Franzius-Institute
Hannover, Germany

INTRODUCTION

It has been demonstrated in earlier publications [1,2,3] that the strength of ice and therefore also the forces exerted by moving ice fields on structures, depends strongly upon the ice temperature. In lakes and rivers drifting of ice generally occurs after breakup of the ice cover, generally following the onset of higher temperatures and ice melting. In coastal regions, on the other hand, drifting ice frequently occurs even during the coldest part of the year. When ice sheets are floating on the water surface, the average temperature in river ice is predicted by Kouzoub (cited by Korzhavin, [1]) to be only 35 percent of the average air temperature (measured in $^{\circ}\text{C}$) during the preceding 24 hours. In some regions, however, ice sheets may lie for many hours or even days on dry ground. Before the floes are lifted by rising water (spring tide or wind floods), the mean ice temperature can approach the air temperature. This happens, for example, at low tides on the tidal flats of the North Sea on the coasts of Holland, West Germany, and Denmark. Similar events occur at the Alaskan coast [4]. A constant temperature throughout the entire ice sheet also occurs at beaches with practically no tide (e.g., the Baltic Sea) after the ice sheets have been pushed out of the water onto flat beaches. At high water stages, this ice will be carried back to the sea where it might encounter structures. When an attempt is made to calculate the forces exerted by these ice floes on structures, it is then important to know the mean ice temperature, and hence also its variation with time.

The time variation of the distribution of temperature in pure ice has already been investigated by Lazier and Metge [5] and McKay [6], using the heat diffusion equation. Lazier and Metge [5] calculated the temperatures by assuming a constant value for the diffusion coefficient. In reality, this quantity is strongly temperature dependent, as is pointed out by Schwerdtfeger [7] for sea ice, and by James [8] for fresh-water ice. Figure 1 shows that this dependency is much more significant for sea ice than for fresh-water ice, especially if the sea ice is warmer than -10°C . At lower temperatures the relationship becomes more similar to that of pure ice. McKay [6] considered the temperature dependency of the diffusion coefficient, but used the diffusion equation derived from the assumption of a constant diffusion coefficient, as will be explained later.

In the present study the exact diffusion equation was solved numerically, taking into account the dependency of the diffusion coefficient on temperature and on salinity, in order to determine the temporal variation of temperature distributions in ice slabs.

MATHEMATICAL MODEL AND NUMERICAL SOLUTION

The heat diffusion equation is

$$\nabla \cdot (\kappa \nabla T) = \frac{\partial T}{\partial t} \quad (1)$$

where κ is the heat diffusion coefficient, T is the temperature, and t denotes time. Equation (1) is a quasi-linear parabolic partial differential equation since the heat diffusion coefficient is a function only of the temperature. When treating κ as a constant, equation (1) reduces to a linear parabolic partial differential equation.

$$\kappa \Delta^2 T = \frac{\partial T}{\partial t} \quad (2)$$

This equation has been used in the studies of Lazier and Metge [5] who assumed the diffusion coefficient to be constant, and of McKay [6] who treated κ as temperature dependent. Since equation (2) has been derived using the assumption of constant κ , a question may arise as to the legitimacy of the use of a temperature dependent value for κ in the same equation.

In the present study, we are concerned with the solution of the one-dimensional form of equation (1)

$$\frac{\partial}{\partial x} \left[\kappa(T) \frac{\partial T}{\partial x} \right] = \frac{\partial T}{\partial t} \quad (3)$$

with the boundary conditions

$$T(x,0) = T_A ; \quad T(0,t) = T_A ; \quad T(h,t) = T_W, \quad t > 0 \quad (4)$$

where h is the ice-sheet thickness, and T_A and T_W are the temperatures of the air and the water under the ice sheet, respectively.

It is convenient to introduce non-dimensional quantities given by

$$T^* = \frac{T - T_A}{T_W - T_A} ; \quad x^* = \frac{x}{h} ; \quad t^* = \frac{\kappa(T_A)t}{h^2} ; \quad \kappa^*(T^*) = \frac{\kappa(T)}{\kappa(T_A)} \quad (5)$$

The substitution of equations (5) into equations (3) and (4) yields

$$\frac{\partial}{\partial x^*} \left[\kappa^*(T^*) \frac{\partial T^*}{\partial x^*} \right] = \frac{\partial T^*}{\partial t^*} \quad (6)$$

subject to the boundary conditions

$$T^*(x^*,0) = 0 ; \quad T^*(0,t^*) = 0 , \quad T^*(1,t^*) = 1 , \quad t^* > 0 \quad (7)$$

Equation (6) was solved numerically using a finite difference approximation of the Crank-Nicolson type, in which the derivatives are centered about the time level $t^*_{n+\frac{1}{2}}$. The numerical scheme used was

$$\frac{\kappa_{i+\frac{1}{2}, n+\frac{1}{2}}^* \delta_x (T_{i+\frac{1}{2}, n+1}^* + T_{i+\frac{1}{2}, n}^*) - \kappa_{i-\frac{1}{2}, n+\frac{1}{2}}^* \delta_x (T_{i-\frac{1}{2}, n+1}^* + T_{i-\frac{1}{2}, n}^*)}{2\Delta x^*}$$

$$= \frac{T_{i, n+1}^* - T_{i, n}^*}{\Delta t^*} \quad (8)$$

where

$$\delta_x T_{i+\frac{1}{2}, n}^* = \frac{T_{i+1, n}^* - T_{i, n}^*}{\Delta x^*} \quad (9)$$

The values of the nonlinear coefficients, $\kappa_{i+\frac{1}{2}, n+\frac{1}{2}}^*$ and $\kappa_{i-\frac{1}{2}, n+\frac{1}{2}}^*$, were computed using a method similar to the projection method suggested by Douglas [9]. The values used were

$$\kappa_{i+\frac{1}{2}, n+\frac{1}{2}}^* = \kappa^* \left\{ \frac{T_{i, n}^* + T_{i+1, n}^*}{2} + \frac{\Delta t^*}{2(\Delta x^*)^2} [\kappa_{i+1, n}^* (T_{i+1, n}^* - T_{i, n}^*) - \kappa_{i, n}^* (T_{i, n}^* - T_{i-1, n}^*)] \right\} \quad (10)$$

$$\kappa_{i-\frac{1}{2}, n+\frac{1}{2}}^* = \kappa^* \left\{ \frac{T_{i-1, n}^* + T_{i, n}^*}{2} + \frac{\Delta t^*}{2(\Delta x^*)^2} [\kappa_{i, n}^* (T_{i+1, n}^* - T_{i, n}^*) - \kappa_{i-1, n}^* (T_{i, n}^* - T_{i-1, n}^*)] \right\} \quad (11)$$

The replacement of the nonlinear coefficient in equation (8) by the values given in equations (10) and (11) results in a set of linear algebraic equations which were solved using the Thomas algorithm for tridiagonal matrices [10].

The computer input data consists of a function $\kappa(T^*)$ obtained from the Gauss interpolation formula applied to the set of discrete values of κ versus temperature for different salinities given by Schwerdtfeger [7] and James [8]. The spatial steps used in the computation were $\Delta x^* = 0.05$ and the initial time step was $\Delta t^* = 0.0025$. The value of Δt^* was increased by 15 percent each time step. It is well known that the Crank-Nicolson scheme, used here, is unconditionally stable for all time steps.

The mean temperature as a function of time is defined by

$$\bar{T}^*(t^*) = \int_0^1 T^*(x^*, t^*) dx^* \quad (12)$$

For each time step the above integral was computed numerically using the Simpson-rule quadrature formula.

The steady state mean-temperature may be written as

$$T_s^* = \frac{\int_0^1 \int_0^{\theta} \kappa(T^*) dT^* d\theta}{\int_0^1 \kappa(T^*) dT^*} \quad (13)$$

For a constant value of the diffusion coefficient one obtains $T_s^* = 0.5$. However, for the case of temperature dependent diffusivity, T_s^* may be larger or smaller than 0.5, for cooling or heating of the ice sheet, respectively. Computations were performed for four different cases: pure ice and sea ice with salinity of 2, 4, and 8 promile. The value of the water temperature used was $T_w = 0^\circ\text{C}$ for pure ice, and $T_w = -2^\circ\text{C}$ for sea ice. The value of the air temperature used was $T_A = -30^\circ\text{C}$. For each case the temperature variation with time was calculated until a steady state condition was reached.

RESULTS AND CONCLUSIONS

The principal conclusions derived from the study may be summarized as follows:

1. The time derivative of temperature decreases with increasing time, giving rise to a significant gradient at the initial stages (figures 2 and 3), especially at the larger values of x^* .
2. The steady-state temperature distribution (the heavier line in figure 2) remains below the $T_s^* = 0.5$ line, which shows that the mean ice temperature is always lower than the arithmetic average of the air and the water temperature when the ice is heated.
3. The mean temperature decreases with increasing salinity (figure 3), for the warming case.
4. An exact expression for the steady-state mean temperature as a function of the thermal diffusivity is given in equation (13). If the relation $\kappa(T) = (8.43 - 0.101T) \cdot 10^{-3} \text{ cm}^2/\text{sec}$, suggested by James [8] for pure ice, is substituted into equation (13) it is found that $T_s^* = 0.47$, which is in very good agreement with the numerical solution.
5. The non-dimensional mean temperature $\bar{T}^*(t^*)$ increases with increasing air temperature (figure 4).
6. The time to approach steady state to a desired degree is nearly independent of the salinity and of the air temperature (see figure 3). However, this time is inversely proportional to h^2 for fixed T_A . For example, the time to reach the steady state condition for pure ice of 50 cm thickness and for $T_A = -30^\circ\text{C}$ is about 24 hrs.

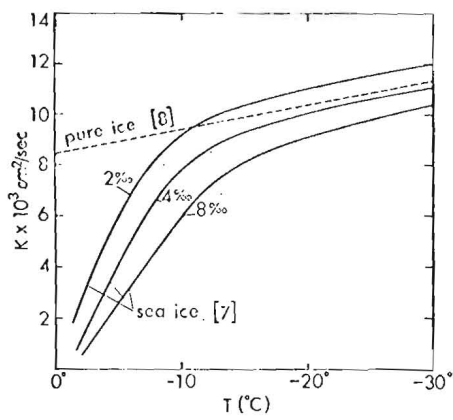


Fig. 1 Thermal diffusivity of pure ice [8] and sea ice [7] as functions of temperature.

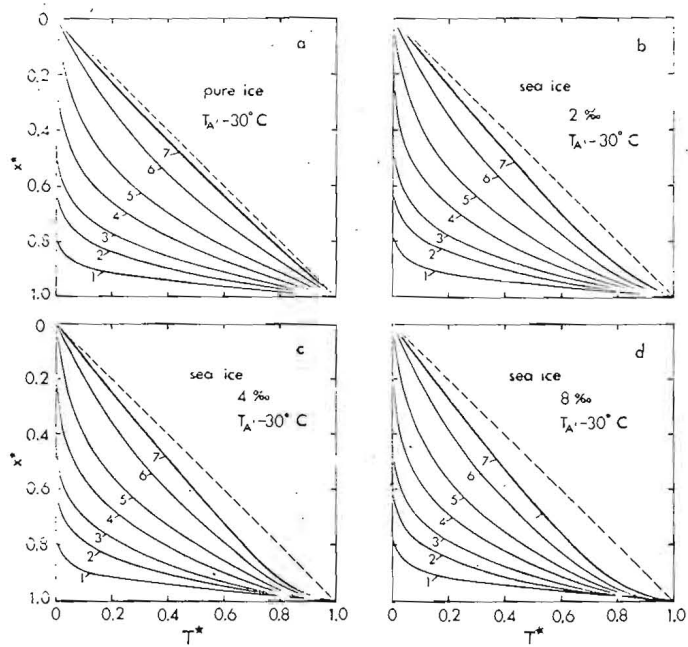


Fig. 2 Temperature variation through the thickness of ice for the following times:

- | | | |
|---------------------|---------------------|---------------------|
| 1 -- $t^* = 0.0025$ | 2 -- $t^* = 0.0090$ | 3 -- $t^* = 0.0185$ |
| 4 -- $t^* = 0.0412$ | 5 -- $t^* = 0.0803$ | 6 -- $t^* = 0.1800$ |
| | 7 -- $t^* = 0.8155$ | |

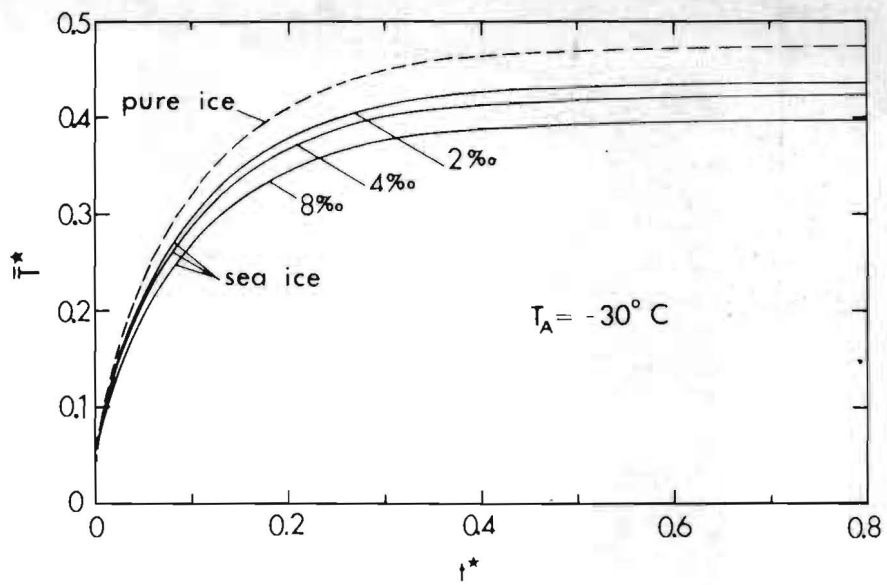


Fig. 3 Mean temperature versus time for pure ice and sea ice

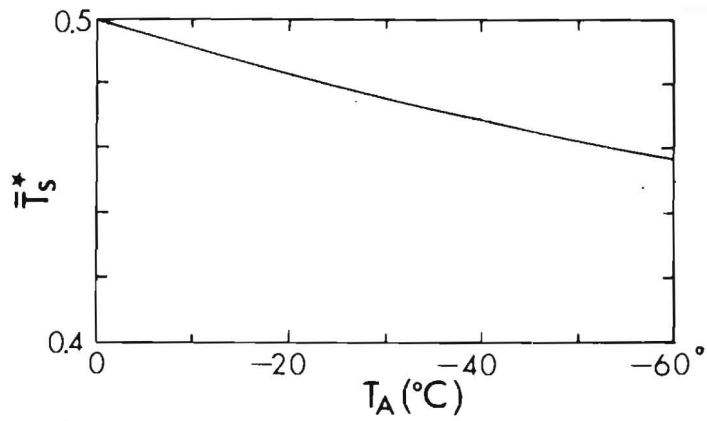


Fig. 4 Non-dimensional mean ice temperature of pure ice related to air temperature (warming case).

ACKNOWLEDGMENT

The work reported herein was supported by the National Science Foundation under Grant X529.

REFERENCES

1. Korzhavin, K.N., "Action of Ice on Engineering Structures," Novosibirsk, U.S.S.R., 1962.
2. Frederking, R. and Gold, L.W., "Ice Forces on Isolated Circular Piles," *Proceedings of POAC Conference*, Trondheim, Norway, 1971.
3. Schwarz, J., "Treibeisdruck auf Pfähle," *Mitteilungen des Franzius - Instituts für Grund- und Wasserbau*, T. U. Hannover, Heft 34, Hannover, Germany, 1970.
4. Bruun, P.M., Johannesson, P., Straumsnes, A.O., "The Interaction Between Ice and Coastal Structures," *Proc. of POAC Conf.*, Trondheim, Norway, 1971.
5. Lazier, S.S. and Metge M, "Temperature Gradients in a Lake Ice Cover," *Proceedings of IAHR Symposium on Ice and Its Action on Hydraulic Structures*, Reykjavik, Iceland, 1970
6. McKay, A.R., "Man-made Ice Structures for Arctic Marine Use," *Proceedings of IAHR Symposium on Ice and Its Action on Hydraulic Structures*, Reykjavik, Iceland, 1970.
7. Schwerdtfeger, P., "The Thermal Properties of Sea Ice," *Journal of Glaciology*, 36, 1963.
8. James, D.W., "The Thermal Diffusivity of Ice and Water Between -40 and 60°C," *Journal of Material Science*, 3, 1968.
9. Douglas, T., *Trans American Mathematical Society*, 89, p484, 1958.
10. Ames, W.F., "Nonlinear Partial Differential Equations in Engineering," Academic Press, 1965.



CALCULATION OF ICE-THERMAL REGIME VARYING
WITH TIME AND ALONG THE LENGTH OF A CANAL-
-CONNECTED CHAIN OF STORAGES

A.P. Braslavsky, Dr. Sc. (Eng.), Head, Hydrophysics Dept	The Kazakh Research Hydrometeorological Institute	Alma-Ata, U.S.S.R.
Ts. A. Nazarov, M. Sc. (Eng.) Vice-Director	The Kazakh Research Institute of Water Economy	Tselinograd, U.S.S.R.

SYNOPSIS

A computerized calculation procedure is presented for a complex ice-thermal regime varying with time and along the length of a canal-connected chain of storages. The technique is based on the consecutive application of the heat balance equation to a number of successive reaches of the waterbody. Heat advection consideration permits to ascertain the location and dimensions of air holes in the ice cover due to heat flux induced by thermal conductivity coefficient variations in the waterbody with an increase in flow velocity and a decrease of water depth in the storage. Calculation of the ice-thermal regime when designing such complex waterbodies is helpful in selecting proper water storage operating conditions and in combatting ice troubles.

RESUME

Le rapport décrit les méthodes de calcul sur l'ordinateur électronique d'un problème compliqué du régime glaciothermique non-uniforme dans l'espace et non-permanent dans le temps des retenues en série liées par les canaux. Les méthodes sont basées sur le principe de l'application successive de l'équation du bilan thermique pour le calcul des processus thermiques ayant lieu sur un nombre de tronçons du système. En tenant compte de l'advection de chaleur on peut déterminer la localisation et les dimensions des ouvertures (polynia) dans la glace qui ont lieu dans les points d'apport de chaleur vers la surface inférieure de la couverture de glace, cet apport étant dû à la variation du coefficient de conductivité thermique de la masse d'eau lors de l'augmentation de la vitesse de l'écoulement imputable à la diminution de la profondeur d'une retenue. Le calcul du régime glaciothermique, effectué au stade du projet, permet de choisir un régime d'exploitation rationnel des retenues et de prévenir les difficultés dues à la glace.

In designing and operating storages and canals connecting them it is necessary to take into account the peculiarities of their ice-thermal regime, especially in the event of a flow directed from the dam to the storage headwaters. Such is the case, e.g., at the Irtysh-Karaganda canal where water will be supplied in the upstream direction along the former river channel of the Shiderta through a chain of storages. Under such conditions air holes can form in winter at the transition from storages to canals owing to heat advection from the deeper layers of the waterbody. This may lead to supercooling of water creating operational problems at the pumping stations.

A water storage with an ice-thermal regime varying with time and along the length can be designed applying the heat balance equation to a number of consecutive storage or canal reaches. The waterbody under design is to be divided into a number of rectangular reaches as nearly uniform as possible. In the absence of ice cover uniform temperatures are assumed to obtain throughout the waterbody, which holds strictly true only for shallow well-mixed storages and canals. In winter thermal stratification is supposed to vary linearly across the depth with 0°C at the under side of the ice cover. The inflowing water temperature for the first calculation reach is prescribed as well as the initial temperature at the boundaries between all the other reaches.

The temperature variation within a unit of length and a unit of time is linear, the day being chosen as the time unit. Calculations were started on July 1st when stabilized water temperatures prevail in waterbodies and watercourses of varying depth.

For the first upstream reach of the waterbody three water temperature values are known: t_i' and t_f' = initial and final temperature at the reach entrance (at the beginning and the end of the day), and t_i'' = initial temperature at the exit. The sought for value is the water temperature at the exit from the reach at the end of the day, t_f'' , found by means of the heat balance equation for the reach considered. For the period when ice phenomena do not occur in the waterbody the equation yields

$$t_f'' = 2 \left[0.5(t_i' + t_i'') + \frac{\Delta\tau}{c\rho H_{av}} (S_p + S_a + S_b + S_{ad} - S_s - S_c - S_{ev}) \right] - t_f'$$

while for the freezing-up period

$$t_f'' = 2 \left[0.5(t_i' + t_i'') + \frac{\Delta\tau}{c\rho H_{av}} (S_b + S_{ad} + S_f - K_t \frac{t_i' + t_i''}{0.25 H_{av}}) \right] - t_f' \quad \text{is valid.}$$

Here $\Delta\tau$ is the duration of the calculation period (days); c and ρ = heat capacity and specific weight of water, respectively; H_{av} = mean water depth in the reach (cm); S_p and S_a = the total solar radiation observed by the water and atmospheric back radiation, respectively; S_b = the heat flux from the bottom of the waterbody into the water; S_{ad} = heat advection; S_s = surface heat ra-

diation; S_c = surface heat transfer due to turbulent convection; S_{ev} = evaporation heat loss; S_f = internal friction heat of the flow (all the values are given in cal/cm²day); K_t = turbulent heat conductivity coefficient of the water-body evaluated from the formula:

$$K_t = 0.012 + 4.36(uH)^{0.8} \quad \text{megacal/m day } ^\circ\text{C.}$$

in which u = flow velocity (m/sec); H = water depth (m).

The calculation relationships for determining the heat balance components are cited mainly from previous work by A.P. Braslavsky.

Account is taken of transformation of parameters of air masses moving over the waterbody and the effect of water surface - air temperature difference on the evaporation and heat flux from the water surface.

The above equations are derived on the assumption that the water stage does not fluctuate in the reach, neither withdrawal nor percolation occur, and heat inflow by precipitation is equal to heat loss through evaporation.

Ice cover thickness is estimated from an empirical relationship proceeding from observation field data on Kazakhstan waterbodies:

$$h_f = 1.8 \left[1 - \exp \left[9.4 \cdot 10^{-6} (A_0 - A) \right] \right] - K_t \frac{0.25(t_i' + t_i'' + t_i' + t_i'')}{3860 H_{av}}$$

where $A_0 = \frac{1}{9.4 \cdot 10^{-6}} \ln \left(1 - \frac{h_i}{1.8} \right)$; h_i and h_f = initial and final ice thickness, respectively (m); $A = S_{p,i} + S_{a,i} + a_7 e_2' + a_8 t_2 - 6.11 a_7 - 654$ cal/cm² day; $a_7 = 12.2(1 + 0.68 W_2)$; $a_8 = 0.575 a_7$; $S_{a,i}$ and $S_{p,i}$ = total solar radiation absorbed by snow and ice cover surfaces, and back radiation, respectively; e_2' = vapour pressure in the air (mb); t_2 = vapour temperature ($^\circ\text{C}$); W_2 = wind velocity 2m above the ice cover. The ice cover will melt provided A is positive. Then h_f is ascertained from the equation

$$h_f = h_i - \frac{A}{80 \cdot 0.92 \cdot 100} \cdot m$$

The daily value of t_f' is calculated consecutively for all the waterbody reaches including the canal connecting it with the next storage. The t_f' values obtained are used as the t_i' values for the next diurnal period. The calculations are continued till the next year break-up date. The water temperature at the end of the last reach of the first storage is accepted as the inflow temperature for the next waterbody. Ice thickness decreases and air holes are liable to form on reaches where heat advection is large in winter. In this case calcu-

- 1) Braslavsky A.P., Studies and calculations of the hydraulic regime of lakes and storages. - Doctor's thesis based on all works published by the author.

lations incorporate such factors as formation of frazil in the air hole, its transport towards and freezing to the under edge of the ice cover or, alternatively, its melting which leads to further enlargement of the hole. Water temperature, t_f'' , is found from the equation derived for ice-free conditions. A negative value of t_f' is indicative of frazil ice production in the air hole. Then applying the heat balance equation and assuming, for the sake of simplicity, heat transfer to take place across the whole surface of the reach, and $t_f = 0^\circ\text{C}$, we have a formula for defining the frazil ice volume:

$$V = 587.5 c_p Q \Delta \tau (t_i'' + t_f'' - t_i' - t_f') - 136 \Delta \tau (1 - K_w) F (S_p + S_a + S_b - S_c - S_{ev} - S_s) + 136 c_p H_{uv} \left(\frac{t_z' + t_z''}{2} - \frac{t_i' + t_i''}{2} \right) F, \text{ m}^3$$

in which Q = discharge (m^3/sec), F = surface area of the reach (km^2).

The volume of frazil ice is estimated and summed up for all non-frozen areas, thereupon the reduction is evaluated in the non-frozen areas due to ice cover formation of frazil ice brought by the flow to the under edge of the air hole. Plunging of frazil ice under the ice cover edge is neglected and the thickness of the newly formed ice cover is assumed to be numerically (m) equal to half of the value of the flow velocity (m/sec) at the point in question. To more accurately assess the conditions at the under edge of the air hole a coefficient, K_w = the ratio between the ice cover area in the reach and its total area, is introduced.

When the temperature of the water flowing towards the lower edge of the air hole is above freezing point, melting of the ice cover sets in. The melted ice volume can be obtained from the equation

$$V_m = \frac{86400 c_p Q (t_f'' + t_i') \Delta \tau}{80 \cdot 0.92 \cdot 2}, \text{ m}^3$$

In case all the frazil in the reach melts, the outflow temperature will be above 0°C , and its value can be determined by

$$t_f'' = \frac{2 \cdot 80 \cdot 0.92 (V_m - V_0)}{86400 c_p Q \Delta \tau} - t_i', \text{ }^\circ\text{C}$$

where V_0 is the volume of ice material in the reach at the beginning of the diurnal period under study.

In keeping with the calculation procedure described above a program for the electronic computer "Minsk-22" was prepared to calculate the water temperature and ice cover thickness of a running water storage. Water temperature, ice thickness and the K_w coefficient values are computerized on the basis of 10-day averages in the absence of, and for 24-hour averages in the pre-

sence of air holes. By analyzing ice thickness distribution over the reservoir reaches and the connecting canals as well as the K_{ω} coefficient values, the air hole conditions, i.e. the periods of frazil ice production causing supercooling of water may be established. By way of example the ice-thermal regime was calculated of the first storage of the Irtish-Karaganda Canal on the Shiderta river. The calculations were performed for two winter periods: a moderately cold (1965-66), and a warm one (1962-63). Computations demonstrated that during the warm winter an air hole was likely to occur, stay open for about a month and a half and produce frazil ice for weeks. During the moderately cold winter only a reduction in the ice cover thickness to 0.5 m was recorded in the region of that air hole, while ice at the dam was 1 m thick.

A good overall correspondence between theoretical and field data was obtained. Storage I on the Shiderta river was first filled in 1970. In the winter of 1970-1971 an air hole appeared, at the site predicted theoretically.

The computation procedure evolved for the determination of the ice-thermal regime of complex waterbodies is of aid in an adequate selection of their operating conditions and in avoiding ice troubles.



ICE SYMPOSIUM 1972
LENINGRAD

TEMPERATURE FIELD OF A CIRCULAR
SURFACE FLOW ARISING DURING PNEUMATIC
INSTALLATION OPERATION

B.S. Borodkin, M. Sc. (Eng.)	The Leningrad Water Transport	Leningrad,
Assistant Professor	Institute	U.S.S.R.

SYNOPSIS

Presented is an abbreviated derivation of the formula for calculating temperatures at an arbitrary point of a circular flow arising on the reservoir surface during pneumatic installation operation.

The calculations are based on the assumption that the flow considered from the kinematic viewpoint is a semiconfined fanwise turbulent jet.

RESUME

Dans ce rapport on donne une déduction abrégée de la formule pour le calcul des températures en un point arbitraire d'un courant circulaire surgissant sur la surface du bassin pendant le fonctionnement de l'installation pneumatique.

Dans le calcul on suppose que, du point de vue cinématique, le courant considéré soit un jet turbulent semi-borné en forme d'éventail.

Surface flows occur during the operation of pneumatic installations utilizing bottom heat, artificial heating with warm water of water areas and in such like cases.

If compressed air or heated water are discharged from individual nozzles widely spaced, the surface current arising at each nozzle has the form of a fanwise jet.

The paper deals with calculation of temperatures in such a jet.

The heat balance equation in polar coordinates for the jet element shaded in Figure 1 may be derived as follows.

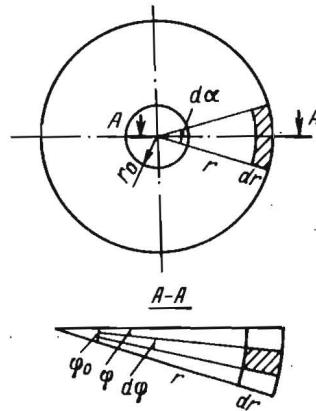


Fig. 1.

The heat increment in the radial direction due to the velocity component u is

$$ds_1 = -c\gamma d\varphi d\alpha dr \frac{\partial}{\partial r} [ur(\Delta\tau + \tau_1)] \quad (1)$$

The heat increment along the normal to the radius due to the velocity component v is

$$ds_2 = -c\gamma d\varphi d\alpha dr \frac{\partial}{\partial \varphi} [vr(\Delta\tau + \tau_1)] \quad (2)$$

The heat increment along the normal to the radius through heat conductivity is

$$ds_3 = d\varphi d\alpha dr \lambda \frac{\partial^2 (\Delta\tau + \tau_1)}{\partial \varphi^2} \quad (3)$$

Equating ds_1 , ds_2 and ds_3 to zero and using the continuity equation

$$\frac{\partial u}{\partial r} + \frac{2u}{r} + \frac{1}{r} \frac{\partial v}{\partial \varphi} = 0$$

we obtain after transformation

$$\frac{\partial}{\partial r} (ur^2 \Delta \tau) + \frac{\partial}{\partial \varphi} (vr \Delta \tau) = \frac{\lambda}{c\gamma} \frac{\partial^2 \Delta \tau}{\partial \varphi^2} \quad (4)$$

in which u = longitudinal velocity component,
 v = transverse velocity component,
 $\Delta \tau$ = excess temperature at an arbitrary point of the jet,
 τ_0 = water temperature in the water area, the jet boundary
 $\varphi = \varphi_0$ neglected,
 c and γ = heat capacity and volume weight of water, respectively,
 λ = coefficient of turbulent heat conductivity.

Taking into account that the longitudinal velocity components exceed considerably the transverse velocity components we may solve the equation

$$\frac{\partial}{\partial r} (ur^2 \Delta \tau) = \frac{\lambda}{c\gamma} \frac{\partial^2 \Delta \tau}{\partial \varphi^2} \quad (5)$$

The longitudinal velocities over the jet section are known to be varying according to the curvilinear law from u_{max} on the jet axis to zero at its boundaries.

However, the solution of Eq.(5) including such a velocity distribution entails serious mathematical difficulties.

Considering this circumstance, calculations in the first stage are performed for the average velocity over the arc

$$u = \frac{A}{r} \quad (6)$$

Then Eq.(5) may be written as

$$\frac{\partial}{\partial r} (r \Delta \tau) = B \frac{\partial^2 \Delta \tau}{\partial \varphi^2} \quad (7)$$

where

$$B = \frac{\lambda}{Ac\gamma}$$

Eq.(7) is solved within the range $0 \leq \varphi \leq \varphi_0$; $r > r_0$ under the following boundary conditions

$$\Delta \tau \Big|_{r=r_0} = \Delta \tau_0 \quad (8)$$

$$\frac{\partial \Delta \tau}{\partial \varphi} \Big|_{\varphi=0} = \frac{S}{\lambda} r = Cr \quad (9)$$

$$\frac{\partial \Delta \tau}{\partial \varphi} \Big|_{\varphi=\varphi_0} = 0 \quad (10)$$

where ξ = heat transfer from the free surface.

The equation is solved in the form of the Fourier series in cosines

$$\Delta T = \frac{A_0(r)}{2} + \sum_{n=1}^{n=\infty} A_n(r) \cos \frac{n\xi}{\psi_0} \cdot \psi \quad (11)$$

where $n = 0, 1, 2, 3, \dots$

The solution of Eq.(7) yields the expression for calculating temperatures at an arbitrary point of the jet

$$\begin{aligned} \Delta T = \Delta T_0 \frac{r_0}{r} - \frac{BC(r^2 - r_0^2)}{2r\psi_0} - \sum_{n=1}^{n=\infty} \frac{2BC}{\psi_0 \left(2 + \frac{Bn^2\xi^2}{\psi_0^2}\right)} \cdot \\ \cdot \left(r - \frac{r_0^2 + \frac{Bn^2\xi^2}{\psi_0^2}}{r_1 + \frac{Bn^2\xi^2}{\psi_0^2}} \right) \cos \frac{n\xi}{\psi_0} \cdot \psi \end{aligned} \quad (12)$$

Hence, formulas for the average temperature over the arc can be easily derived

$$\Delta T_{av} = \Delta T_0 \frac{r_0}{r} - \frac{BC(r^2 - r_0^2)}{2r\psi_0} \quad (13)$$

or

$$T_{av} = T_0 \frac{r_0}{r} + T_1 \left(\frac{r - r_0}{r} \right) - \frac{BC(r^2 - r_0^2)}{2r\psi_0} \quad (14)$$

Calculations according to formula (12) showed that jet temperature variations are strongly affected by the first term incorporating jet expansion. Two other terms of the formula related to heat transfer exert but a slight effect on temperature variations of the jet.

CONTENTS

K.F. Voitkovsky, V.N. Golubev, Dependence of Mechanical Properties of Ice on its Structure	3
Ph.R. Johnson, The Modulus of Elasticity of Sea Ice Shown by Direct Tension and Compression Tests of Small Specimens. .	8
D.E. Nevel, The Ultimate Failure of a Floating Ice Sheet. .	17
R. Frederking, Preliminary Results of Plane Strain Compression Tests on Columnar-Grained Ice	23
V.V. Bogorodsky, V.P. Gavriilo, A.V. Gusev, Z.M. Gudkovich, A.P. Polyakov, Stressed Ice Cover State due to Thermal Wave and Related Underwater Noise in the Ocean	28
B.A. Savelyev, V.N. Golubev, M.N. Laptev, I.B. Savelyev, Structural Features of Ice Adhesion to Solids	34
R.C. Byrd, M. Yerkes, W.M. Sackinger, T.E. Osterkamp, Prediction of Sea Ice Physical Properties by Use of Radar . . .	39
C.R. Neill, Force Fluctuations during Ice-Floe Impact on Piers	44
R.Y. Edwards Jr., J.W. Wheaton, Experimental Determination of Ice Impact Loads on Marine Vehicles	51
D.S. Carter, Brittle Fracture of Polycrystalline Ice under Compressive Loadings	62
M. Drouin, Laboratory Investigation on Ice Thermal Pressures	72
M.S. Uzuner, J.F. Kennedy, Hydraulic Criterion for Submergence of Ice Blocks	81
Shin-etsu Kamada, Behaviour of Water-Stage in the River Closed with the Ice Cover	86
V.I. Sinotin, Specific Features of Ice Jam Formation at the End of the Backwater Curve. Some Quantitative Regularities. . . .	91
K.N. Korzhavin, On Wind Drift of Ice Floes	96
S.S. Lazier, M. Metge, Observations on Thermal Cracks in Lake Ice	99
B.V. Proskuryakov, V.P. Berdennikov, Ice-Dam Studies on Models	105
M. Drouin, L. Simard, B. Michel, Ice Floes Velocities in the St. Lawrence River from Oblique Pictures	109
V.A. Koren'kov, Ice Passage through Hydraulic Structures (Field Observation Data)	117

G.D. Ashton, Field Implications of the Formation of Ice Ripples	123
W.D. Hibler, S. Ackley, W.F. Weeks, A. Kovacs, Top and Bottom Roughness of a Multi-Year Ice Floe	130
R.O. Ramseier, D.F. Dickins, A New Approach to Field and Laboratory Tests of Tensile, Compressive, and Flexural Strength of Polycrystalline, Fresh Water Ice	143
D.F. Panfilov, Steady Motion of Packed Fine-Fragmented Ice Masses in a Straight River Reach	148
G. Frankenstein, A. Assur, Israel River Ice Jam	153
S.N. Bulatov, B.M. Ginzburg, I.V. Balashova, Calculation of Thawing Ice Cover Strength and Freeze-up and Break-up Periods in Reservoirs	158
B. Michel, Static Growth of Black Ice in Cold Regions	163
E.V. Kanavin, Problems with Sludge Ice Connected with the Planning and Utilization of Water Power in Norway	171
G.P. Williams, Frazil Ice during Spring Break-up	179
M.V. Kuuskoski, On Frazil Ice Measurements in the Kemi River	184
V. Matoušek, Utilization of a Water Reservoir to Control Winter Phenomena on a River	196
Ph.H. Burgi, Ice Problems in Winter Operation - Bureau of Reclamation Experience	202
S.M. Aleinikov, R.A. Gutkin, V.M. Chesnokov, Winter Operation of Heating Systems of Hydromechanical Equipment of Hydraulic Structures	209
V. Balanin, A. Dytman, M. Zhidkikh, E. Zugrova, L. Bykov, Navigation Lock Equipment for Operation at Negative Air Tempe- ratures and Lock Classification	214
K.A. Andrianov, L.M. Khanashvili, G.J. Chogovadze, D.G. Pagava, M.I. Topchiashvili, A.G. Zelentsov, On the Appli- cability of Different Electrically-Conductive Polymeric Composi- tions in Low-Temperature Heaters	219
V.P. Zakharov, M.M. Bellinson, I.N. Shatalina, Specific Features of Ice Conditions in Rivers and Reservoirs of Central Asia	224
J.V. Danys, Effect of Ice Forces on Some Isolated Struc- tures in the St. Lawrence River	229
L. Bergdahl, Two Lighthouses Damaged by Ice	234

$$\frac{\partial u}{\partial r} + \frac{2u}{r} + \frac{1}{r} \frac{\partial v}{\partial \psi} = 0$$

we obtain after transformation

$$\frac{\partial}{\partial r} (ur^2 \Delta \tau) + \frac{\partial}{\partial \psi} (vr \Delta \tau) = \frac{\lambda}{c\gamma} \frac{\partial^2 \Delta \tau}{\partial \psi^2} \quad (4)$$

in which

u = longitudinal velocity component,

v = transverse velocity component,

$\Delta \tau$ = excess temperature at an arbitrary point of the jet,

τ_1 = water temperature in the water area, the jet boundary

$\psi = \psi_0$ neglected,

c and γ = heat capacity and volume weight of water, respectively,

λ = coefficient of turbulent heat conductivity.

Taking into account that the longitudinal velocity components exceed considerably the transverse velocity components we may solve the equation

$$\frac{\partial}{\partial r} (ur^2 \Delta \tau) = \frac{\lambda}{c\gamma} \frac{\partial^2 \Delta \tau}{\partial \psi^2} \quad (5)$$

The longitudinal velocities over the jet section are known to be varying according to the curvilinear law from u_{max} on the jet axis to zero at its boundaries.

However, the solution of Eq.(5) including such a velocity distribution entails serious mathematical difficulties.

Considering this circumstance, calculations in the first stage are performed for the average velocity over the arc

$$u = \frac{A}{r} \quad (6)$$

Then Eq.(5) may be written as

$$\frac{\partial}{\partial r} (r \Delta \tau) = B \frac{\partial^2 \Delta \tau}{\partial \psi^2} \quad (7)$$

where

$$B = \frac{\lambda}{Ac\gamma}$$

Eq.(7) is solved within the range $0 \leq \psi \leq \psi_0$; $r > r_0$ under the following boundary conditions

$$\Delta \tau \Big|_{r=r_0} = \Delta \tau_0 \quad (8)$$

$$\frac{\partial \Delta \tau}{\partial \psi} \Big|_{\psi=0} = \frac{S}{\lambda} r = Cr \quad (9)$$

$$\frac{\partial \Delta \tau}{\partial \psi} \Big|_{\psi=\psi_0} = 0 \quad (10)$$

where \dot{S} = heat transfer from the free surface.

The equation is solved in the form of the Fourier series in cosines

$$\Delta \bar{T} = \frac{A_0(r)}{2} + \sum_{n=1}^{n=\infty} A_n(r) \cos \frac{n\pi}{\psi_0} \cdot \psi \quad (11)$$

where $n = 0, 1, 2, 3, \dots$

The solution of Eq.(7) yields the expression for calculating temperatures at an arbitrary point of the jet

$$\begin{aligned} \Delta \bar{T} = & \Delta \bar{T}_0 \frac{r_0}{r} - \frac{BC(r^2 - r_0^2)}{2r\psi_0} - \sum_{n=1}^{n=\infty} \frac{2BC}{\psi_0 \left(2 + \frac{Bn^2\pi^2}{\psi_0^2}\right)} \\ & \cdot \left(r - \frac{r_0^2 + \frac{Bn^2\pi^2}{\psi_0^2}}{r_1 + \frac{Bn^2\pi^2}{\psi_0}} \right) \cos \frac{n\pi}{\psi_0} \cdot \psi \end{aligned} \quad (12)$$

Hence, formulas for the average temperature over the arc can be easily derived

$$\Delta \bar{T}_{av} = \Delta \bar{T}_0 \frac{r_0}{r} - \frac{BC(r^2 - r_0^2)}{2r\psi_0} \quad (13)$$

or

$$\bar{T}_{av} = \bar{T}_0 \frac{r_0}{r} + \bar{T}_1 \left(\frac{r - r_0}{r} \right) - \frac{BC(r^2 - r_0^2)}{2r\psi_0} \quad (14)$$

Calculations according to formula (12) showed that jet temperature variations are strongly affected by the first term incorporating jet expansion. Two other terms of the formula related to heat transfer exert but a slight effect on temperature variations of the jet.

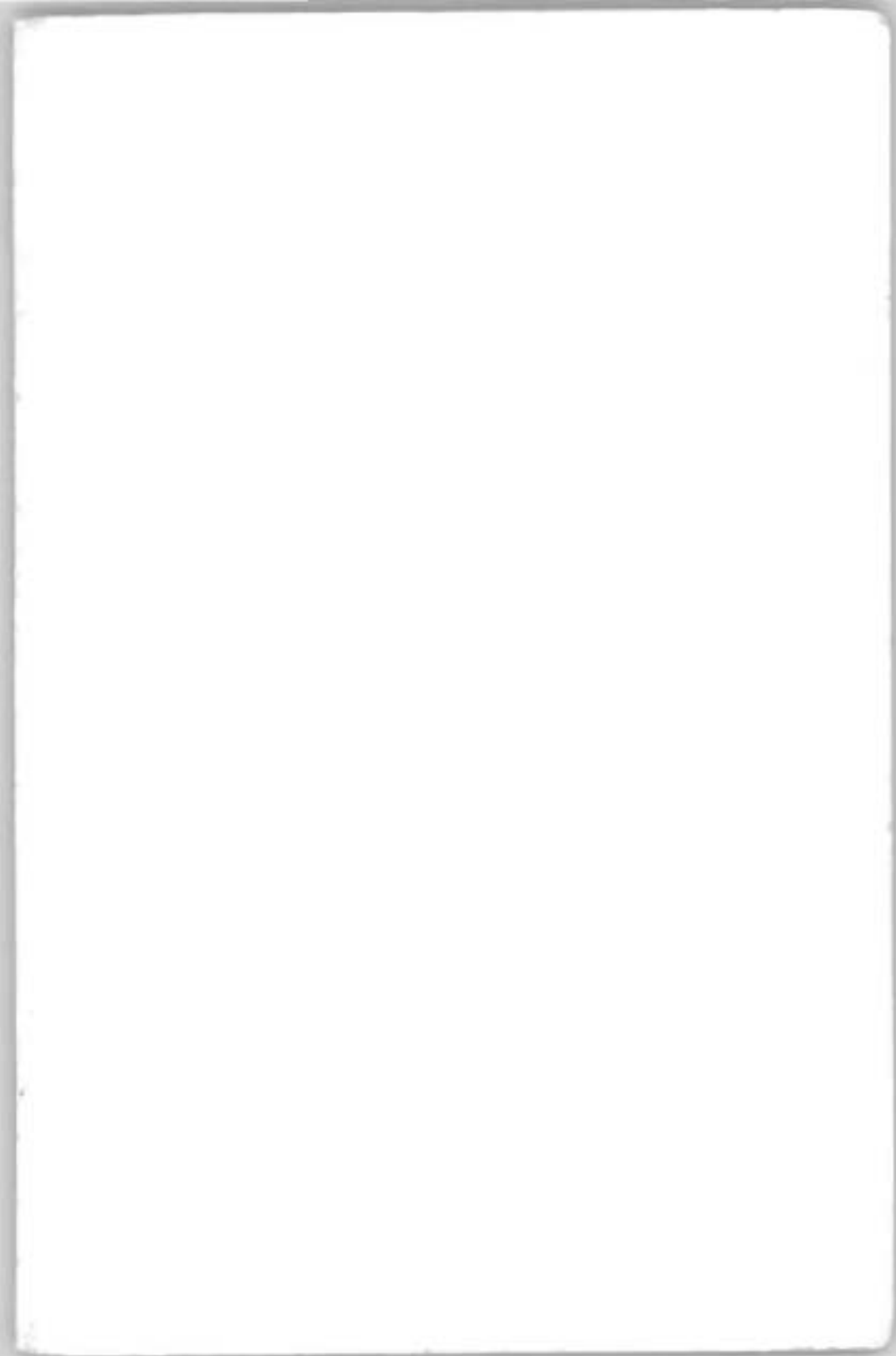
CONTENTS

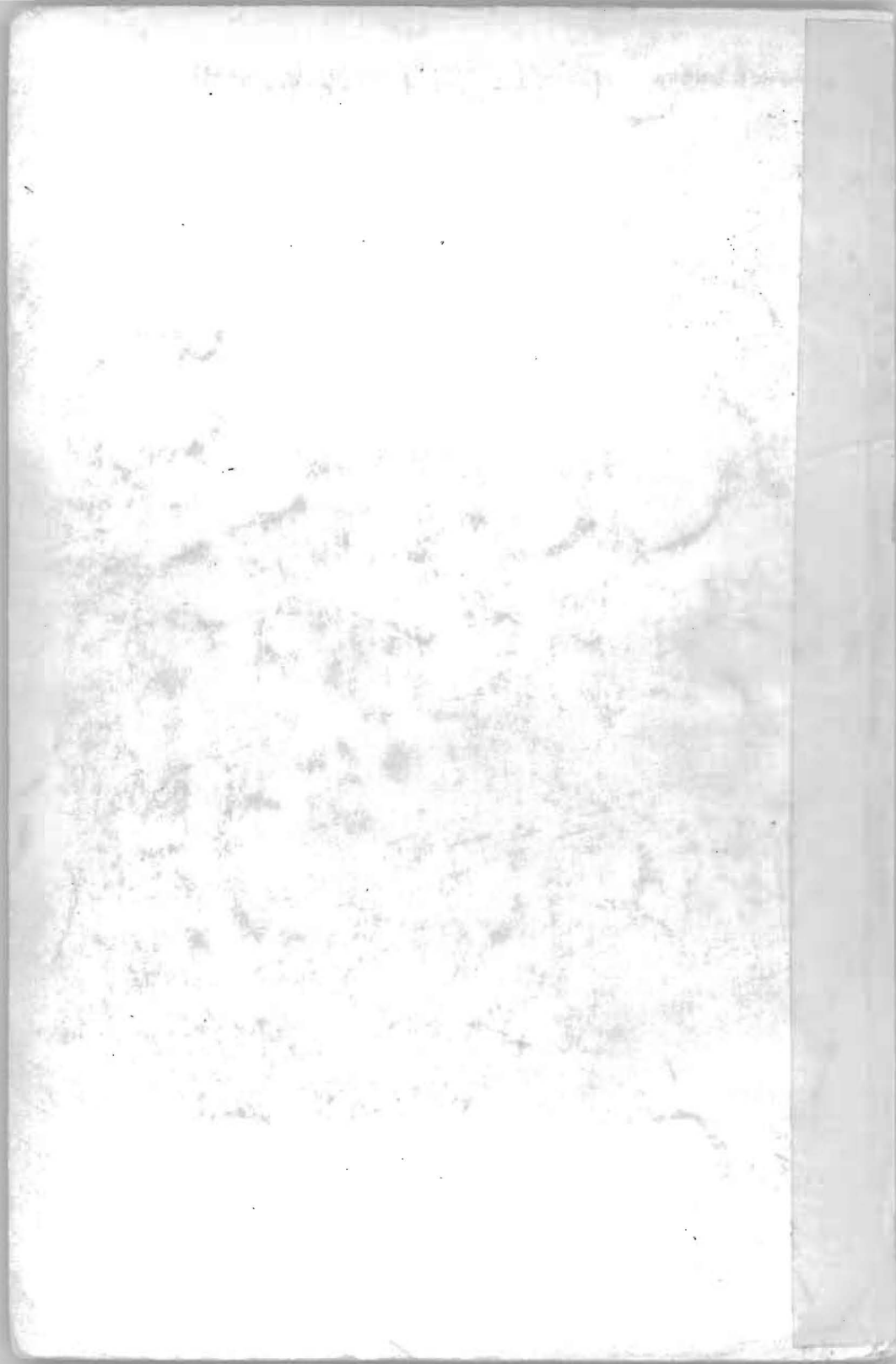
K.F. Voitkovsky, V.N. Golubev, Dependence of Mechanical Properties of Ice on its Structure	3
Ph.R. Johnson, The Modulus of Elasticity of Sea Ice Shown by Direct Tension and Compression Tests of Small Specimens. .	8
D.E. Nevel, The Ultimate Failure of a Floating Ice Sheet. .	17
R. Frederking, Preliminary Results of Plane Strain Compression Tests on Columnar-Grained Ice	23
V.V. Bogorodsky, V.P. Gavriilo, A.V. Gusev, Z.M. Gudkovich, A.P. Polyakov, Stressed Ice Cover State due to Thermal Wave and Related Underwater Noise in the Ocean	28
B.A. Savelyev, V.N. Golubev, M.N. Laptev, I.B. Savelyev, Structural Features of Ice Adhesion to Solids	34
R.C. Byrd, M. Yerkes, W.M. Sackinger, T.E. Osterkamp, Prediction of Sea Ice Physical Properties by Use of Radar . . .	39
C.R. Neill, Force Fluctuations during Ice-Floe Impact on Piers	44
R.Y. Edwards Jr., J.W. Wheaton, Experimental Determination of Ice Impact Loads on Marine Vehicles	51
D.S. Carter, Brittle Fracture of Polycrystalline Ice under Compressive Loadings	62
M. Drouin, Laboratory Investigation on Ice Thermal Pressures	72
M.S. Uzuner, J.F. Kennedy, Hydraulic Criterion for Submergence of Ice Blocks	81
Shin-etsu Kamada, Behaviour of Water-Stage in the River Closed with the Ice Cover	86
V.I. Sinotin, Specific Features of Ice Jam Formation at the End of the Backwater Curve. Some Quantitative Regularities. . . .	91
K.N. Korzhavin, On Wind Drift of Ice Floes	96
S.S. Lazier, M. Metge, Observations on Thermal Cracks in Lake Ice	99
B.V. Proskuryakov, V.P. Berdennikov, Ice-Dam Studies on Models	105
M. Drouin, L. Simard, B. Michel, Ice Floes Velocities in the St. Lawrence River from Oblique Pictures	109
V.A. Koren'kov, Ice Passage through Hydraulic Structures (Field Observation Data)	117

G.D. Ashton, Field Implications of the Formation of Ice Ripples	123
W.D. Hibler, S. Ackley, W.F. Weeks, A. Kovacs, Top and Bottom Roughness of a Multi-Year Ice Floe	130
R.O. Ramseier, D.F. Dickins, A New Approach to Field and Laboratory Tests of Tensile, Compressive, and Flexural Strength of Polycrystalline, Fresh Water Ice	143
D.F. Panfilov, Steady Motion of Packed Fine-Fragmented Ice Masses in a Straight River Reach	148
G. Frankenstein, A. Assur, Israel River Ice Jam	153
S.N. Bulatov, B.M. Ginzburg, I.V. Balashova, Calculation of Thawing Ice Cover Strength and Freeze-up and Break-up Periods in Reservoirs	158
B. Michel, Static Growth of Black Ice in Cold Regions	163
E.V. Karavin, Problems with Sludge Ice Connected with the Planning and Utilization of Water Power in Norway	171
G.P. Williams, Frazil Ice during Spring Break-up	179
M.V. Kuuskoski, On Frazil Ice Measurements in the Kemi River	184
V. Matoušek, Utilization of a Water Reservoir to Control Winter Phenomena on a River	196
Ph.H. Burgi, Ice Problems in Winter Operation - Bureau of Reclamation Experience	202
S.M. Aleinikov, R.A. Gutkin, V.M. Chesnokov, Winter Operation of Heating Systems of Hydromechanical Equipment of Hydraulic Structures	209
V. Balanin, A. Dytman, M. Zhidkikh, E. Zugrova, L. Bykov, Navigation Lock Equipment for Operation at Negative Air Tempe- ratures and Lock Classification	214
K.A. Andrianov, L.M. Khananashvili, G.I. Chogovadze, D.G. Pagava, M.I. Topchiashvili, A.G. Zelentsov, On the Appli- cability of Different Electrically-Conductive Polymeric Composi- tions in Low-Temperature Heaters	219
V.P. Zakharov, M.M. Bellinson, I.N. Shatalina, Specific Features of Ice Conditions in Rivers and Reservoirs of Central Asia	224
J.V. Danys, Effect of Ice Forces on Some Isolated Struc- tures in the St. Lawrence River	229
L. Bergdahl, Two Lighthouses Damaged by Ice	234

A.I. Pekhovich, Thermal Calculations in Prediction of Ice Action on Hydraulic Structures	239
Ya.L. Gotlib, F.F. Razzorenov, N.M. Sokolnikov, V.M. Zhidkikh, Thermal Regime of Deep Reservoirs in Siberia and Investigation of their Thermal Characteristics	246
V.M. Zhidkikh, Yu.A. Popov, Pressure Conduit Icing Studies and Anti-Icing Techniques	252
Ö. Štarošolszky, The Application of Heat-Transfer Relationships to Watercourses	257
J. Schwarz, T. Miloh, On the Time Dependent Temperature Variation within Ice Sheets	262
A.P. Braslavsky, Ts.A. Nazarov, Calculation of Ice-Thermal Regime Varying with Time and along the Length of a Canal-Connected Chain of Storages	270
B.S. Borodkin, Temperature Field of a Circular Surface Flow Arising during Pneumatic Installation Operation	275

ВНИИГ. 20/УІ-1972. Зак.331.





Bib 28-3893-3909

U. S. ARMY CORP OF ENGINEERS
HANOVER, NEW HAMPSHIRE 03752

I·A·H·R SYMPOSIUM
ICE AND ITS ACTION
ON HYDRAULIC STRUCTURES

LECTURES
PAPERS AND DISCUSSION
RECORDS OF SYMPOSIUM

LENINGRAD · USSR
26-29 SEPTEMBER 1972





28-3893

28-3909

U. S. ARMY CORP

OF THE ARMY
ENGINEERING LABORATORY
Kempshire 03755

I·A·H·R SYMPOSIUM
ICE AND ITS ACTION
ON HYDRAULIC STRUCTURES

LECTURES
PAPERS AND DISCUSSION
RECORDS OF SYMPOSIUM

•

LENINGRAD · USSR
26-29 SEPTEMBER 1972

Papers and discussions:

Slesarenko, Yu. E., Frolov, A. D. Comparison of elasticity and strength characteristics of salt-water ice	85
Frolov, A. D., Slesarenko Yu. E. Characteristics of elasticity of sea ice of different compositions	88
Ergin, V. P. Effect of ice structure and mineralization on the mechanical properties of the fresh-water ice cover	91
Assur, A. Structures in ice infested waters . .	93
Sinyavskaya, V. M., Dlk P. G. Field observations on static ice pressure against hydraulic structures	98
Kopalgorodski, E. M., Vershinin, S. A., Nifontov, S. A. Model investigations of the effect of an ice field pushed against the piles of off-shore oil platforms	100
Triquet, C. Processus de formation des accumulations de frazil en amont d'un barrage réservoir	103
Herva, M. Some observations about the break-up of ice cover on the river Kemi above the Isohaara power dam	108
Sokolov, I. N. On ice passage through hydraulic structures	110
Slissky, P. M. Specific features of ice floe behaviour in the vicinity of ice retaining structures	113
Karnovich, V. N. Ice jams and adequate preventive measures	115
Shlygin, I. A. Studies on the effect of ice cover on tidal wave propagation in the water area of a tidal power plant	117
Chizhov, A. N. Field data on ice damming and ice jamming	120

Liamas, J. Penetration of ice blocks in the stilling basin of a dam	123
Donchenko, R.V. Estimation of the variation in the ice regime on regulated river reaches	131
Rozhnoy, R. Ice trouble prevention on the Danube river	134
Votruba, L. Ice-pressure on tower structures in the reservoir	135
Timchenko, V.M. Investigation of heat inflow to a melting ice cover on rivers	141
Yamaoka, I. Ice troubles on hydraulic structures of the Hokkaido Development Bureau	143
Fokeev, V.V. Application of pulse water jets and vortex funnels for the discharge of surface ice and frazil through hydraulic structures	144

PREFACE

The 2nd International Symposium "Ice and its Action on Hydraulic Structures" organized by the Technical Committee on Ice Problems and the Soviet National Committee of the International Association for Hydraulic Research was held in Leningrad, September 26-29, 1972.

The technical program of the Symposium included the following subjects:

1. Structure and physico-mechanical properties of ice, including procedures and equipment for their measurement both in the laboratory and in the field.
2. Freezing and break-up in rivers and reservoirs, including ice jamming and ice damming.
3. Ice regime and ice control in the vicinity of hydraulic structures, including preventive measures against harmful effect on the structures and methods of extending the navigation period.

The contributions to the above subjects presented by foreign and soviet specialists in the field of ice engineering were published in English and Russian in the pre-Symposium period.

Besides papers, invited lectures were delivered on the advances in ice engineering research in the U.S.A., Canada and the U.S.S.R. as well as on some special problems concerning mainly physico-mechanical characteristics of ice. The Symposium provided a wide forum for exchange of opinions on the problems considered and an opportunity for discussion.

The present volume comprises the invited lectures, the papers which were received after the deadline, the discussions, and finally the records of the Symposium.

WELCOMING ADDRESS

by

P. Neporozhny

Minister of Power and Electrification of the U.S.S.R.

I would like to bid a cordial welcome to the participants of the Symposium on behalf of the U.S.S.R. Ministry of Power and Electrification.

Due to the present advances in hydraulic construction, water transport and development of the Extreme North of our planet the engineering profession is faced with a good many urgent ice engineering problems which are covered by the Ice Symposium.

The discussions at the Symposium must serve as a basis in furthering research on ice engineering and in contributing to its progress.

May success attend the activities of all the Symposium participants.

WELCOMING ADDRESS

by

M. F. Skladnev

Chairman of the Organizing Committee of
the 2nd International Symposium on
"Ice and its Action on Hydraulic Structures"

President of the IAHR Soviet National Committee

Ladies and Gentlemen, dear Colleagues and Comrades,

We are gathered here today to commence the activities of the International Symposium on "Ice and its Action on Hydraulic Structures" sponsored by the International Association for Hydraulic Research.

It affords me the greatest pleasure to welcome the honoured guests and the Symposium participants on behalf of the Organizing Committee and the IAHR Soviet National Committee.

The decision to choose Leningrad as the site of the 2nd Ice Symposium was passed at the 1st Symposium held in Iceland in 1970. Soviet scientists spent the two intervening years in making ready for the present Symposium, the necessary preparatory work being conducted under the Local Organizing Committee.

The wish to participate in the Symposium was expressed by 170 research engineers hailing from 14 different countries, 60 participants coming from outside this country. A total of 47 papers was approved of, including 29 from abroad. The accepted papers were published in the 1st volume of the Symposium Proceedings. A program is worked out for inspection visits to laboratories in Leningrad, and the route of a study tour to Novosibirsk-Irkutsk-Bratsk-Moscow comprising visits to the Siberian Branch of the U.S.S.R. Academy of Sciences, the Irkutsk, Novosibirsk, and Bratsk Hydropower Projects as well as the Baikal Lake. In addition a social events' program is evolved.

I would like to avail myself of the opportunity to express our gratitude to the President of the IAHR Technical Committee on Ice Problems, Mr. Michel, for his most kind attention and the assistance rendered

during the preparations for the Symposium. I consider it my pleasant duty to thank the representatives of the Municipal and Communist Party Authorities for their great help.

We trust that the stay of the Symposium participants in Leningrad may prove both profitable and pleasant.



M. SKLADNEV, Chairman of the Organizing Committee,
President of the IAHR Soviet National Committee
greets the Symposium participants

OPENING ADDRESS

by

B. Michel

President of the IAHR Committee on Ice Problems

Your honor Mr. Goloubovitch, representing the Municipal Authorities,
Mr. Skladnev, chairman of the Organizing Committee,
colleagues of the International Association for Hydraulic Research,
Ladies and Gentlemen

It is a very great privilege for me to open this second International Symposium on "Ice and its Action on Hydraulic Structures" on behalf of the Committee on Ice Problems of the IAHR and to tell our hosts how pleased I am with all other foreign participants to be again in this great country to discuss the subject of ice.

Some of you present today have not had the opportunity to come in contact with, or do not have specific knowledge of the activities of the Section on Ice Problems of the IAHR. I would like to take this opportunity to refer briefly to our objectives and to the past activities of our group.

The purpose of the Section for Ice Problems is to foster a bond between those concerned with ice phenomena in general and with ice problems in connection with hydraulic structures.

This objective is attained by:

- a) exchange of information and publication of results of research
- b) discussion on research in progress
- c) collaboration of research organizations in pursuing relevant research

The Section was created by the IAHR at the Montreal Congress of 1959 after a very successful seminar on Ice Problems. It set up lectures in London in 1963 and a very active and well attended Seminar was held here in Leningrad at the General Congress of 1965. Another Seminar on Ice was organized for the Congress of 1967 in Colorado.

Renewed and increased interest was shown for ice problems at the end of the sixties when accelerated development had to be made of

difficult river sites for hydroelectric exploitation during winter months and for problems related to navigation in ice and construction of off-shore structures in the Arctic.

Our first International Symposium outside of the IAHR Congresses was held in Iceland in 1970 and its success opened the door for the acceptance of the invitation of Mr. Skladnev for this second one, beginning today.

Another important task of our Committee has been to draw up an acceptable set of definitions and a terminology for ice phenomena. Much confusion was apparent in the definition of terms at the first seminar on ice problems which was held in Montreal and in the following ones. We will hear today the last part of this work relating to the Russian and French translations of the terminology.

I would now like to express my thanks, those of the members of the Committee on Ice Problems and on the members of the IAHR to those who have worked very hard on the program and the very appreciated arrangements for the stay of the participants in Leningrad.

We are particularly grateful to the Chairman of the Organizing Committee, Mr. M. Skladnev, Director of the B. E. Vedenev All-Union Research Institute of Hydraulic Engineering. I know that from the amount of correspondence we had that he had put a tremendous personnel effort in the organization of this Symposium. He had been assisted by Messrs V. V. Balarin, B. V. Proskuryakov, V. I. Sinotin and S. M. Aleinikov who are outstanding scientists in ice research and have contributed from the beginning in 1960 to the work of our Committee. May I give, on your behalf, our warmests expression of gratefulness to our Russian colleagues.

With these introductory remarks and, bearing in mind, that the main objectives of this Symposium is an exchange of ideas, views and experiences in our field of ice research in order to advance our knowledge, I now take pleasure in declaring this Symposium on Ice and its Action on Hydraulic Structures, in session.



B. MICHEL, President of the IAHR Technical Committee on Ice Problems
declares the Symposium in session

PROGRAM OF SYMPOSIUM SESSIONS

Tuesday, 26 September (Morning Session)

- 09,00 Welcoming addresses
- 09,30 Communication on Ice Terminology of the IAHR Committee on Ice Problems
- 10,15 Lecture by Prof. K. N. Korzhavin - Ice Engineering and Hydroelectric Development - the U.S.S.R. Experience
- 10,45 Refreshment interval
- 11,15 K. F. Voitkovsky, V. N. Golubev, U.S.S.R. - Dependence of Mechanical Properties of Ice on its Structure
- 11,30 Ph. R. Johnson, U.S.A. - The Modulus of Elasticity of Sea Ice Shown by Direct Tension and Compression Tests of Small Specimens
- 11,45 D. E. Nevel, U.S.A. - The Ultimate Failure of a Floating Ice Sheet
- 12,00 R. Frederking, Canada - Preliminary Results of Plane Strain Compression Tests on Columnar Grained Ice

Tuesday, 26 September (Afternoon Session)

- 14,15 Lecture by Dr. T. Carstens - Structure and Physico-Mechanical Properties of Ice
- 14,45 V. V. Bogorodsky, V. P. Gavrilov, A. V. Gusev, Z. M. Gudkovich, A. P. Polyakov, U.S.S.R. - Stressed Ice Cover State due to Thermal Wave and Related Underwater Noise in the Ocean
- 15,00 B. A. Savelyev, V. N. Golubev, M. N. Laptev, I. B. Savelyev, U.S.S.R. - Structural Features of Ice Adhesion to Solids

- 15,15 T. Nuttall, Canada - Plane Strain Tests on River Ice
- 15,30 B. Ross, U.S.A. - Drilling Platforms in an Arctic Environment
- 15,45 Refreshment interval
- 16,15 R. C. Byrd, M. C. Yerkes, W. M. Sackinger, T. E. Osterkamp, U.S.A. - Prediction of Sea Ice Physical Properties by Use of Radar
- 16,30 C. R. Neill, Canada - Force Fluctuations during Ice-Floe Impact on Piers
- 16,45 R. Y. Edwards, Jr., J. W. Wheaton, U.S.A. - Experimental Determination of Ice Impact Loads on Marine Vehicles
- 17,00 D. S. Carter, Canada - Brittle Fracture of Polycrystalline Ice under Compressive Loadings
- 17,15 M. Drouin, Canada - Laboratory Investigation on Ice Thermal Pressures
- 17,30 Discussion

Wednesday, 27 September (Morning Session)

- 09,00 Lecture by Dr. A. Assur - Ice Engineering in the American Experience
- 09,30 M. S. Uzuner, J. F. Kennedy, U.S.A. - Hydraulic Criterion for Submergence of Ice Blocks
- 09,45 Shin-etsu Kamada, Japan - Behaviour of Water-Stage in the River Closed with the Ice Cover
- 10,00 V. I. Sinotin, U.S.S.R. - Specific Features of Ice Jam Formation at the End of the Backwater Curve. Some Quantitative Regularities
- 10,15 K. N. Korzhavin, U.S.S.R. - On Wind Drift of Ice Floes.
- 10,30 S. S. Lazier, M. Metge, Canada - Observations on Thermal Cracks in Lake Ice
- 10,45 Refreshment interval
- 11,15 B. V. Proskuryakov, V. P. Berdennikov, U.S.S.R. - Ice-Dam Studies on Models
- 11,30 M. Drouin, L. Simard, B. Michel, Canada - Ice Floes Velocities in the St. Lawrence River from Oblique Pictures

- 11.45 V. A. Koran'kov, U.S.S.R. - Ice Passage through Hydraulic Structures (Field Observation Data)
- 12.00 G. D. Ashton, U.S.A. - Field Implications of the Formation of Ice Ripples

Wednesday, 27 September (Afternoon Session)

- 14.15 W. D. Hibler, S. Ackley, W. F. Weeks, A. Kovacs, U.S.A. - Top and Bottom Roughness of a Multi-Year Ice Floe
- 14.30 R. O. Ramseier, D. F. Dickins, Canada - A New Approach to Field and Laboratory Tests of Tensile, Compressive, and Flexural Strength of Polycrystalline, Fresh Water Ice
- 14.45 D. F. Panfilov, U.S.S.R. - Steady Motion of Packed Fine Fragmented Ice Masses in a Straight River Reach
- 15.00 A. Assur, U.S.A. - Structures in Ice-Infested Waters
- 15.15 G. Frankenstein, A. Assur, U.S.A. - Israel River Ice Jam
- 15.30 S. N. Bulatov, B. M. Ginzburg, I. V. Balashova, U.S.S.R. - Calculation of Thawing Ice Cover Strength and Freeze-up and Break-up Periods in Reservoirs
- 15.45 Refreshment interval
- 16.15 B. Michel, Canada - Static Growth of Black Ice in Cold Regions
- 16.30 E. V. Kanavin, Norway - Problems with Sludge Ice Connected with the Planning and Utilization of Water Power in Norway
- 16.45 G. P. Williams, Canada - Frazil Ice during Spring Break-up
- 17.00 C. Têquet, Canada - Processus de formation des accumulations de frazil en amont d'un barrage réservoir
- 17.15 T. E. Osterkamp, U.S.A. - Frazil in Production in a Small Stream
- 17.30 M. V. Kuuskoski, Finland - On Frazil Ice Measurements in the Kemi River
- 17.45 Discussion

Thursday, 28 September (Morning Session)

- 09.00 Lecture by Prof. B. Michel, - Ice Management in Hydraulic Design - Recent Canadian Experience
- 09.30 V. Matoušek, Czechoslovak Socialist Republic - Utilization of a Water Reservoir to Control Winter Phenomena on a River
- 09.45 Ph. H. Burgi, U.S.A. - Ice Problems in Winter Operation - Bureau of Reclamation Experience
- 10.00 I. Yamaoka, Japan - Ice Control for Intake Structures of Reservoirs in Hokkaido
- 10.15 S. M. Aleinikov, R. A. Gutkin, V. M. Chesnokov, U.S.S.R. - Winter Operation of Heating Systems of Hydromechanical Equipment of Hydraulic Structures
- 10.30 V. V. Balanin, A. O. Dytman, M. I. Zhidkikh, M. I. Zugarova, L. S. Bykov, U.S.S.R. - Navigation Lock Equipment for Operation at Negative Air Temperatures and Lock Classification
- 10.45 Refreshment interval
- 11.15 K. A. Andrianov, L. M. Khananashvili, G. I. Chogovadze, D. G. Pagava, M. I. Topchiashvili, A. G. Zelentsov, U.S.S.R. - On the Applicability of Different Electrically-Conductive Polymeric Compositions in Low-Temperature Heaters
- 11.30 V. P. Zakharov, M. M. Beilinson, L. N. Shatalina, U.S.S.R. - Specific Features of Ice Conditions in Rivers and Reservoirs of Central Asia
- 11.45 M. Herva, Finland - Effect of Fine Materials in Water on Ice Formation
- 12.00 L. Votruba, Czechoslovak Socialist Republic - Les effets des glaces sur les tours dans les réservoirs

Thursday, 28 September (Afternoon Session)

- 14.15 J. V. Danys, Canada - Effect of Ice Forces on Some Isolated Structures in the St. Lawrence River

- 14.30 L. Bergdahl, Sweden - Two Lighthouses Damaged by Ice
- 14.45 Jose Llamas, Canada - Pénétration des blocs de glace dans un bassin de dissipation d'énergie à l'aval d'un barrage
- 15.00 Keith C. Arnold, Canada - Harmful Effects of Glacier Ice on Potential Pipeline Routes in the Queen Elizabeth Islands
- 15.15 A. I. Pukhovich, U.S.S.R. - Thermal Calculations in Prediction of Ice Action on Hydraulic Structures
- 15.30 Refreshment interval
- 16.00 Ya. L. Gotlib, F. F. Razzorenov, N. M. Sokol'nikov, V. M. Zhidkikh, U.S.S.R. - Thermal Regime of Deep Reservoirs in Siberia and Investigation of their Thermal Characteristics
- 16.15 V. M. Zhidkikh, Yu. A. Popov, U.S.S.R. - Pressure Conduit Icing Studies and Anti-Icing Techniques
- 16.30 Ö. Starošolszky, Hungarian People's Republic - The Application of Heat-Transfer Relationships to Watercourses
- 16.45 J. Schwarz, T. Miloh, U.S.A. - On the Time Dependent Temperature Variation within Ice Sheets
- 17.00 A. P. Braslavsky, Ts. A. Nazarov, U.S.S.R. - Calculation of Ice-Thermal Regime Varying with Time and along the Length of a Canal-Connected Chain of Storages
- 17.15 B. S. Borodkin, U.S.S.R. - Temperature Field of a Circular Surface Flow Arising during Pneumatic Installation Operation
- 17.30 Discussion
- 18.30 Closing Session

Friday, 29 September

- 09.00 Technical excursions to research establishments in Leningrad (the B. E. Vedenev All-Union Research Institute of Hydraulic Engineering, the Arctic and Antarctic Research Institute, and the State Hydrological Institute). Sightseeing tour of the city.

LIST OF PARTICIPANTS
OF THE 2nd ICE SYMPOSIUM
Leningrad, 1972

CANADA

1. Cammaert, A.B. Engng Faculty, Memorial University of
Newfoundland, Newfoundland
2. Croasdale, K.R. B. Sc. Eng., C. Eng. Research Engineer,
Imperial Oil Ltd., 339, 50th Ave S. E.
Calgary, Alberta
3. Danys, J.V. Superintendent of Civil Engng, Ministry of
Transport, Marine Services, Place de Ville,
Tower "C", Ottawa
4. Drouin, M. D. Sc., Research Associate, Civil Engng
Department, Laval University, Quebec 10,
Quebec
5. Ferguson, D.J. Engineer, Section Head, the St. Lawrence
Seaway Authority, P. O. 200, St. Laurent,
Montreal 379, Quebec
6. Frederking, R. Ph. D., Research Off., National Research
Council of Canada, Ottawa, Ontario, K1A,
OR6 X
7. Hhatiuk, J. Petroleum Engineer - Sen. Projects Engineer,
Exploration and Production Department, Gulf
Oil Canada Ltd. P. O. Box 130, Calgary,
Alberta
8. Jazrawi, W. Ph. D. Eng., Arctic Off-shore Engineer,
Imperial Oil Ltd. 500, 6th Ave, S. W.,
Calgary, Alberta
9. Lariviere, R. Engr, Manager, Hydraulics Service, Hydro-
Quebec, 16th Floor, Stock Exchange Tower
Building, Victoria Sq., Montreal, Quebec

10. Lawrie, Ch. J. R: B. Sc. (Eng.), P. Eng. - Research & Development Engineer, Ministry of Transport, 20 G, Tower "C", Place de Ville, Ottawa K1A Ontario ON7 X
11. Llamas, J. Prof. of Hydrology, Civil Engng Department, Laval University, Quebec 10, Quebec
12. Metge, M. Grad. Student, Queen's University, Ellis Hall, 28 Maitland Street, Kingston, Ontario
13. Michel, B. President of the IAHR, Committee on Ice Problems, Dr. Eng., Laval University, Quebec 10, Quebec X
14. Neill, Ch. R. Hydraulic Engineer, Research Council of Alberta, 11315-87 Ave, Edmonton, Alberta
15. Nuttall, J. B. Associate Professor, University of Alberta, Edmonton, Alberta
16. Swann, L. F. Bachelor of Science, Civil Eng. - Chief. Design Division X
17. Ramseier, R. O. Research Scientist, Project Leader, Dept. of the Environment, Inland Waters Branch, 562 Booth Street, Ottawa, Ontario
18. Triquet, C. Eng., M. Sc., Water Resources Management Plans Coordinator, Quebec's Department of Natural Resources, 1640 Boul. de l'Entente, Quebec 6, Quebec
19. Wigle, T. E. Engineer-River Control, the Hydro Electric Power Commission of Ontario, 620 University Ave, Toronto, Ontario

CZECHOSLOVAK SOCIALIST REPUBLIC

20. Matoušek, V. Candidate of Science, Head of Department, Povodi Ohre, Celakovskeho 28, Chomutov X
21. Sikora, A. Dipl. Ing. C. Sc., Director of the Water Research Institute, Bratislava, Karlovska 9

22. Stančíková, A. Dipl. Ing., Research worker, Water Research Institute, Bratislava, Karloveska 9
23. Votruba, L. Prof., Dept. of Civil Engng, Technical University, Praha 6, Zikova 4

FINLAND

24. Airaksinen, K. Naval Architect, Icebreaking Laboratory, Wärtsilä, Helsinki Shipyard, Box 132, 00151 Helsinki 15
25. Herva, M. A. Planning Engineer, Civil Eng., Pohjolan Voima Oy, Isokatu 14, Oulu X
26. Kuuskoski, M. V. Diploma Engineer, Director, Imatran Voima Osakeyhtio, P. O. Box 10138, 00101 Helsinki 10
27. Mäkinen, E. K. Naval Architect, Head, Icebreaking Laboratory, Oy Wärtsilä, Helsinki Shipyard, Box 132, 00151 Helsinki 15
28. Korri, P. E. Res. Engr, Rauma-Repola Oy, 26100 Rauma 10.
29. Rekonen, T. G. Civ Eng., Mikohkatu 2, Helsinki 10

FRANCE

30. Ramette, M. Ingénieur, Chef de Division Hydraulique Fluviale, E. D. F. Laboratoire National d'Hydraulique, 6 Quai Watier 78, Chatou

GERMAN DEMOCRATIC REPUBLIC

31. Lauber, R. Dr. rer. nat. Ministerium für Wasserwirtschaft (FAS)
32. Seeger, U. Dipl.-Ing. Oberflussmeisterei "Oder" Frankfurt/O, Karl-Marx-Str 162
33. Honecker, A. Ing. Direktor, Wasserstrasseninspektion 102 Berlin Poststr. 22/23

GREAT BRITAIN

34. Richardson, H. Secretary-General, International Glaciological Society, Cambridge CB2 1ER X

HUNGARIAN PEOPLE'S REPUBLIC

35. Törőcsik, G. National Water Authority, Budapest V
36. Rozsnyói, P. National Water Authority, Budapest V
37. Starosolszky, O. Dr. Eng., Deputy Head of Dept. for Water Resources, National Water Authority, Budapest I, Fo ut., 48-50
38. Zsilák, E. Civ. Engineer, Senior Design Officer, Design Office for Hydraulic Engng "VIZITERV", Budapest V, Münnich F. ut., 26

ICELAND

39. Freysteinsson, S. Civil Engineer Thoroddsen & Partners, Consulting Engrs, Armuli 4, Reykjavik X

NORWAY

40. Tesaker, E. Engr, River and Harbour Laboratory, Klæbovn 153, Trondheim

SOCIALIST REPUBLIC of ROUMANIA

41. Bondar, C. Dr. Eng., Institute of Meteorology and Hydrology - Bucharest
42. Armencea, G. Research Engineer, Institute for Hydroenergetic Studies and Design - Bucharest, Galats Str., 5-7.

SWEDEN

43. Bergdahl, L. M. Research Engineer, Chalmer's University of Technology, Division of Hydraulics, CTH, Fack, S-40220, Goteborg
44. Henriksson, M. E. Civil Engineer, Swedish State Power Board, the Hydraulic Laboratory, S-81071, Alvkarleby

SWITZELAND

45. Lemcke, B. Scientist-Managing Director, Institute CERAC SA, Ch. des Grandes Pieces, 1024 Ecublens

U.S.A.

46. Ackley, S. F. Research Physicist, U.S. Army Cold Regions Research & Engineering Laboratory, Lyne Rd 1, Hanover, New Hampshire 03755
47. Ashton, G. D. Dr., Hydrologist, U.S. Army Cold Regions Research & Engineering Laboratory, Hanover, New Hampshire 03755
48. Assur, A. Chief Scientist, U.S. Army Cold Regions Research & Engineering Laboratory, Hanover, New Hampshire 03755 X
9. Edwards, R. Y., Jr. Vice President for Research, ARCTEC, Incorporated, Suite 255, Wilde Lake Village Green, Columbia, Maryland 21044
0. Ehrlich, N. A. Engineer, Domestic Icebreaking Project Off., U.S. Coast Guard Res. and Development, 400 7th St., S.W., Washington, D.C. 20590
1. Frankenstein, G. E. Civil Engineer, U.S. Army Cold Regions Research & Engineering Laboratory, P.O. Box 282, Hanover, New Hampshire 03755 X

52. Gerwick, B. Prof. of Civil Engng, University of California, Berkeley, California 94720
53. Kennedy, J. F. Director, Institute of Hydraulic Research, the University of Iowa, Iowa City, Iowa 52240
54. Louie, D. S. H. Chief Hydraulic Engr, Harza Engineering Co., 150 South Wacker Drive, Chicago, Illinois 60606
55. Marshall, E. M. Glaciologist, University of Michigan, Ann Arbor, Michigan 48104 X
56. Nevel, D. E. Research Civil Engineer, U.S. Army Cold Regions Research & Engineering Lab., P.O. Box 282, Hanover, New Hampshire 03755 X
57. Wilson, G. E. Assistant Administrator-Development, St. Lawrence Seaway Development Corp. P. O. Box 5403, Fair Lawn, Ohio 14313
- U.S.S.R.
58. Agalakov, S. S. Project Leader, the S. Ya. Zhuk All-Union Design and Research Institute "Hydroproject", Leningrad Branch, Leningrad
59. Aleinikov, S. M. Scientific Secretary of the Organizing Committee, Head of Research Group, the B. E. Vedenev All-Union Research Institute of Hydraulic Engineering, Leningrad
60. Amirov, K. A. M. Sc., Head of Department, the Kazakh Research Institute of Power Engineering, Alma-Ata.
61. Balanin, V. V. M. Sc., Rector, the Leningrad Water Transport Institute, Leningrad
62. Berdennikov, V. P. M. Sc., Senior Research Worker, the State Hydrological Institute, Leningrad

63. Bogorodsky, V. V. Corresponding Member of the Academy, the Arctic and Antarctic Research Institute, Leningrad
64. Borodkin, B. S. Associate Professor, the Leningrad Water Transport Institute, Leningrad
65. Braslavsky, A. P. D. Sc., the Kazakh Hydrometeorological Research Institute, Alma-Ata
66. Bulatov, S. N. D. Sc., Head of Department, the Hydrometeorological Research Center of the U.S.S.R., Moscow
67. Butyagin, I. P. M. Sc., Head of Chair, the Novosibirsk Institute of Water Transport Engineers
68. Bykov, L. S. M. Sc., Chief Engineer, the Authority of the Canal named after Moscow, Moscow
69. Chesnokov, V. M. Chief Engineer, the "Lengidrosta" Design Office, Leningrad
70. Chizhov, A. N. M. Sc., Head of Laboratory, the State Hydrological Institute, Leningrad
71. Chogovadze, G. I. M. Sc., Director, the Georgian Research Institute of Power Engineering and Hydraulic Structures, Tbilisi
72. Dvorzhnyak, N. A. Director, the "Lengidrosta" Design Office, Leningrad
73. Faiko, L. I. M. Sc., Scientific Secretary, the Institute of Physico-Technical Problems of the North, the Siberian Division of the Academy of Sciences of the U.S.S.R., Yakutsk
74. Gindin, A. M. Deputy Head of Department, the State Committee of the Council of Ministers of the U.S.S.R. for Science and Engineering, Moscow
75. Ginzburg, B. M. D. Sc., Head of Department, the Hydrometeorological Research Center of the U.S.S.R., Moscow

76. Gotlib, Ya. L. M. Sc., Chief Hydrologist, the S. Ya. Zhuk All-Union Design and Research "Hydroproject", Moscow
77. Grigoryev, Yu. A. Director, the S. Ya. Zhuk All-Union Design and Research Institute "Hydroproject", Leningrad Branch, Leningrad
78. Gusev, A. V. M. Sc., Senior Research Worker, the Arctic and Antarctic Research Institute, Leningrad
79. Gutkin, R. A. Chief Design Engineer, the "Lengidrostal" Design Office, Leningrad
80. Ivanov, L. V. M. Sc., Head of Laboratory, the "Lenmornii-project" Institute, Leningrad
81. Ivanov, N. P. Chief Engineer, the Volgo-Baltic Canal Authority, Leningrad
82. Ivanov, N. S. D. Sc., Director, the Institute of Physico-Technical Problems of the North, the Siberian Division of the Academy of Sciences of the U.S.S.R., Yakutsk
83. Khrapatyi, N. G. M. Sc., Head of Chair, the Far Eastern Polytechnical Institute, Vladivostok
84. Kopaigorodsky, E. M. M. Sc., Head of Laboratory, the Moscow Institute of Building Engineering, Moscow
85. Koren'kov, V. A. M. Sc., Senior Research Worker, the B. E. Vedeneev All-Union Research Institute of Hydraulic Engineering, Leningrad
86. Korzhavin, K. N. D. Sc., Head of Chair, the Novosibirsk Institute of Railway Transport Engineers, Novosibirsk
87. Kudoyarov, L. I. M. Sc., Chief Engineer of the Central Board, the U.S.S.R. Ministry of Power and Electrification, Moscow

88. Kuperman, V. L. M. Sc., Chief Engineer of the Central Board, the U.S.S.R. Ministry of Power and Electrification, Moscow
89. Kuz'min, I. A. M. Sc., Chief Expert, the S. Ya. Zhuk All-Union Design and Research Institute "Hydroproject", Moscow
90. Marusenko, Ya. I. M. Sc., Associate Professor, the Ukrainian Institute of Water Economy Engineers, Rovno
91. Matkov, A. B. Chief Hydrologist, the S. Ya. Zhuk Design and Research Institute "Hydroproject", the Central Asian Branch, Tashkent
92. Mamadzhanov, D. R. Senior Research Worker, Tajik Research Department of Power Engineering, Dushanbe
93. Melkumyan, T. A. M. Sc., Senior Research Worker, the Georgian Research Institute of Hydraulic Engineering and Reclamation, Tbilisi
94. Mikhailov, A. V. D. Sc., Prof., Head of Chair, the Moscow Institute of Building Engineering, Moscow
95. Morosov, M. L. Head of Research Group, the S. Ya. Zhuk All-Union Design and Research Institute "Hydroproject", Leningrad Branch, Leningrad
96. Morozov, G. A. M. Sc., Director, the Siberian Research Institute of Hydraulic Engineering and Reclamation, Krasnoyarsk
97. Nazarov, Ts. A. M. Sc., Senior Research Worker, the Kazakh Research Institute of Water Economy, the Tselinograd Branch, Tselinograd
98. Nezhikhovsky, R. E. M. Sc., Senior Research Worker, the State Hydrological Institute, Leningrad
M. Sc., Associate Professor, the Gorki

99. Panfilov, D. F. M. Sc., Associate Professor, the Gorki Institute of Building Engineering named after V. P. Chkalov, Gorki
100. Panov, V. V. M. Sc., Head of Laboratory the Arctic and Antarctic Research Institute, Leningrad
101. Pekhovich, A. I. M. Sc., Senior Research Worker, the B. E. Vedeneev All-Union Research Institute of Hydraulic Engineering, Leningrad
102. Piotrovich, V. V. D. Sc., Professor, the Hydrometeorological Research Center of the U.S.S.R., Moscow
103. Popov, E. G. D. Sc., Professor, Deputy Director, the Hydrometeorological Research Center of the U.S.S.R., Moscow
104. Popov, L. I. Chief Expert, the State Committee of the Council of Ministers of the U.S.S.R. for Science and Engineering, Moscow
105. Popov, Yu. A. M. Sc., Senior Research Worker, the Siberian Central Research Institute of Railway Construction, Novosibirsk
106. Potapov, V. M. M. Sc., Head of Chair, the Moscow Institute of Water Economy Engineers, Moscow
107. Proskuryakov, B.V. D. Sc., Professor, the Leningrad Hydrometeorological Institute, Leningrad
108. Ptukhin, F. I. M. Sc., Associate Professor, the Novosibirsk Institute of Railway Transport Engineers, Novosibirsk
109. Rool, E. I. M. Sc., Deputy Chief Engineer, the S.Ya.Zhuk All-Union Design and Research Institute "Hydroproject", Moscow
110. Rosanov, N. S. D. Sc., Professor, Deputy Director, the B. E. Vedeneev All-Union Research Institute of Hydraulic Engineering, Leningrad

111. Rossinsky, K. I. M. Sc., Head of Department, the Institute of Water Problems, the Academy of Sciences of the U.S.S.R., Moscow
112. Rozhkov, N. P. Deputy Head of Department, the S. Ya. Zhuk All-Union Design and Research Institute "Hydroproject", Moscow
113. Sapir, I. L. Chief Engineer, the S. Ya. Zhuk All-Union Design and Research Institute "Hydroproject", Moscow
114. Savelyev, B. A. D. Sc., Prof., the Moscow State University named after M. V. Lomonosov, Moscow
115. Semenov, V. M. Head of Department, the S. Ya. Zhuk All-Union Design and Research Institute "Hydroproject", Moscow
116. Shatalina, I. N. M. Sc., Junior Research Worker, the B. E. Vedenev All-Union Research Institute of Hydraulic Engineering, Leningrad
117. Shtern, E. P. M. Sc., Head of Hydraulic Structures Service, the "Lenenergo" Leningrad
118. Simakov, G. V. M. Sc., Head of Chair, the Leningrad Polytechnical Institute, Leningrad
119. Sinotin, V. I. Vice-Chairman of the Organizing Committee, M. Sc., Head, the River and Reservoir Winter Regime Laboratory, the B. E. Vedenev All-Union Research Institute of Hydraulic Engineering, Leningrad
120. Sinyavskaya, V. M. Director, the S. Ya. Zhuk Design and Research Institute "Hydroproject", the Volgograd Branch, Volgograd
121. Skladnev, M. F. Chairman of the Organizing Committee of the 2nd Ice Symposium, M. Sc., Honoured Scientist, Director, the B. E. Vedenev All-Union Research Institute of Hydraulic Engineering, Leningrad

122. Smagin, I. F. Head of Department, the "Gipromorneft" Institute, Baku
123. Sokol'nikov, N. M. Head of Section, the S. Ya. Zhuk All-Union Research and Design Institute "Hydroproject", Leningrad Branch, Leningrad
124. Sokolov, A. A. D. Sc., Professor, Director, the State Hydrological Institute, Leningrad
125. Sokolov, I. N. M. Sc., Senior Research Worker, the B. E. Vedenev All-Union Research Institute of Hydraulic Engineering, Leningrad
126. Stolyarov, A. V. Head of Department, the U.S.S.R. Ministry of Power and Electrification, Moscow
127. Terentyev, L. I. Head of Department, the S. Ya. Zhuk All-Union Design and Research Institute "Hydroproject", Moscow
128. Topchiashvili, M. I. Head of Laboratory, the Georgian Research Institute of Power Engineering and Hydraulic Structures, Tbilisi
129. Treushnikov, Yu. V. M. Sc., Chief Engineer of the Board, the R.S.F.S.R. Ministry of Inland Water Transport, Moscow
130. Tsykin, E. N. M. Sc., Head of Laboratory, the Institute of Geography, the Academy of Sciences of the U.S.S.R., Moscow
131. Vasiliev, O. F. Corresponding Member of the Academy of Sciences of the U.S.S.R., Head of Department, the Institute of Hydrodynamics, the Siberian Division of the Academy of Sciences of the U.S.S.R., Novosibirsk
132. Vel'ner, Kh. A. D. Sc., Prof., the Tallin Polytechnical Institute, Tallin
133. Voitkovsky, K. F. D. Sc., Prof., the Moscow State University named after M. V. Lomonosov, Moscow

134. Zakharov, V. P. Academician, the Kazakh Research Institute
of Power Engineering, Alma-Ata
135. Zarubaev, N. V. D. Sc., Prof., the Leningrad Polytechnical
Institute, Leningrad
136. Zhidkikh, V. M. M. Sc., Senior Research Worker, the
B. E. Vedeneev All-Union Research
Institute of Hydraulic Engineering, Leningrad

X: Participant of the Study Tour, September 30 - October 8, 1972.

M i n u t e s
of the Joint Meeting of the LAHR Technical Committee
on Ice Problems and the Soviet Organizing Committee
held on 25 September 1972

Persons present: B. Michel (Canada), A. Assur (U.S.A.),
T. Carstens (U.S.A.), M. Kuuskoski (Finland), S. Freysteinnsson (Iceland),
M. Skladnev (U.S.S.R.), K. Korzhavin (U.S.S.R.), V. Balanin (U.S.S.R.),
V. Sinotin (U.S.S.R.), S. Aleinikov (U.S.S.R.)

Doctor B. Michel opens the meeting and informs the Committee that all the members of the LAHR Technical Committee on Ice Problems who were able to come to the meeting are present. Messrs H. Oudshoorn and Kivisild (Canada) and Yamaoka (Japan) wrote that they were unable to attend the meeting. President B. Michel declares the meeting open.

Item 1 on the agenda

Doctor B. Michel, Chairman, says that a temporary secretary should be nominated due to Mr. H. Oudshoorn's absence. The Chairman suggested that Mr. V. Balanin act as temporary secretary. The suggestion is adopted.

Item 2 on the agenda

Doctor B. Michel, Chairman, moves to listen to the report of Mr. M. Skladnev, Chairman of the Organizing Committee of the 2nd Ice Symposium and gives him the floor.

Mr. M. Skladnev informs the meeting that the Organizing Committee started its activities immediately after the offer of the U.S.S.R. of calling the 2nd Ice Symposium in Leningrad had been approved of in Reykjavik (Iceland). More than 170 participants take part in the Symposium, 60 foreign scientists among them. 47 papers are published in the Proceedings, including 29 from abroad. 4 lectures will be delivered at the Symposium by Messrs B. Michel, A. Assur, T. Carstens, and K. Korzhavin. After the Symposium volume II of the Proceedings will be issued containing lectures and discussions. The Symposium program includes inspection tours of ice laboratories in Leningrad, as well as the Study Tour to Novosibirsk, Irkutsk and Bratsk, where the participants will visit the Academic

township and two hydroelectric plants. In addition, social events are envisaged and a special program for ladies is arranged. The Chairman emphasizes the great assistance rendered by Doctor B. Michel in the preparatory work and expresses his gratitude to him.

Doctor B. Michel, Chairman, touches upon the activities of the Organizing Committee headed by Mr. M. Skladnev and suggests to approve the program of the Symposium.

The program is approved.

Item 3 on the agenda

Doctor Michel states that the period of office of five members of the Technical Committee on Ice Problems has expired: Prof. I. Yamaoka, Dr. H. Oudshoorn, T. Carstens, K. Korzhavin, H. Kivisild. It is necessary to form a committee for nominating new members. Mr. B. Proskuryakov (U.S.S.R.) was named Chairman of the Nomination Committee.

Doctor Assur (U.S.A.) and Doctor Kuuskoski (Finland) propose J. Kennedy and Dr. Palosuo as members of the Committee.

The following members of the Nomination Committee were approved: Dr. B. Proskuryakov (Chairman), Dr. J. Kennedy, Dr. Palosuo.

Item 4 on the agenda

Dr. B. Michel, Chairman, informs the meeting that three suggestions have been received as to the place of holding the next Symposium: from the Hungarian National Committee offering to arrange a Symposium on River Hydraulics and River Ice in Budapest in January, 1974; from the U.S. Army Corps of Engineers Laboratory offering to organize a Symposium on the problems concerning river and lake ice and extending the navigable season in Hanover; from the Alaska University suggesting that the next Symposium be held in Fairbanks in August, 1974, its basic problems being sea ice and coastal engineering. After a discussion Mr. Michel moves that the third Ice Symposium be organized in 1975, that the sessions are to be begun in Hanover (U.S.A.) where problems of river and lake ice and prolongation of the navigation period are to be discussed, and the second part of the Symposium is to take place in Fairbanks (Alaska, U.S.A.) where marine ice and coastal engineering problems are to be considered.

A decision is adopted to take an active part in the Symposium to be convened under the joint auspices of the IAHR Hungarian National

Committee and the Hungarian Section of the IANIG. An additional meeting of the Technical Committee on Ice Problems is scheduled for 10.30 a.m. on Wednesday September 27, 1972 with the aim in view to refine the program of the Symposium because of the absence of Dr. Ö. Starosolszky at the present meeting.

Item 5 on the agenda

Dr. Michel, Chairman, suggests to adopt the following list of Chairmen and Secretaries for the Symposium Sessions:

- 26.09.72 - Morning Session: Chairman - Dr. Assur
Secretary - Mr. K. Zvorykin
- 26.09.72 - Afternoon Session: Chairman - Dr. M. Kuuskoski
Secretary - Mr. K. Zvorykin
- 27.09.72 - Morning Session: Chairman - Dr. T. Carstens
Secretary - Mr. Yu. Dolgoplov
- 27.09.72 - Afternoon Session: Chairman - Dr. S. Freysteinson
Secretary - Mr. Yu. Dolgoplov
- 28.09.72 - Morning Session: Chairman - Dr. K. Korzhavin
Secretary - Mr. V. Koren'kov
- 28.09.72 - Afternoon Session: Chairman - Mr. V. Balanin
Secretary - Mr. V. Koren'kov

The above list of Chairmen and Secretaries has been adopted.

Item 6 on the agenda

Chairman B. Michel speaks of the development of ice terminology in English, French and Russian and suggests that Mr. V. Balanin make a report on the subject of the Symposium.

The proposition has been approved.

M i n u t e s
of the Meeting of the IAHR Technical Committee
on Ice Problems
held on 27 September, 1972

Persons present: B. Michel (Canada), A. Assur (U.S.A.), T. Carstens (U.S.A.), K. Korzhavin (U.S.S.R.), M. Kuuskoski (Finland), S. Freysteinnsson (Iceland), M. Skladnev (U.S.S.R.), V. Balanin (U.S.S.R.), K. Zvorykin (U.S.S.R.), O. Vasiliev (U.S.S.R.) J. Kennedy (U.S.A.), Ö. Štarošolszky (Hungary).

Item 1 on the agenda

Dr. O. Štarošolszky informs the meeting of the suggestion of the IAHR Hungarian National Committee to convene an International Symposium on river hydraulics, ice, and inland navigation in Budapest in January, 1974. The Symposium will be organized under the auspices of the IAHR Technical Committees on Ice and Fluvial Hydraulics. The Hungarian National Section of the IANAC will also take part in preparations for the Symposium.

Dr. B. Michel, Chairman, expresses his thanks to Dr. Ö. Štarošolszky for the invitation on behalf of the Hungarian National Committee and proposes to participate in the Symposium. Then he suggests that the scope of the problems on the agenda be limited to hydraulic and ice phenomena associated with inland navigation.

Dr. O. Vasiliev emphasizes the necessity of considering ice problems related to navigation when designing not only low- and medium-head hydro plants, but also high-head hydro plants.

Dr. B. Michel, Chairman, moves to adopt the following decision:

To approve the initiative of the IAHR Hungarian National Committee as to arranging a joint symposium in the field of fluvial hydraulics, ice and navigation; to take part in the Symposium; to recommend the Organizing Committee when formulating the final agenda to limit to hydraulic and ice phenomena associated with navigation in unregulated rivers and in those regulated by low-, medium- and high-head plants.

The proposition is adopted.



Meeting of the LAHR Technical Committee on Ice Problems

M i n u t e s

of the Meeting of the Nomination Committee held
on 27 September 1972

Members of the Nomination Committee J. F. Kennedy (U.S.A.), E. Palosuo (Finland) and B. Proskuryakov (U.S.S.R.), Chairman, discussed the candidates proposed for the next term of the activity of the IAHR International Ice Committee.

The following candidates were unanimously recommended for adoption by the second IAHR International Ice Symposium:

A. Assur	(U.S.A.)
V. Balanin	(U.S.S.R.)
M. Kuuskoski	(Finland)
P. Larsen	(Sweden)
B. Michel	(Canada)
I. Sokolov	(U.S.S.R.)
T. Tabata	(Japan)
R. Frederking	(Canada)
S. Freysteinnsson	(Iceland)
O. Starosolszky	(Hungary)

At the closing meeting of the Symposium held on 28 September, 1972 all the persons mentioned above were unanimously elected members of the IAHR Committee on Ice Problems.

CLOSING REMARKS

by

B. Michel

President of the IAHR Committee on Ice Problems

As this Second International Symposium on Ice and its Action on Engineering Structures draws to a close, I wish to take this opportunity to express my sincere appreciation to the authors of the 50 papers that were presented and those who participated so actively in the discussions of the papers.

I cannot but be impressed by the tremendous accomplishment that have been made in the field of ice science since our first seminar on ice in Montreal in 1959. This Symposium shows that great depth has been attained in analysis of ice phenomena, that scientific methods are thoroughly used in all ice research studies and are applied to the practical solution of engineering problems. To me it seems that we have attained a level of excellence that was attained by geotechnical sciences when the mechanics of material was applied with foundation engineering to form the applied science of soil mechanics. However our applied science of ice is even broader because it combines not only the solid and fluid mechanics aspects of the ice phenomena but also its thermal aspects. The triple base of our ice science makes it very difficult of approach to newcomers and layman and I have always admired the determination if not courage of our ice scientist in dealing with the intricate multidisciplinary studies that are required to solve any ice problem. Congratulations to the braves who have presented the results of difficult research work at this Symposium.

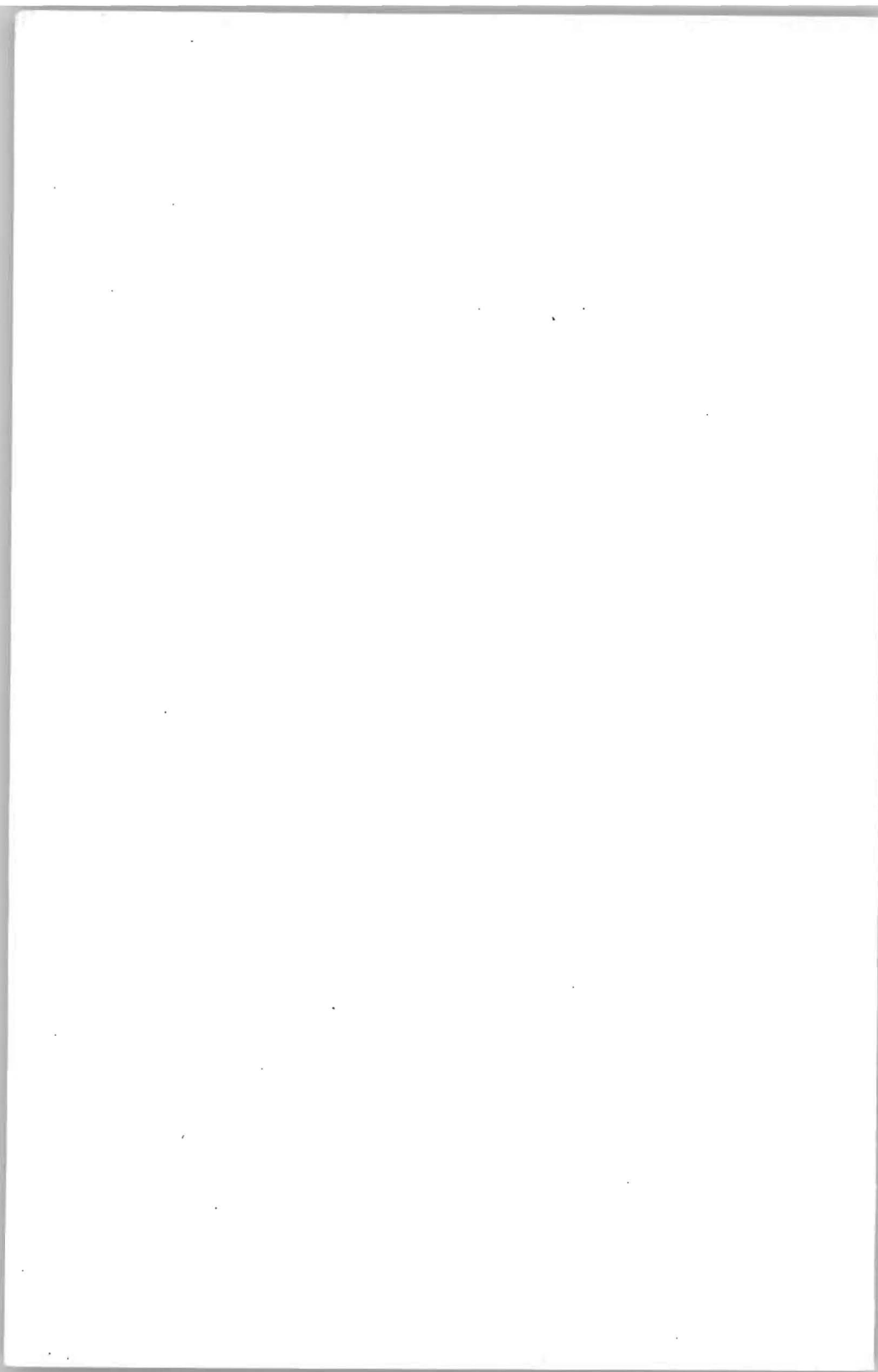
I extend my deepest appreciation to the members of the Organizing Committee who worked so diligently and faithfully on the organization of this Congress. Without their cooperation and willingness to accept numerous tasks, the Congress would not have been possible. I do not want to forget the organization of the Social Activities and in particular the unique representation that was given to us at the Russian Circus.

I also want to thank the Guest Lectures, the Chairman of each session that have made the Symposium so successful. I would not like to forget the operators of equipment and the translators who did such a magnificent job during the meetings.

We will surely remember forever this wonderful city of Leningrad and we owe our utmost gratitude to the B. E. Vedenev All-Union Research Institute, particularly its director Mr. M. Skladnev for hosting this Symposium.

In conclusion, let us have a good hand for all our fellow colleagues of the U.S.S.R.

LECTURES



STRUCTURE AND PHYSICO-MECHANICAL

PROPERTIES OF ICE

Torkild Carstens
Visiting Professor of
Ocean Engineering

Fairbanks,
Alaska
U.S.A.

SUMMARY

Because of its low melting point and large crystals, ice has provided scientists with a convenient material for the study of crystal structure. On the other hand, the anisotropy of this structure and the rheological effects of the low melting point have proved to be serious obstacles to the experimental determination of ice strength.

Our knowledge of the structure of broken-up ice fields in nature is largely descriptive and therefore insufficient for prediction of ice action.

The need for in situ stress observations to supplement laboratory strength data is recognized and a first generation of field instruments is now being developed.

RESUME

A cause du point de fusion bas et de la large taille des cristaux, la glace a donné aux savants un matériau adapté à l'étude de la structure cristalline. Par contre, l'anisotropie de cette structure et les effets rhéologiques du point de fusion bas sont des obstacles sérieux à la détermination expérimentale de la résistance de la glace.

Notre connaissance de la structure des champs de glace dans l'échelle géophysique est largement descriptive et ainsi insuffisante pour nous permettre de prédire l'action de la glace. La nécessité de mesurer la contrainte in situ pour suppléer aux données sur la résistance obtenues en laboratoire est reconnue, et une première génération d'instruments de travail est en train d'être développée.

1- INTRODUCTION

In the context implied by the title of the present paper, the term structure commonly refers to crystallographic structure, the geometric or morphologic properties of ice crystals. Much can be deduced about strength and stiffness of ice from a study of this type of small-scale or infrastructure. Good, recent references on the relations between crystal structure and mechanical properties are WEEKS and ASSUR 1969, LAVROV 1969, and MASER 1972.

The study of infrastructure has proved particularly useful for interpreting the results of laboratory tests on small samples of ice. However, for estimating forces on hydrotechnical structures, we must know the mechanical behavior of single ice floes, ensembles of ice floes, and pressured ice fields.

Figure 1 illustrates the scale of various ice phenomena.

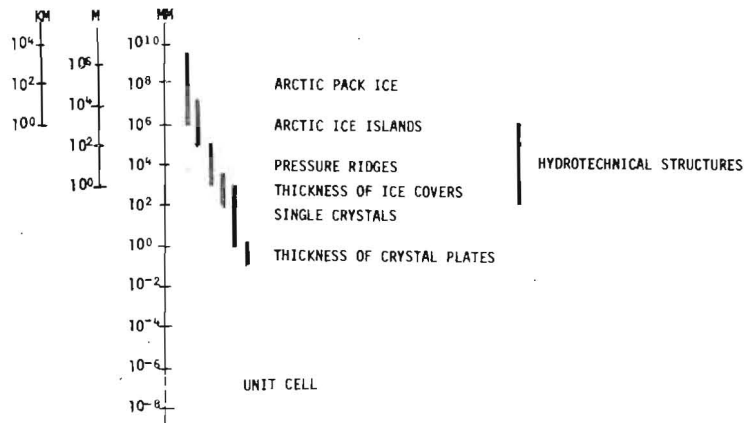


Figure 1. Length scale of ice phenomena.

The lower end of the scale, from the unit cell of order 1 \AA (10^{-10} m) through the individual monocrystals of order 10^{-3} to 1 m to annual ice covers of order 1 m , has been well studied. This brings us up to the scale of hydrotechnical structure shown to the right in Figure 1.

Overlapping in size with man-made structures, we find a set of natural ice structures such as pressure ridges and ice jams, which are major hazards to navigators and to river valley communities. These structures consist of ice covers that are fractured and piled up by horizontal forces due to wind and current.

In large bodies of water, such destruction of the ice cover causes extensive fields of hummocked ice. The formation and deformation of sea ice is a topic of intensive scientific research at present. There is also an upsurge of interest in the engineers' problem of predicting ice push at specific target areas.

A crucial question in this type of research is the length scale. For the simpler cases, the largest length scale entering any particular ice problem is limited by the topography of the immediate surroundings. On an open coast, as we move away from the target area, the local conditions have less influence on

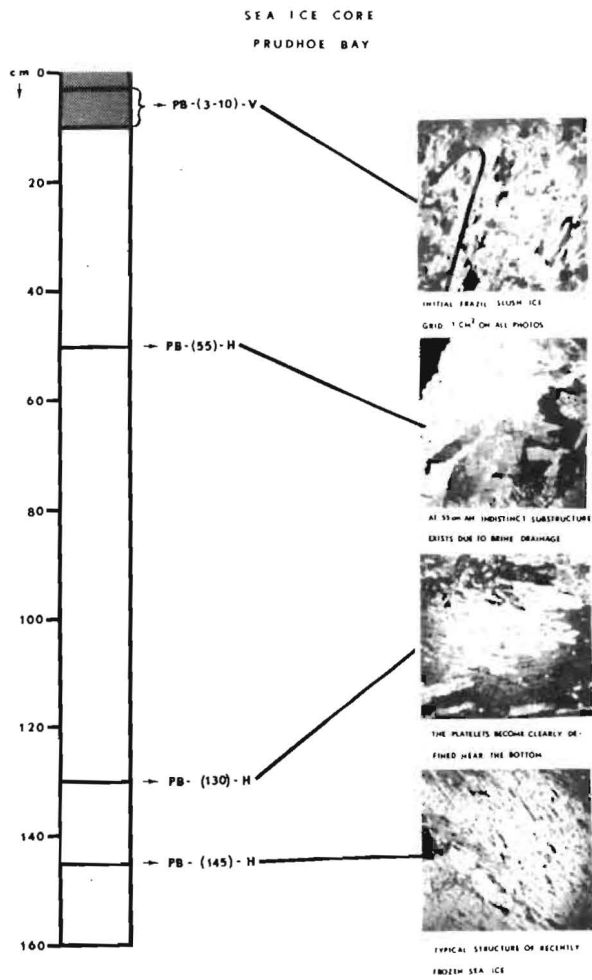


Figure 2. Sea ice structure (Seifert 1972)

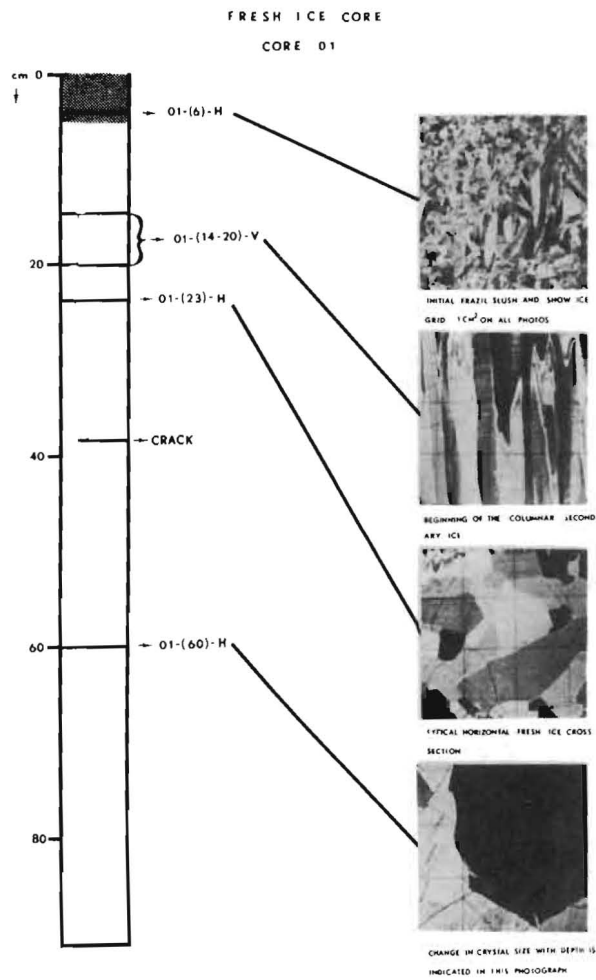


Figure 3. Fresh ice structure (Seifert 1972)

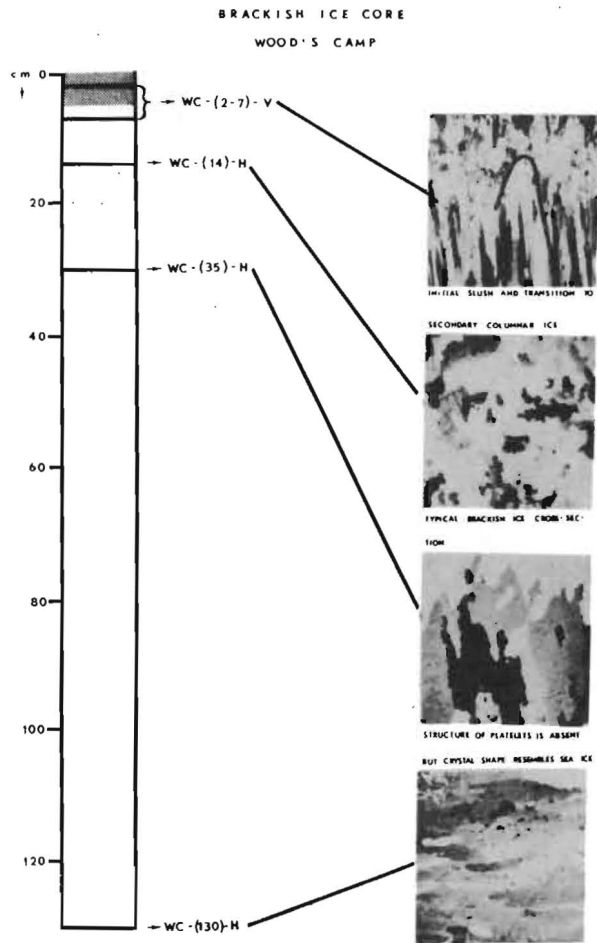


Figure 4. Brackish ice structure (Seifert 1972)

ii. Preferred Growth Direction. Growth rate is another anisotropic molecular property of ice. During freezing, the unit cells stack themselves up much more readily in the basal plane than along the c axis. On an absolutely calm water surface, the first skim of ice would therefore consist of plates with vertical c axis. Ripples and turbulence normally cause the initial plates or disks to freeze in tilted positions, setting the stage for a competition between favorably and unfavorably oriented crystals. Figure 6 shows this initial condition, and Figure 7 illustrates how the unfavorably oriented crystals are closed off from the melt.



Figure 6. Initial skim of ice disks on sea water (Weeks and Assur 1969).

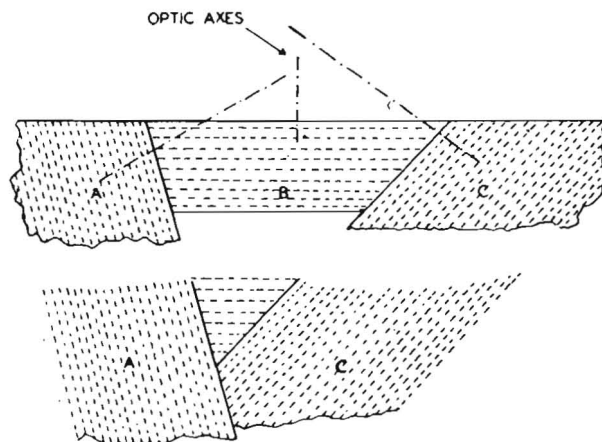


Figure 7. Preferred growth orientation (Pounder 1965).

The subsequent race is eventually won by crystals with horizontal c axis, while the other crystals are closed off from the melt.

iii. Stress Concentrators. Natural water always contains both dissolved minerals and gases and suspended solids and gas bubbles. All or most of such

impurities are expelled from the plates of pure ice during freezing and deposited in thin layers between the plates.

Sea ice, which is rich in minerals, develops a system of vertical brine channels between the plates. Frequently, a rather regular pattern of brine channels is seen, such as in Figure 2.

iv. Crack Nucleators. The failure strength of even the purest ice is several orders of magnitude less than the expected strength based on the number of atomic bonds in the unit cell. This discrepancy is explained by imperfections in the crystals. The most common types of imperfections are the edge dislocation and the screw dislocation shown in Figure 8.

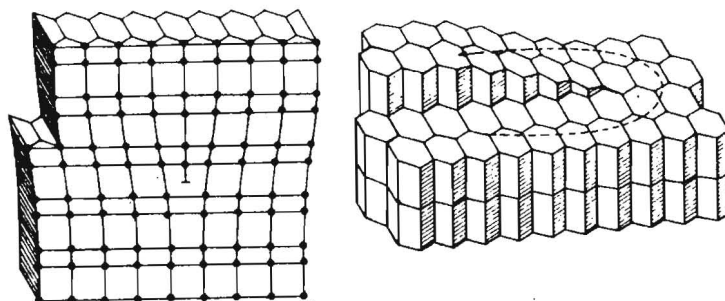


Figure 8. Schematic of dislocations (Carter 1971).

To cause slip in imperfect crystals, it is only necessary to break a small number of bonds compared with the number for a perfect crystal. Dislocations, therefore, propagate readily under, for instance, thermal stress.

According to KNIGHT 1967, dislocations tend to interact and propagate to positions that minimize the internal strain energy. Striations in monocrystals are due to a high density of dislocations that may well have been driven together by internal stresses. In any case, striations form weak zones and are potential crack nucleators.

B. ENVIRONMENTAL EFFECTS

The strength of ice also depends on the previous history of the ice, which is imposed by the environment. The *thermal history* of the ice determines, among other factors, the size of its crystals and, for sea ice, its porosity. In small samples of all types of ice, there is a marked dependence of strength on temperature.

The *stress history* is most evident when it has caused failure of the ice. However, the ice remembers not only those stress events that lead to failure, but probably its entire stress history.

A monocrystal subjected to stress with a component normal to the c axis will slip as indicated in Figure 9.

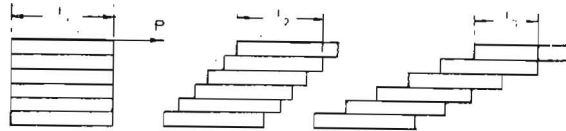


Figure 9. Work softening in monocrystal (Lavrov 1969).

Each loading will decrease the ultimate strength of the crystal by reducing its effective cross-sectional area.

In a monocrystal, the so-called basal glide of Figure 8 goes unchecked until failure under a sustained or repeated load, even if the load is gradually reduced. This type of behavior is known as *work softening*.

Work softening of an ice sheet is conceivable if shear stress acts along the basal planes. This action is illustrated in Figure 10 which explains the peculiar deformation observed under long-term or repeated point loading of a beam as a case of basal glide, resulting in a plastic hinge.

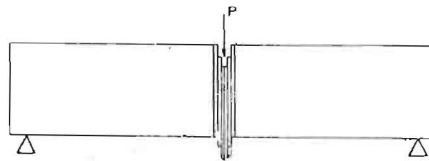


Figure 10. Plastic hinge in beam (Lavrov 1969).

3- POLYCRYSTALS AND ICE SHEETS

A. STRESS HISTORY

The type of deformation illustrated in Figure 10 could also, and more likely, result from slip along weak crystal boundaries, if these boundaries were lined up with the direction of the applied shear stress. This is the case for vertical loading of spring ice (candled ice). Before attempting lake crossings late in the season, a test of the shear strength is therefore advisable.

However, a more general type of response to repeated loading is *work hardening*. Each successive loading steepens the experimental stress-strain curve, indicating an increased stiffness or hardening of the ice.

The mechanism behind work stiffening is understood from pictures of deformed ice such as Figure 11.

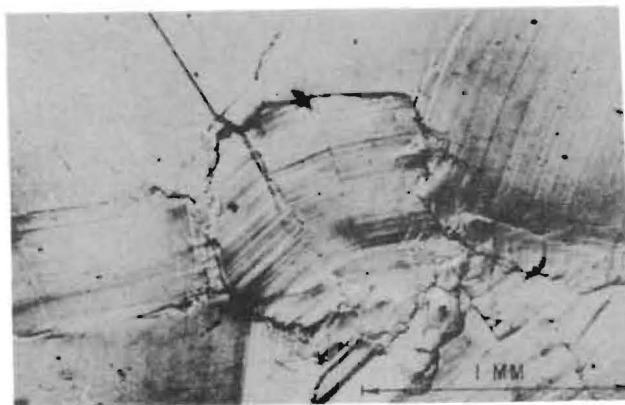


Figure 11. Deformation of polycrystal (Gold 1965).

Unlike the slip in monocrystals, basal glide within the individual crystals making up a polycrystal is checked at their boundaries. The neighboring crystals usually have a different c axis orientation and so offer firm resistance to further slip upon contact.

When applied to ice sheets, the arguments used above lead to the conclusions that vertical preloading is likely to reduce the ice stiffness and strength. Horizontal stress should stiffen the ice sheet and make it more brittle, without appreciably lowering the ultimate strength.

These conclusions seem justified for the predominating type of sea ice as well as lake ice, that is, with columnar crystals and horizontal c axis. Undoubtedly, they are too general and need additional qualifications. However, the point to be made here is that prestressing does affect both the infrastructure of the ice crystals and the structure of the ice fields.

Stress Sources. Many stress-producing processes work continually on the ice sheet, producing transient as well as locked-in stresses: Wind stress on its upper surface; current stress on its lower surface; thermal stresses due to expansion and contraction with changes in temperature; flexural stresses due to water waves, or barometric pressure waves, or loading by snow and water; collision stress due to contact with other ice fields, or for moving ice fields, fixed boundaries.

Pressure ridges are only the most spectacular result of ice stress, preserving a record of stress events exceeding the failure strength. Other familiar stress-induced features are thermal cracks, also representing an irreversible change of the structure of an ice sheet.

B. THERMAL HISTORY

I have listed thermal cracks as a permanent result of the stress history of an ice sheet. I could equally well say that thermal cracks are a lasting result of the thermal history of the ice. In fact, it is nearly impossible to separate completely the effects of stress history and thermal history on the structure of an ice field.

A fairly clear-cut case of a temperature effect on structure is the brine drainage in sea ice. The initial trapping of expelled salts depends on the rate of freezing and usually amounts to about one-third of the salt source or

1.0-1.2 percent. Within one or two weeks, about half of this amount has drained out under normal conditions in the Arctic. The remaining 0.5-0.6 percent are more or less permanently trapped until the ice thaws. Multi-year ice loses most of its salts in the first thawing season and has only a residual salinity of less than one part per thousand.

The effect of the salts on the infrastructure is seen in Figure 2. The freshly frozen sea ice (bottom of Figure 2) is full of brine channels. The upper layers have the same structure, but the porosity is less as most of the brine has drained away.

Figure 3 shows a similar pattern for brackish ice.

A more irregular system of brine drainage channels has also been observed by LAKE and LEWIS 1970, indicating an inclined brine transport towards major vertical drains as shown in Figure 12. This drainage pattern repeated itself every 12-15 cm and extended about 90 cm up from the interface.

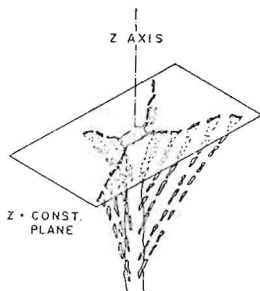


Figure 12. Coarse drainage structure in sea ice (Lake and Lewis 1970).

4- FRACTURED ICE COVERS

Fractured ice has been described by many ingenious models. When piled up in jams or pressure ridges, it has been compared with a granular material. When drifting in large fields, it has been compared with anything from an elastic plate to a viscous fluid (CAMPBELL 1968).

All these ideas represent, of course, functional rather than physical models of fractured ice.

A. PRESSURE RIDGES

The structure of pressure ridges has been studied for almost a century. WEEKS and KOVACS 1970, summing up the state of the art, could add only relatively few observations to what Russian investigators have reported a generation ago (ZUBOV 1943).

The documented knowledge of pressure ridges deals exclusively with morphological and isostatic conditions. No direct observations of the strength of pressure ridges or of hummocked ice fields have been made. As icebreaker operators are well aware of, pressure ridges have strength properties entirely different from flat ice covers. Inference from icebreaker experience is problematic, however.

B. ICE JAMS

The river equivalent of a pressure ridge in lakes or the sea is an ice jam. For floating (wet) jams held by natural arching between the river banks, or by man-made booms, a workable theory is developed by Canadians (MICHEL 1971) on the assumption that jammed ice behaves like a granular material.

The more hazardous grounded (dry) ice jams are at present unpredictable.

C. ICE HISTORY

Even more so than for flat ice covers, the structure of a ridged or hummocked ice field must depend on its thermal and stress histories. The consolidation of pressure ridges in the Arctic Ocean is a case in point. Over several years, melting and refreezing transform a high ridge of low strength into a lower ridge of higher strength. Leaving aside stress events causing renewed failure, the ridge eventually disappears, and the ice cover becomes flat again.

5- TESTING OF ICE

The objectives in testing materials for their physical and mechanical properties may be more or less general depending on the outlook of the researcher. Scientists, driven by pure curiosity, are likely to take an interest in any property they can observe. It is not necessary that the result of their testing can be used for anything; a mere mapping of nature is a legitimate end result in itself.

Engineers, on the other hand, are more selective in their research. For them, testing is a means to an end; they are mission-oriented and, therefore, in a sense narrow-minded.

Both groups of researchers face the same two fundamental problems: The first problem is to obtain a fair sample, and the second problem is to subject that fair sample to a fair test. However, the constraints put on the engineer in defining a fair sample and designing a fair test are more severe. In fact, the engineer frequently finds that he cannot apply a scientist's test results for reasons described below:

A. THE SAMPLE PROBLEM

The methods that have evolved for experimental determination of ice strength, are mostly methods developed for testing of other solids, especially construction materials. These methods have been rather faithfully copied and adapted to freezing temperatures.

i. Size. The test samples are cylinders, cubes, and beams of small size, often less than 10 cm. This size is adequate for materials consisting of small crystals so that the test specimen contains several hundred crystals. But the correct interpretation of the test results becomes problematic when the sample contains only a few crystals or if it is cut from one single crystal.

The same criticism must be made of in situ tests on small samples taken with conventional small bore ice corers.

The scaling problem created by the low ratio of crystal size to sample size is one which ice mechanics shares with rock mechanics. To ease the scaling by increasing the sample size appears more feasible for ice than for rocks because of the lower ice strength.

The drive towards larger and more representative test specimens led Russian investigators to the in situ "piano-key" test in the thirties. Cantilever beams are sawed out of an ice cover and loaded until flexural failure. The in

situ flexure test on cantilevered beams has been widely used ever since. Figure 13 shows the testing of the largest beams to date, $b \times h \times l = 32' \times 5' \times 45'$ cut in the Bering Sea ice with a trench digger (TAURIAINEN 1970).



Figure 13. Large cantilever beam testing (Tauriainen 1970).

ii. Structure. In situ tests, apart from lending themselves to larger samples, also offer the right ice. The tests are made not on artificial ice or ice from some other location than the one we are concerned with. Thus, the ice is frozen from the proper melt and not some other, subjected to an authentic ensemble of thermal and stress events, including the initial freeze-up. In short, we are testing a fair sample.

B. THE TEST PROBLEM

The set of properties we are trying to uncover in a test programme includes the failure strength when the samples are subjected to a variety of loadings: Compression, tension, flexure, shear. Of equal importance are, in most cases, the rather complex strain properties. While the modulus of elasticity and the Poisson ratio may adequately account for the response of ice to low loads at high load rates, some measure of the observed plastic flow is otherwise required.

i. Analysis. With a few exceptions such as a plane tension test, it is no easy task to design an experiment that will yield unambiguous answers. For instance, in a material as plastic as ice, a steep stress gradient is likely to be smoothed rather quickly. Any theoretical analysis which presumes strong stress gradients should, therefore, be looked at with suspicion.

ii. Indices. It is seldom possible to measure directly the desired quantity and often difficult to measure any other quantity which bears a known analytical relation to the former. We are then forced to work with a third category of observed quantities, a so-called index or indicator. A good index is easy to measure and correlates statistically with the sought after quantity. When estimating ice properties we mostly work with indices, such as temperature and salinity, which are indices of strength.

If we use a simplified theory when interpreting test results, the derived property, say flexural strength, is itself no more than an index. A good example is given by BUTKOVITCH 1958, who observed that test results on flexural and tensile strength are ranked consistently according to the method of testing.

$$\sigma_{rt} > \sigma_{fl} > \sigma_t > \sigma_{isc}$$

where the subscripts have the following meaning:

- rt* - ring tensile test
- fl* - flexural beam test
- t* - plane tension test
- isc* - in situ cantilever beam test

The ordering shows the expected decrease of strength with increasing sample size for polycrystals. One can also argue that flexural strength should not exceed tensile strength since a bending failure is triggered by a tension failure. Therefore, $\sigma_{fl} > \sigma_t$ is an erroneous result, and a number of reasons have been suggested to explain this anomaly (MASER 1972). They are all tied to either the method of testing or of analysis, and so the real flexural strength is still unknown, and σ_{fl} is merely an index.

C. MISSION-ORIENTED TESTS

The application of general small sample test strength to engineering design involves a problematic scale-up and an a priori choice of failure mechanism. A more direct approach is clearly desirable, and the most direct way is to build a test structure as similar to the proposed structure as one can afford, at the actual site.

Such a highly mission-oriented test programme was undertaken prior to the design of oil platforms in Cook Inlet, Alaska (PEYTON 1966). Figure 14 shows the test pile, which is subjected to a very special ice regime:



Figure 14. Test piles, Cook Inlet, Alaska (Peyton 1966).

Another well-conceived set of mission-oriented tests led KORZHAVIN 1971 to a design formula for ice forces on bridge piers. The basic tests were small-scale compression tests of 7 cm cubes, subjected to strain rates observed in river ice during breakup. Thus, by observing the failure mechanism and the loading rates in nature, the conditions for which ice strength was needed, were duplicated in a laboratory. The final scale-up of the test results is made by a reasonably sound use of elastic plate theory.

A third example of a very interesting test method is that of CROASDALE

1971, who described a "nutcracker" designed to trigger crushing failure in situ.

Natural Ice Stress. A recent development pioneered by Japanese scientists is the use of embedded sensors to monitor stress and strain in an ice field, by methods resembling those used in soil and rock mechanics. In the absence of a test structure, which is expensive, information on the response of shorefast ice to impact by drifting pack ice seems the next best way to predict ice forces on a marine structure.

By locating sensors close to the failing boundaries of the ice sheet, the effect of stress history on failure strength can be investigated.

Surveys of ice stress can be used to locate areas protected by shore and bottom topography from the most intense ice push.

Figure 15 shows the sensors used by a team from the University of Hokkaido

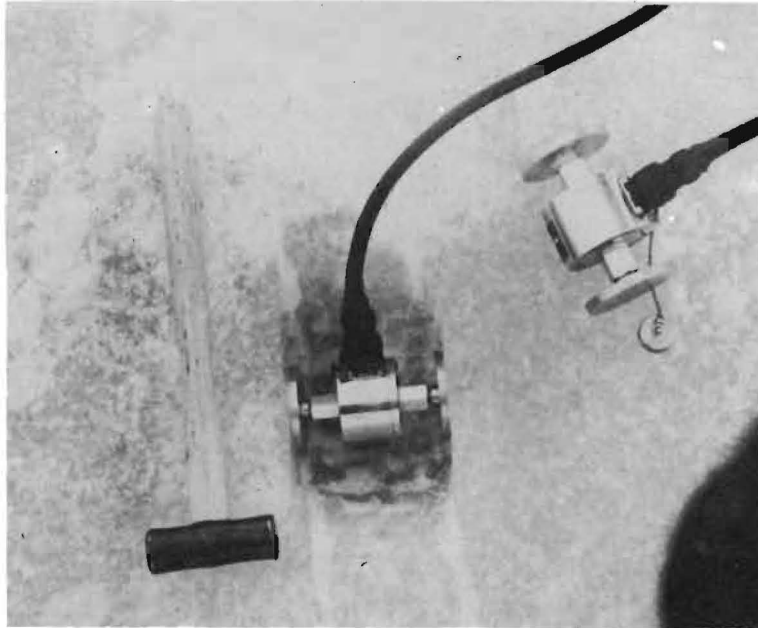


Figure 15. Stress sensors for in situ experiments.

Figure 16 shows a way of calibrating sensors by perturbing the natural stress field. An air bag is placed in a slot and inflated. The sensors, which have positions that permit the orientation of the principal stresses to be obtained, pick up the known stress perturbation (NELSON and TAURIAINEN 1972).



Figure 16. Calibration of embedded sensors.

6- CONCLUSIONS

Our knowledge of ice structure is much better on the molecular scale than on the geophysical scale.

Ice physicists have the advantage of working in close cooperation with metallurgists and others who concern themselves with freezing from impure melts. A fruitful exchange of ideas and research results has taken place between scientists interested in very analogous processes of crystal structure and strength for many different materials. Largely because of this fortunate circumstance, we have a good working knowledge of the structure of ice crystals.

The complex rheological properties of ice, with its large anisotropies, has made the mapping of ice strength an exasperating task. The dependence of ultimate strength on strain rate is still incompletely known for almost any type of stress. However, on a laboratory scale, encouraging progress is being made.

Those studying the larger natural ice structures such as drifting ice fields are in a less fortunate position than the laboratory physicists. The gathering of data is difficult, expensive and time-consuming, and no close analogies exist for the analysis.

Our understanding of these geophysical ice problems has therefore progressed slowly, so at present there is a quantum jump between what the molecular physicist and the geophysicist know about their respective ice structures.

The present advance of technology in the Arctic is hampered by the lack of knowledge of the properties of large-scale ice phenomena. The engineers, searching for rational design criteria, have recently moved out on the ice with new instruments and new ideas. This is encouraging, and we may anticipate efficient new test methods within a few years, provided the effort is continued.

However, a chief characteristic of dynamic ice phenomena, and indeed of all geophysical processes, is their extreme variability. Therefore, we must take into account not only large length scales and work over appropriate areas. Perhaps more important still, we must have patience to wait out long sampling periods to cover the large time scales that are also involved.

7- ACKNOWLEDGEMENT

This survey paper was written while the author was a visiting professor at the University of Alaska, Fairbanks. On that campus, ice is always a favored subject of discussion, and the author wishes to thank his Alaska colleagues, C. E. Behlke, C. S. Benson, P. R. Johnson, A. R. McKay, R. D. Nelson, T. E. Osterkamp, and E. F. Rice for sharing their experience with him.

8- REFERENCES

- BUTKOVICH, T.R. 1958. Recommended Standards for Small-Scale Ice Strength Tests. Trans. Eng. Inst. Canada, 2, p. 112-115.
- CAMPBELL, W.J. 1966. Sea Ice Dynamics; in Arctic Drifting Stations, ed. JE Sater, The Arctic Institute of North America, 1968.
- CROASDALE, K.R. 1970. The Nutcracker Ice Strength Tester and its Operation in the Beaufort Sea. IAHR 1st Ice Symposium, Reykjavik.
- GOLD, L.W. 1965. The Initial Creep of Columnar-Grained Ice. Can. Journ. Physics, 43, p. 1414-1422.
- KORZHAVIN, K.N. 1962. Action of Ice on Engineering Structures. (In Russian) Transl. Defense Documentation Center, Cameron Station, Alexandria, Virginia 1971.
- KNIGHT, CH.A. 1967. The Freezing of Supercooled Liquids. p. 108-111. D. van Nostrand Co. Inc.
- LAVROV, V.V. 1969. Deformation and Strength of Ice. (In Russian) Transl. Nat. Tech. Info. Serv., Springfield, Va. 22151, 1971.
- MASER, K.R. 1972. An Analysis of the Small-Scale Strength Testing of Ice. Ph.D. thesis, MIT Rep. No. MITSG 72-6.
- MICHEL, B. 1971. Winter Regime of Rivers and Lakes. CRREL Monograph 111-B1a, p. 90-99.
- NELSON, R.D. and TAURIAINEN, M. 1972. Natural Sea Ice Stress Measurements. Progress report, IAEE, University of Alaska.
- PEYTON, H.R. 1966. Sea Ice Strength. Geophys. Inst., University of Alaska, Rep. UAG R-182.
- SEIFERT, R.D. 1972. The Structure of Shorefast Ice off the North Slope of Alaska. M.S. thesis, University of Alaska.
- TAURIAINEN, M.J. 1970. Port Clarence Sea Ice Testing. The Northern Engineer, vol. 2, no. 1.
- WEEKS, W.F. and ASSUR, A. 1969. Fracture of Lake and Sea Ice. CRREL Res. Rep. 269.
- WEEKS, W.F. and KOVACS, A. 1970. On Pressure Ridges. CRREL
- ZUBOV, N.N. 1943. Arctic Ice. (In Russian) Transl. Nat. Tech. Info. Serv., Springfield, Va. 22151, 1948.

GENERAL RESEARCH RESULTS OBTAINED
IN THE U.S.S.R. ON ICE-THERMAL CONDITIONS
IN THE VICINITY OF HYDRAULIC STRUCTURES

K.N. Korzhavin, The Novosibirsk Institute of Novosibirsk
Prof. D. Sc. (Eng.) Railway Transport Engineers U.S.S.R.

I. A BRIEF REVIEW OF ICE-THERMAL CONDITIONS ON THE RIVERS
IN THE U.S.S.R.

The widely varying physiographical characteristics of the geographical zones to be encountered in this country engender pronounced differences in winter conditions along corresponding river reaches. In the southern regions of Turkmenia, for example, an ice cover forms only during exceptionally severe winters, while, as a general rule, only frazil is produced leading to frequent ice jam formation and sharp rises of the water stage.

Relatively tranquil (though prolonged spring and autumn ice runs and the formation of a stable ice cover are characteristic for the lower reaches of the Volga, the Don, the Dnieper, and other rivers of the European part of the country.

The ice regime of a number of large Siberian rivers possesses specific features of its own, viz.: due to temperature drops occurring simultaneously over large areas ice production develops at a great rate in autumn and is accompanied by ice jamming and repeated ice runs; low air temperatures and a long winter are conducive to the formation of a thick and strong ice cover which can exert a considerable pressure on hydraulic structures. The majority of Siberian rivers running north makes for severe spring ice-runs, with ice jams causing abrupt rises in water stages.

In the Amur River basin, where winters are severe and snowfalls insignificant, frazil ice formation proceeds at a great rate, the autumn ice-run is protracted, that in spring tranquil, the small amount of snow in the area precluding the occurrence of heavy spring floods.

The diversity of ice-thermal conditions is so great that ice-cover thicknesses range from 0.25 m (in the South of the European part of the U.S.S.R. and Central Asia) up to 2.0 m (in the North of the Asiatic part of the country). It takes more than a hundred days for the ice-run to be completed over the whole territory of the country.

II. BASIC EXPERIMENTAL FINDINGS ON THE ICE-THERMAL REGIME

The severity of the climate in the greater part of the U.S.S.R. necessitates systematic investigation into the ice-thermal conditions of both natural and regulated waterbodies. The main experimental results obtained lately with a view to promote the extensive development of hydropower, water resources and transport in this country will be treated here.

1. Change in ice-thermal conditions caused by a hydroelectric plant

Creation of storages is known to induce marked changes in the ice-thermal regime of a waterway. Recognition of these variations in the design, construction and operation of hydraulic structures results in a more accurate evaluation of the polynya dimensions upstream and downstream from the power plant, the determination of the probable ice discharges, the establishment of the effect of water temperature in deep storages on the thermal stress condition of concrete structures, the choice of an optimal elevation for water intakes, and the solution of other important engineering problems. Worthy of note are in this connection the investigations conducted by B. V. Proskuryakov, K. I. Rossinsky, A. G. Kolesnikov, V. V. Piotrovich, L. G. Shulyakovsky et al. who evolved calculation procedures that are in sufficiently good agreement with field observation data.

Research has been carried out into the thermal parameters of soils and the varying boundary conditions on the air-water interface.

Mention should be made of the interesting investigations by A.I. Pekhovich and V.M. Zhidkikh who worked out solutions to a great number of vital hydrothermal problems with reference to water storages and suggested some nomographs and charts which substantially simplify calculations.

Of great value are field observations on ice-thermal conditions in some water storages (viz. the Bratsk, the Novosibirsk, the Ust'Kamenogorsk, etc.) performed by V.V. Piotrovich, N.M. Sokol'nikov, V.M. Samochkin, S.N. Bulatov et al. in different regions of the country. Significant results were obtained in evaluating the ice regime of water storages. Ice thickness was found to differ only slightly as against that in unregulated situations, but the ice structure pattern was shown to be more regular. The ice cover of water storages is observed to fracture more readily due to solar radiation than that of rivers, and its strength to deteriorate sharply, which is favourable to detaining the ice in the reservoir. Investigations indicate that at upstream velocities of less than 0.4-0.5 m the ice does not accumulate in front of the outlets but decays in situ. In studying ice damming and ice jamming phenomena upstream from structures ice accumulations during the spring break-up were sometimes recorded not at the end of the backwater of the hydro-power plant, but rather at the end of the backwater during the ice-cover formation in autumn.

2. Evaluation of ice impact on structures

The necessity of damming rivers which are numbered among the largest on our planet, viz. the Ob', the Yenisei, the Angara, the Volga, etc. induced Soviet researchers to make very careful estimates of the ice impact on spillway and bridge piers, water intake structures and navigation facilities.

Numerous studies permitted to elucidate the physical aspect of the phenomena and resulted in evolving calculation techniques adequate under prototype conditions.

Coming into contact with the ice cover the vertical cutting edge of the pier apron penetrates into the ice sheet for about 0,1-0,5 m causing local crumpling and subsequent failure, with two or three concussion cracks forming to outline the so-called ice cantilevers, the latter break off at a distance equal to from 3 to 6 ice thicknesses. The width of the lead cut by the apron in the ice scarcely exceeds the width of the apron. The process is further complicated by fragmentation and splitting of ice causing ice pressure on the pier to vary with time. The phenomenon appears to have been described in the publications of foreign researchers as well.

The decay pattern of an ice floe is chiefly governed by its kinetic energy content, as well as by the shape, dimensions and material of the pier. With a sufficiently strong ice cover the width of the pier section subjected to ice pressure (due to fragmentation of ice in the contact zone) is not more than 0,5-0,6 of the maximum width of the pier. An inclined apron is more effective cutting the ice sheet from below and inducing failure through flexure or (less frequently) by shear, thus facilitating ice passage.

The solution to the problem of ice impact on the structure requires an insight into the mechanical and physical properties of ice during the ice-run. Comprehensive investigations by I.P. Butyagin, K.N. Korzhavin, F.I. Ptukhin, V.V. Lavrov, K.F. Voitkovski, I.S. Pestchanski, V.A. Koren'kov et al. permitted to establish that:

- 1) the ultimate compressive and bending strength of river ice is reduced from 1,5-3 times by the beginning of the break-up period;
- 2) owing to local crumpling ice pressure on the structure may be increased from 1,8 to 2 times;
- 3) the character of the deformation rate effect on the ultimate strength of ice depends on the absolute value of the deformation rate;
- 4) the ultimate strength both in flexure and compression is reduced inversely to the specimen's dimensions; the scale effect arising through greater probability of failure due to stress concentrations (at cavities and cracks) in specimens of large dimensions;
- 5) the significance of the pier configuration in plan was brought out by tests on river ice resistance to the penetration of variously

shaped plates. The effect is described by the shape coefficient, m .

Analysis of possible schemes of interaction between the pier and the ice points to the fact that a vertical pier is subjected to peak ice pressures when it cuts a large ice sheet, or when an ice floe stops at the structure after a local failure at the contact, while on a pier featuring an inclined apron maximum pressures develop with the ice floe falling in flexure.

Evaluation of the effect produced by an inclined apron reveals that it reduces the magnitude of the horizontal pressure component and facilitates fragmentation of the ice sheet. Hence selection of the pier configuration depends on the spacing of spillway or bridge spans. With short spans the choice of piers with an inclined apron seems advisable after a careful economic estimate. The vastness of the territory of the U.S.S.R. makes it expedient that the country be divided into six zones with different climatic coefficients, A ranging from 0.75 to 2.25.

The ice strength values adopted in the design (with A equal to unity) are at crushing $R_1 = 45-75 \text{ ton/m}^2$ in flexure $R_2 = 0.5 R_1$

The calculation procedures recommended in this country for determining the horizontal component of the dynamic ice action on massive piers assume the following form:

a) when a large ice sheet is broken by a vertical pier

$$H_1 = A m R_1 B h \quad (1)$$

b) when an ice floe of an area, Ω , moving at a velocity, V , stops at a vertical pier

$$H_2 = 0,43 v h \sqrt{A R_1 m \Omega \operatorname{tg} \alpha} \quad (2)$$

c) at a pier with an inclined apron

$$H_3 = A R_2 h^2 \operatorname{tg} \beta \quad (3),$$

where B is the maximum pier width; 2α is the apron taper; β is the angle of the apron; h is the calculated ice thickness.

The minimum pressure found from formulae (1) and (2) is accepted as the design pressure for vertical piers. The relationships

obtained are verified by means of field observations on peak dynamic ice pressures. Actual ice pressures were measured by F.I. Bydin, Gamayunov, K.N. Korzhavin, V.A. Koren'kov by means of special instrumentation; installation of dynamometers specially modified for the purpose was suggested by Davidenkov, whereas B.V. Zylev proposed to use the interaction between the icebreaker and the ice sheet as an analogue of the dynamic ice pressure against a structure. Application of dynamometer panels at the Krasnoyarsk Hydropower Project seems to merit attention, as well as Korzhavin's suggestion to make use of the kinematic approach which permits to evaluate the interaction between a large ice sheet and the structure by the decrease in the ice sheet velocity after impact against the pier. The method was implemented upwards of 50 times at the structures of the Novosibirsk, the Bratsk and the Krasnoyarsk hydroelectric plants as well as on a number of major bridges in Siberia.

At the Reykjavik Symposium a paper was presented by Soviet researchers on the relationship of structure deformation and the design value of ice pressure. Without going into the problem in detail we shall only state that the technique described in the paper permits to define the range wherein it is expedient to make allowance for structure deformations.

3. Evaluation of static ice action on structures

Static ice action on structures owing to thermal expansion of the ice cover has been and remains the subject of research in the U.S.S.R.

The most comprehensive studies were carried out by B.V. Proskuryakov whose original approach to the problem permitted to get an adequate description of the process. Proceeding from the basic assumption that pressures developed due to the thermal expansion of ice exceed its yield point, he regards ice within the range of plastic deformations as a viscous fluid. The approach was further refined by N.N. Petrunichev, V.P. Berdennikov and A.I. Pekhovich to make it suitable for introduction into engineering practice, and was incorporated into Building Codes and Standards acting in this country.

Recently A.B. Ivchenko and A.E. Yakunin who treat ice as an elasto-viscous body performed experiments in flumes, at the Novosibirsk water storage, and at Lake Baikal and received some noteworthy results. A considerable amount of work is being done on investigating ice pressure on the gates of a power plant dam on the Volga, and another in Siberia, which can be expected to throw some light on this unexplored problem and to evaluate the effectiveness of corrective measures against static ice action on dam gates. The problem being rather abstruse, prototype observations should be undertaken on a more extensive scale.

4. Ice passage through structures and bridges, both under construction and in service

Erection of hydroelectric plants on large rivers under severe climatic conditions in the U.S.S.R. focused the attention of research engineers on this problem. During the construction of power plants observations were conducted permitting to identify the key factors affecting the process, viz. the size and the velocity of drifting ice floes, the dimensions of spans used for ice passage, water level differences, the strength and thickness of the ice cover, the type of structures, etc.

Long-term studies by N.M. Sokol'nikov, O.F. Vasiliev, F.I. Bydin, B.V. Pospelov, S.S. Agalakov, Ya.L. Gottlieb, V.A. Koren'kov, I.N. Sokolov, D.F. Panfilov, K.N. Korzhavin, V.K. Troinin et al. led to evolving practical recommendations based on experience and theoretical considerations, on ice passage through river channel contractions, unfinished dam blocks, bottom outlets, temporary tunnels and bridge spans.

Assuming that no ice floe accumulation will take place at the structure provided the kinetic energy of fragmented ice masses in the main flow is sufficient for breaking the ice sheet adjacent to the piers, relationships were derived for determining optimum span dimensions. For instance, the minimum bridge span ensuring trouble-free ice passage may be found from the formula

$$l > \frac{0.7 KB}{\rho V^2} \quad (4)$$

where K is specific ice pressure, ton/m^2 ; B is width of pier, m ; V_0 is surface velocity of flow, m/sec ; p is ice concentration. Similar relationships taking into account the shape of the calculated drop-down curve were obtained for ice passage through unfinished dam blocks and through spillway outlets.

5. Hydraulics of flow under the ice cover

Several procedures generally based on applying the Chezy formula in different parts of the river cross-section are now in use for hydraulic calculations of flow under the ice cover. However, because of scarcity of data available on the regularities in the flow distribution under the ice cover, certain assumptions have to be made which may introduce errors into the calculation results. By extending to both parts of the velocity diagram the law of velocity distribution in open channel flow obtained by A.K. Nikitin

$$\frac{V}{V_*} = 6.45 \lg \frac{y}{\delta} + 5.6 + 2.8 \frac{y}{4/\delta} \quad (5)$$

(here δ is the bottom layer thickness) V.I. Sinotin deduced a relationship

$$\frac{h_1}{H} = 0.6 \lg \frac{n_1}{n_2} + 0.5 \quad (6)$$

which permits to plot a velocity curve and estimate the reduced roughness coefficient from the expression

$$n_{ult} = \frac{n_1}{1.67 [(0.6 \lg \alpha + 0.5)^{1.75} + \alpha (0.5 - 0.6 \lg \alpha)^{1.75}]} \quad (7)$$

where n_1 and n_2 are the roughness coefficients of the channel bed and the under surface of the ice, respectively; $\alpha = \frac{n_1}{n_2}$; H is the depth of the flow; h_1 is the distance of V_{max} from bottom.

The assumption of Academician N.N. Pavlovsky that the distribution of flow velocities under the ice cover is similar to that for

peak flow discharge conditions proved to be valid. Investigations into the problem are being continued.

6. Ice as a construction material

Application of ice and snow as construction materials is far from being a novelty. Considerable experience has been accumulated in this field in our country on a number of major engineering structures. A 40 m-high dam of frozen pulp, mooring facilities constructed of ice on the Yenisei River (the volume of the structure is in excess of 11 000 m³), which were completely inundated during the flood, and some other structures may be cited as examples.

Studies by N.A. Tsytoich, K.F. Voitkovsky, V.V. Balanin, G.A. Pchelkin, A.A. Bubyri' et al. demonstrated the feasibility of construction and long-term operation of structures built of ice. A stability design theory for ice structures permitting to evaluate the rate and magnitude of deformations inherent in a given time interval was elaborated by K.F. Voitkovsky. An approximate design method was also worked out using solutions to problems of the elasticity theory.

A procedure based on the mechanics of frozen bodies was evolved by N.A. Tsytoich for the approximate evaluation of the strength of the ice core of a rockfill dam.

Introduction of reinforcement into an ice structure was proposed as a means of enhancing its strength and prolonging its life. The thermal regime of and construction techniques for ice structures were studied by V.I. Sinotin, Yu.E. Gavrish et al. There is no doubt whatever that structures built of ice should and will be more extensively utilized in the future.

7. Combatting of ice troubles

Ice jams and ice dams which occur on the majority of rivers in this country are a serious hazard causing floods and endangering the safety of hydraulic structures. Ice dam formation was studied on a number of large rivers, viz. the Yenisei, the Ob', the Volga, the Dniester, the North Dvina, the Tom', the Lena, etc. Comprehensive studies on

ice jams were executed on the Angara, and on some Caucasian and Central Asian rivers as well (A.M. Estlfeev, V.V. Balanin, L.G. Shulyakovsky, Yu.A. Popov, V.I. Sinotin, V.N. Karnovich, V.P. Berdennikov, R.I. Stcherbakova, V.P. Zakharov, I.Ya. Liser et al.).

Research is under way on problems of forecasting the period when and the site where ice dams and jams are liable to form, the rise in the water stage, etc. Several research programs have been carried out lately to elaborate techniques for promoting more efficient ice passage.

Recently recommendations on corrective and preventive measures to alleviate ice troubles were developed at the VNIIG (Leningrad). The principles underlying the measures for eliminating ice-jam and ice dam formation and field observation procedures are detailed, the effectiveness is compared of techniques for reducing ice strength, such as, blackening of the snow-ice cover, chemical and mechanical methods, aviation and blasting, the latter being widely used.

Hydraulic and thermal control of storages is considered with the aim in view to combat ice jam and ice dam formation. The corrective measures recommended in particular are: utilization of the discharge from tributaries, and of warm water releases from power plants, raising to the surface of warmer water from the lower layers (research by V.V. Balanin, B.S. Borodkin, G.I. Melkonyan), with instructions on their application adduced.

8. Development of field observation techniques and instrumentation

In the U.S.S.R. extensive studies of the ice-thermal regime of water storages and waterways both under natural and regulated conditions are performed at present.

Methods for the calculation of the thermal regime of water storages were developed (by A.I. Pekhovich, B.V. Proskuryakov, V.M. Zhidkikh, K.I. Rossinski, S.N. Kritski, M.F. Menkel', A.G. Kolesnikov, V.V. Piotrovich, N.M. Sokol'nikov, S.N. Bulatov, V.V. Balanin et al.) including classification of storages, choice of the initial temperature distribution, thermal conditions at the surface and the bottom of a

waterbody, and procedures for finding solutions to basic hydrothermal problems.

Proceedures are elaborated for the evaluation of mechanical and physical properties of the natural ice cover by I.P. Butyagin, V.K. Morgunov, V.V. Bogorodski, V.A. Koren'kov, V.M. Samochkin, F.I. Ptukhin, V.P. Berdennikov, et al. Observations are conducted on the dynamics of ice conditions making use of aviation and photography; hydraulic integrators and electronic computers being utilized for treating observation data and forecasting ice-thermal mechanisms. In conclusion, I would like to draw attention to the work conducted with the object of extending the navigable season, and controlling ice troubles during winter operation of the hydraulic machinery of power plants.

ICE MANAGEMENT IN HYDRAULIC DESIGN
RECENT CANADIAN EXPERIENCE

Bernard Michel, Dr. Eng.
Professor of Ice
Mechanics

Université Laval

Quebec, Canada

SYNOPSIS

Ice has been considered in the past to be a particular problem to be dealt with by hydraulic engineers, once all the other aspects of an engineering design were covered. It was seen as a secondary factor that would require only small corrective measures. In the very last few years, there has been a few Canadian developments where ice has become the dominant factor and had to be taken into account right at the start of the feasibility studies. In many cases the way of dealing with ice has been termed the technique of ice management. We will describe briefly in this summary paper three recent examples of ice management in major Canadian projects.

RESUME

Dans le passé, les ingénieurs hydrauliciens ont toujours considéré la glace comme un problème particulier qui devait être résolu une fois que toutes les autres questions étaient traitées. C'était un facteur secondaire qui ne requerrait que des corrections mineures. Il est apparu, dans les toutes dernières années, que la glace était le facteur dominant dans certains développements canadiens et qu'on devait en tenir compte dès le début dans les études de praticabilité technique. Dans ces cas la façon de résoudre les problèmes de glace a été appelée la technique du "management de la glace". Nous décrivons brièvement dans cet article-thème trois exemples récents du management de la glace pour des projets importants au Canada.

1- INTRODUCTION

Up to ten years ago ice was considered to be a specific problem to be dealt with locally as it would affect engineering structures. This would apply for instance to blocking by ice of an intake, to flooding with an ice jam at a particular site or to ice loading on a bridge pier or a wharf. No overall planning was deemed necessary as ice questions were concerned. Recently, new projects have come up in which engineers had to deal with ice as the main factor affecting the design of their structures. This has brought up a new concept in ice engineering; the concept of overall management of ice that would start well before the design of engineering works so that it would play the same role that hydraulics has played in hydraulic structures. We will give in this paper three recent examples of ice management in Canadian projects: the control of ice in the Niagara River, the ice management of the Chaudière River and the integrated control of ice in the St. Lawrence ship channel. In the last two of these projects ice is the major factor affecting the engineering works and was recognized as such right from the beginning.

2- ICE CONTROL FOR THE NIAGARA POWER PLANTS

Hydro-electric developments have been done more or less steadily at Niagara Falls since 1900 and the power installations of Ontario Hydro and the Power Authority of the State of New York have a combined capacity of the order of 4½ million kilowatts which ranks this site among the largest of the developed power sites of the world¹.

The Niagara River connects lake Erie to lake Ontario as can be seen on Figure 1. The river itself is too shallow and fast to form an ice cover so that lake Erie and the upper Niagara River produce vast quantities of ice every winter. All that enters the river and is formed therein must pass over the fall and down river to lake Ontario. In a normal winter the entire surface of lake Erie (26,000 square km) tends to become completely ice covered. In natural conditions a vast quantity of ice would come down the Niagara River from the lake in the early winter until the pieces became large enough to form a natural ice bridge at the neck of the lake. Under those conditions ice would drift in the river in quantity from a few km to perhaps 50 sq. km in one day. With a severe storm that would break the ice arch in lake Erie, as much as 100 sq. km. of ice would have entered the river. This ice is a mixture of slush, brash and floes piles together by wind and waves. The difficulty in passing such material down a river which is less than 10 feet deep in many areas could well be imagined.

The upper Niagara River is 29 km long and the flow velocity ranges from 1 m/sec to 3 m/sec. Maximum depth is around 9 m and average depth about 4 m. The average winter flow is approximately 5400 cu. m/sec so that no natural ice cover forms on the river. The whole stretch is thus a giant refrigerator where immense quantities of frazil and anchor ice are formed. The frazil which is formed moves and compresses on the surface to make ice pans with frazil underneath and as much as 2.5 m thick has been observed.

The general solution to the ice problems at Niagara has come progressively with time as more and more experience was gained and as the capacity was being raised up.

This general solution to this major ice problem contains the following elements

1- A non-obstructive diversion system for power production with special water intakes that are placed laterally along the river edge forming no obstruction to the river flow in order to let water in at the lower strata and keep the floating ice moving out in the upper stratas of the flow.

2- A control structure that can block part of the river width with gates and which is situated downstream of the intakes. This structure can raise the water level to let jams or big ice floes off the ground and to start them moving.

It has 18 sluices with gates 100 feet wide which open downwards to allow the ice to pass over the top.

3- An ice boom at the outlet of lake Erie to prevent most of the ice to move downstream in the upper river at the beginning of winter².

4- Channel excavations to provide greater depths and widths to keep the ice moving.

5- A program of ice control using two small icebreakers to destroy jams and grounded iceballs. There is a special organization for ice control working 24 hours a day that operates the structures and ships in order to keep the ice moving downstream at all times while providing the minimum flow over the fall specified by treaty in order to use the maximum for power production.

In conclusion it might be said that these hydro-electric plants at Niagara Falls have been specially designed to operate with free surface flow in winter. They are the biggest plants of that type in the world and they operate very successfully in winter with an overall combination of special structures and an efficient ice control organization. The main problem encountered has been the flow retardation caused by anchor ice formation which may cause, at times, large reduction in power production. Extensive research, started about five years ago, is being done by Ontario-Hydro on this question.

3- OVERALL PLAN FOR ICE CONTROL ON THE CHAUDIÈRE RIVER

The Chaudière River in the Province of Quebec was one of the best known Canadian river where damages caused by ice floods were important every year mainly in the numerous villages along its path. (Figure 2). Before the realization of the 5-year plan by the Quebec Government these were estimated at \$220,500 per year.

The profile of the river was found to be the main cause for the flooding. The river divides itself in four main sections (Figure 2). In the upper Chaudière the slope is steep and this, coupled with the fact that the river flows from the south to the north, leads to sudden breakup and movement of ice floes. There is then a middle stretch of small slope followed by dead waters. Because of the small velocities in these areas and the numerous bed irregularities the evacuation of the moving ice is very difficult. In fact important ice jams were formed every year in this section, where most of the important villages are located, because the moving ice floes would stop in front of the continuous ice cover still well in place. The last section is fast flowing again and the ice would usually move easily to the river mouth in the St. Lawrence River.

The overall plan to alleviate ice jams was essentially based on two basic ideas: prevent the ice from the upper Chaudière to get to the critical zone and correct the major irregularities of the bed in this latter zone to accelerate the departure of the ice³.

The main control structure is a dam 650 feet long and 40 feet high, (Figure 2) designed specifically for ice retention and set at the foot of the upper Chaudière reach but just upstream of the city of St. Georges which was heavily affected by floods every year. The dam retains all ice that is formed upstream and no flooding has occurred at St. Georges since its construction. As could be expected the level rises as much as 15 feet at the limit of backwater with ice accumulations. Another effect is the delay in the disappearance of ice downstream of the dam which has time to rut in place much more, before the general break-up.

To improve the ice conveyance of the river in the middle Chaudière⁴ and the dead water reach, more than twelve local remedial works were carried on. This includes dredging of the river bed, elimination of islands, blocking of secondary channels, blasting of protruding rocks, alignment of shores, corrections of curves and construction of walls and protected berms.

Although it was considered that the reduction of icy floods would be only

50% in the dead water stretch, no such flood has happened since the completion of the plan in 1967, so the efficiency is at this time 100% for the purposes of ice management.

4- ICE MANAGEMENT IN THE ST. LAWRENCE RIVER

Winter navigation on the St. Lawrence River between Montreal and the Gulf and St. Lawrence was practically inexisting ten years ago and is now a lucrative venture that keeps river ports busy with activity twelve months a year. The growth in traffic can well be demonstrated by the phenomenal growth of winter cargo handled in the Port of Quebec City and shown on Figure 3.

This development has been rendered possible by an extensive ice management program combining the use of ice control works and the management of an ice-breaker fleet from an ice controlling central operated by the Ship Channel, Division of the Department of Transport in Montreal.

Under natural conditions, the navigation can usually proceed to Quebec City without much difficulty except for the occasional help of icebreakers. A fleet of 12 icebreakers patrol the river between Montreal and the Gulf and they usually operate in conditions of good visibility for daylight work. They are now being instrumented to navigate at all times with precise range positioning system. From Quebec City to Montreal the ice conditions are severe and jams would form in natural conditions mainly from lake St. Pierre to Montreal.

The principle of operation of ice control works in the Montreal area is to keep stable as much as possible of shorefast ice during winter months, leaving the minimum amount of open water surface in the shipping channel. Thus a minimum amount of ice is produced in the limited width of the channel and this ice is usually of small size.

The main ice control work is a massive ice control dam⁵ built at a cost of \$19 million upstream of Montreal in the Laprairie Basin (Figure 4) to retain as much as ice as possible in the basin and out of Montreal Harbor. This structure was built first for the Canadian Universal and International Exposition in Montreal in 1967 to prevent winter flooding of the EXPO site. This structure is almost 7000 feet long and consists of 72 reinforced concrete piers, between fitted removable 85 feet long floating stop-logs. The stop-logs are dropped to the river at the beginning of winter to accelerate the formation of continuous shorefast ice on the basin and reduce to a minimum the amount of ice flowing out of the basin.

Downstream from Montreal the control works are essentially lateral booms (Figure 4) to retain the ice in secondary channels and along the shores. More than 14,000 feet of these booms made of B.C. fir timbers are set in place mainly in lake St. Peter. Artificial islands have also been built to stabilize the shorefast ice.

In the winter of 1970 the ship channel was practically opened all winter to Montreal. In 1971, it was closed 6 days when a storm broke a large area of shorefast ice south of lake St. Pierre which drifted and rafted through the ship channel. In a general manner it is now considered that navigation in winter from the Gulf to Montreal takes an average of four days compared with three days during the summer months.

The ships using the St. Lawrence are increasing in size because larger, high-horsepower ships with reinforced hulls have less difficulty breaking through the ice. The opening of the St. Lawrence River to navigation twelve months a year has changed completely the economics of transportation in the area and many industries are now being established in the St. Lawrence valley because of that favorable factor.

5- CONCLUSIONS

The review of these three projects where ice is the main factor affecting engineering design shows that we are entering an area of ice engineering where extensive use is to be made of existing knowledge and further large scale research will be required to develop ice-minded engineering solutions.

There is little doubt that ice management will be needed on a large scale if we are going to open up winter navigation along most of the coast of a large country like Canada which is presently ice bound most of the year. There is also renewed interest in developing low head run-of-river power-plants for power hungry North America. These projects have not found easy support in the past in Canada because of the extensive ice problems they set up that may often require new designs. Ice is also a direct remedy to thermal pollution. In the same line of thought, a bold proposal was recently made⁶ in Canada to control local climate by ice control in the Gulf of St. Lawrence.

So we consider that ice management techniques are just starting to develop in our country for large scale engineering projects and this may well be one of the big challenge of our times.

REFERENCES

- 1- Foulds, D.M. (1967)- "Niagara River Ice Control". Eastern Snow Conference.
- 2- Bryce, J.B. (1968)- "Ice and River Control". Proc. ASCE, Journal of the Power Division, Vol. 94, No. 2.
- 3- Ministère des Richesses Naturelles du Québec (1965)- En Collaboration. "Plan d'ensemble des travaux remédiateurs de la rivière Chaudière". R.1, 18 pages et ill.
- 4- Ménard, R., Mathieu, B. (1967)- "La lutte contre les inondations: l'aménagement de la rivière Chaudière au Québec". Le Génie Civil, T. 144, No. 2, p. 154 - 157.
- 5- Donnelly, P. (1968)- "An outline of the design and operation of the Montreal ice control structure". Proc. Conference "Ice pressures against structures". Tech. Memorandum No. 92, National Research Council of Canada, p. 171-195.
- 6- Stewart, P.W., Dickie, L.M. (1971)- "Etude sur les sciences et la technologie de la mer". Etude Spéciale No. 16 du Conseil des Sciences du Canada. 189 pages.

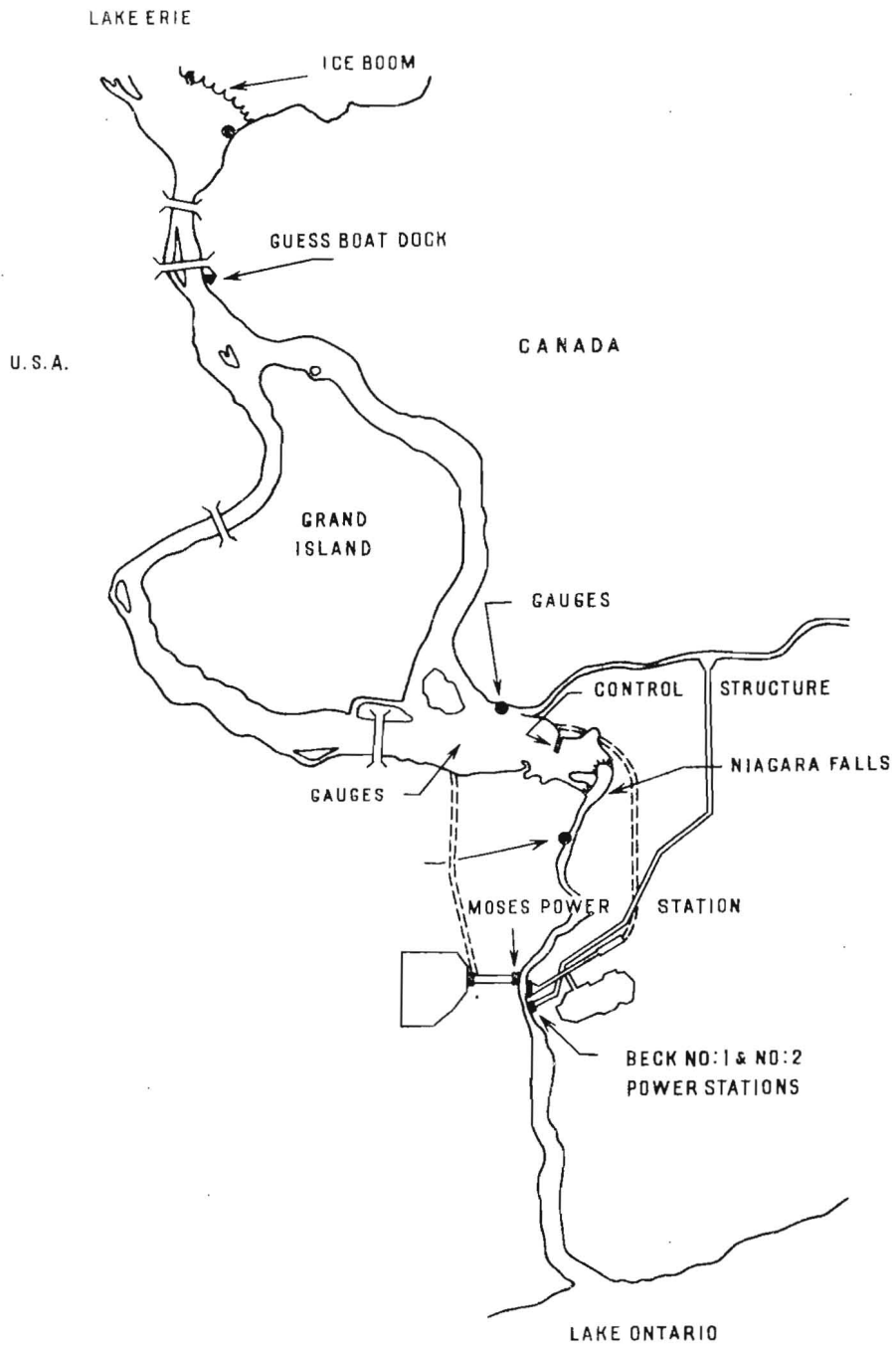


FIGURE I—NIAGARA RIVER AND POWER INSTALLATIONS

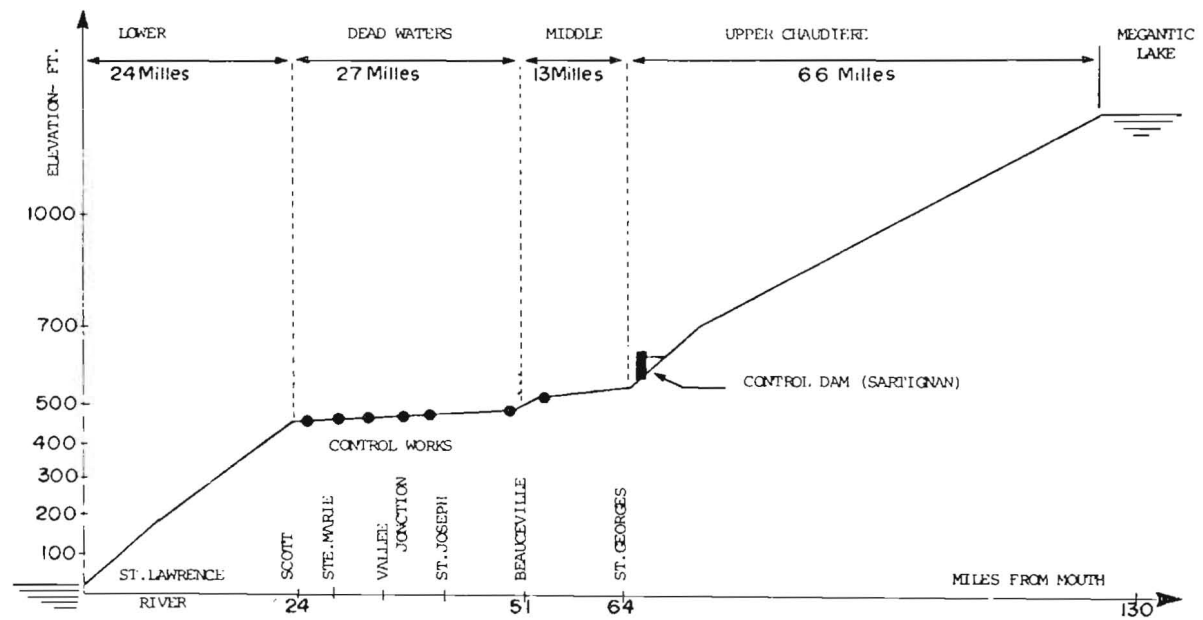


Figure 2. - Profile of Chaudiere River with ice control works.

CARGO TONNAGE (JAN-FEB-MARCH)

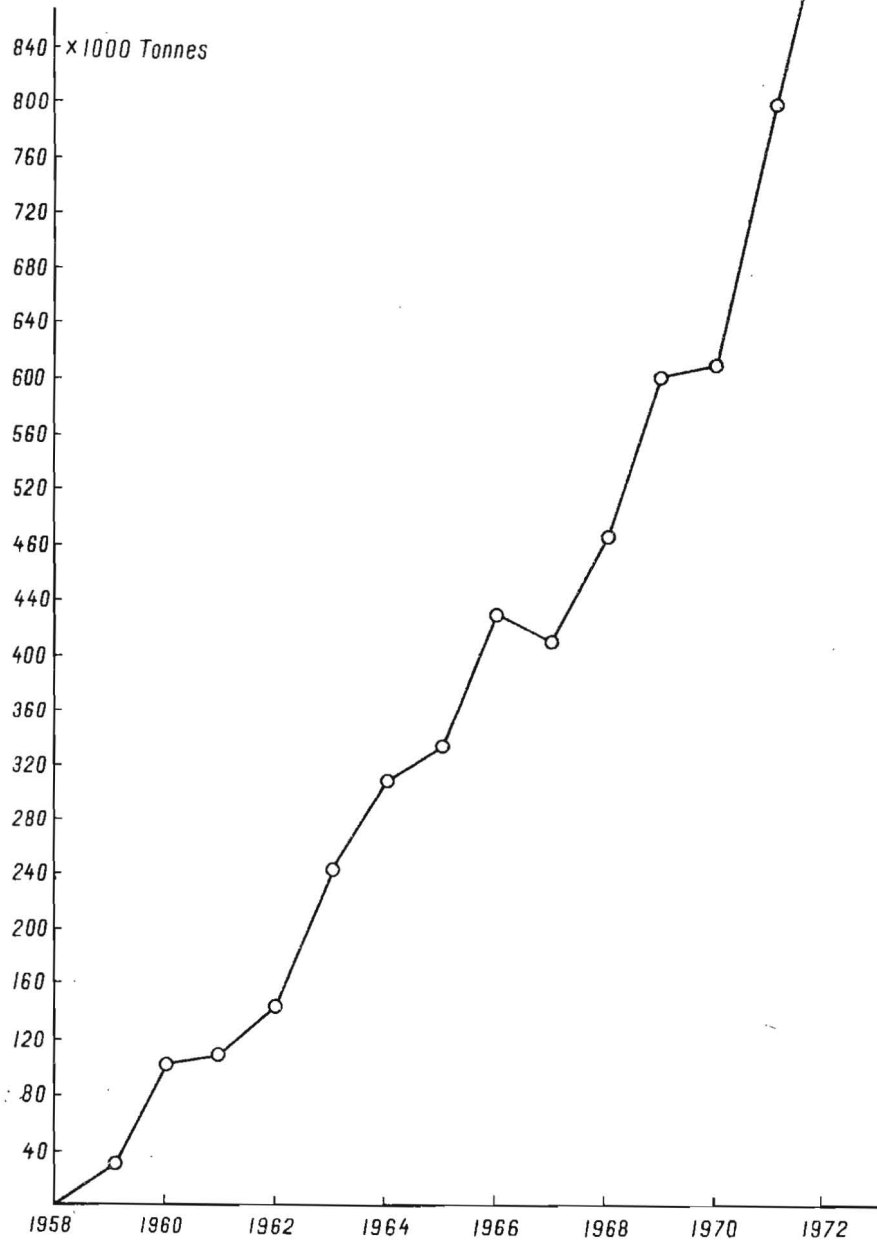
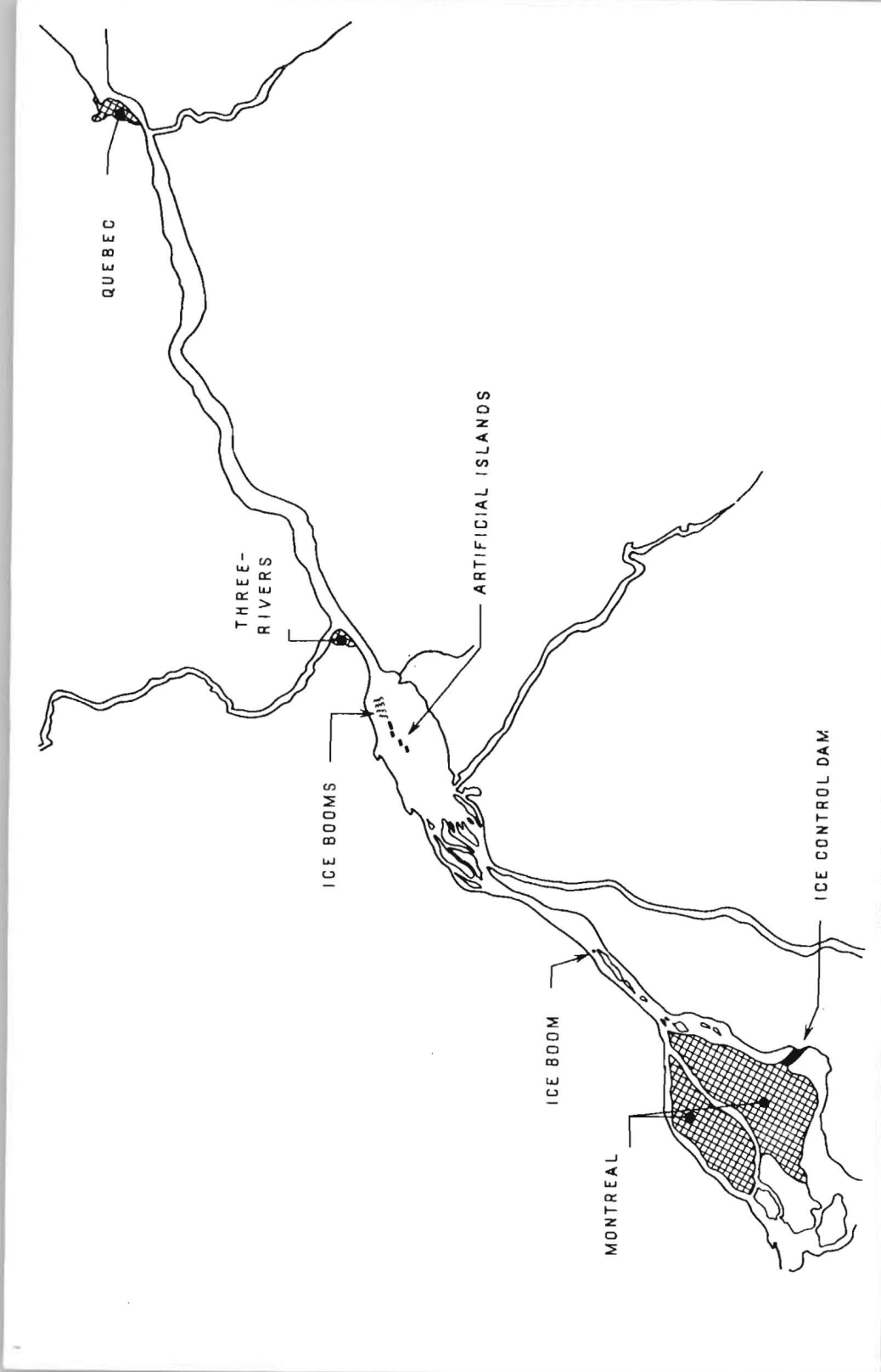


FIGURE 3-WINTER NAVIGATION AT QUEBEC CITY



ICE ENGINEERING IN THE AMERICAN EXPERIENCE

A. Assur, Chief Scientist USACRREL U.S.A.

Ice Engineering research in North America has been conducted by a number of government laboratories, academic institutions and industrial interests. The Cold Regions Laboratory of the Corps of Engineers represents the largest concentrated effort primarily devoted to permanent and seasonal cold regions. It closely cooperates with groups doing related work in the United States and Canada, thus providing important background material for the civilian economy.

Over the last 20-30 years significant advances have been made. Early work by ACFEL (Arctic Construction and Frost Effect Laboratory) and SIPRE (Snow, Ice and Permanent Research Establishment), predecessors of CRREL (Cold Regions Research and Engineering Laboratory), dealt largely with load carrying capacity of ice sheets and development of special drilling equipment for the field. Loads leading to first cracking as predicted by classical theory can be significantly exceeded without imminent danger to the load. This chain of thought over the years led to the development of a failure theory based upon wedges, the results of which agree closely with recent laboratory experiments published in the Russian literature. Other approaches tried were based upon plastic collapse and various yield theories. In-situ tests were introduced.

An early difficulty was the special treatment necessary for sea ice. As a result of trying to solve these problems significant advances were made in the petrology of sea ice, phase composition, computation of brine volume as a function of salinity and temperature, relation of properties to brine volume, brine separation during growth etc. A series of mechanical tests were made.

Other work dealt with resonance oscillations of ice sheets. Other contributions to ice engineering included machines for leveling of pressure ridge and rough spots, protection from deterioration and repair of ice surfaces. Weakening of ice sheets by a bubbler and other systems paid off in extending shipping.

Ice jam mechanics and control of jams by explosives for prevention of floods was another extension of capabilities.

Work on ice breakers eventually led to joint US-Canadian cooperation on the two cruises of SS Manhattan.

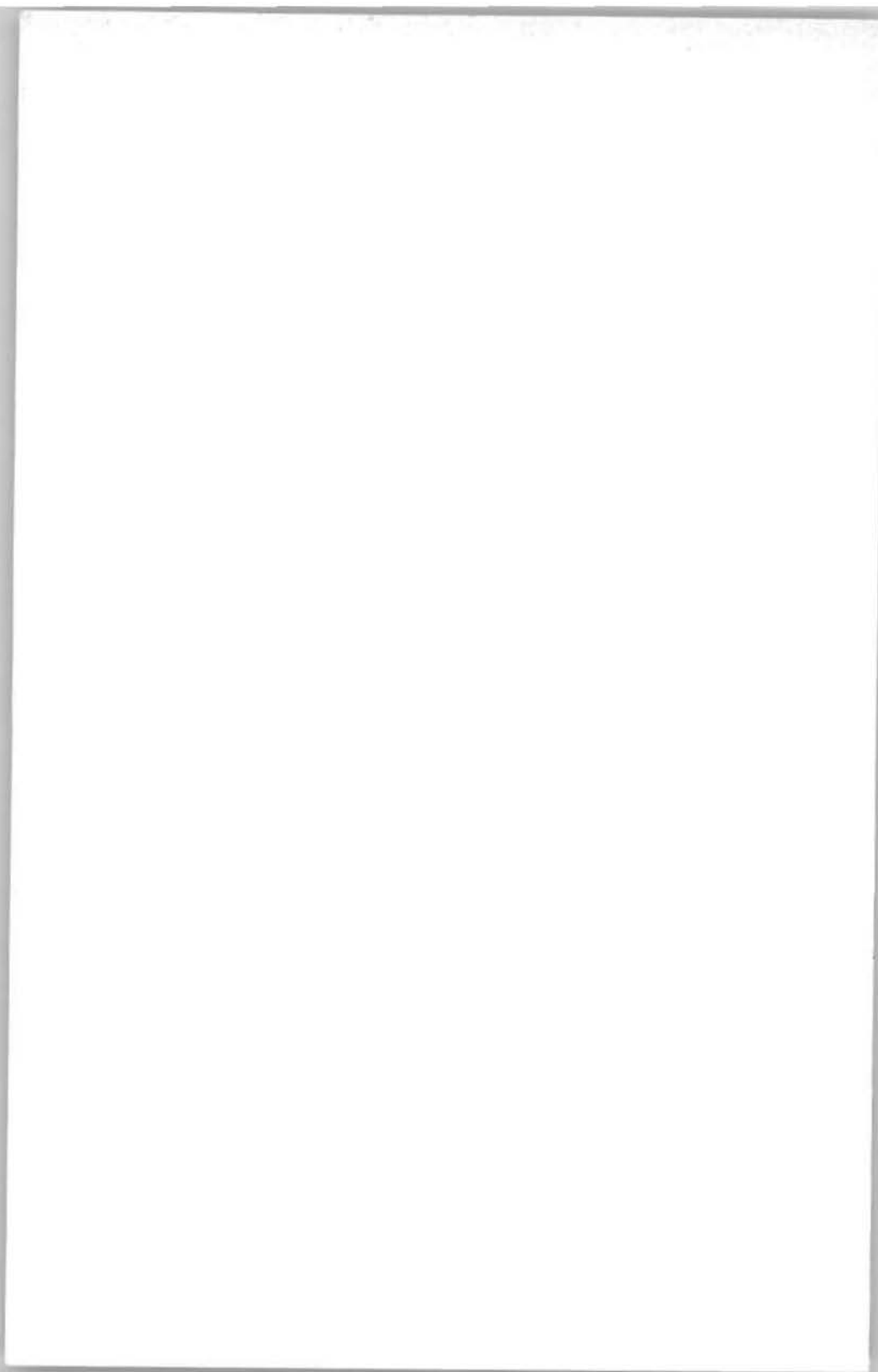
The action of ice on offshore installations, terminals, bridge piers, and causeways became a matter of concern which led to additional efforts in the American scientific community.

More recent efforts include lifting forces of ice, ice action on vertical walls and piles, sloping surfaces, mechanics of broken-up ice masses, ice accumulations and pressure ridges.

Efforts to extend the navigation season lead to artificial weakening of ice sheets, studies on barges, ice control in locks, ice adhesion etc.

Movement of sea ice is considered by the AIDJEX project which in turn will lead to advances in ice engineering. Other work is being done in ice hydraulics, glacier management, study of ice-dammed lakes etc. Russian publications in ice engineering were very helpful throughout these years of efforts.

PAPERS AND DISCUSSIONS



COMPARISON OF ELASTICITY AND STRENGTH
CHARACTERISTICS OF SALT-WATER ICE

Yu. E. Slesarenko
A. D. Frolov

The Moscow State University
The Moscow Geological Survey
Institute

Moscow
U.S.S.R.

A basic trend in studying physico-mechanical properties of ice is associated with establishing correlations between individual characteristics in order to devise simpler and more effective techniques for an indirect evaluation of the properties whose investigation is labour-consuming. Emphasis should be placed on the factors affecting many ice properties. Such a factor for salt-water and sea ice is the content and distribution of the liquid phase whose physico-chemical transformations are responsible for a change in the position of intergranular zones, which in its turn alters the cohesion of ice, and consequently, its elasticity and strength. As an example let us consider NaCl ice. Weeks /R. 1/ adduces experimental data on the relationship between the ring tensile strength and the liquid phase content. Using the ultrasonic pulse method, we have also determined the elastic properties versus the liquid phase content. Figure presents averaged experimental relationships between different parameters and the liquid phase content. The curves obtained allow to draw the following conclusion: ice of more perfect elasticity (higher values of the Young modulus and lower values of the effective viscosity $\frac{1}{\nu}$) has a higher strength.

CONCLUSIONS

1. There is a fairly distinct linear correlation between elasticity and strength characteristics of salt-water ice, which confirms the feasibility of elaborating an indirect procedure for estimating the strength by acoustic measurements.

2. Increase in ice cohesion with decreasing of the liquid phase content affects the strength and rigidity (elasticity) of ice in a different manner.

3. We consider it more expedient to compare different properties of ice in terms of the liquid phase content as opposed to the attempts of correlating them versus such individual factors as temperature, salinity, density, etc.

REFERENCES

1. Weeks W.F., Tensile strength of NaCl ice. - Journal of Glaciology, 1962, v.4, N 31.

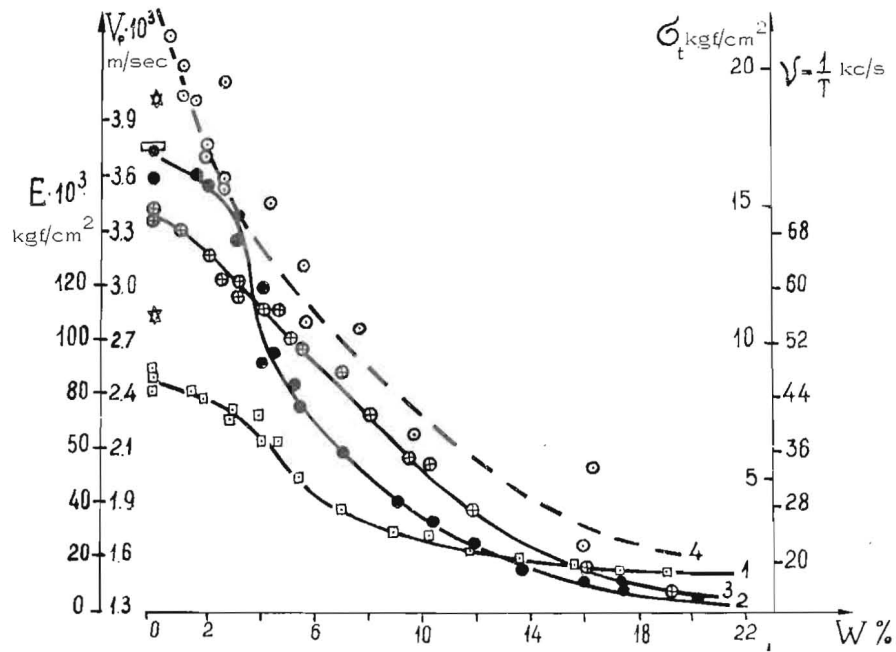


Fig. 1. Elasticity and tensile strength (σ_t) of salt-water ice versus the liquid phase content (W)

- 1 - the Young modulus, E
- 2 - elastic wave propagation velocity, V_p
- 3 - signal frequency, ν , corresponding to the elastic wave
- 4 - tensile strength, σ_t

CHARACTERISTICS OF ELASTICITY OF SEA ICE
OF DIFFERENT COMPOSITIONS

A.D.Frolov The Moscow Geological Survey Institute Moscow
Yu.E.Slesarenko The Moscow State University U.S.S.R.

Due to small values of ultimate ice elasticity (0.5 kg/cm^2) its characteristics may be most accurately established by dynamic tests, viz. by the ultrasonic pulse method. The authors have applied the latter method to obtain a systematized body of data on ice of various salinity. Based on the wave gauge records a series of the time curve records was constructed corresponding to different phases of longitudinal and elastic Rayleigh waves, proceeding from that V_p and V_R velocities and wave signal periods with subsequent determination of the elasticity modulus and signal frequency.

Fig. 1 shows the dependence of ice elasticity on its temperature and salinity. The above experiments should be concentrated on establishing ice salinity rather than the brine from which various types of ice are formed under different conditions.

It follows from the graphs that the characteristics considered vary regularly. The left-hand sides of the graphs that represent small values of the elasticity modulus, the velocities V_p and V_R , and large values of the signal periods ($T = \frac{1}{\nu}$) are characteristics of the ice conditions when the complex modulus of elasticity is greatly dependent on the imaginary part, i.e. the importance of the viscosity of ice is highly prominent.

The right-hand sides of the graphs describe ice conditions of much more perfect elasticity (rigidity) when it is susceptible to brittle failure.

The character of variation in the elasticity modulus and the signal periods of sea ice follows the phase diagram and is mainly governed by the variation in the liquid phase content and by the precipitation of solid salts, namely, the hydrate of Glauber's salt (at -8.2°C) and the sodium chloride (at -22.9°C).

In this manner, the study of the dynamic characteristics of ice elasticity and viscosity allowed different ice conditions to be evaluated, which are to be considered while developing the methods for breaking the ice.

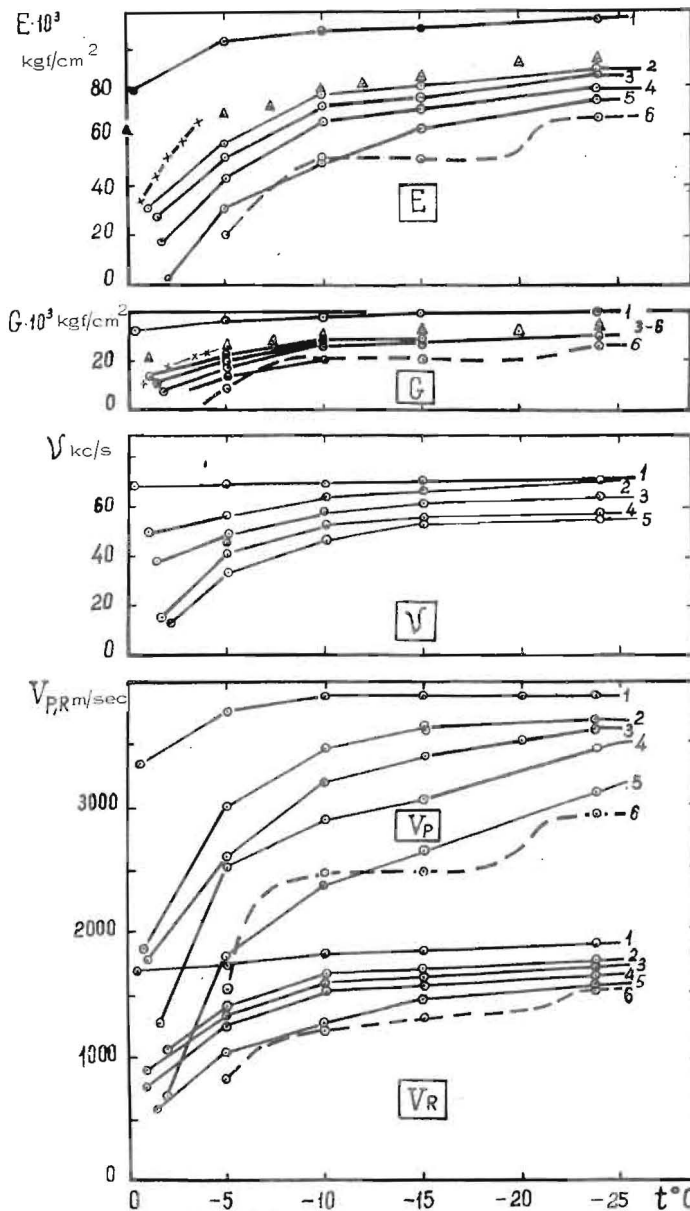


Fig. 1 Characteristics of elasticity of fresh, sea and salt water ice of different salinity versus temperature
 E = Young's modulus; G = shear (rigidity) modulus; ν = signal frequency of wave "R"; V_{PR} = propagation velocity of longitudinal and Rayleigh (R) waves; 1 = fresh water ice; 2,3,4,5 - NaCl - ice of 4.0, 5.5, 9.0, 11.5% salinity, respectively; 6 = sea ice of 18.5% salinity; $\Delta\Delta$ = pack ice (after Bogorodski); $\times\times$ = one-year ice (after Lin'kov).

EFFECT OF ICE STRUCTURE AND MINERALIZATION ON
THE MECHANICAL PROPERTIES OF THE FRESH-WATER ICE COVER

V.P.Ergin The Siberian Research Institute Novosibirsk
Engineer of Power Engineering U.S.S.R.

During the years 1967-71 the author was studying the physico-mechanical properties of the ice-cover on the reservoir of the Novosibirsk hydropower project (Under K.N.Korzavin, Dr. Sc. (Eng.)).

Investigations into ice of predominantly layered structure provided new information on the ice cover strength.

The results obtained in particular showed that:

1) The mechanical properties of the fresh-water ice cover are largely governed by the salt content in the water. The strength of the ice formed of water with a low-salt content is substantially higher than that of the ice formed of water with a high-salt content, the former displaying higher strength at sub-zero temperatures and disintegrating more slowly during the spring breakup.

The ice strength was evaluated as a function of water salt content and temperature and of solar radiation.

2) The strength of the layered ice (with the principal optical axes being horizontal), all other things being equal, was found to be considerably higher than that of ice of polar structure (with the principal optical axes being vertical).

3) In the range of the ice crystal sizes considered (cross-sections of 0.5 to 100 cm^3 and larger) no marked relation between the ice strength and the crystal size was found.

4) Great regional and year-to-year variations in the ice strength of the ice cover on rivers in the U.S.S.R. are observed.

The above findings are a sufficient ground for a revision of the existing concepts on mechanical and rheological properties of ice in the ice cover on rivers, reservoirs and of ice in general.

The investigations described are of great significance for solving many ice-engineering problems, particularly for prediction of ice conditions in rivers and reservoirs.

STRUCTURES
IN ICE INFESTED WATERS

Dr. Andrew Assur, U.S.A. Cold Regions Research Hanover
Chief Scientist and Engineering Laboratory New Hampshire
03755 U.S.A.

SYNOPSIS

A method is presented to calculate the effective ice load on vertical structures depending upon width of structure related to ice thickness and fundamental ice properties (anisotropic semirestrained crushing strength, Young's modulus, Poisson's ratio, internal friction). The basic equation satisfies the theoretical indentation solution for a narrow pile and approaches exponentially the crushing value for a straight wall. Both extremes appear as simple intercepts on a plot which furthermore can be linearized. The concept is compared with largely Russian test material and equations which show good agreement.

Internal friction must be considered in the analysis since it increases possible ice forces. Due to this local indentation forces by ice can be higher as previously assumed for the design of ships.

Buckling instability introduces complications in model tests.

For structures in the field the random configuration of ice collars must be considered. For this a complete solution is still not available.

One of the unresolved problems confronting the designer of structures in ice infested waters is the effect of the width of the structure B in relation to the ice thickness h on the nominal ice pressure $\sigma_n = P/Bh$ with P the total load. Narrow structures will indent the ice with high resulting loads, wide structures will be subjected to much less ice pressure. The following equation is suggested to take care of this effect

$$\Delta S = \Delta S_0 \left(\frac{1-\eta}{2} + \eta 2^{-\beta} \right) \quad (1)$$

$$\Delta S = S-1; S = \sigma_n / \sigma_{\infty}; \Delta S_0 = S_0-1; S_0 = \sigma_0 / \sigma_{\infty}$$

$\sigma_0, \sigma_{\infty}$ is σ_n for $B/h = 0$ or $B/h = \infty$ respectively.

$\sigma_0 = \sigma_{\perp} S_1; \sigma_{\infty} = \sigma_{\parallel}$ where σ_{\perp} is the crushing strength perpendicular to growth direction G with a test conducted to prevent deformation along G , σ_{\parallel} parallel to growth with no deformation in one direction \perp to G . See Fig. 1a and b for the distinction. S_1 is the Prandtl indentation factor (eq. 5).

$$\beta = \beta / \beta_0; \beta = B/h; \beta_0 - \text{value of } \beta \text{ where } \frac{\Delta S}{\Delta S_0} = \frac{1}{2}$$

$$\eta = \begin{cases} +1 & \text{for } 0 \leq \beta \leq 1 \\ -1 & \text{for } 1 \leq \beta \leq \infty \end{cases} \quad \text{an interruptor to distinguish} \quad (2)$$

between two domains.

The "interruptor" η is introduced here for purposes of better definition. Eq. (1) properly satisfies boundary conditions. For $\beta=0$ (thin pile) it reduces to the two-dimensional case of Prandtl's indentation equation taking the ice anisotropy into account as shown below. For $\beta \rightarrow \infty$ (straight wall) it approaches exponentially the crushing value of ice with one side, perpendicular to growth, confined.

We plot $S = f(\beta)$ in the domain $\eta=1$ and $S = f(1/\beta)$ in the domain $\eta=-1$. In such a way the entire plot for $0 \leq \beta \leq \infty$ can be shown as a simple graph from $0 \leq \beta \leq 1$ and continuing with $1 \geq 1/\beta \geq 0$. The resulting plot (Example in Fig. 4) is almost linear in a wide range which is the principal advantage. The intercepts, $\sigma_0 = \sigma_{\perp} S_1$, and $\sigma_{\infty} = \sigma_{\parallel}$ are easily obtained. Eq. (1) ties forces exerted on structures to fundamental constants of ice (strength, elasticity, internal friction).

Eq. (1) can be linearized by the expression

$$\Delta S = \frac{1}{2} (1-\eta - \eta \beta^{\beta_0}) \quad (3)$$

and plotting ΔS versus $1/\beta$ in the domain $\eta=1$. Eq. (3) becomes simply linear interpolation between $\sigma_{\perp} S_1$, and σ_{\parallel} (Example in Fig. 2)

$$\Delta S = \Delta S_0 2^{-\beta} \quad (4)$$

the case of (1) for $\eta=1$ was briefly mention by Assur(1971) with instructions for $\eta=-1$.

Assur, A. (1971): Forces in moving ice fields, Trondheim, Proc. 1st Intern. Conf. Port and Ocean Engineering and Arctic Conditions (POAC) VI:112-118

This paper compares the applicability of eq. (1) largely upon the basis of Russian test material.

Fig. 1a illustrates the action of ice with vertical crystals against a vertical wall. It is difficult to tear the crystals lengthwise or across. Fig 1b shows the action of the ice edge against a narrow vertical object. Prandtl type sliplines develop along grain boundaries.

Therefore $\sigma_1 > \sigma_{\infty}$. Tests with small samples should be conducted to prevent deformation along one axis and allowing slippage in the other direction. The

anisotropy may be especially pronounced in case of sea ice.

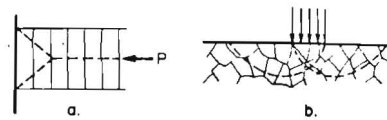


Fig.1

Prandtl's equation for indentation by a trunkated wedge can be presented as

$$S_1 = A + \frac{1}{2} + \frac{1}{\sin \mu} \left(A - \frac{1}{2} \right) \quad (5)$$

with $A = \frac{1}{2} e^{2\theta \tan \mu}$. μ - angle of internal friction, θ angle between side and axis of wedge. For $\mu = 0$; $S_1 = 1 + \theta$. For Fig. 1a $\theta = 0$ and $S_1 = 1$, for Fig. 1b $\theta = \pi/2$ and $S_1 = 2.5708$, the classical value used for the design of bearing pads on concrete for bridge supports. This is a minimum value since internal friction is neglected. It should not be used for ice since actual indentation values can be much higher. Afanas'ev (1972) mentions $\mu = 15 \rightarrow 25^\circ$. Our own measurements (Chamberlain, person. commun.) give $16 \rightarrow 20^\circ$. Table 1 gives some values for S_1 depending upon wedge angle θ and internal friction angle μ .

Table 1

	0	15°	30	45	60	75	90°
15	1	1.3663	1.7877	2.2726	2.8306	3.4726	4.2113
20	1	1.4119	1.9103	2.5132	3.2428	4.1256	5.1937
25	1	1.4655	2.0596	2.8181	2.7864	5.0224	6.6003

This line of reasoning is also important, but neglected, for the design of ice-strengthened ships against local indentation by ice. Assume piece of ice having the shape of a trunkated wedge with $\theta = 60^\circ$. Local indentation force can be 3.43 times the usually assumed full crushing strength of ice ($\mu = 20^\circ$).

Korzhasin (1962) effectively used $S_1 = 2.5$ independent of $\beta = B/h$, a value which is too low for narrow objects, and too high for wide structures. It may be just right for his type of structures (piers). Korzhavin's experimental data show a distinct effect of β . These data are plotted in Fig. 2 using linearized equ (2).

Afanas'ev V.P. (1972): Davlenie l'da na vertikal'nye pregrady /Ice pressure on vertical obstacles/ Transportnoe stroitel'stvo 7:47-48

Korzhasin K.N. (1962): Vozdeistvie l'da na inzhenernyye sooruzheniia /Action of ice on engineering structures/ Novosibirsk

With $\beta_0 = 1$ a sharp break occurs.
 $\beta = 0.2$ gives a linear plot with
 $\sigma_{\infty} = 53$ and $\sigma_0 = 154 \text{ kg/cm}^2$
 $S_0 = 3.38$. Using equ. (1), $\mu = 15^\circ$,
 $S_1 = 4.21$ and $\sigma_{\perp}/\sigma_{\parallel} = 1.25$ could
be assumed.

The value 10.9 kg/cm^2 plotted
at $1/x$ is a crushing value for unrestrained
cubes. We prefer prismatic samples
with a length to side ratio > 2.5

Using model tests on thin ice sheets
in the laboratory difficulties can occur
due to buckling instability which would
not occur on thicker ice sheets in nature.
Assur (1972) has shown how to use
equ. (1) and (3) in such a case. Plot-
ting equ. (3) versus $1/x$ one obtains an
intercept for $x = \infty$. This is not
 $\sigma_{\infty} = \sigma_{\perp}$ but a value affected by
buckling.

Fig. 3, for example shows \bar{R}
values computed from experimental
data by Afanas'ev (1971), who ob-
served buckling in a number of
instances. According to Hetenyi
(1946) $N_1 = C\sqrt{\kappa EJ}$ for a
buckling load which, for a plate
with cylindrical buckling, we prefer
to write as $N = c\kappa\sqrt{E\ell}$ (6)

$C = 1$ for a semiinfinite beam
with a free end, $C = 2$ with a
hinged or fixed end. In nature
or experiment $C = 2$ (or slightly
below) because of restraint.

κ - density of water; $\ell = D/\kappa$
(action radius); $D = Eh^3/12(1-\mu^2)$
(flexural rigidity). E, μ -
Young's modulus and Poisson's
ratio of ice.

Setting $E = \alpha\sigma_f$, σ_f -
flexural strength and rearrang-
ing terms

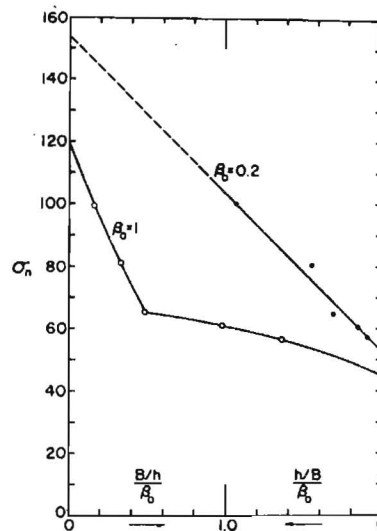


Fig. 2

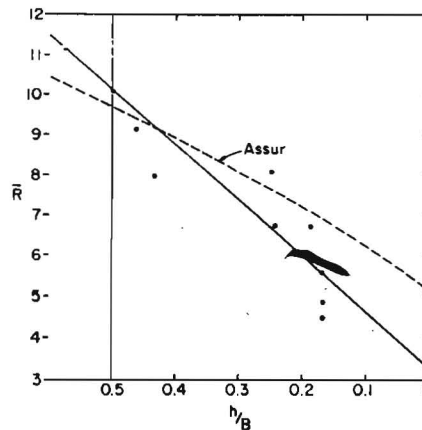


Fig. 3

Assur A. (1972): Ice pressure on structures, USACRREL TN
72-1-11 (Unpubl)

Afnas'ev V.P. a.o. (1971) Davlenie l'da na morskije otdel'no stoiashchie
opory /Ice pressure on separate piers in ocean waters/ Leningrad, Arkt. i
Antarkt. Inst. Tr. 300; 61-80

Hetenyi M. (1946): Beams on elastic foundations, Ann Arbor

$$N = h \sigma_f \sqrt{\frac{a}{3(1-\mu^2)}} \frac{\kappa h}{\sigma_f} = h \sigma_f R \quad (7)$$

with

$$R = \frac{\sigma_n}{\sigma_f} = \frac{P}{h \sigma_f} \quad (8)$$

\bar{R} average of several tests. Plotting \bar{R} computed from Afanas'ev's data in Fig. 3 according to equ. 2 in the domain $\beta = -1$ we obtain an intercept $\bar{R} = 3.25$ for $\beta \rightarrow \infty$ (straight wall case). Using equ. (3) and assuming for Afanas'ev's case $a = 2750$, $\mu = 1/3$, $\kappa = 1$, $h = 0.03$ m, $\sigma_f = 3.0$ t/m^2 (h, σ_f - thickness and flexural strength of model ice) $\bar{R} = 3.21$ in almost exact agreement with theory.

Our equ. (1), satisfying theoretical boundary conditions, gives the line marked "Assur" in Fig. 3 with $\bar{R} = 5.17$, $\mu = 19^\circ$, $S_0 = 4.97$ and $s = \frac{4.97}{1.25} = 3.98$. With assumed $\frac{\sigma_n}{\sigma_u} = 1.25$ the crushing to flexural strength ratio becomes $5.17/1.25 = 4.14$ which is reasonable.

Recently Afanas'ev (1972) suggested the empirical equation

$$S = \sqrt{1 + 5/\gamma} \quad (9)$$

(our notations)

for the effect of $\gamma = h/B$ upon ice forces exerted on structure, valid in the range of experiments $\gamma = 1/2 \rightarrow 1$. Fig. 4 shows a comparison with our equ. (1), satisfying theoretical boundary conditions, with $S_0 = 4$ and $\beta_0 = 1$. In the range of its validity the agreement with Afanas'ev is very close.

It should be pointed out that for actual field structures in ocean waters a random ice collar must be considered. Assur (1971) has given a few indications how such a problem could be approached. However, even that approach gives a "high loading bracket". In fact simultaneous breaking does not occur on a large structure at once, which was already pointed out by Korzhain (1962). A "low bracket" solution of this stochastic problem will be given in a subsequent paper.

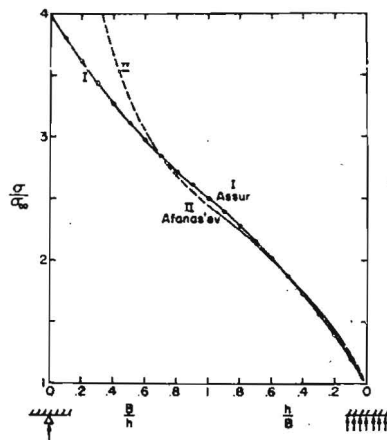


Fig. 4

Afanas'ev V.P. (1972): Davlenie l'da na vertikal'nye pregrady /Ice pressure on vertical obstacles/ Transportnoe stroitel'stvo 3:47-48

FIELD OBSERVATIONS ON STATIC ICE PRESSURE
AGAINST HYDRAULIC STRUCTURES

V.M. Sinyavskaya The Volgograd Branch of the Volgograd
P.G. Dik "Gidroprojekt" Research Institute U.S.S.R.

The discussions by Metge of observations on thermal cracks in lake ice, by Votruba on ice pressure due to thermal expansion on intake towers and a number of others are indicative of a lively interest in field observations on static pressure of ice against hydraulic structures. In this connection the following three points will be raised:

1. In reservoirs upstream from water retaining structures typical patterns of ice cracking are observed, the cracks tending to concentrate along the boundaries of a transit flow and reverse current zones.

A knowledge of different patterns of ice fields upstream from the structure provides a basis for better prediction of ice loading on structures. Some basic data on the point in question can be obtained from hydraulic model tests carried out for specific hydropower projects, with the given boundary conditions reproduced on the models.

2. Continuous in-situ records of both ice temperatures and static pressures on the Volzhskaya and the Mamakanskaya dams showed a fairly close correlation of data, regardless of other factors (cracking, etc.) varying.

A need is felt in extensive observations on ice temperatures under various climatic and hydrologic conditions to include the measured data into design formulae.

3. As evidenced by our field observations, in spring, when the strength of the ice in the leads near the piers of retaining structures is affected by changes in the water level, quasi-static ice pressure as

a result of thermal expansion of an ice field is exerted on the hydraulic gates. Sometimes this is the maximum ice pressure observed throughout the winter period.

In his paper A. Assur pointed out that large-scale modelling is a promising research tool. This trend in ice studies appears to be very interesting and important. Though the interpretation of observation data is complicated owing to the combined effects of various factors, these data are of great value in solving engineering problems, optimizing theoretical solutions and verifying scientific hypotheses.

MODEL INVESTIGATIONS OF THE EFFECT OF AN ICE FIELD
PUSHED AGAINST THE PILES OF OFF-SHORE OIL PLATFORMS

E.M. Kopaigorodsk, M.Sc.(Eng.)	The Moscow Institute of Civil	
S.A. Vershinin, M.Sc.(Eng.)	Engineering named after	Moscow
S.A. Nifontov, Engr	V.V. Kuibyshev	U.S.S.R.

Future development of off-shore production of oil in freezing seas calls for designing and constructing new types of supports for oil platforms. Prediction of ice effects on such structures is of primary importance. An analytical solution to the problem using conventional theories of mechanics of continua proved impracticable because of insurmountable mathematical difficulties. Therefore the most feasible solutions should be sought through laboratory model studies of the action of an ice field on the structures considered.

The effect of ice on isolated cylindrical supports ϕ 325 mm (piles) and ϕ 8000 mm was studied on scale models.

Ice is generally assumed to be an anisotropic statistically-nonhomogeneous material consisting of individual elements (crystallites) of varying strength and geometry.

In the case considered herein the ice block tends to fail along certain planes. Let a mesh with a Δh^p spacing equal to the mean linear dimension of the ice specimen be layed out across the plane of failure (the external plane of sliding). The limit force exerted on a pile by an ice field at failure can be given as a sum of random values:

$$P^p = \sum_{i=1}^n \sigma_i^p (\Delta h^p)^2 n_{ix} = \sum \tilde{A}_i ,$$

where n_{ix} are direction cosines and σ_i^p are stresses related to the value of "i" of the platform.

The mean value of A_i and the dispersion D_A are taken as governing parameters. The statistical characteristics of a given ice field depend largely on the specimen size. The linear dimensions of ice fields and those of the prototype structure are reduced on the models α times, the resulting ice pressure on the model pile being:

$$P = \sum_{i=1}^n \sigma_i^m (\Delta h)^2 n_{ix} = \sum \tilde{A}_i / \alpha^2 \beta_i,$$

To obtain a statistic similarity of prototype and model ice, their basic statistical characteristics of the dimensionless frequency distribution of strengths must coincide. As evidenced by experimental data, this condition is satisfied for:

$$\frac{\delta^p}{h^p} = \frac{\delta^m}{h^m} = idem,$$

where δ is the cross-section of a crystal.

The mathematical expectations and dispersions will be:

$$\bar{A}^m = \frac{\bar{A}^p}{\beta \alpha^2} \quad D_A^m = \frac{D_A^p}{\beta^2 \alpha^4}$$

An average force acting on the structure is finally obtained as:

$$\bar{P}^p = \bar{P}^m \alpha \beta$$

Model tests on cylindrical supports to a scale of 1:20 carried out in an ice flume at the Arctic and Antarctic Research Institute permitted to establish some major regularities in the failure of an ice field as function of the physico-mechanical properties of ice and the geometry of the structure.

The dimensionless value of $\frac{h}{d}$ (where h is the ice thickness and d is the diameter of the pile) was found to be the main geometric parameter governing the average value of the limit ice pressure along the contact with the pile.

The pattern of an ice field failure around models of small-diameter piles, $\frac{h}{d} \approx 0.1 \div 0.2$, differs greatly from that around large-diameter piles, $\frac{h}{d} = 1 \div 5$. In the first case the ice field regarded as a plate becomes

unstable, whereas in the second case shear strains inside the ice field are mainly responsible for the failure. Accordingly, the average values of contact stresses in Case 2 are many times those in Case 1.

PROCESSUS DE FORMATION DES ACCUMULATIONS DE FRAZIL
EN AMONT D'UN BARRAGE RESERVOIR

Claude Triquet, Service de l'Amenagement hydraulique, Québec
ing., M.Sc. Ministère des Richesses naturelles Canada

Frazil accumulations upstream of two small reservoir dams situated in the Province of Québec, Canada, are formed in very different ways since many years, even though the two dams and reservoirs are quite similar in dimensions and shape. In one case the accumulation starts right at the dam, completely filling the reservoir, and in the other part the accumulation starts only at the upstream of the reservoir. The possible causes of such differences are analysed qualitatively.

Les accumulations de frazil à l'aval de deux petits barrages-réservoirs situés dans la Province de Québec, Canada, se forment de façon très différente depuis plusieurs années, bien que les deux barrages et réservoirs sont à peu près semblables quant à leurs dimensions et leurs formes. Dans un cas l'accumulation commence au barrage même, remplissant complètement le réservoir, et dans l'autre l'accumulation ne commence qu'à la partie aval du réservoir. Les causes possibles pouvant provoquer ces différences sont analysées qualitativement.

INTRODUCTION

Frazil ice is generally defined as a mass of ice crystals formed in a turbulent flow which is in a supercooled condition. The process starts with the supercooling of water which is at the origin of frazil for-

mation. In turbulent flow, the supercooling effect is extended in depth to the whole flow cross-section, so the crystallisation process takes place in the whole section. Frazil crystals then agglomerate into flocks which after a while flow up to the water's surface. Water imprisoned between crystals freezes at the surface, and soon the upper parts of the flocks form solid ice crusts. Those ice cakes evolve into the well known form of pancake ice, which in turn form the ice cover by well known processes. (1) (2) (3) (4)

A particular aspect of ice behaviour during ice cover formation is created at the foot of uncovered rapids when the fluvial stretches downstream of it are covered. In that case the oncoming ice, because of the relatively short distance under which it travels and the great turbulence of the water, mostly if not entirely consists of frazil flocks. At the foot of the rapids those flocks, due to the high velocity of the flow, are carried under the cover until they reach a section of sufficiently low velocity where they are deposited on the underside of the cover. The local accumulation of frazil thus developed narrows the flow section until the water gains enough speed to carry the flocks farther downstream. Considerable amounts of frazil thus accumulate over great distances under the cover. (5)

(1) Morphology of frazil ice.

B. Michel, Conference on the physics of snow and ice, Hokkaido University, Sapporo, Japan, August 14-19, 1966.

(2) Theory of formation and deposit of frazil ice.

B. Michel, Eastern Snow Conference, Proceedings 1963.

(3) Observations cryologiques sur la rivière Chaudière.

C. Triquet, Publication R-1A, Direction générale des Eaux, Ministère des Richesses naturelles.

(4) Ice cover progression in the Caudiere River.

B. Michel, C. Triquet, Eastern Snow Conference, Proceedings 1966.

(5) Les métamorphoses du frazil en rivière.

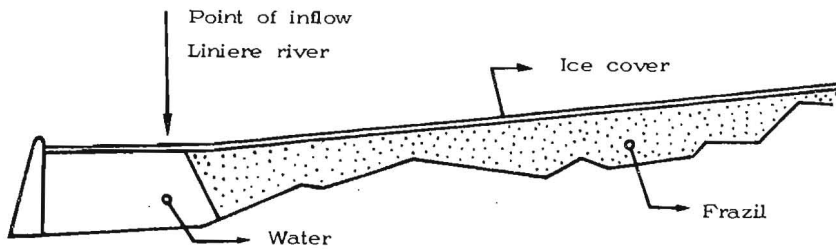
B. Michel.

FRAZIL ACCUMULATIONS AT THE DAMS

At one of the dams (the Charny dam), the process described above is followed and consequently its reservoir has been completely filled with frazil every winter; at the other one (the Sartigan dam) a different process is followed. The principal characteristics of the dams and reservoir are as follows:

	Charny dam	Sartigan dam
Height	25 feet	35 feet
Length at the top	1000 feet	750 feet
Reservoir capacity at mean level	45×10^6 cubic feet	40×10^6 cubic feet

The differences between the characteristics of the two dams are too small to account for the difference in frazil accumulation processes, more so if we consider that the general shapes of the two reservoirs are also quite similar. Difference in weather conditions also are negligible, the two dams being in the same climatic region. Since the Charny dam follows the more logical process of accumulation, we will describe the type of accumulation observed at the Sartigan dam and then analyse the causes which could explain that particular case.



Vertical scale : 50 '/in Horizontal scale : 2000 '/in

State of frazil accumulation at Sartigan dam
during the winter 1967-68

As can be seen from the previous graph, the accumulation at the Sartigan dam starts approximately 2000 feet upstream of the dam itself; from soundings taken during the winters 1967-68, 1968-69, 1969-70, the accumulation was always formed approximately the same way, including a small tunnel (not shown on the graph) free of frazil by which passed the winter flow.

ANALYSIS OF CAUSES

One feature at the Sartigan dam which does not exist at the Charny dam is a tributary falling in the main river in the critical zone. As shown on the graph, the Liniere River falls approximately at the upstream end of the accumulation: it does not bring any frazil in the main stream since an accumulation of frazil starts a little upstream of its point of inflow on a natural obstacle. That inflow could possibly affect the process of accumulation by the sideways current it induces, although that is doubtful since that sideways current is concentrated at the point of inflow and affects only a small percentage of the main stream's cross-section.

Another important difference between the two cases is the topographical conditions upstream of the dams. In the Charny case, rapids with a high degree of turbulence extend for 24 miles upstream, so ice arriving at the dam is still under the state of frazil flocks; in many places in the rapids section there are local breaks in the slope where frazil accumulates. Consequently the length of rapids actually bringing flocks to the dam is only a few miles, with the result that the concentration of flocks reaching the dam is relatively low. In the Sartigan case, rapids with also a high rate of turbulent extend for about 65 miles upstream: local breaks in the slope are scarce and the reach of uninterrupted rapids immediately upstream of the dam extends for some 10 to 15 miles. Flocks reach the dam zone at a very high concentration: from surface observations flocks in that zone were so concentrated that they occupied almost 90% of the water surface. The way the accumulation possibly develops is that, after the first flocks have participated in forming the solid ice cover up to the section where the accumulation starts, their very high concentration forces them to cluster in very large masses of flocks which, because of their spongy texture, cling together strongly. There probably is a critical degree of concentration of the flocks at

which, for a given range of discharge conditions, the flow is unable to carry their clustered masses under a cover because of their size and because those masses have strong clinging characteristics. They consequently block the cross-section without the aid of a physical obstacle and the accumulation progresses upstream.

CONCLUSION

The present text treats of a particular case and in qualitative form only: a campaign of measurement of precise and detailed topography and of the progression of frazil accumulation in time and space could not, unfortunately, be carried because of financial constraints, and because of the obvious difficulties in measuring processes occurring under water. The matter is thus treated mainly from visual observations, but it still represents a valuable piece of information in the not too well known field of frazil accumulations processes. A good knowledge of those processes could be useful, particularly in the cases where it is wanted to control those accumulations by forcing them to occur where they will not do any damage. Some measurements of the process of accumulation of frazil ice in time and space have been made last winter by Hydro-Quebec, in relation with the hydro-electric development of James Bay: those measurements will certainly bring very useful information on the question.

SOME OBSERVATIONS ABOUT THE BREAK-UP OF ICE COVER
ON THE RIVER KEMI ABOVE THE ISOHAARA POWER DAM

Matti Herva
Planning Engr

Pohjolan Voima Oy

Finland
Oulu

SUMMARY

Two serious break-ups of ice cover on the River Kemi at the Isohaara power station are described with aid of pictures (slides).

The first one, occurred in May 1956, seemed very dangerous but both the earth and concrete dams were able to withstand the impact of ice.

The second one, occurred in May 1963, caused the collapse of the trash racks, driven frozen frazil slush into the space between them and the turbine. The machines were stopped and the break lasted two weeks.

The break-up of May 1963 is an extreme event until now. The building of the Taivalkoski dam will prevent the reoccurrence of the dangerous break-ups.

With the aid of slides I will describe to you the two types of winter ice cover, which could have been observed on the River Kemi in northern Finland. The place of observations is situated at the latitude of 65.5 degrees north, where the mean annual temperature is 1°C above zero. The River Kemi has a catchment area of 52 000 km².

The Isohaara power plant was built during the late 1940's. It has a nearly 20 km long reservoir whose backwater ends at the lower part of the Taivalkoski rapids. Up to now 40 kms of this river above Taivalkoski has been undeveloped. There are several smaller rapids with relatively fast reaches of the river. Further upstream other power plants have been built, which have involved some construction work, e.g. the riverbed has been dredged and earth embankments have been built.

In 1956, from May 12th, the break-up of the ice cover on the river below the Taivalkoski rapids was very strong. The ice on the reservoir above Isohaara dam had partially maintained its strength. The increased speed of flow below the ice cover moved the ice against the shores and dams. We see how the ice has crushed against the riverbank and the dikes forming big piles of ice. At the power station some pictures have been taken showing how the ice floes have risen against the concrete dam or on the crest of the earth dam. The power station was able to run during the whole break-up period and remain undamaged.

In 1963, on May 8th, the second aggregate of the Isohaara power station had to be stopped. The reason for this interruption were the enormous ice masses, which had entered the intake of the turbine, broken the trash racks and shut the chamber between the trash racks and the turbine. The spring flood had on May 6th broken its way through the Taivalkoski reach, which had been filled by slush-ice during the icing period in November 1962. At the Isohaara power station the masses of ice against the dam could not be seen. Above the water or the ice could be seen several ice-berg like floes. These were broken from the huge ice accumulations formed on the Taivalkoski area in the winter before the spring of 1963 when the water level rose because of the increasing flood discharge. In the last slides you see the Taivalkoski reach of the River Kemi taken the same day that the accident described above happened at Isohaara power station.

ON ICE PASSAGE THROUGH HYDRAULIC STRUCTURES

I.N.Sokolov, Sr Res.Offr The B.E.Vedeneev Leningrad, U.S.S.R.
All-Union Research
Institute of Hydraulic
Engineering (VNIIG)

The paper by V.A.Koren'kov presents the results of field observations on ice passage through hydraulic structures. Based on the field data on ice routing through some hydro plants in the U.S.S.R., V.A.Koren'kov established some dimensionless similarity criteria and relationships between them permitting to determine the restricted channel width and that of the unfinished spillway span, as well as some other parameters. The above criteria are obtained using dimensional analysis. It is essential to execute field inspections on passing of ice through structures with a view to derive similar design relationships since at present no complete general equations are available for describing the process in question. In the existing equations of the destruction of ice fields valid for some particular cases (K.N.Korzhasin, B.V.Proskuryakov, D.F.Panfilov et al), different coefficients are also usually defined from field or laboratory test data. Therefore prior to undertaking field investigations, one should consider the equations describing the interaction between an ice block and the water, the banks, structural elements and the air. This will permit to more completely include all the factors affecting ice discharge both during field investigations and while processing the data in order to derive design relationships.

As to the equations adduced by V.A.Koren'kov, it should be noted that:

1) the quantity B in the right-hand side of Eq. (2) is an erratum, therefore it should be excluded,

2) the quantity L in Eq. (2) whose numerical value should be sometimes predetermined may be approximately assumed from field data equal to $1.4 b_r$. Excluding B from and including $L = 1.4 b_r$ into the right-hand side of Eq. (2), we have

$$\frac{b_r}{B} = \frac{0.72}{1 + 0.35 \frac{B}{h} \cdot \frac{V_i^2}{R_f} \cdot \frac{\gamma_i}{g}}$$

where all the quantities are the same as in Eq. (2), i.e.

$\frac{b_r}{B}$ is the ratio of the restricted channel width to the total river width in front of the structure;

$\frac{B}{h}$ = river width-to-ice thickness ratio;

V_i = velocity of approach of ice floes to the restriction;

R_f = ultimate bending strength of ice determined on cantilever ice specimens of $b \times h \times 3h$;

$\frac{\gamma_i}{g}$ = ratio of the volume weight of ice to the acceleration of gravity.

If $\frac{b_r}{B}$ varies from 0.3 to 0.6 and $\frac{B}{h}$ between 100 and 1300, $\frac{V_i^2}{R_f}$ should be of the order of magnitude of 0.02-0.03.

Proceeding from the field results, we derived a formula for estimating $\frac{b_r}{B}$ as a function of $\frac{B}{h}$ only within the above range

$$\frac{b_r}{B} = 0.50 - 0.133 \cdot 10^{-3} \frac{B}{h}$$

With $\frac{B}{h}$ increasing from 100 to 1300, $\frac{b_r}{B}$ decreases from 0.49 to 0.33.

As regards the submergence of ice floes arrested against a floating ice cover (see the paper by M.S. Uzuner and J.F. Kennedy, and the discussion by P.M. Slisky), worthy of note is that this process as proved experimentally may develop in two forms:

- a) an ice floe is swept under the ice cover with its leading edge;
- b) an ice floe is submerged by rotating against the ice cover.

The latter situation is frequently observed when an ice floe moving at a high velocity comes to rest against the ice cover, and the wave

generated at the farther edge runs up on the floe and floods it. Thereupon the floe becomes unstable and is submerged by overturning.

The stability of an ice floe against the cover is governed by the ratio of forces acting on the floe and dependent on the flow and ice floe velocities, on the floe sizes and on some other quantities. Submergence of ice floes by rotation and without it is thoroughly investigated by V.F.Tsilikin in laboratory.

References

1. V.A.Koren'kov, Ice passage through hydraulic structures (field observation data). - IAHR Symposium "Ice and its action on hydraulic structures", Leningrad, 1972, p.117-122.

2. M.S.Uzuner, J.F.Kennedy, Hydraulic criterion for submergence of ice blocks. - IAHR Symposium "Ice and its action on hydraulic structures", Leningrad, 1972, p.81-85.

3. V.F.Tsilikin, Study of submergence of ice floes under partially opened spillway gates. - Izvestia VNIIG, v.76, Energia, 1964.

SPECIFIC FEATURES OF ICE FLOE BEHAVIOUR
IN THE VICINITY OF ICE RETAINING STRUCTURES

P.M. Slissky, M.Sc. (Eng.) Moscow Institute of Moscow, U.S.S.R.
Power Engng

Theoretical and experimental studies of certain phenomena occurring during the interaction between the flow, the ice and the structure, such as sweeping of ice under the structure were conducted at the Hydraulics Laboratory of the Moscow Institute of Power Engineering. Identical problems are considered in the paper by M.S. Uzuner and J.F. Kennedy. We carried out a more general investigation into the sweeping of ice under a structure with a vertical ice deflector which may be immersed in the flow at a depth other than the draught of the ice floe.

The problem was solved by constructing three static equilibrium equations: equations of total force projections on the horizontal and vertical axes, and the momental equation. However, from these three equations one cannot obtain for the ice floe under limit equilibrium conditions the four unknowns, viz. the draught of the downstream end of the floe, its trim, the pier response, and the flow velocity. The additional condition of the limit equilibrium of the ice floe is obtained proceeding from the assumption that the momental equation has two roots, and at a certain trim the solution reaches an extreme value. Hence the system of equations may be closed on the additional condition that the derivative of the momental equation with reference to the trim value be equal to zero. Thus a closed system of equations is set up corresponding to the limit equilibrium of the ice floe. The assumptions adopted by Uzuner and Kennedy which affect the rigorousness

of analysis are: 1) the application of the experimentally established fact that the moment the ice floe becomes unstable, the submergence of its upper surface is initiated; 2) determination of the flow depth from Bernoulli's equation.

Our own solution permits to draw the important conclusion that the ice floe does not remain motionless after stopping at the structure, but continually changes its trim due to a variety of causes, e.g. shedding of eddies in the flow round the end face of the ice floe, waves on the free surface of the flow, in case the ice floe fluctuations result in a trim of a value larger than either of the roots of the equation the ice floe will be swept under at a flow velocity less than the maximum one. Therefore, strictly speaking, one should not seek to determine the velocity at which the ice will be underturned, but rather the probability of its underturning at a given velocity. Hence the considerable scatter of experimental points even though the experimental routine be strictly adhered to.

The set of four equations constructed being too complicated for application in practice, a simplified approach was developed based on the assumptions that with the ice floe in the state of limit equilibrium no flooding of its upper surface occurred, and the draught of the downstream end of the floe was similar to that in still water. The former assumption is identical to the one accepted by Uzuner and Kennedy. Under the said assumptions the velocity is found from the momental equation.

Theoretical calculation data received by means of the simplified technique display a satisfactory agreement with experimental findings. However, for long narrow ice floes of low density, ρ^i , the basic assumption does not hold: our experiments indicated that such ice floes remained stable even with the upper surface submerged to a considerable depth. The range wherein the basic assumption is valid has not been established yet.

the backwater of a reservoir may be eliminated by inducing headwater level fluctuations. The method was checked up experimentally on the Dubossary reservoir and proved adequate.

Prof. B. Michel suggests that ice jams should be prevented by constructing special trestles for ice crushing and small dams for holding of ice. Note that ice crushing to eliminate ice jams is quite rational. Ice jams develop if ice floe dimensions exceed a certain river width section. From our viewpoint dam construction is not very promising since it is associated with costly concrete spillways.

Prof. E.G. Popov recommends to hold back ice on a narrow innavigable river by erecting groups of piles which may also serve as bridges. Prof. V.V. Piotrovich proposes to arrest ice on a river by a system of training dykes damming part of the river channel.

If the local topography is suitable, a bypass canal may be cut for lowering the ice-jam stage. The sill of such a canal should be within the backwater from the jam, and the lower end should be directed to the flood plane lake or to the river downstream, i.e. below the ice jam.

In conclusion it should be noted that based on the study of ice preventive measures advanced by Soviet and foreign scientists, the B.E. Vedeneev VNIIG devised complex schemes for flood control in the lower reaches of the Danube and Dniester Rivers.

STUDIES ON THE EFFECT OF ICE COVER ON TIDAL WAVE
PROPAGATION IN THE WATER AREA OF
A TIDAL POWER PLANT

I.A. Shlygin, Eng. The S.Ya. Zhuk "Gidroproject" Moscow, USSR
Institute

In 1968 the experimental Kislogubskaya water power plant, the first tidal plant in the Soviet Union, was commissioned in Motovsky Bay, in the Barents Sea. Favourable operation experience as well as the results of investigations performed there point to the significance of tidal power development for the future.

At present the feasibility of construction of large tidal power plants in the White and Okhotskoye Seas is contemplated. The hydroelectric potential of these seas is considerable. However all the regions promising from the point of view of tidal power development are characterized by severe ice conditions.

The results of exploitation and research carried out in the Kislaya Guba, Lunbovsky and Mezensky Bays since 1959 up to the present moment indicate that here the ice conditions do not present unsurmountable obstacles to constructing power plants. However all the investigations performed were confined to the direct action of ice on the structure : piling-up, friction, dynamic impact, etc, while in the design of large tidal power plants the indirect ice action, in particular, effect of ice cover on the tide range are to be also taken

into account.

The effect of ice cover on the tidal wave has been relatively long studied by oceanologists.

The necessity of adequate calculation methods was emphasized by Prof. N.N. Zubov in the 1930ies-1940ies. Prof. Zubov pointed out the fact that in some areas of tidal seas, e.g. in the Mezensky Bay the stable ice cover decreases the tide range by 2.5-3 times as compared to that in summer. In the central part of the White Sea only fragmented ice is observed, but it also reduces the range of the tidal wave by 1.5 to 2 times at Arkhangelsk.

Later-on the problem of the ice cover effect on the amplitudes and phases of tidal wave components was to some extent solved for Arctic Seas in the works by I.V. Maksimov. Were established the coefficients, M_2 and K_1 , taking account of the variation of wave parameters at different water depths.

In a general case the amplitude of the tidal wave at the end section of its path under the ice cover equals

$$A_1 = A \sqrt[4]{\frac{H}{H_1}} - \eta S \ell$$

where A_1 and A are tidal wave amplitudes at the initial and final sections of the way, respectively

H_1 and H are water depth at the initial and final sections of the path

η is coefficient of wave "damping"

ℓ is path length under the ice cover

S is ice cover thickness.

According to Maksimov the ice cover causes occasionally an increase in the tidal wave amplitude due to varying of the parameters of the amphidromic system of the sea covered with ice. But the problem is not acute for relatively small water areas of tidal power plants where the influence of the ice cover on the amphidromic system is negligible.

Though long wave propagation under the ice had been for years studied by fluvial hydraulics specialists, the problems correlating amplitudes and phases of long waves propagated with and without the ice cover were considered to be of secondary importance.

The tidal plant design group of the Gidroproekt Institute, the Leningrad Department, performed a study on the tidal wave propagation in the Kislaya Guba both in the presence and absence of the ice

cover under comparable initial conditions.

The experiments were carried out in winter and in summer conventional devices being used for determining surface elevations. Practically analogous patterns of tidal wave propagation with and without the ice cover were established. The theoretical treatment of the results obtained only proved that the ice cover does not affect the wave propagation in the almost circular water basins of about 1 km² area and 35 m depth which was the case in Kislaya Guba.

The morphometric parameters of water areas promising for the construction of large tidal power plants are quite different: the Mezensky Bay has 800 sq. km area and 5-10 m depth, the Penzhinsky Bay is more than 6 000 sq. km and 10-15 deep. It is obvious that at large tidal power plants with water areas exceeding thousands of square kilometers of 10 to 15 m depth the ice cover will significantly affect the tidal wave propagation.

The problem is most important in designing tidal power plants because its proper solution will determine the output of electric power under winter conditions.

To solve the problem in question means to derive theoretical and empirical design equations for tidal wave propagation over water areas of tidal power plants with and without the ice cover.

References

1. Zubov N.N. Dynamic oceanology, Gidrometeoizdat, 1938.
2. Investigation of unsteady flow in the Svir River under winter and summer conditions, Gidrometeoizdat, 1963.
3. Maksimov I.V. On the dependence of tide elements on the ice cover of the sea. Uchenye Zapiski VAMU, Vyp. 4, 1953.
4. Ruppert M.L. On the influence of the ice cover on the velocity of release wave propagation, Trudy GGI, Vyp. 117, 1964.

FIELD DATA ON ICE DAMMING AND ICE JAMMING

A.N.Chizhov The State Hydrological Institute Leningrad, U.S.S.R.

At present the mechanism of ice damming is being investigated, with the physico-mechanical and hydraulic conditions of the process taken into account. Analytical, experimental and model studies are aimed at determining the critical parameters of ice dams and the flow for predicting the scale of the above phenomenon under different conditions.

According to the mechanism of their formation, ice dams are divided into those caused by hummocking and those formed by ice blocks being submerged by the stream and swept under the ice edge. In the application of investigation results on the ice-damming mechanism the phenomenon under study is to be referred to either of the above groups. Therefore it should be useful to summarize the great body of field data accumulated in the U.S.S.R., to describe typical schemes of the formation and occurrence of ice dams and jams. For a better understanding of the problem it is necessary to draw a distinction between the phenomena of ice damming and ice jamming in conformity with the terminology adopted in the U.S.S.R.

Ice jams form of frazil and slush ice in supercooled water during the freeze-up period at low water stages and sub-zero air temperatures, while ice dams form of thick but rather weak ice floes during the spring at the break-up period associated with floods at above-zero water and air temperatures. These features account for the difference between the mechanisms of ice jamming and ice damming.

The main types of the mechanism of ice jamming and ice damming can be established based on observation data obtained in different seasons

on various rivers in the U.S.S.R.

Ice jams are peculiar to the majority of large and medium rivers in this country. During the formation of an ice cover relatively high water stages are frequently observed at different river stretches. However, inundations due to ice jamming are comparatively rare because of low water stages at this period.

Ice jamming is most commonly associated with the progression of the ice cover edge upstream, its extension rate decreasing in the river reaches with strong currents. Part of frazil or ice blocks are swept under the ice edge restricting the river cross-section. A similar process takes place during the formation of ice bridges, some growing to such an extent as to obstruct the passage of ice under them. With the development of a sufficient high backwater ice jamming ceases in both cases. Then ice blocks stop against the ice edge and freeze together to extend the ice cover.

Similarly, ice jams due to sweeping frazil under the ice cover occur downstream from large polynyas remaining unfrozen for a long time. In contrast to ice accumulations of large ice blocks, frazil ice jams deteriorate with the decrease in the discharge of frazil under the ice cover.

Ice jamming in mountain rivers has its specific features. A backwater is created by an ice bridge with frazil ice frozen to its under side, frazil ice accumulations come to rest against the ice cover edge. With the progression of the frazil ice cover upstream ice pushes occur intermittently, and the thickness of the cover increases many times over with each push due to the looseness of the frazil. As the backwater zone propagates upstream, new accumulations of ice stop against the ice edge. During ice pushes part of frazil ice is entrained by the flow under the ice jam which is in a state of dynamic equilibrium, frazil accumulations being destroyed and forming again beneath the whole length of the jam. The destruction of the ice jam commences when the frazil discharge decreases, with a consequent decrease in the growth of the ice jam length. The thickness of the jam increases together with its length, reaching in some rivers from 10 to 15 m.

Mention should be made of the ice-jam stage rise due to increased production of bottom ice. Such ice jams, however, are usually not very large.

The phenomenon of ice damming is inherent in many rivers in the U.S.S.R. The process attains its maximum scale and frequency on the rivers in which the break-up and spring flood progress towards the river

mouth. Ice damming is mainly due to hummocking of either ice fields and large ice floes, or of fragmented ice fields.

At the early stage of the break-up ice pushes set in motion large ice fields, which break-up and form hummocks when stopped. This is the period when the head of the ice dam is formed, creating a backwater zone with slow currents.

The ice fields and ice floes floating downstream come to rest against the ice cover edge. As soon as the length of the ice field thus formed reaches a magnitude at which the drag force of the flow exceeds the stability of the ice blocks, intensive hummocking and haphazard rafting occur in the already broken ice field. These two types of hummocking are characteristic of the majority of ice dams. However, in rivers channels with a slight fall a single-layer ice cover of fragmented ice may extend over scores of kilometers.

The fundamental difference in the ice damming process on different rivers lies in the conditions under which ice obstacles engendering ice dams form. On large plain rivers and at the end of the backwater zones of reservoirs massive ice dams usually develop as a result of a delayed break-up at individual reaches. On rivers of medium size ice dams are due to blocking of the river channel by ice fields and large floes in places whose particular shape hampers ice passage during ice pushes.

The description of ice damming presented herein is by no means complete. For instance, the cases of ice damming and ice jamming downstream from hydropower plants and ice damming from consolidated masses of floating ice from a broken upstream ice dam are not considered here.

PENETRATION OF ICE BLOCKS IN THE
STILLING BASIN OF A DAM

José Llamas, Ph.D.
Professor of Hydrology

Université Laval

Québec
Canada

SUMMARY

The stilling basin of a dam is usually designed in order to dissipate the kinetic water energy. However, when the ice blocks pass over the spillway their penetration in the basin can be greater than the design depth and under this condition the impact with the downstream revetment may damage seriously the structure. The stilling basin is created naturally by the downstream level of water or by a sill. In this case the length of the basin must be greater than the horizontal path of the ice block. The objective of this study is to evaluate the block trajectory and determine the main factors affecting the block position under several hydraulic and structural conditions.

RESUME

Les bassins à l'aval des déversoirs sont conçus pour dissiper de façon optimale l'énergie cinétique de l'eau par la formation d'un ressaut hydraulique. Or, lorsque des blocs de glace accompagnent l'eau dans la chute, il est possible, et l'expérience l'a souvent montré, que la pénétration de la glace soit plus grande que la profondeur du bassin, et, par conséquent, ces blocs risquent d'endommager et même de détruire complètement le radier aval. Quelquefois, il arrive que ce bassin de dissipation est créé naturellement par la profondeur aval de la rivière. Dans ce cas on peut dissiper l'énergie cinétique de l'eau au moyen de blocs de béton situés à quelque distance en aval du point d'intersection du radier avec le parament aval du déversoir. Dans ces conditions, il est nécessaire d'étudier aussi la trajectoire horizontale des blocs de glace pour éviter l'impact avec les dissipateurs.

1- INTRODUCTION

The penetration phenomenon is illustrated on figure I which shows a typical section of a spillway and the trajectory of the ice block.

In order to calculate this trajectory, the following hypothesis has been considered:

- a) The velocity of the ice block at the intersection with the basin level is the same as the velocity of falling water at this point. That means that no contact exists between the block and the spillway face. This hypothesis is a realistic one because the phenomenon occurs late in spring and at this time the discharge is usually high.
- b) Only the blocks having simple forms, like cubes or rectangular parallelepipeds, are considered in this study.
- c) The water velocity in the stilling basin is supposed to be zero. In this condition the block trajectory is not affected by any external component.
- d) Regarding the trajectory computations, the block mass is supposed to be concentrated in its center of gravity. In this case, no time occurs between the first contact of the block with the basin level and its total submersion.

2- PENETRATION MECHANISM

The movement of the ice block in the basin is governed by two main forces: the lifting force and the drag force.

The lifting force depends on the difference between the water and ice densities.

$$P = V(\gamma_w - \gamma_{ic})$$

Where V = volume of ice block (ft^3)
 γ_w and γ_{ic} are respectively the densities of water and ice (lb/ft^3).

The drag force depends on block velocity and block dimensions

$$F = C_d \rho A \frac{v^2}{2}$$

v is the relative velocity of the block with respect to the water velocity (ft/sec)

C_d = coefficient of drag resistency (dimension less)

ρ = density of the fluid ($\text{lb}\cdot\text{sec}^2/\text{ft}^4$)

A = area projected on a plane perpendicular to the motion of the block (ft^2).

The coefficient C_d depends upon Reynolds (low and intermediate velocities) and Mach Numbers (high velocities). The following table illustrates the variation for certain geometric shapes.

Form.	C_d	A	AC_d
	2.00	l	$2l$
	1.60	$l\sqrt{2}$	$2.26l$
	1.39	$l\sqrt{2}$	$1.94l$

3- DIFFERENTIAL EQUATION OF THE MOTION

Beginning with the Newton's law $F = ma = m \frac{dv}{dt}$ the equations of the block motion can be derived

a) Downward movement:

$$Kv^2 + P = \frac{mdv}{dt} \quad \text{with} \quad v = \frac{dz}{dt}$$

z is the depth of the block at time t .

$$\frac{m d^2z}{dt^2} - K \left(\frac{dz}{dt}\right)^2 - P = 0$$

With initial conditions:

$$v = -\sin\alpha \sqrt{2gH} \quad \text{and} \quad z = 0 \quad \text{at} \quad t = 0$$

Where

H is the total head

α is the slope of the spillway

b) Upward movement:

$$\frac{m d^2z}{dt^2} + K \left(\frac{dz}{dt}\right)^2 - P = 0$$

Initial conditions: $z = z_{\min}$ and $v = 0$ at $t = 0$

c) Horizontal movement:

$$\frac{m d^2x}{dt^2} - K \left(\frac{dx}{dt}\right)^2 = 0$$

Initial conditions: $v = \cos\alpha \sqrt{2gH}$ at $t = 0$

The solutions of these differential equations are:

a) Downward:

$$v = \sqrt{P/K} \operatorname{tg} \frac{(t+C_1)\sqrt{KP}}{m}$$

with

$$C_1 = \frac{m}{\sqrt{KP}} \operatorname{arctg} (-\sqrt{2gH} \sqrt{K/P} \sin\alpha)$$

The depth of block is

$$z = \frac{-m}{K} \ln \cos \frac{(t+C_1)\sqrt{KP}}{m} + C_2$$

with $C_2 = \frac{m}{K} \ln \cos \frac{C_1\sqrt{KP}}{m}$

b) Upward:

$$v = \sqrt{K/P} \left[\exp \frac{2\sqrt{KP}t}{m} - 1 \right] \div \left[\exp \frac{2\sqrt{KP}t}{m} + 1 \right]$$

$$z = \frac{m}{K} \ln \left[\exp \frac{\sqrt{KP}t}{m} + \exp \frac{-\sqrt{KP}t}{m} \right] + C$$

where $C = z_{\min} - \frac{m \ln 2}{K}$

c) Horizontal:

$$v = \frac{-m}{K(t+C_1)} \quad \text{with} \quad C_1 = \frac{-m}{K\sqrt{2gH} \cos \alpha}$$

$$x = \left| \frac{-m}{K} \ln (t+C_1) \right| + C_2 \quad \text{with} \quad C_1 = \frac{m}{K} \ln C_1$$

The trajectories and velocities of different ice blocks and water heads were calculated in APL language in IBM-360 computer. The results are shown on figures 2 to 10.

In order to verify the theoretical study and also to emphasize the influence of the main parameters of the ice and the spillway with the block trajectory, and the block impact upon the revetment, a series of experiments were performed on a scale model. One of the objectives of this experimental study was to find the design criteria to minimize or eliminate the possible damages on the dams due to block impact.

The experiments brought out the following facts:

a) The risk of impact increases (in this order) with

- the length of ice block
- the reduction of water head
- the thickness of block
- the ice density (small effect).

b) The radius of the transition between the downstream face of the spillway and the basin (cylindrical transition), has no effect on the impact.

c) The risk of impact in a spillway having cylindrical transition, under free and submerged discharge, are roughly the same.

Figure 11 shows the spillway of Sartigan Dam (Chaudière River, Quebec) and the trajectory of an ice block having standard dimensions. In this case the observation of the block path particularly the impact point gave a very good agreement between the prediction (computed by theory) and the real situation.

REFERENCES

- 1- Streeter, Victor L. - Fluid Mecanic (1962) McGraw-Hill Book Company Inc. N.York
- 2- Pouse, Hunder - Engineering Hydraulics (1949) John Wiley & Son Inc. N.York
- 3- Richesses Naturelles - Plan d'ensemble des travaux rémédiateurs de la rivière Chaudière. Rapport R-1 (1965) Quebec
- 4- Llamas, José et Demers, Claude: "Etude sur la pénétration des blocs de glace". Ministère des Richesses Naturelles, Québec. Rapport R-8 (1969).
- 5- Gallez, Bernard: "Etude du passage de blocs de glace au-dessus des barrages déversoirs". Rapport non-publié (1971), Sherbrooke.

TRAJECTORY OF ICE BLOCK

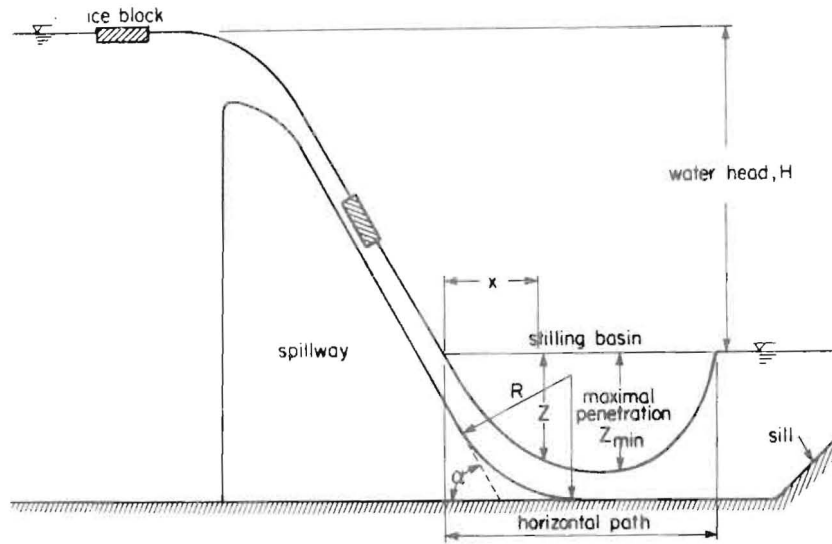


Figure 1

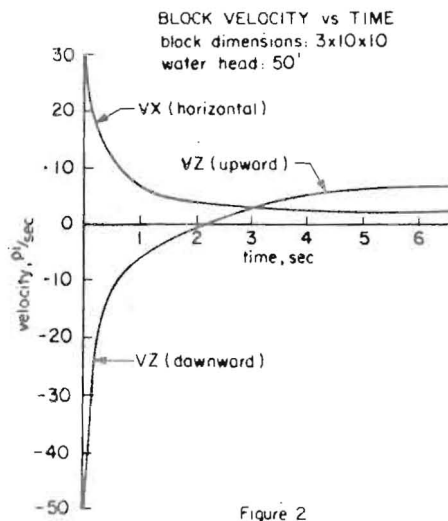


Figure 2

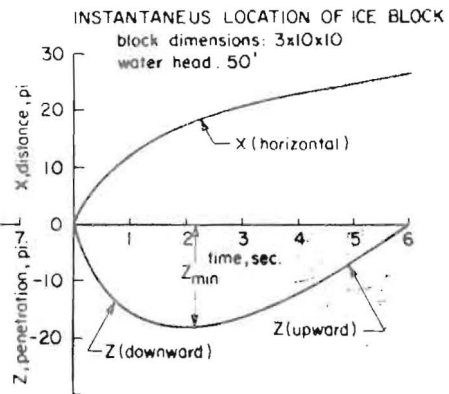
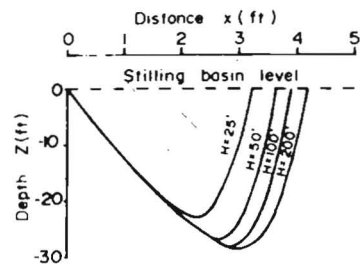
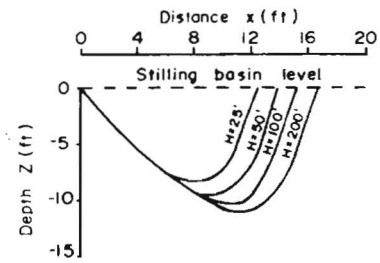


Figure 3



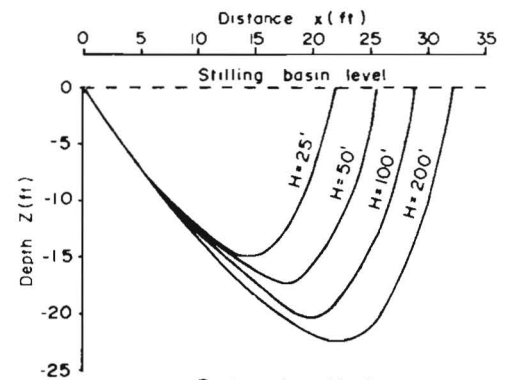
Cubic block
Dimensions: 1' x 1' x 1'

Figure 4



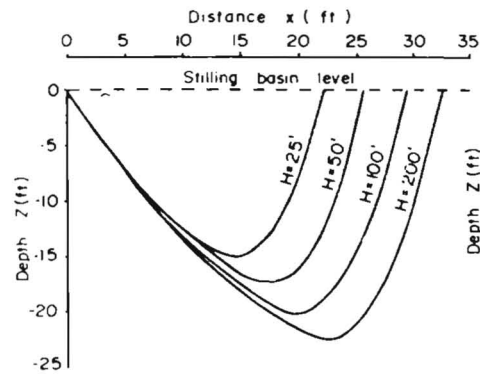
Rectangular block
Dimensions: 1' x 5' x 5'

Figure 5



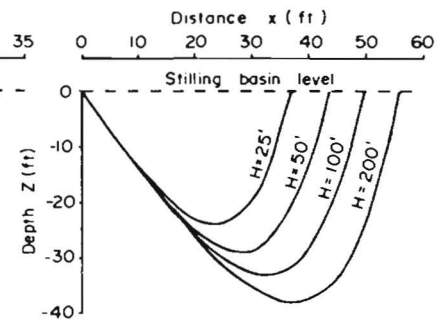
Rectangular block
Dimensions: 1' x 10' x 10'

Figure 6



Rectangular block
Dimensions: 3' x 10' x 10'

Figure 7



Rectangular block
Dimensions: 3' x 20' x 20'

Figure 8

ICE BLOCK TRAJECTORY
IN A STILLING BASIN

Parameters:

- Water head H (ft)
- Block dimensions

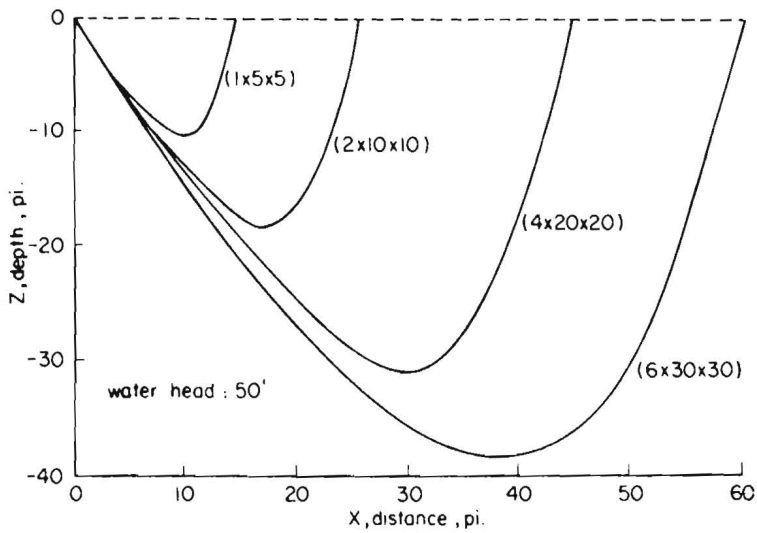


Figure 9

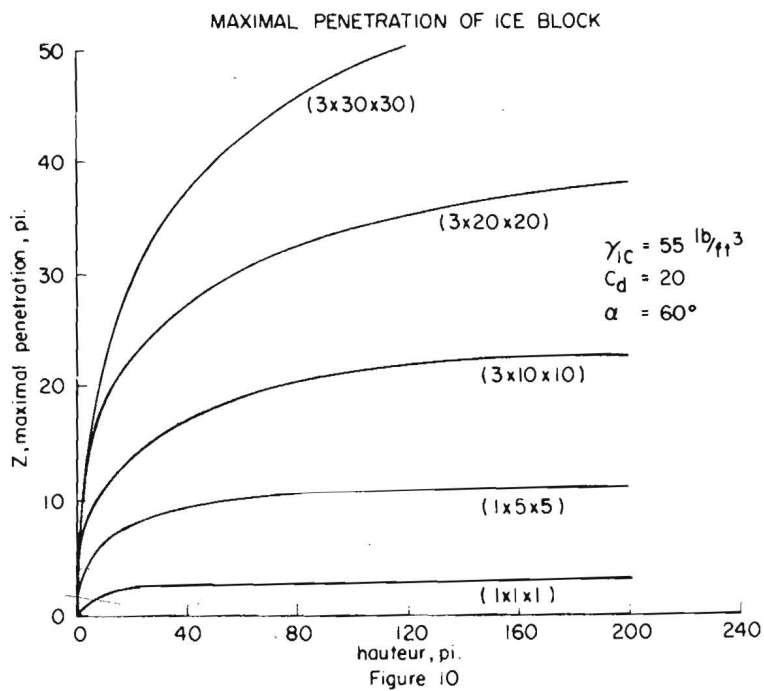


Figure 10

SARTIGAN SPILLWAY (CHAUDIERE RIVER)

TRAJECTORY OF ICE BLOCK (1.5' x 10' x 10')

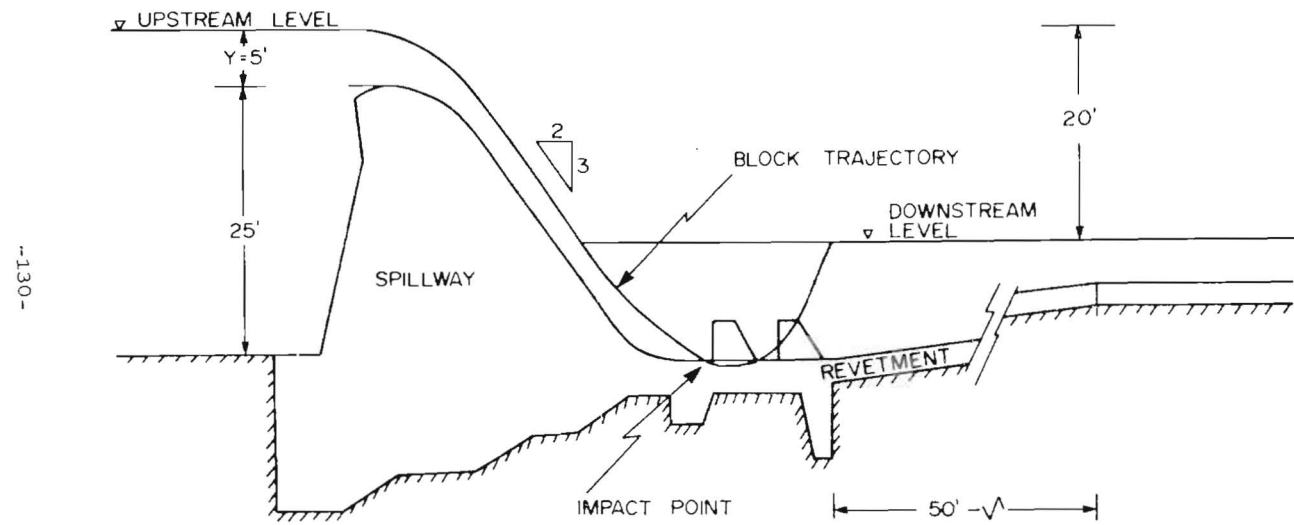


Figure 11

SCALE 1" = 10'

ESTIMATION OF THE VARIATION IN THE ICE REGIME
ON REGULATED RIVER REACHES

R.V. Donchenko, M.Sc.(Eng.) GGI Leningrad, U.S.S.R.

The specific pattern of the ice regime is governed by the changed hydraulic and morphologic characteristics on regulated river reaches.

At the end of the backwater due to abruptly decreasing velocities at the transition from fluvial to reservoir regime ice dams and ice jams are likely to form.

The ice conditions downstream from structures are unstable during the whole winter with a sequence of different ice phenomena replacing one another.

As compared to rivers, water storages are characterized by a much wider range for coefficients of water masses mixing, viz. from $0.1 \text{ cm}^2/\text{sec}$ for no-wind situations and up to $800-1000 \text{ cm}^2/\text{sec}$ at wind velocities exceeding 15 m/sec . Hence different freezing processes occur depending on the rate of ice generation, the place (the water surface or deep-water layers) where the ice is produced, the type of ice (surface or underwater ice) and the length of the freeze-up period that ranges between 1 to 3 or 10 to 15 days.

Frazil ice production takes place in storages at wave forces above 2. A special program for studying frazil ice formation carried out at the Kakhovka water storage during the winters of 1969/70 and 1970/71 indicated that frazil ice was produced with surface heat loss to the atmosphere of more than $200 \text{ cal/cm}^2/\text{day}$ and mixing of water masses in excess of $20 \text{ cm}^2/\text{sec}$, which results in vertical heat exchange accompanied by mechanical disturbances precluding agglomeration

of ice crystals. Turbulent mixing is conducive to supercooling of the waterbody (the maximum supercooling recorded was $-0,04^{\circ}\text{C}$), hence ice is formed at different depths: in the waterbody and at the bottom. The combined effect of the heat transfer and of turbulent mixing on the ice formation pattern across the depth may be given as

$$P_z = \frac{S}{\sqrt{\eta \cdot m}} \frac{ch \frac{H-z}{\sqrt{\eta \cdot m}}}{Sh \frac{H}{\sqrt{\eta \cdot m}}}$$

The uniform distribution of the ice formation rate across the depth depends on wave height and the heat flux density per unit depth. For the Kakhovka water storage conditions the ratio between the depth of intensive ice generation and the wave height is 0,11. At a 3,2 m wave height of 1% probability the correlation between bottom and surface ice formation is 1:3. In the Kakhovka water storage frazil is produced in the form of irregularly shaped or rounded plates of a 0,5 to 1 cm diameter up to 1 mm thick, and a fall velocity from 2 to 4 cm/sec. With the ice production rate increasing, and due to mechanical clustering of individual plates, the fall velocity grows and frazil rises to the surface as sludge balls of 30 to 50 cm diameter and a density of 0,30 to 0,40 g/cm^3 . The frazil flocs cluster together forming a frazil cover which drifts across the reservoir under the action of the wind, the wind velocity being from about 0,10 to 0,40 cm/sec. At high wind velocities frazil ice ridges from 2 to 3 m high form at the leeward shore. Mixing decreases inversely to ice concentration, a frazil ice cover being formed of frazil accumulations. As a rule there is a 1 to 5 m thick layer of floating frazil with a density from 0,22 to 0,40 g/cm^3 underneath the ice cover.

Intensive frazil ice production can be observed in some other water storages of the Dnieper cascade (viz. those named after V.I.Lenin, and the Kremenchug) and serious difficulties ensue in the operation of hydroelectric plants. Conditions of frazil generation downstream from dams materially differ from those in natural water bodies due to enlarged water discharges and later ice formation commencement.

Data obtained downstream from the Volga hydropower plant named for the XXIIInd Congress of the CPSU revealed that the ice cover was formed after the development of a chain of ice jams. As compared to natural conditions the total ice volume in the ice jams increased two or three-fold, simultaneously the mean velocity of the ice cover edge

drift along the length of the downstream pool dropped to 8,5 km/day. The rise in water stage due to ice jams is a function of the water discharge. The larger the water discharges, the greater the rises in water stages and heads. The peak mean diurnal heads range from 2,2 to 4,4 m (for a site 19 km downstream from the power plant) and from 2,4 to 5,0 (for a site 63 km downstream).

With water discharges growing $1\frac{1}{2}$ to 2 times larger, the winter discharge coefficients in the vicinity of the dam (19 km downstream) increased only slightly as against natural conditions, while at remote sites the coefficients were diminished.

Regulation of the power plant winter operation regime with reference to the ice phenomena development is one of the corrective measures for alleviating ice troubles.

ICE TROUBLE PREVENTION ON THE DANUBE RIVER

Dr. R. Rozhnoy Water Resources Department Budapest, Hungary

This contribution deals with the description of preventive measures against ice troubles on the Danube river.

Frequent floods due to ice jams cause considerable damage to the national economy of the Hungarian People's Republic. During the recent decades (in the years of 1940, 1941, 1956) devastating floods occurred on the Danube.

The problem of combatting such floods may be solved in the two following ways: either through modification of the river bed morphology by regulating the water course, or through active demolition of the ice cover.

The most effective methods of river ice destruction used in the Hungarian People's Republic are the application of ice breakers and of blasting.

The development of the ice breaker fleet in the country has commenced since 1954. At present the ice breaker fleet of the Hungarian People's Republic numbers 20 modern ships, which provide a continuous ice passage, delay the beginning of freeze-up and prevent ice jamming during the ice run. In the freeze-up period ice breakers ensure an ice-free navigation channel 30 to 40 m wide in the solid ice cover and keep it throughout the winter. Besides, ice breakers destroy ice jams. During the severe autumn ice runs on the Danube river, when heavy ice jams up to 4 m thick form that cannot be demolished by ice-breakers, blasting is applied. The Hungarian Water Resources Department has developed a series of up-to-date blasting methods.

ICE-PRESSURE ON TOWER STRUCTURES IN THE RESERVOIRS

Dr. Ladislav Votruba, Prof., Ing., Dr. Sc. Technical University Prague
of Prague C.S.S.R.

In the Czechoslovak as well as the world-wide construction of dams the designs of tower structures fulfil as a rule several functions: those of the lower outlet, spillway, water intake and hydroelectric power plant. These so-called combined plants are economically advantageous: during the recent two decades, a number of them have been built in Czechoslovakia. About half of them have the form of towers about 60 metres high, with outside diameters ranging between 5 and 20 metres.

It is chiefly the horizontal forces that represent a threat to the stability of such towers. With them is also classed the ice-pressure, the static moment of which with respect to the critical profile by the bottom of the reservoir is, for the length of the lever of force ranging between 20 and 50 metres, great indeed. This load calls for a robust steel reinforcement of the tower. From the angle of the economy of the structure it is therefore essential to have a precise knowledge of the pressure of ice on a high tower standing isolated in a reservoir and separated by a distance of a few dozens of metres from the dam or from the bank.

To know the pressure of ice on the tower is also of importance in the cases when the tower is well protected against the effect of ice. In Czechoslovakia we have been successful in using pneumatic protection, i.e. protection by bubbles of compressed air from a piping surrounding the tower several metres below the water level. In one case where such a protection was not installed, subsequent pumping of the water around the tower from the lower strata of the reservoir was resorted to.

FAILURE OF THE TOWER STRUCTURE OF THE KORYČANY DAM

On January 24, 1963, in the lower section of the tower of the Koryčany earth dam, 25 metres tall, built on the Stupávka water stream, a horizontal crack was observed. The works were put into operation in 1957 (Fig. 1).

The tower has a circular cross-section with an inner diameter of 340 cm and thickness of the concrete wall of 70 cm. An armature chamber, 110 cm wide, with a 20 cm concrete wall is attached to the tower.

The crack formed on elevation 297.60, with the water level at 305.60, therefore no more than 8 metres below the ice sheet. The crack affected two thirds of the circumference of the tower in the direction towards the reservoir.

The static pressure of the ice was the immediate cause of the crack. After the ice had been cut, the tower assumed its original position and the crack closed. It is of course possible that also other forces concurred, such as the uplift in the construction joint of the wall, the eccentric pressure of the ice sheet in the vertical direction.

The thickness of the ice was 49 centimetres, the thickness increasing in the direction toward the reservoir. The crack formed after a sudden temperature increase from -17°C to -2°C within 24 hours.

Fig. 2 illustrates the scheme of action of forces on the Koryčany tower structure, and table No. 1 tabulates the results of the calculation of stresses in the footing bottom of the structure, and in the cross-section of the crack.

Table No. 1
Stresses from ice-pressure P in the Koryčany tower structure

Dimensions /m/	Load G, P, W_x Stresses σ_1, σ_2	For
	$l_p = 18.6 \text{ m}$	$x_p = 8.0 \text{ m}$
$t_1 = 0.2$	$G = 468 \text{ Mp}$	277 Mp
$d_1 = 2.2$	$l_G = 2.62 \text{ m}$	2.62 m
$t_2 = 0.7$	$P = 48 \text{ Mp}$	111.3 Mp
$d_2 = 3.4$	$l_p = 18.6 \text{ m}$	8.0 m

Dimensions /m/	Load G, P, W_z Stresses σ_1, σ_2	For
	$l_p = 18.6$ m	$z_p = 8.0$ m
$h = 21.0$ (12.4)	$W_z = 91$ Mp	78.3 m
$H = 18.6$ (8.0)	$\sigma_1 = + 8.2$ kp/cm ² $\sigma_2 = - 12.9$ kp/cm ²	+ 10 kp/cm ²

Symbols: G - gravity

W_z - upward lift

For a footing bottom at the depth of $H = 18.6$ metres, and for the ice-load $P = 48$ Mp (10 Mp/m) we obtain tensile stress at point l $\sigma_1 = 8.2$ kp/cm².

For a cross-section in the place of the crack, at the depth $H = 8.0$ m and for the assumed low strength of the concrete in the construction joint of 10 kp/cm², we obtain the required ice-pressure $P = 111.3$ Mp, i.e. 23.2 Mp/m.

Detailed analyses were not carried out inasmuch as the scheme of action of the ice-pressure on an isolated tower structure was not known.

The reconstruction was simple: cement grouting of the crack from short holes. The experience gained at Koryčany resulted in the conclusion that the tower structure should be protected against ice-pressure, even though the latter be not very high.

DISCUSSION OF THE PROBLEM OF ICE-PRESSURE STABILITY OF TOWER STRUCTURES

In the case of a deep reservoir with a low through flow, as the most adverse effect of the ice on the overall stability of the tower structure we regard ice-pressure that is due to the temperature increase of the ice sheet.

In general, ice-pressure on a tower structure is different from that acting on a plane wall having the same width, and it is not possible to

determine it unambiguously beforehand. The following simplifying assumption can be introduced:

a) The planar problem in a vertical cross-section normal to the face of the dam (Fig. 3a). This assumption is the simplest to solve. From sector L_1 (between the structure and the dam) and sector L_2 (between the structure and the end of the dam backwater) the structure shall be acted upon by the difference in pressures $P_1 - P_2$.

The following will come into play:

- the length of sectors L_1 and L_2 ,
- rigidity of support at points A and D,
- different thicknesses of the ice in sectors AB and CD,
- rigidity of structure proper,
- system of cracks in the ice sheet.

b) Planar problem in horizontal cross-section at the level of the ice sheet (Fig. 3b).

From the schematic ground plan it is evident that:

- the resultant of all the pressures acting upon the structure may have an arbitrary direction, as a result of the rigidity of the support of the ice sheet along its circumference and the distance of the structure from the banks;
- the overall pressure of the ice does not have to be the result of the ice sheet width alone, equal to the diameter of the tower, for a rigid structure may draw on to itself the pressure of ice from a greater width.

c) Passive resistance of the ice sheet against the direction of the resultant of the ice-pressure. We are facing force P_2 from the supposition a), which may acquire a variety of values theoretically within the entire range $0 \leq P_2 \leq P_1$, evidently augmented in the sense of supposition b).

There are three possible methods of solution of the problem:

- theoretical calculation
- laboratory research
- measurement in the field

In the theoretical calculation, if the problem is to be mastered analytically, a number of simplifying premises have to be resorted to. The reciprocal action between the ice sheet and the tower structure must be solved by iteration.

Also the laboratory research of the pressure of ice on the tower structure exhibits numerous simplifications. On our model (Fig. 4) we

modelled the ice sheet by a slab from low-module modurite. The increases of air temperature were modelled by means of infrared radiators. We measured absolute deformations of the ice sheet and tower, and stresses in the ice sheet and the tower wall. The model permits, in particular, to inquire into the influence of different degrees of rigidity of the support of the ice sheet upon the "banks".

Measurement in the field entails difficulties, but this method alone can yield dependable results. We prepare measurements of horizontal and vertical shifts of points on the ice cover of several reservoirs where we can expect a slight change in the level in course of several winter weeks. In our country no such measurements have as yet been carried out, nor do I know the results of similar measurements from international practice.

CONCLUSION

The problem of the ice-pressure upon isolated tower structures in the reservoir has not as yet been satisfactorily solved. The failure of the structure of the Koryčany dam bears testimony to the importance of the problem. Work was begun on the investigation of the stresses in a tower structure caused by ice by three different methods: theoretically, on a model, and by measurements in the field.

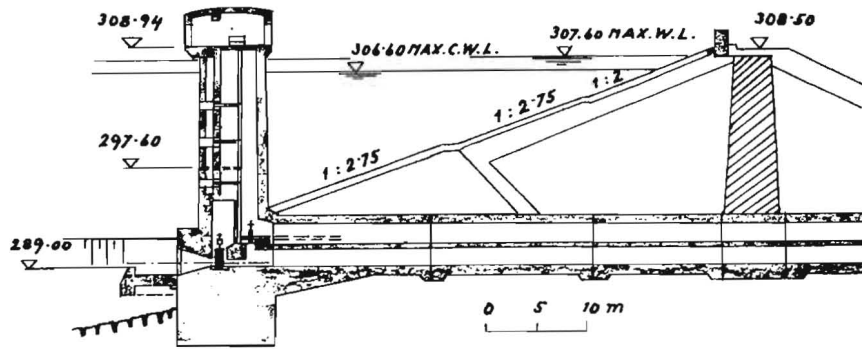


Fig. 1 Tower structure of the Koryčany dam

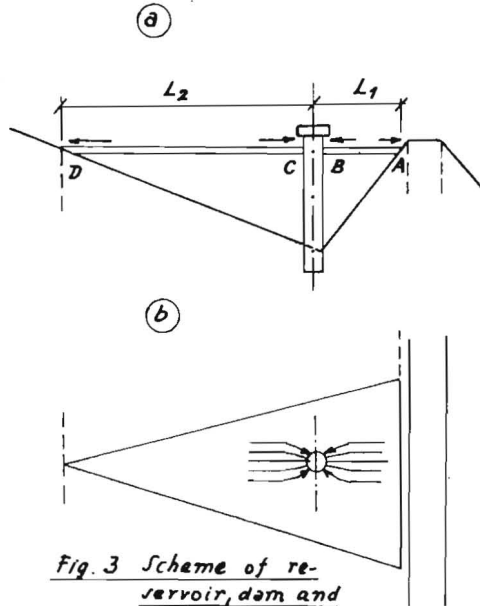


Fig. 3 Scheme of reservoir, dam and structure

- a) Vertical cross-section normal to the face of the dam
- b) Ground plan

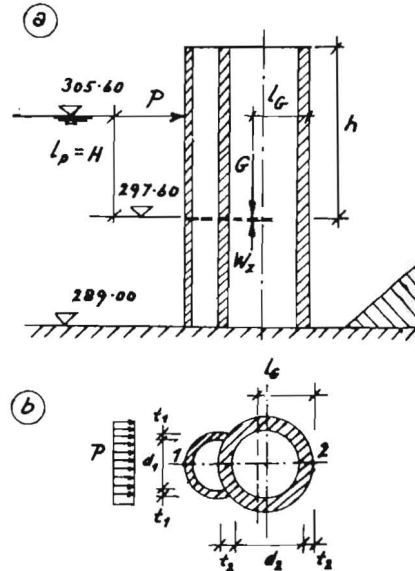


Fig. 2 Diagram of forces acting upon the structure of the Koryčany dam

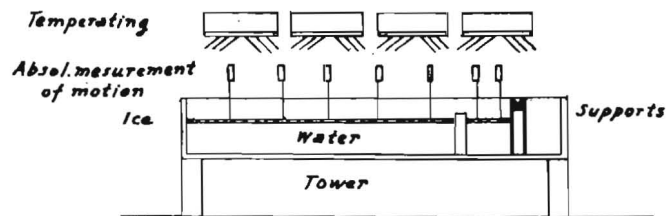


Fig. 4 Scheme of model

INVESTIGATION OF HEAT INFLOW TO A MELTING
ICE COVER ON RIVERS

V.M. Timchenko
M. Sc. (Eng.)

The Far Eastern Research
Hydrometeorological Institute

Vladivostok
U.S.S.R.

The break-up dates on rivers depend largely upon the intensity of the heat inflow to the ice cover from the environment, the contribution of heat transferred from the water masses to the under side of the ice cover in spring being of great significance.

The methods of determination of all the components of the heat flow to the under side of the ice cover, other than the heat transferred by snowmelt are well known. Therefore it should be emphasized that an acute need is felt of the evaluation of the amount of heat incoming from snowmelt, which is an intricate problem, since no information is available concerning the methods of its calculation. The problem in hand presents difficulties mainly because of scarcity of observation data on water temperatures in seasonal streams required for a better understanding of the temperature regime of snowmelt runoff.

Field measurements of the heat flow to the under side of the ice cover in the Ussuri river showed that a considerable amount of heat is transferred to the river with the runoff during intensive snowmelt, its contribution being in some cases several times that from other components of the heat water balance.

The total amount of the heat inflow to the under side of the ice cover was estimated by well-known formulae of thermodynamics based on the mean water temperature measured over the cross-section, the flow rate and the depth. Then the heat inflow components were estimated, namely, penetrating solar radiation heat transferred from the ground waters and the river bed, as well as the heat due to energy dissipation of the undercover flow. The difference between the total heat inflow and

the sum of the above heat components is assumed to be the heat inflow from thawing waters.

The relationship between the magnitude of the heat inflow and the rate of snowmelt runoff was analyzed.

The effect of water temperature in seasonal streams on the magnitude of the heat inflow to the under side of the melting ice cover was evaluated.

dispenses with the need in special structures for the passage and accumulation of frazil.

During a study into the vortex-type flow on a dam model a permanent vortex funnel was obtained.

A plate (which we termed a vortex producer panel) obstructed the forward flow and caused the formation of a vortex funnel. The specific features of motion in the funnel modify the free surface and circulation patterns, etc.

To evaluate the flow velocity measurements were performed both in the funnel and upstream from it. The data recorded were used to plot velocity distribution curves showing the fluid velocity in vortex funnels to increase both when approaching the center line, and with the depth.

The central portion of the funnel (the so-called "core") free from the fluid has a non-uniform section diminishing downward.

The fluid velocity (V , m/sec) in the vortex funnel is given by the formula

$$V = \frac{A}{2\pi} \sqrt{\frac{Q^2}{(r^2 + z^2)^2} + 39,4 \frac{V_0^2 \cdot B}{r^2}},$$

- where Q is the water discharge, m^3/sec ;
 r = distance from the axis of the funnel to the point considered, m ;
 z = the vertical coordinate of the point considered, m ;
 V_0 = velocity of the flow approaching the vortex producer panel, m/sec ;
 A = coefficient including the velocity increment across the flow depth;
 B = width of the vortex panel, m

$$B = b \left(\frac{\Delta h}{H} \right)^k \cdot F$$

- herein b is the width of the flow;
 Δh = drop in the water stage level in front of the trash rack, m ;
 H = flow depth at the entrance, m ;
 k, F = coefficients governed by the approach velocity [R. 1].

The increased flow velocities in the funnel make it eminently suitable for combatting frazil and ice troubles at hydroelectric plants.

The method described does not call for electric heating of the trash rack, and ensures steady operation of the hydraulic turbines at constant pressures [R. 2].

The design of the vortex producers is both simple and economical. Flat rectangular plates, i.e. vortex producers are mounted at right angles to the flow in front of the trash racks. Large vortex funnels sometimes extending throughout the total depth of the flow form beyond them. A single vortex producer is provided in forebays with vertical walls and one penstock. In forebays with a dividing pier either two plates are to be installed, one in each chamber, or a single T-shaped vortex producer that generates two funnels rotating in opposite directions is mounted at the dividing pier. The above device is utilized with sloping forebay walls.

The 20-year experience obtained at the Verkhne-Varzob hydro-power plant indicates that the vortex funnels exerted a marked favourable effect on winter operation conditions.

The Burdzharskaya hydroelectric plant was equipped with vortex producers in 1952. Since then frazil has been every year passed through the turbines by means of funnels.

Two vortex funnels for the discharge of fragmented and frazil ice through the turbines are envisaged at the Kiev pumped-storage plant. With this aim in view two 6 m wide and 14.25 m high vortex producer panels are to be assembled and attached to the vertical reinforced concrete channel walls by hinges. The panels revolving on a vertical axis will be controlled by a screw mechanism. In summer the device will not obstruct the flow being stored in a specially designed recess.

Comparison of the potential economic effect of the various ice control measures at the Kiev pumped storage plant proved the discharge of fine-fragmented ice and frazil through the turbine units to be simplest, most effective and convenient in operation [R. 3].

Tests conducted at the head structures of the Dzauzhikau power plant revealed the feasibility of using vortex funnels for passing logs through dam bottom outlets.

References

1. Fokeev V.S., Breaking of ice for navigation purposes, River Transport, 1969, N 4.
2. Fokeev V.S., Vortex funnels and their application at power plants, "Energia", 1964.
3. Shmulson B.D., The Kiev pumped storage plant, Gidrotekhnicheskoe Stroitelstvo, 1972, N 4.

ВНИИГ. 3/УШ-73 г. Зак. 419.

